ENVIRONMENTAL MINING IMPACT ON SOILS AROUND THE ABANDONED KGWAKGWE MANGANESE MINE, BOTSWANA

Ekosse Georges-Ivo Ekosse

Thesis submitted in fulfillment of the requirements for the Degree

Doctor of Philosophy in Soil Mineralogy

Discipline of Soil Science

School of Agricultural and Environmental Sciences

University of the North

Sovenga

South Africa

April 2004

ENVIRONMENTAL MINING IMPACT ON SOILS AROUND THE ABANDONED KGWAKGWE MANGANESE MINE, BOTSWANA

Ekosse Georges-Ivo Ekosse

Thesis submitted in fulfillment of the requirements for the Degree

Doctor of Philosophy in Soil Mineralogy

Discipline of Soil Science

School of Agricultural and Environmental Sciences

University of the North

Sovenga

South Africa

Supervisor: Prof. P. Fouche

April 2004

DECLARATION OF INDEPENDENT WORK

I, EKOSSE GEORGES-IVO EKOSSE, do hereby declare that this thesis hereby submitted to the UNIVERSITY OF THE NORTH, SOVENGA, SOUTH AFRICA for the degree of DOCTOR OF PHILOSOPHY IN SOIL MINERALOGY has not been previously submitted by me for a degree at any university; that it is my own work in design and execution, and that all material contained therein has been duly acknowledged.

…… ……..

SIGNATURE OF STUDENT DATE

DEDICATION

In memory of Anthony Gabriel Litange Ekosse,

My Father, Teacher, Counselor and Mentor

ACKNOWLEDGEMENTS

I am particularly grateful to my supervisor and Head of the Discipline of Soil Science and Acting Director of the School of Agricultural and Health Sciences, University of the North, Prof P.S. Fouche for the tireless academic, technical, logistical, moral and spiritual support given to me all through out the time the research project was executed. I also thank Mr. B. Mashatola for academic and logistical support and assistance with fieldwork. Their timely field visits to the study site threw more light and directional understanding on the research work. I am also grateful to other members of staff of the Department of Soil Science, University of the North who were contributory to my success includes Ms. P. Shaker, Mr. F. Madiba, and the secretarial staff. The following individuals and laboratories are acknowledged:

- Mr. G. Rabalone, Faculty of Science, University of Botswana, for assistance with some aspects related to physico-chemical analyses.
- Prof. B. Vink, Department of Geology, University of Botswana, for discussions on manganese mineralogy in the Kgwakgwe Mn oxide ore abandoned mine.
- Dr. A. Jordaan and Mr. S. Coetzee, Electron Microscopy Unit, University of Botswana, for assistance with some aspects related electron microscopy.
- Dr. J. C. Ngila, Ms. Nchindo and Mr. Kiptu, Department of Chemistry, University of Botswana, for assistance with different aspects related to chemical analyses.

- Ms. B. Mazibuku, for assistance with some aspects related to Remote Sensing and GIS skills and maps.
- My team of field assistants (Katlherelo, Simon and John) who assisted with some aspects of fieldwork.
- Ms. V. Ngole, Department of Environmental Science, University of Botswana for logistics, moral and technical support.
- Prof. J. S. Nkoma, Department of Physics, University of Botswana, for moral and academic support.
- Physico-chemical analyses were conducted at the Soils Laboratory, Department of Environmental Science, University of Botswana.
- Mineralogical tests were performed at the X-Ray Diffraction Laboratory and the Electron Microscopy Laboratory, both of the Faculty of Science, University of Botswana.
- Chemical analyses were done at the Chemical Instrumentation Laboratory, University of Botswana.
- The different software packages used in this study were provided by the X-Ray Diffraction Laboratory, and the Department of Geology, University of Botswana.

I cannot list all the individuals, institutions and organizations that have over the years been a very strong pillar of support for me. Without them I could not have attained this level of academic pursuit. Of special mention are Prof. H. H. Murray, Indiana University, Bloomington, USA for teaching me applied clay mineralogy

and being my mentor, Drs. E and B Morton for the continuous extension of their right hand of fellowship to me, and Dr. E. Mondoa for a lifelong relationship of friendship and perpetual support that has spanned from elementary school days.

On the family side, different levels and forms of support and encouragement were received from Timothy Ekosse, Emmanuel Ekosse and Comfort Ekosse; Ma Theresa Ekosse, Dr. Mbako Ngombe and all my siblings, the many wonderful nephews and lovely nieces, and to all my cousins who have identified themselves with me over the years.

Finally I am most grateful and thankful to God the Father, the Lord Jesus Christ and the Blessed Holy Spirit for giving to me the strength, finances, knowledge, courage and the faith to pull through the program. God has been my shield and my salvation. All Glory goes back to Him!

ABSTRACT

This research study focuses on environmental mining impact of soils around the abandoned Kgwakgwe Mn mine in Botswana. The thesis contains five chapters: introduction, methods and analytical techniques, results, interpretation and discussions, and conclusions. The physico-chemical properties, mineralogical identification and characterisation and chemical properties of soils and related geological materials as well as the chemical properties of the soils and leaves of plants around the abandoned mine were investigated in order to determine the mining impact on the surrounding soils. It mentions field research components, which included observation and sampling of surface soils, related geological materials and leaves of plants for different laboratory analyses. Methods, techniques and instrumentation for physico-chemical, mineralogical and chemical analyses are explained. Physico-chemical properties studied on soil samples included particle size distribution (PSD), pH, electrical conductivity (EC), soil colour, and descriptive petrography. Identification of minerals contained in soil samples which included both < 53 μm and < 4 μm size fractions were performed employing X-ray powder diffraction (XRPD) techniques. The < 4 μm size fractions of soil samples were further characterised using the environmental scanning electron microscope (ESEM) to which was fitted with an X-ray energy dispersive spectrometer (EDS). Chemical analyses for iron (Fe) and manganese (Mn) concentration levels in soil and leaf samples were measured with the flame atomic absorption spectrometer (FAAS). Determination of exchangeable bases (Na, K, Ca and Mg), cation echange capacity (CEC) and percent base saturation,

P, Cl, SO_4 and CO_3 concentrations were performed only on the soil samples. The exchangeable bases, CEC and percent base saturation were determined using the ammonium acetate method which included flame photometry for K and Na, and AAS for Ca and Mg. The Olsen method was applied to determine P concentrations. Furthermore analyses for Cl and SO_4 were done using ion chromatography, whereas the calcimeter was used to determine CO_3 concentrations. A Quickbird 2.4 m – 2.8 m resolution with zero cloud cover multispectral standard imagery of the study area was processed to characterise the vegetation cover. The laboratory results were processed using Geographical Information Systems (GIS), and Remote Sensing (RS) techniques with the integrated Land and Water Information System (ILWIS), Geosoft Oasis Montaj and ArcGIS software packages. Microsoft Excel was used for statistical and graphical presentation of data analyses. The particle size distribution of soil samples revealed the average wt % of the soil fractions as follows: the < 4 μm fraction was between o.3 wt % and 30.58 wt %, and the < 53 μm fraction was between 11.05 wt % and slightly above 100 wt %. Soil pH ranged from 2.92 to 7.26 with very acidic soils located close to the mine workings. Electrical conductivity values were significantly low, and the range was from 49.1 $\mu S cm^{-1}$ to 123.5 $\mu S cm^{-1}$. Dark brown to reddish brown soil colour was indicative of very high Fe and Mn levels in the soils. Bulk soil samples consisted of quartz, SiO_2; haematite, Fe_2O_3; goethite, $Fe^{+3}O(OH)$; bixbyte, Mn_2O_3; braunite, $Mn^{+2}Mn_6{}^{+3}SiO_{12}$ ramsdellite, MnO_2; pyrolusite, MnO_2; cryptomelane, $K_{2-x}Mn_8O_{16}$; sanidine, $K(Si_3Al)O_8$; microcline, $KAlSi_3O_8$; whereas the < 4 μm

fraction was made up of kaolinite, $Al_2Si_2O_5(OH)_4$ illite, $KAl_2Si_3AlO_{10}(OH)_2$; and muscovite $KAl_2Si_3AlO_{10}(OH)_2$. The range of concentration levels of Fe in soils was from 1116 μg g^{-1} to 870766 μg g^{-1} with a mean of 17593 μg g^{-1} and for Mn in soils was 35 μg g^{-1} to 24907 μg g^{-1} with a mean of 1088 μg g^{-1}. The values for Na concentration in the soil samples ranged from 0.1 $cmol_ckg^{-1}$ to 89.1 $cmol_ckg^{-1}$, with a mean of 0.44 $cmol_ckg^{-1}$, and for K concentration in the soil samples values ranged from 0.1 $cmol_ckg^{-1}$ to 163.6.1 $cmol_ckg^{-1}$, with a mean of 0.82 $cmol_ckg^{-1}$. The values for Ca concentration in the soil samples ranged from 0.3 $cmol_ckg^{-1}$ to 1139 $cmol_ckg^{-1}$, with a mean of 5.68 $cmol_ckg^{-1}$, and values for Mg concentration in the soil samples ranged from 0.3 $cmol_ckg^{-1}$ to 1655.3 $cmol_ckg^{-1}$, with a mean of 8.26 $cmol_ckg^{-1}$. The CEC values in the soil samples from the study area ranged from 1.1 $cmol_ckg^{-1}$ to 29.2 $cmol_ckg^{-1}$, with a mean of 8.2 $cmol_ckg^{-1}$, and values for percent base saturation in the soil samples were from 33.77% to 100 % with a mean of 82.10 % $cmol_ckg^{-1}$. Values obtained for P_2O_5 in some randomly chosen soil samples from the study area were from 0.51 $mgkg^{-1}$ to 6.02 $mgkg^{-1}$. The values for Cl concentration in the soil samples ranged from 0.2 $mgkg^{-1}$ to 11.9 $mgkg^{-1}$, with a mean of 7.63 $mgkg^{-1}$, and for SO_4 concentration in the soil samples values ranged from 2.1 $mgkg^{-1}$ to 47.5 $mgkg^{-1}$, with a mean of19.36 $mgkg^{-1}$. The values for CO_3 concentration (measured in terms of $CaCO_3$ equivalent) in the soil samples ranged from 5.1 gkg^{-1} to 59.1 gkg^{-1}, with a mean of 40.98 gkg^{-1}. For the leaves, the range of concentration levels of Fe contained in them was from 101.2 μg g^{-1} to 3758 μg g^{-1} with a mean of 637 μg g^{-1} and for Mn in leaves, the range was from 26.2 μg g^{-1} to 3611.5 μg g^{-1} with a mean of

598.4 μg g^{-1}. The TOC values were between 0 wt % to 7.9 wt %. High acidity of soils is reflected by on-going neomineralisation activities which at some places are depicted by the formation of dead zones. Other observable phenomena were stunted growth of plants, and the yellowing of their leaves as a result of high concentrations of Fe and Mn in their organic systems. The gridded soil and vegetation maps for Fe and Mn show anomalies in different parts of the study area. Where Mn is high, the Fe is low and vice versa. Manganese was high at the mine workings and in the northwestern part of the study area. Iron on the other hand is very low in the mine working area and is high on the northern part of the study area. The mineral genesis is explained and a model is advanced for the Mn interplay in the soils and environment around the Kgwakgwe abandoned Mn oxides ore mine. Remediative measures for reclamation of the contaminated soils and appropriate land use of the area have been suggested. It is anticipated that these useful recommendations to stakeholders which have been suggested, and the direction for further research if adhered could bring solution to some of the environmental pollution problems in the study area.

TABLE OF CONTENTS

LIST OF FIGURES

Figure ----------Page No.

LIST OF TABLES

Table----------Page No.

LIST OF ACRONYMS

AAS	Atomic absorption spectrometry
BRQF	Black Reef Quartzite Formation
EC	Electrical Conductivity
EDS	Energy Dispersive Analysis
EIA	Environmental Impact Assessment
ESEM	Environmental scanning electron microscopy
ESEM-EDX	Environmental scanning electron microscopy with X-ray dispersive spectrometry
FAAS	Flame atomic absorption spectrophotometry
GPS	Global positioning system
HVM	High Vacuum mode
ICDD	International Center for Powder Diffraction Data
ILWIS	Integrated Land and Water Information System
KVF	Kanye Volcanic Formation
KCBF	Kgwakgwe Chert Breccia Formation
KS	Kgwakgwe Shale
LN	log normal
LVM	Low Vacuum mode
Ma	million year
MSS	Multi spectral
N	Normal
NDVI	Normalised difference vegetation index

OM	Optical Microscopy
PAM	Particulate air matter
PS	Particle size
PSA	Particle size analyser
PSD	Particle size distribution
RSD	Relative standard deviation
SD	Standard deviation
SUTW	Super Ultra Thin Window
TDS	Total dissolved salts
TOC	Total organic carbon
TDG	Taupone Dolomite Group
USA	United States of America
USA-EPA	United States of America – Environmental Protection Agency
USDA	United States Department of Agriculture
WHO	World Health Organisation
XRPD	X-ray powder diffraction
cm	centimetre
esd	euhedral spherical diameter
pH	hydrogen ion concentration
ppb	parts per billion
ppm	parts per million
rpm	revolutions per minute
wt %	weight percent

^{o}C	degree Celsius
μg /g	micrograms per gram
μm	micro metre
μScm^{-1}	micro siemens per centimetre

CHAPTER ONE

INTRODUCTION AND LITERATURE SURVEY

1.1 BACKGROUND

Manganese (Mn) and iron (Fe) concentrations in soils are having a growing interest because of the implications resulting from their high concentration levels. Plants require nitrogen (N), phosphorus (P), potassium (K), calcium (Ca), magnesium (Mg), sulfur (S), iron (Fe), manganese (Mn), copper (Cu), zinc (Zn), and boron (B) in varying amounts, but if quantities of these elements are high, they become harmful to the plants. Manganese and Fe are among the common metals found in soils, and could occur at levels considered to be contaminants/pollutants when present in higher concentrations. Both Mn and Fe are important constituents in plants and animals, provided their toxicity levels of ionic concentrations are not exceeded. Plants require Mn and Fe from soils, whereas animals obtain theirs from plants if herbivores, or from herbivores if they are carnivores. Aquatic plants and animals obtain their Mn and Fe supplies from waterbodies.

Manganese (Mn) occurrence in soils is mostly in the form of Mn minerals in chemical combinations with oxygen: its oxides MnO_x, common forms include pyrolusite MnO_2, cryptomelane KMn_8O_{16} and bixbyite $(Mn,Fe)O_3$ (Bohn *et. al*., 2001). Other MnO_x present in soils are manjiorite $(Na,K)Mn_8O_{16}.xH_2O$ and hausmannite Mn_3O_4 (Ekosse and Vink, 1998). The oxides are usually black. Ions of transition metals have the same size as that of Mn, making isomorphous

substitution easy (Bohn, mcNeal and O'Connor, 2001) for these elements to be retained in oxides and hydroxides of Mn.

Iron (Fe) occurrence in soils is mostly in the form of Fe minerals in chemical combinations with oxygen: its oxides Fe_xO_y, and the common forms being hematite (Fe_2O_3) and magnetite (Fe_3O_4) (Bohn *et. al*., 2001). Its hydroxyoxide form, goethite (FeO. OH) is also very common. Hematite is pink to bright red, magnetite is reddish brown, and goethite is brown to dark yellowish brown.

Manganese (Mn) occurrences at Kgwakgwe hill are associated with goethitic ochre and kaolin (Ekosse and Mulaba, 2003; Ekosse and Nkoma, 2002; Lanznicka, 1992). Both the goethitic ochre and kaolin have never been mined for any known economic applications (Ekosse and Modisi, 1999). Manganese mining, which started in 1957 (Aldiss, Tombale, Mapeo and Chiepe, 1989), has been suspended over two decades ago. Previous studies carried out at Kgwakgwe area focused on origin of the Kgwakgwe Chert Breccia (Modisi, 1995), manganese oxides (Mn oxides) as evidence for shallow aqueous palaeo-environment (Ekosse and Vink, 1998), provenance of argillaceous sediments (Ekosse, 2001; Ekosse and Nkoma, 2002), and the geology and mineralogy of the manganiferous, ferruginous and argillaceous sediments (Ekosse and Vink, 2001).

No known studies have so far been conducted to physico-chemically, mineralogically and chemically characterise the soils, and to appraise the Mn mining impact on the surrounding surface sedimentary environments. This research project aimed at investigating the physico-chemistry, mineralogy and soil chemistry of the surface sediments occurring at Kgwakgwe in an attempt to determine soil genesis, and evaluation for possible small scale agricultural activities. Furthermore, the impact of manganese mining on the surrounding surface sediments was determined. Aspects of mine rehabilitation were also addressed.

1.2 STATEMENT OF PROBLEM

Kgwakgwe is within the periphery of Kanye township, the capital of the southeastern District, Botswana. Kanye is one of the few major towns/cities of Botswana with a current population of over 65 000 inhabitants (Figure 1.1) (National Census, 1991). The inhabitants of the surrounding villages are engaged in agro-pastoral activities. Recent complaints from villagers and cattle grazers within the periphery of Kgwakgwe regarding drop in agro-pastoral yield has called for the need to characterise the surface soil. The characterisation exercise aimed at ascertaining the genesis of the soil and appraises its suitability for agro-pastoral activities.

Minerals of Mn occur within the Kgwakgwe Shale of the Neoarchaean Transvaal Supergroup (Carney, Adliss and Lock, 1994). Small scale mining of Mn oxides

started in 1957 and continued for well over thirty years intermittently at Kgwakgwe by a number of South African based mining companies. Due to limited high grade quality and associated high cost of mining, the exploitation of Mn oxides was suspended. However, the abandoned mine workings have not been rehabilitated. During mining of Mn ore, a lot of anthropogenic activities were carried out to the extent that aeolian, aquatic and terrestrial distribution of the mineral covered a wider area than the mining premises. Consequently, concentration levels of Mn in soils within contaminated areas may have increased. It was therefore necessary to fully understand migratory pathways of ions of Mn and to determine contamination of surrounding soils in the area.

Figure 1.1: A closer view of part of Kanye township (Photograph taken from the Adventist Hospital, Kanye)

In this study of mining impact on soils at Kgwakgwe, Botswana, an investigation of the physico-chemical, mineralogical and chemical properties of the soil as well as the chemical properties of the vegetation was conducted. Furthermore, the digital version of Multispectral Quickbird Imagery: resolution 2.4-2.8m for the study area was used for overlying laboratory analytical results and data interpretation. The satellite data was interpreted to identify suitable land cover classes mainly of most stressed, moderately stressed, mildly stressed and non stressed vegetation cover, abandoned mine workings, and Mn-contaminated soils.

1.3 AREA OF STUDY

The location, geology, geomorphology, hydrology, climate, soils and vegetation of the area are briefly discussed below.

1.3.1 Location of the study area

The research project is around Kgwakgwe area, 4 Km south of Kanye township, (Figure 1.2), in the southeastern part of Botswana. Kgwakgwe is located between latitudes 24^{o}59' and 25^{o}02', and longitudes 25^{o}17' and 25^{o}20'. Kgwakgwe Hill (Figure 1.3) is where the manganiferous and ferruginous sediments occur, and mining took place. The area is accessible by road from Gaborone and Lobatse, and there are many motorable tracks which serve the lands and cattle posts closeby.

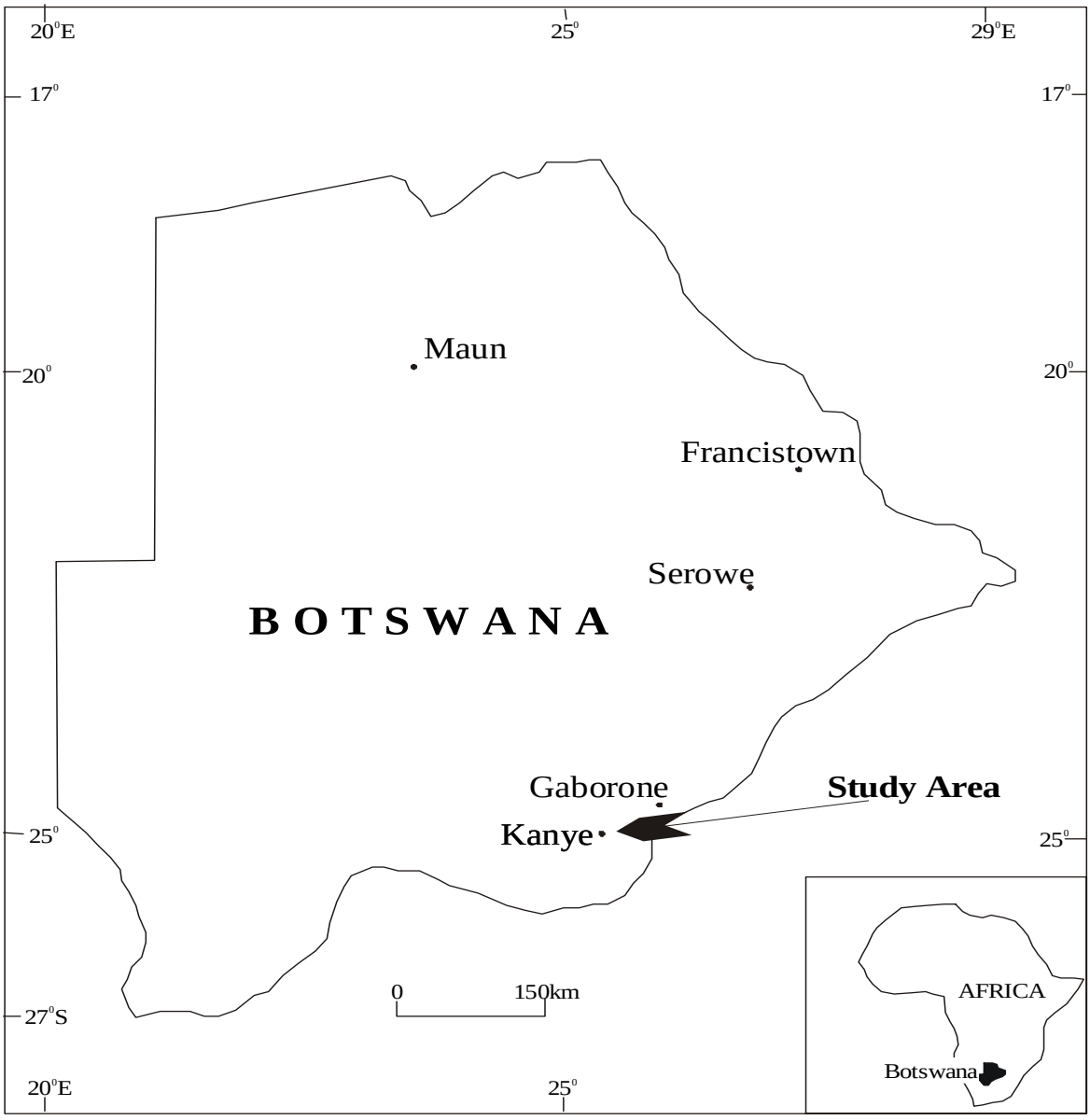

Figure 1.2: Map of Botswana showing location of proposed study area

Figure 1.3: Kgwakgwe Hill viewed from a distance of about 2km

1.3.2 Geology of the study area

The geology of the Kgwakgwe Basin is extensively discussed in Aldiss *et. al*., 1989; Carney *et. al.,* 1994; Modisi, 1995; Vink and Ekosse, 1998; Ekosse and Modisi, 1999; and Ekosse and Nkoma, 2002. The geology of the area where the Mn mineralisation occurred is presented in Figures 1.4 and 1.5. The rocks of the Kgwakgwe basin are of the Paleoproterozoic Transvaal Supergroup, capped by the younger Waterberg Group, and underlain by an older Kanye Volcanic Formation (KVF) (Table 1.1).

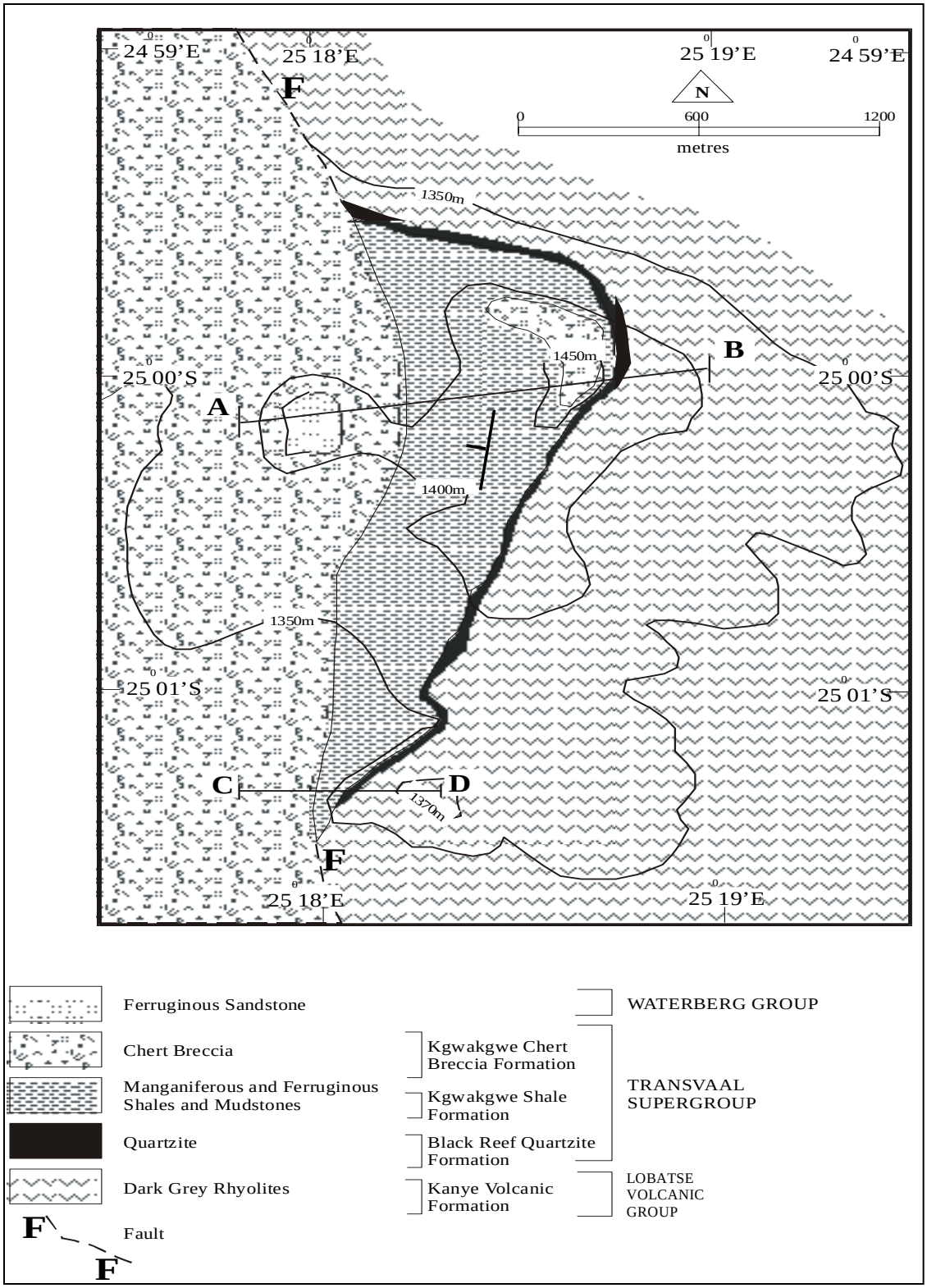

Figure 1.4: Geology map of the Kgwakgwe area where Mn mineralisation occurs (after Ekosse and Modisi, 1999; Ekosse and Vink, 1998; 2001).

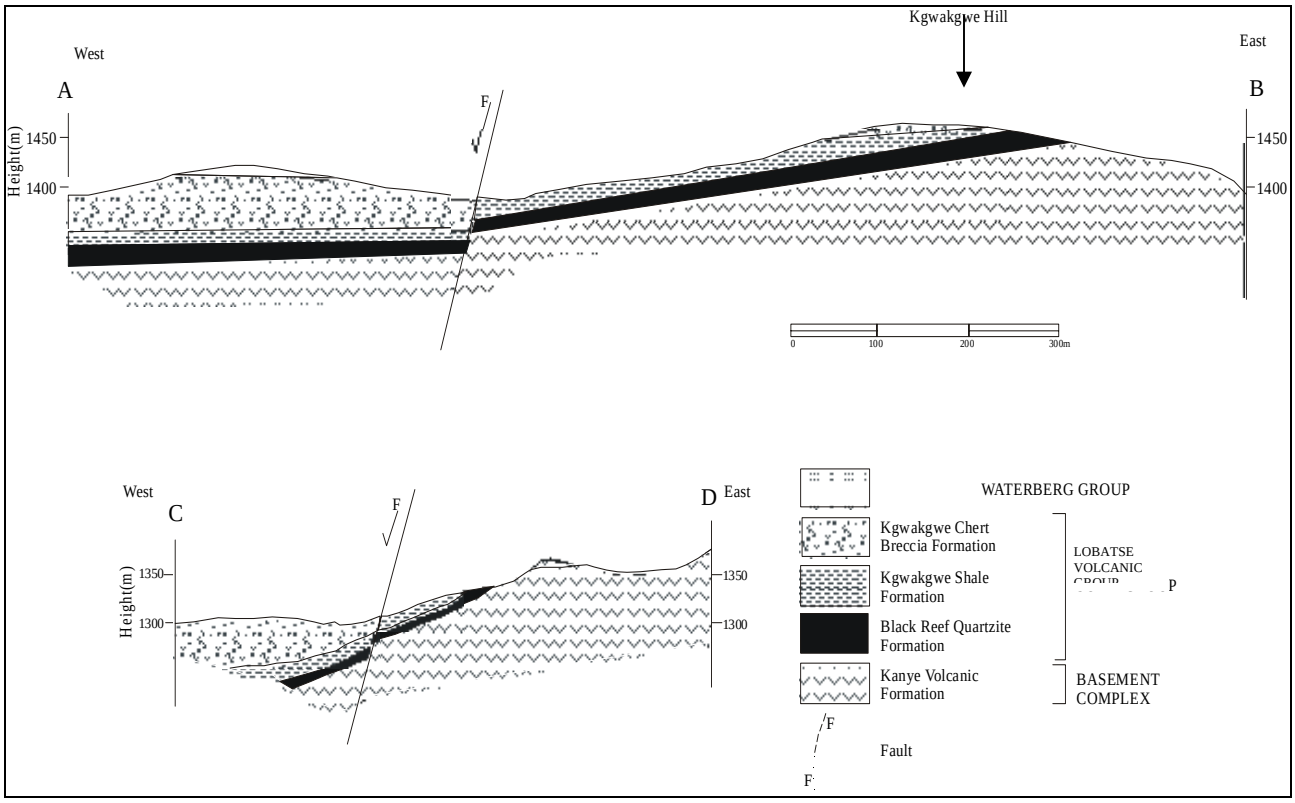

Figure 1.5: Cross section of A-B and C-D in Figure 1.4 (after Ekosse and Modisi, 1999; Ekosse and Vink, 1998; 2001).

The Black Reef Quartzite Formation (BRQF) as indicated in Table 1.1, is the lowest stratigraphic unit of the Transvaal Supergroup and overlies the rhyolites of the KVF with unconformity (Table 1.2). The BRQF consists mainly of conglomerates, coarse to medium grained sandstone, arkoses, and interbedded siltstones and shales, with sediments displaying plain bedding, graded bedding and cross bedding. The Kgwakgwe Shale (KS) succeeds the BRQF, and it consists of varicoloured manganiferous and ferruginous shale units belonging to the Taupone Dolomite Group (TDG).

Table 1.1: Lithostratigraphy of the Kgwakgwe basin (modified after Vink and Ekosse, 1998; Ekosse and Modisi, 1999; Ekosse and Vink, 2001).

Lithology	**Formation**	**Group**	**Supergroup**	**Age**
Sandstones		Waterberg		1700 Ma
Chert clast breccia	Kgwakgwe Chert Breccia	Taupone Dolomite	Transvaal	2500 Ma
Varicolored manganiferous and ferruginous shale	"Kgwakgwe Shale"			
Quartzite, shale conglomerate	Black Reef Quartzite			
Feldspathic rhyolites	Kanye Volcanic	Lobatse Volcanic (LVG)		2780 Ma

The manganiferous and ferruginous shales and siltstones are directly underlain by the BRQF, which is the basal formation of the rocks of the Transvaal Supergroup in large parts of South Africa, extending northwards into Botswana. The TDG as indicated Table 1.1, represents the lower part of the Paleoproterozoic (Carney *et al*., 1994) of the Transvaal Supergroup in Botswana and South Africa (Tombale, 1986) having an age of 2500 - 2000 Ma (where Ma is million year). The lower section of the TDG, being the host rock of the Mn oxides and kaolin occurrences, may be close to 2500 Ma old.

Table 1.2: Stratigraphy of the Kanye – Jwaneng area 2a (after Tombale, 1986); 2b, the Kgwakgwe area (this research area); 2c, area close to the water pumping station located 2km south of Kgwakgwe

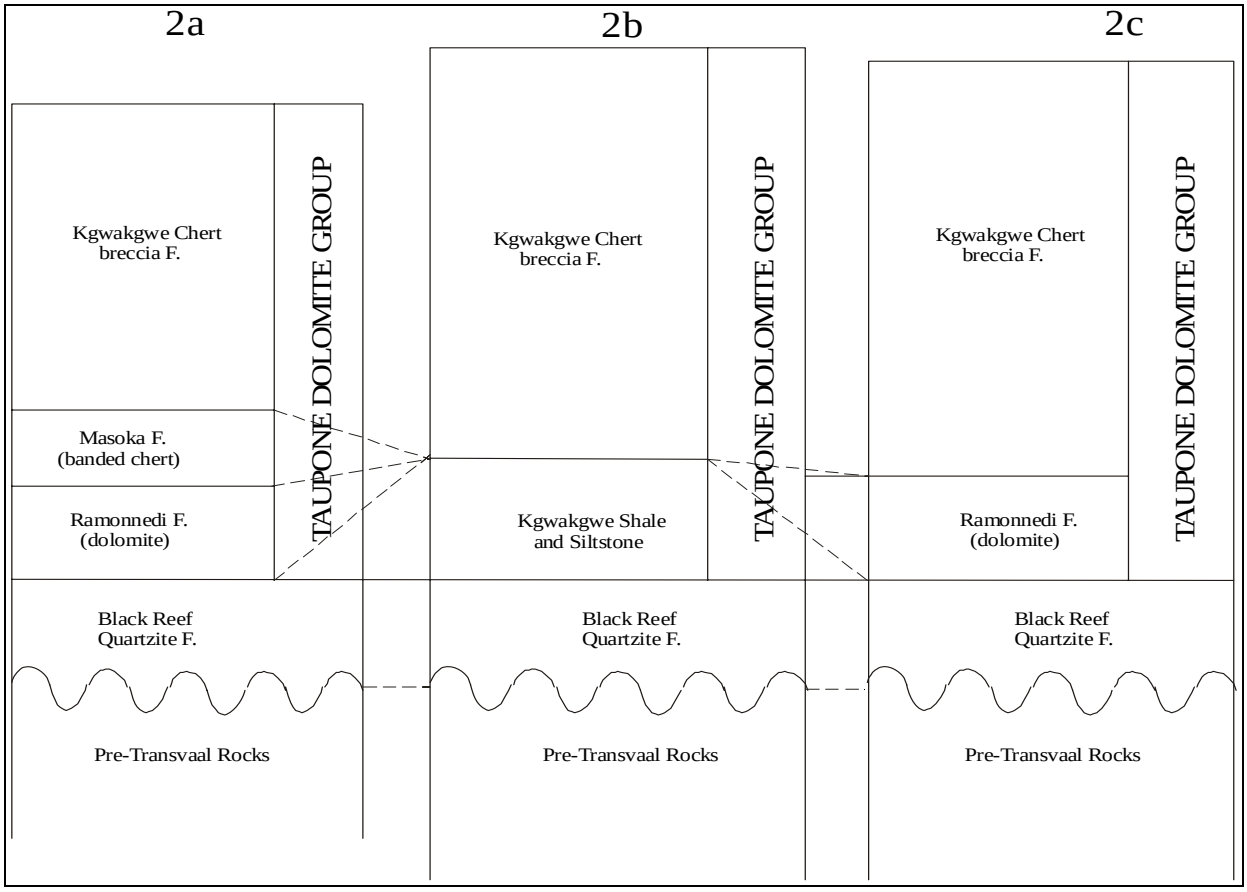

The Kgwakgwe Chert Breccia Formation (KCBF) directly overlies the KS and siltstones (Table 1.1). The BRQF, the TDG and the KCBF dip about 10^{o} to the WNW, and west of Kgwakgwe Hill and are truncated by a N-S trending fault zone. To the west of the fault, the KCBF is partially overlain by much younger sandstones of the Waterberg Group as shown in Figure 3a, for which a lower age limit of 1920 ± 40 Ma is accepted (SACS, 1980; Carney *et al.,* 1994).

The stratigraphy of the Kanye-Jwaneng area as shown in Table 1.2 section 2a has been described by Tombale (1986). Table 1.2 section 2b depicts the stratigraphic sequence in the Kgwakgwe Hill area. In the study area, the manganiferous and ferruginous shales and siltstones are located directly on top of the BRQF. They are overlain by the KCBF. The dolomite of the Ramonnedi Formation and the banded chert of the Masoke Formation are absent. Table 1.2 section 2c illustrates the stratigraphy located 2 km south of Kgwakgwe Hill where most of the soil samples used in this study were obtained. At this area, the BRQF is overlain by the dolomite of the Ramonnedi Formation. The maximum thickness of the manganiferous shales and siltstones is not more than 20 m. The shale is overlain by the chert breccia of the KCBF. The Kgwakgwe manganiferous and ferruginous shales are locally strongly folded, strongly contorted and jointed. In the south of the deposit they are brecciated, resulting in total disappearance of any original stratification.

1.3.3 Geomorphology and hydrology of the study area

Kgwakgwe area adjoins Kanye township, which is situated on a plateau with an altitude ranging from 1300 m, and 1400 m above mean sea level. The plateau consists of igneous rocks, and makes contact with dolomitic plains, part of which this study area covers. Elongated hills on the eastern edge of the dolomite complex area are formed by pinkish to whitish quartzites of the Black Reef Quartzite Formation.

Chert breccia caps most of the hills around Kgwakgwe. The dolomitic rocks, which are less resistant to weathering, become predominant in the flat areas. Quite distinctly are the positive relief chert rich dolomites, which alternate with the negative relief chert free dolomites.

The Transvaal Dolomite has been identified in the study area as the main aquifer body. No prominent surface river is found in the study area. Excessive run-off of storm water after torrential rains are typical of the environment. Cattle and game drink from stream water, which may contain high concentrations of Mn (Figure 1.6). During the dry season, the streams are void of running water.

Small streams in the area flow east into the Notwane River, which is part of the Limpopo River System, some flow northwest into the Makgadikgadi Pans, whereas others flow southwest into the Molopo drainage system. The margins of the drainage channels on the flat lying terrains have been affected very extensively by soil erosion. There are several large areas that have been rendered derelict due to erosional activities resulting in exposure of bedrock, and the formation of gullies some of which could be as deep as 3 m.

Figure 1.6: A closer view of cattle drinking from stream water suspected to be Mn contaminated

1.3.4 Climate of the study area

The southeastern Botswana, which includes the study area is climatically characterised with hot and wet summers, and dry, cold short winter seasons. Recorded temperature values from 1958 to 1985 indicated an average maximum temperature of 40.9 ^{o}C, and an average minimum of 2.2 ^{o}C, and an average mean temperature of 14 ^{o}C (Bhalotra, 1987).

Rainfall is similar to the type occurring at semi-arid regions characterised by heavy thunderstorm activities. Most of the rainfall occurs between the months of

October and April (Bhalotra, 1987). Thunderstorm activities are usually short-lived, and are followed by long dry spells. Between 1925 and 1985, monthly average annual rainfall recorded was 177 mm/year in August, and high of 345.5 mm in December (Bhalotra, 1987). Between 1975 and 1976, the highest ever-recorded annual rainfall amount of more than 700 mm/yr was obtained. Between 1983 and 1986 as well as in 1993, the region experienced severe drought, with a recorded average rainfall of 300 mm/yr.

1.3.5 Soils of the study area

The soil types at the study area vary with changes in topographic elevations and underlying rocks. The ferric luvisols and calcic luvisols are associated with lowland areas having ephemeral streams. The soils are characterised as moderate, moderate-well to well drained, brown to yellowish brown sandy loam to sandy clay soils (Mitchell, 1976; Remmelzwaal, 1988). They overlie the granitic, rhyolitic and doleritic rocks of the Basement Complex and dolerite intrusions. The soils at Kgwakgwe (Figure 1.7) are high in Mn and Fe from the Mn oxide orebodies. The soils are exposed to erosion, and are suspected to be contaminated with Mn from old mine workings (Figure 4).

Figure 1.7: Exposed soil at Kgwakgwe area, reflecting Mn and Fe contamination

The Mn content in soils is derived from the parent materials, and usually the element is associated with Fe because of their ability to isomorphically substitute one another in the crystal lattice structure of minerals. Most common form of its existence in soils are in the oxide forms and the minerals are birnessite, $(Na_{0.7}, Ca_{0.3})Mn_7O_{14}.2.8H_2O$); pyrolusite, MnO_2; manganite, $Mn^{3+}OOH$ and hausmannite, Mn_2O_4. The element can exist in oxidation states of Mn(II) to Mn(VII) of which Mn(II) and Mn(IV) occur the most (Smith, 1990).

1.3.6 Vegetation cover of the study area

Timberlake (1980) described the vegetation cover of the area as having depressions of thicket and shrub savannah on dark clayey soils. Acacia is the dominant vegetation cover at the Kgwakgwe area. Acacia plants in the area include *Acacia tennispina*, *Acacia mellifera*, *Acacia karoo*, *Acacia hereroense*, *Acacia caffra* and *Acacia tortills*. Other dominant species are *Combretum apiculatum*, *Euclea undulata* and *Terminalia sericea*. Interspersed areas of hardveld are covered with woodland and tree savannah type vegetation on less acid soils. These plants include *Rhus lancea*, *Rhus leptodictya*, *Ziziphus mucronata*, and *Tarchonanthus camphorates*. There are possibilities of high Mn in soils affecting vegetation and possibly causing sparse vegetation cover (Figure 1.8).

Figure 1.8: Acacia-dominated sparse vegetation cover at the Kgwakgwe area

1.4 MOTIVATION FOR STUDY

Manganese deposits and occurrences in Botswana are found in Kgwakgwe, Lobtase, Otse, Ramotswa and Tsabong (Ekosse and Vink, 2001; Vink and Ekosse, 2002; Adliss *et. al*., 1989), and of past mining activities, which were carried out at Kgwakgwe, Lobtase, and Otse (Adliss *et. al*., 1989). Because the Mn ore deposit at Kgwakgwe was vast compared to the other mining areas, exploitation activities were carried out for over thirty years intermittently. Consequently, the surrounding environment and more especially the soils, became easily susceptible for Mn pollution.

At the time of inception of the Mn mining project at Kgwakgwe, no environmental impact assessment (EIA) studies were conducted, and no environmental mitigation programmes were put in place. Mining companies were interested in making maximum profit at the least possible investment costs. As a result of Mn exploitation activities not being properly carried out, its negative effect on the environment around the abandoned mineral deposit is today considered to be problematic. These negative effects apart of waste accumulation, which often are a source of ecological danger, could also be associated with pollution of soils, surface and ground waters, and atmospheric air. A contrast of concentrations of Mn and Fe in soils substantially increases in the areas around the abandoned mine.

Complaints have been made by the inhabitants of the area regarding sparse vegetation cover, and the researcher has conducted several field visits to substantiate the fact. The surrounding land has lain fallow for several years without any usage. With increasing population growth at Kanye, recent expansion has been directed towards Kgwakgwe. In this regard, there is building pressure from the local community land board for the allocation of more land including that of the study area. Unfortunately, because of its closeness to the abandoned mine which was neither rehabilitated nor decommissioned, there is reluctance from local authorities to assign any specific application to the land. It is thought that the findings from this study may advise on possible land use.

1.5 RESEARCH QUESTIONS

The research questions, which this study attempted to answer, include the following:

- What are the physico-chemical properties of the surface soils around the abandoned Kgwakgwe Mn mine, and the Mn ore?
- What mineral occurrences in the Mn ore, the country rocks and soils are found both at the abandoned soils and mine? Can the soils be mineralogically characterised?
- What are the levels of concentrations of Mn and related elements such as Fe in Mn ore?
- What are the levels of concentrations of Mn and related elements such as Fe in the soils?

- How do the concentrations of Mn in soil effect the surrounding vegetation?
- Can a hypothesis be postulated based on physico-chemistry, mineralogy, and chemistry regarding the genesis of the Mn ore?
- Can a hypothesis be postulated based on physico-chemistry, mineralogy, and chemistry regarding the soils around the abandoned Mn mine?
- Can the surfacial extent of Mn contamination be extrapolated in the area as a result of past mining activities?
- Can the suitability of the soils around the abandoned Kgwakgwe mine be determined for agro-pastoral activities?
- Can an understanding be deducted on possible health and environmental hazards of Mn contamination and/or pollution around Kgwakgwe?

1.6. AIMS AND OBJECTIVES

The aims and objectives addressed in this study were as follows:

- Determination of the physico-chemical properties of the surface soils around the abandoned Kgwakgwe Mn mine, and the Mn ore.
- Identification and characterisation of the mineral occurrences in the Mn ore, the country rocks (which are mainly granitic, rhyolitic and doleoritic rocks), and soils both at the abandoned mine and surrounding surface sedimentary environments.
- Determination of the levels of concentrations of Mn and related elements such as Fe in Mn ore.

- Determination of the levels of concentrations of Mn and related elements such as Fe in surface soils.
- Postulation of a hypothesis based on physico-chemistry, mineralogy, and chemistry regarding the genesis of the Mn ore.
- Postulation of a hypothesis based on physico-chemistry, mineralogy, and chemistry regarding the soils around the abandoned Mn mine
- Extrapolation of the surfacial extent of Mn contamination in the area as a result of past mining activities and other contemporaneous mineralogical and geochemical processes.
- Determination of the suitability of the soils around the abandoned Kgwakgwe mine for agro-pastoral activities by comparing its physico-chemical properties, mineralogical and chemical characteristics obtained at the study site to levels in published literature.
- Discussions on the possible health and environmental hazards of Mn contamination and/or pollution around Kgwakgwe area by comparing concentration levels in soils obtained at the study site to levels in published literature.

1.7 RESEARCH HYPOTHESIS

This study will be conducted under the broad hypothesis that the mining of Mn ore at Kgwakgwe has had negative impact on the surrounding soils.

1.8 SOURCES OF MANGANESE AND IRON CONTAMINATION IN SOILS

Manganese and Fe are naturally occurring and present in varying amounts in most soils and rocks, as well as in surface and groundwater (Iron and manganese, 2002). Alloway and Ayres (1997) have discussed sources of metals contamination in soils including Mn and Fe. These sources are briefly mentioned below:

- Geochemical sources are the main sources of Mn and Fe occurring as primary minerals mainly in igneous rocks and, secondary minerals in metamorphic and sedimentary rocks. The weathering of these rocks causes Mn and Fe ions to occur in regoliths and eventually become chemical constituents of soils.
- In the atmosphere and hydrosphere, Mn and Fe particles occur in parts per billion (ppb). In seas and oceans, Mn nodules occur in great quantities. The nodules could be mined for their Mn contents.
- Due to mining of Mn and Fe from their orebodies, they may be introduced into the environment in high concentration levels causing them to be classified as contaminants and eventually pollutants if levels increase.
- Metallurgical industries whereby Mn and Fe are processed for different industrial applications have been identified as sources of Mn and Fe contamination into the soils.

- Agricultural materials such as pesticides and Mn based fungicide, as well as corrosion of metals objects made of Fe (wire fences, galvanized roofs and animal sty) could provide Mn and Fe ions into surrounding soils.
- Fossil fuel combustion could provide a wide range of metals including Mn and Fe through emission into the environment as particles, or accumulated in ash and transported by air, eventually contaminating soils and waters. The particles could also be leached in situ into the soils below the ash.
- Other sources of Mn and Fe contamination in soils include waste disposal sites, chemical plants and electronics factories. They handle both primary raw and semi-processed materials containing Mn and Fe, releasing contaminated waste either directly or indirectly into soils.

Levels of concentrations of Mn and Fe in different materials and environment are given in Table 1.3. Studies carried out by Purdey (2000) indicated that Mn levels in soils could be traced to volcanic activities. Toxic levels of Mn have been recorded at levels up to 1886 ppm in pine needles (Sisler, 1996), and more generally in soil matrices (Purdey, 2000). High Mn values could be related to acid rain (Sisler and Huffinan, 1993) as a result of airborne pollutants found around industrial areas (Barrick and Schoettle, 1996). These pollutants are widely recognised to blow onto prevailing air currents, whereby the warm air is forced to rise up and rapidly cool causing the pollutant particulates to fall back to earth as

an integral component of the rain. Increased soil acidity unlocks certain soil cations, such as Mn and aluminium (Al), rendering them more available for uptake into the vegetation horizon (Park, 1987).

Table 1.3: Concentration levels of manganese and iron in different materials and environments (Alloway, 1990).

No	Different materials and environments	Concentration levels of Mn (ppm)	Concentration levels of Fe (ppm)
1.	Earth's crust	950	
2.	Ultramafic igneous rock	1040	
3.	Mafic igneous rock	1500	
4.	Granitic igneous rock	400	
5.	Limestone	620	
6.	Sandstone	460	
7.	Shales/Clays	850	
8.	South Pole Atmosphere	0.01	0.84
9.	Europe Atmosphere	9-210	130-5900
10.	Near Volcano	55-1300	1000-10000
11.	Fresh Water	0.02-130	10-1400
12.	Sea Water	0.03-21	0.03-70

1.9. ENVIRONMENTAL IMPLICATIONS OF MANGANESE AND IRON CONTAMINATION

Manganese and Fe particles are released into the atmosphere through varying anthropogenic and natural activities. Anthropogenic activities including mineral exploitation are having negative impacts on the environment. Issues of metal pollution are becoming increasingly common especially in mining and processing areas (Reichman, 2000). The main sources of metal pollution include the direct release of metals in tailings and waste rock dumps, and release from emissions in the different processing stages. Depending on the metal mine, mitigation procedures range from almost non-existent to sophisticated long-term remediation programs. From industrial operations, their ions percolate into soils and dilute in water bodies. These displacements of Mn and Fe result in different environmental implications affecting the soils, vegetation, surface and groundwater, and human beings and animals.

Of particular concern to the community is the exploitation of minerals. This is because the mining activities have the ability to cause sickness and death in plants, animals and humans as a result of soils, water and air pollution. Plants are of particular concern because they extract metals from polluted soils and mine wastes making them available to animals, including livestock, and humans who feed on the plants and animals (Reichman, 2000). Iron occurs as an integral element in Mn orebodies. At Kgwakgwe, Fe bearing minerals (both goethite and

hematite) (Ekosse and Modisi, 1999), have been identified in substantial quantities. Although it is very essential in the blood, Fe may have some adverse effects to the physical environment. In the oxidation of sulphides of Fe, acidic solutions are created which tend to decrease adsorption and promote mobility of metals in soils, water and sediments. Although many metals, including Mn, Fe and Al are essential for plant health, they could be toxic if their concentration levels are high. High toxic levels of heavy metals in plants are manifested by reduced and stunted growth and, in extreme cases, death.

From the Exploration State through to the post closure or mine decommissioning state, mining of ore bodies has the potential of causing serious environmental impact. As mining is carried out, the land surface is disturbed, affecting to varying degrees the groundwater, surface water, soils, vegetation, wildlife, air quality and cultural resources. Elevated Mn and Fe concentrations in the environment have wide ranging impacts on animals and plants as well as human beings. The environmental implications affecting each of these classes of environmental bodies are briefly discussed.

1.9.1 Soils

Manganese and Fe in soils and mine wastes exist in many forms, including as components of minerals, being bonded to organic matter and as dissolved ions in the water phases of soil. It is known that plants absorb metal-ions from the soil (Reichman, 2000). However in Botswana, there are no regulations based on

bioavailable soil fractions and total soil metal, which are indicative of pollution. Many mines aim to return the postmining landscape to a self-sustaining native ecosystem, which unfortunately has not been done at Kgwakgwe. On metal contaminated sites rehabilitators have a few options, which include liming the soil to reduce acidity thus making the metals substantially unavailable to plants and allowing plants with high metal tolerance (Reichman, 2000) to grow in polluted areas. However, utilising these options is contingent on information about how tolerant plants are to the bioavailable fraction of various metals. This study of the soil mineralogy and chemistry of Mn minerals and to a certain extent Fe minerals, will focus on distribution of Mn and Fe on the soils around the abandoned Kgwakgwe Mn mine in Botswana.

Metal pollution in soils is a widespread international problem resulting form mining and ore refinement, nuclear processing and the industrial manufacture of a variety of products including batteries, metal alloys and electrical components (Roane, Perpper and Miller 1994). Poor industrial waste disposal practices associated with industrialization and technological development have made contamination to become a global problem. Many metal-contaminated sites occur worldwide that pose very serious health risks (Roane, *et al*. 1994).

Soil contamination with metals including Mn and Fe may disrupt the physical, chemical, and biological balance of the soil (Alloway, 1990). Manganese can be found in high concentrations in contaminated soils (Roane, *et al*. 1994). Soil

parameters such as pH, organic matter, particle size, permeability, soil moisture, bulk density and particle density can drastically affect the rate of metal absorption. Whereas sand and gravel are the most favorable soil types for metal-ion leaching, clays are the least favorable. Another factor, which affects the soil absorption rate of metals, is the chemical interaction of the soil and metal (Alloway, 1990). Iron exists in many forms in soils. Iron content in soils affects plant growth, and promotes soil acidity (Ptacek and Bowles, 1992).

Isomorphous substitution of Mn and Fe in clay minerals occurs in mostly the octahedral sheet of 2:1 clays such as smectites, nontronites and Mn rich clays. Sources of Mn and Fe are mainly from Mn and Fe rich orebodies with low weathering activities whereby the ions stay for a long period of residence in the environment. In high leaching environments, whereby 1:1 clays such as kaolin occur, Mn and Fe ions are relatively low. Structural contamination of these minerals in soils and claybodies is possible through isomorphous substitution in both the tetrahedral and octahedral sheets. In well aerated soils rich in oxygen, both Mn and Fe ions are oxidised becoming part of the soil solids.

1.9.2 Vegetation

Rocks and soils contain varied amounts of manganese (Mn) and iron (Fe). Manganese content in soils is linked to its role as micronutrients in plants and as an enzyme activator in the synthesis of glycoproteins and fatty acids, and bone development in animals (Smith, 1990). Manganese and Fe are required for

healthy plant growth. Manganese and Fe are required for electron transport and photosynthesis by plants. Plant roots have Mn and Fe absorption mechanisms that provide sufficient Mn and Fe for healthy growth in most soils. In some acid soils however, solution Mn and Fe concentration levels may be very high. Many plants will then absorb more Mn and Fe than required by their systems internally. If they do not have some internal mechanism to control cellular Mn and Fe concentrations, toxicity effects occur. Under Mn and Fe toxicity conditions, the evidence indicates cell Mn and Fe concentrations very high, such that control of the Mn and Fe activated enzymes is lost (Helyar, 2002). The normal regulation of plant biochemistry is sufficiently upset to cause cell chlorosis, and in the extreme, death.

Iron is a constituent of many organic compounds in plants and is essential for synthesizing chlorophyll. High levels of Mn can induce its deficiency. High Fe levels can also cause Mn deficiency. Injury due to high soil Fe concentrations is not common under neutral or high soil pH conditions. Toxic situations occur primarily on acid soils (< pH 5.0) and where excess soluble Fe salts have been applied as foliar sprays or soil amendments.

The first symptoms of Fe toxicity are necrotic spots on the leaves (Vitosh *et. al*., 1994). Symptoms are more severe in the older leaves that have had the longest time to accumulate Mn and Fe. With the sudden onset of high levels of Mn and Fe, the symptoms can be most prominent in the younger leaves. The most

common symptom is the formation of chlorotic grading to dead spots on the leaf. These spots are frequently near the ends of xylem vessels, so tend to be near the leaf margin and in interveinal positions. Lucerne, cowpea, lupins, barley and perennial ryegrass all tend to develop leaf spots (Helyar, 2002) due to high Mn. High Mn and Fe also interact with the uptake of other nutrients such as Zn, Ca and Mg.

Some Fe rich, low pH, low Mn soils create an environment in which an interaction between the Fe and Mn in the soil reduces Mn uptake by plants. The symptoms observed on the plants are of Mn deficiency, but excessive available Fe in the soil causes the low plant uptake of Mn. The addition of Fe chelates or Mn chelates, which rapidly convert to the Fe form under these soil conditions, aggravates the situation by increasing the amount of available Fe and without solving the Mn deficiency problem (Vitosh, Warncke and Lucas 1994).

Metal toxicity in plants can cause shortening of roots, leaf scorch, nutrient deficiency and increased vulnerability to insect attack. Unless removed completely from the soil through intervention by leaching, metal will persist indefinitely (Roane, *et al.* 1994). The main role of Mn in the plant is as an activator of enzymes associated with phosphorus reactions, and with the plant energy system. Plants normally control the rates of these reactions within cells, by varying the Mn concentration at the reaction sites. High Mn restricts the survival of rhizobium in the soil (Heylar, 2002).

Leaf crinkling and cupping is a symptom of Mn toxicity in rape, beans and soybeans. The cupping is thought to be caused by Mn accumulation in the leaf margin area, slowing the growth of that area relative to the rest of the leaf. With oats and fescue, Mn toxicity causes interveinal yellowing giving stripy leaves (Helyar, 2002). This is thought to be due to manganese induced iron deficiency.

1.9.3 Surface water and groundwater

Manganese and Fe contents in water has been discussed extensively in the World Health Organisation (1984) guidelines. Water percolating through soil and rock can dissolve minerals containing Fe and Mn and hold them in solution. Their presence in water results in staining as well as offensive tastes and appearances. The two elements are common elements found in the earth's crust. Surface waters (rivers and reservoirs) do not usually contain high concentrations of Mn and Fe because the oxygen rich water enables both minerals to settle out as sediments.

In deep wells, where oxygen content is low, the Fe and Mn bearing water is clear and colorless, but on exposure to air, becomes colored with visible solids due to oxidation of the Fe and Mn ions. Oxidation of dissolved Fe particles in water changes the Fe to white, then yellow and finally to red-brown solid particles that settle out of the water. Manganese usually is dissolved in water, although some shallow wells contain colloidal black Mn oxides (World Health Organisation,

1984). These sediments are responsible for the staining properties of water containing high concentrations of Fe and Mn. Iron pipes may be a source of Fe contamination in pipe borne water. These precipitates or sediments may be severe enough to plug water pipes.

Iron and Mn can affect the flavor and color of food and water. They may react with tannins in coffee, tea and some alcoholic beverages to produce a black sludge, which affects both taste and appearance. Manganese is objectionable in water even when present in smaller concentrations than iron. Iron will cause reddish-brown staining of laundry, porcelain, dishes, utensils and even glassware. Manganese acts in a similar way but causes a brownish-black stain. Soaps and detergents do not remove these stains, and use of chlorine bleach and alkaline builders (such as Na^{+} and CO_3^{2-}) may intensify the stains (World Health Organisation, 1984).

1.9.4 Human beings and animals

Manganese is an essential trace element and has a daily nutritional requirement of about 50mg kg^{-1} of body weight. Amongst other functions, Mn plays a role in bone mineralisation, protein and energy metabolism and metabolic regulation. The rate at which it is absorbed varies according to actual intake, chemical form and the presence of other metals in the diet. In infants and young animals, very high absorption rates have been observed.

According to the World Health Organisation (1984), no convincing evidence of toxicity in humans associated with the consumption of Mn in drinking waters exists although only limited studies are available. At high levels of exposure not expected to occur in drinking waters but in contaminated soils and vegetation, Mn can be associated with a Parkinson-like disease and some reproductive effects that include impotence and decreased fertility amongst males. People with lung disease, individuals with Fe deficiency or people with liver disease are more susceptible to the adverse effects of Mn contamination.

Human exposure to high levels of these metals causes a wide range of medical problems such as heart disease, liver damage, cancer, neurological problems, and central nervous system damage. Chronic levels of Mn poisoning occurring via inhalation of Mn dust affects the central nervous system. Symptoms include speech disturbances, sleepiness, and cramping and weakness of legs. The victim has a stolid mask-like appearance, and could be given to uncontrollable laughter, euphoria, and spastic gait with tendency to fall while walking. The situation can be reversed if identified early. Individuals with Fe deficiency as well as children are at the greatest risk of being affected by Mn toxicity (World Health Organisation, 1984).

1.10 REMEDIATIVE MEASURES

1.10.1 Phytoremediation and phytomining

Phytoremediation and phytomining are suggested phytotechniques in controlling metal concentrations in soils. Bioremediation by using plants is phytoremediation. Phytoremediation is defined as the use of green plants to remove heavy metals and contaminants from the soil. The heavy metals most commonly associated with phytoremediation are Pb, Cd, Zn, Ni, or radioactive isotopes such as Ur or Co (Comis, 1996), but this does not rule out that Mn and Fe could not be associated with the technique. Siderophores are plants, which accumulate Fe in their system (Cunningham, Berti and Huang, 1995). The use of plants in metal contaminated soils is a recent technique not quite thirty years old in its application (Cunningham, *et al*. 1995). The plants take up the toxic metals or isotopes through their roots and transport them to the stems or leaves. Researchers are hoping that one day these metal-scavenging plants, called hyperaccumulators, could be grown in contaminated soils and be harvested like hay (Ekosse and Nkoma, 2002). The metal could then be recovered and recycled when burned and the ash is collected (Comis, 1996).

There are plants that tolerate excessive concentrations of metals in soils by absorbing, translocating and storing the metals in a nontoxic way. Many of these plants have evolved on metal-rich soils. Research over the last two decades has shown that certain specialised plants have the ability to accumulate up to 3% (by

dry weight) of heavy metals and up to 25% (by dry weight) in sap/latex with no apparent damage to the plant. Almost all of these plants have been found on metalliferous soils. These soils are either natural or man made soils. The accumulation of metals is dependent on the plant, type of metal and environmental conditions (Cunningham, *et al.* 1995).

Phytoremediation of metal contaminated soil as explained by Chaney, Brown, Li, Angle, Homer and Green (1995), offer a lower cost method of soil remediation and some of the extracted metals may be recycled for value. Phytoremediation as explained by Nedelkoska and Doran (2000) is the process whereby plant metals hyperaccumulators (PMH) are applied to clean up soils and/or water bodies. The objective of phytoremediation also referred to as bioremediation, botanical-bioremediation, and green remediation by Chaney *et al*. (1995), is to use plants to make soil contaminants non-toxic.

1.10.2 Phytostabilisation

Phytostabilisation is a recently developed technique aimed at rendering ions to species that are "environmentally friendly". It has been suggested by Ekosse, van den Heever and de Jager (2003), and Ekosse, van den Heever, de Jager and Totolo (2003b) that the technique could be applied to reduce Cu, Ni, Fe, Co and Cr in soils around the Selebi Phikwe Ni-Cu mine, Botswana. An example of the application of phytostabilisation is in reducing available Cr^{6+} by rendering Cr into the insoluble Cr^{3+} form. The Cr^{6+} constitutes as much as 40 wt % to 66 wt %

of total Cr released into the environment as indicated by WHO (1993) and discussed by Van den Heever and Frey (1996). By redox alterations insoluble Mn and Fe can be removed from soils.

1.10.3 Biotechnology

There are on going research endeavours as mentioned by Chaney *et al*. (1995) and Salt *et al*. (1996), geared at developing synthetic plants, clones and resins with very high capabilities for heavy metals extraction from soils, atmosphere and water. Fundamental characterisation of mechanisms and cloning of genes as mentioned by Chaney *et al*. (1995, 1997), for phytoremediation in higher plants is expected soon. The development of specialised plant hyperaccumulators of heavy metals and their possible use as metallophores to aid in phytoextracting heavy metals in soil will decrease heavy metal toxicity.

1.10.4 Related remediative aspects

Both soil vapor extraction and bioventing are applied to soils contaminated with volatile gases and liquids (Bioremediation, 2003). Whereas soil vapor extraction depends on physical forces in separating the contaminants from the soil matrix, bioventing uses ambient air, nutrients and soil moisture to stimulate growth of microorganisms in the contaminated soils. The microorganisms digest the contaminants, thereby remediating the soil.

Often the treatment for Fe and Mn is the same for hydrogen sulfide, allowing removal of all three contaminants in one process. Treatment of Mn and Fe depends on the form in which they occur in untreated water, soils and vegetation. Therefore, accurate testing is important before considering options and/or selecting treatment equipment.

CHAPTER TWO

METHODS, INSTRUMENTATION AND ANALYTICAL TECHNIQUES

2.1 METHODOLOGY

The research study was carried out in two main phases: fieldwork and laboratory analyses. The two phases are discussed in corresponding sections below.

2.2 FIELDWORK

The fieldwork for this study was based on observations and collection of samples for laboratory analyses. Five investigatory field visits were carried out during the months of April and May of 2002 in an attempt to understand the research problems and defining the study. After a number of field visits by the researcher spanning a couple of months, there was a comprehensive field visit by the Project Supervisor and colleague, which focused on problems being encountered and giving academic guidance/direction. A Pentax Espio 738 S regular zoom camera with colour films and a Hewlett Packard photosmart 850 digital camera with memory card were used to take photographs, which reflected different aspects of the research. A Global positioning system (Garmin GPS 12XL with its accessories) and a Silva compass with clinometer aided in navigation and location of geographic coordinates. A Ward's 10X hand lens and a Busnell 7 X 35 wide angle 13-7307 binoculars were used for field study. Also, E 3-22P Eastwing 22 oz rock pick geological hammer, shovel, trowel, machete, sampling bags were used to obtain the different samples.

More specifically, the fieldwork component of this research embodied field observations of exposed outcrops of Mn orebodies, mine workings, surface soils, and leaves within the abandoned mine and its surroundings, and sampling of these materials for laboratory analyses. A hand lens was used in the field to have a closer look at hand specimens of Mn oxide ore, manganiferous and ferruginous shales, soils and leaves. Exposed soils at the study area were observed in terms of soil colour and texture. The environment was visually inspected for Mn oxide dust particles, in order to note any significant quantity, as well as attempts for possible observation of vegetation cover. The shape and length of the leaves as well as colour were observed. Other observations included leaves sites where leaves were stunted. All the observations were carried out at the sampling sites on the same days and time that samples were obtained for laboratory analyses.

2.2.1 Sampling

Sampling was done over a period of one month with the aid of four research assistants, all students of the Environmental Science Department, University of Botswana. There were two sampling areas, which included a chosen control site located 4 km south of the study area. Coordinates for soil samples are given in Table 2.1 (Appendix A). Table 2.1: X and Y coordinates of sampling points for soils at the study site. The coordinates and the grids for both soil and leaf samples on the satellite image are presented in Figures 2.1 and 2.2 respectively.

Figure 2.1: Satellite image of the study area showing grid where soil samples were obtained

The control site had an area of 900 m^2 (300 m X 300 m). This control site was chosen because it was at the other side of a paleotopographic barrier where Mn mineralisation has not occurred (Ekosse and Vink, 1998). The soil lithology and vegetation cover of the control sampling site were very similar to those of Kgwakgwe area.

Detailed soil grid of 2 km X 2 km was established, of which the one for vegetation was made from. Soil samples were taken at 100 m intervals, and vegetation samples obtained at 200 m interval. The coordinates are given in Table 2.1. To make the grid a base point of known location was marked. Gridding is an interpolative method used to create a two dimensional surface of distribution of

point data. Point interpolation is performed on randomly distributed point values to create a raster map in which each pixel has a value calculated on the input point values. The result is an equally spaced grid of values in a specified co-ordinate system. This technique is often used to display geochemical data in environmental studies.

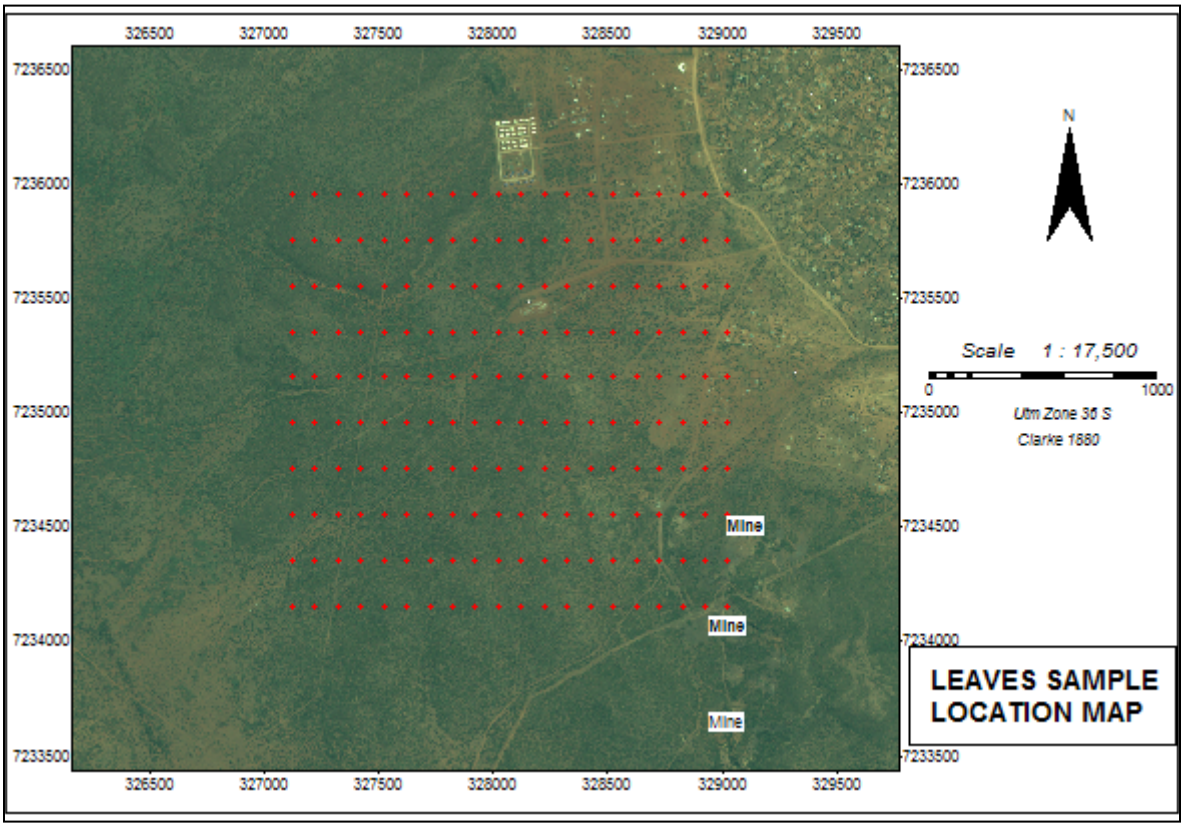

Figure 2.2: Satellite image of the study area showing grid where vegetation samples were obtained

2.2.1.1 Soil samples

Random techniques highlighted in Jewell *et al.,* (1993) and judgmental techniques described in Crépin and Johnson (1993) were used in obtaining soil

samples from both the study and control sites. Figure 2.3 reflects the soil sampling points. Details of sampling have been explained in section 2.2.1. A total of 400 samples were collected from the study site and nine samples from the control site for analyses. Grab soil sampling method as explained by Tan (1996, 1998) was used to obtain the samples with the aid of a machete, a trowel and/or a shovel. Soil samples were taken at a depth of between 0 cm and 20 cm. Each sample was placed in a 20 cm x 30 cm polythene bag and transported to the Geology Departmental Laboratories, University of Botswana, Gaborone where it was placed in an oven at 60 ^{o}C overnight for the release of surface soil moisture, and later analysed.

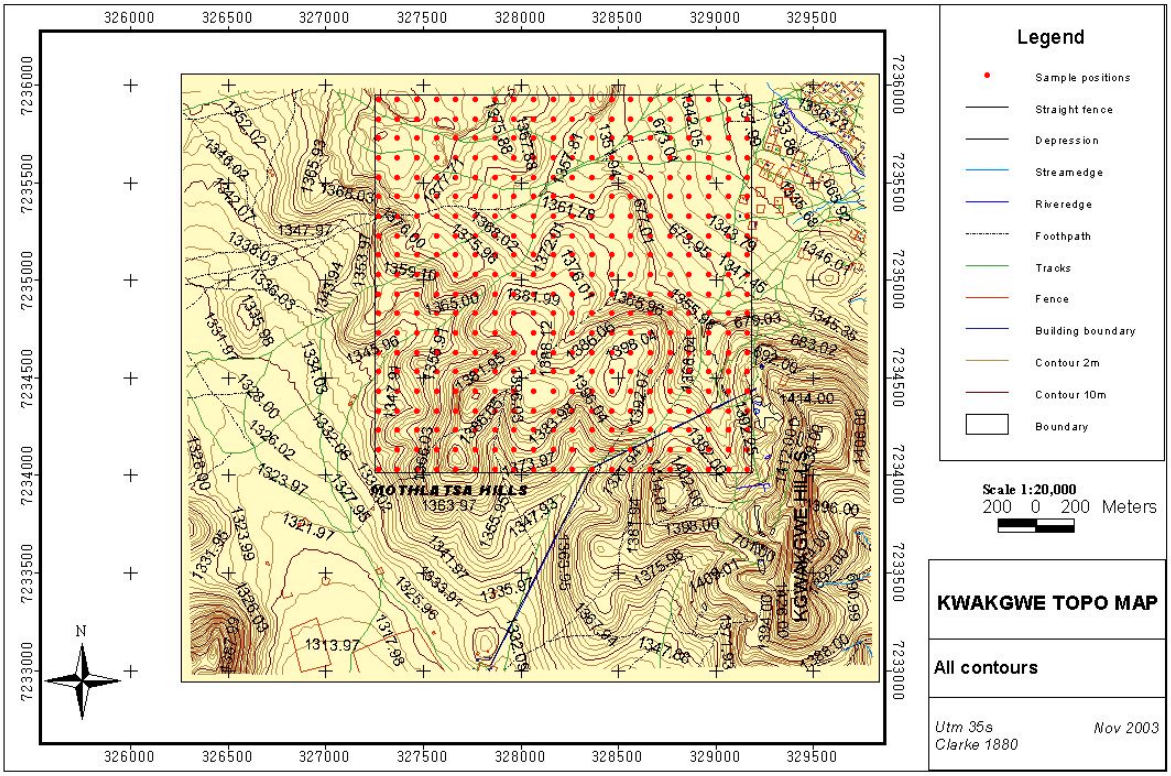

Figure 2.3: Soil sampling points located on topographic map of the study area

2.2.1.2 Vegetation samples

Vegetation samples in this study refer to leaves of *Combretum apiculatum*, *Euclea undulata* and *Terminalia sericea*. Mature dark green leaves with leaf diameter ranging from 2 cm to 4 cm within both the study and control sites were harvested for laboratory analyses. Between 100 and 200 leaves depending on the leaf diameter, which constituted a sample set, were sampled per sampling area. A total of 200 sample sets from the study area and four sample sets from the control site were obtained during the sampling period. The leaf samples were transported to the Geology Departmental Laboratories, University of Botswana, Gaborone for analyses and processing. Samples were aerated for one week or more, until there was release of moisture from the leaves.

2.2.1.3 Other geological materials sampled

Table 2.2 summarises the number of samples obtained for the different geological materials. Sources of Mn and Fe ions at the Kgwakgwe area are the manganiferous and ferruginous shale, Mn oxide ore, Mn wad, and tectonised manganiferous chert breccia. In order to better understand Mn contamination trends, it was considered appropriate to perform some analyses on Mn source materials. In this regard, hand grab samples of the manganiferous and ferruginous shale, Mn oxide ore, Mn wad, and tectonised manganiferous chert breccia from the Kgwakgwe area were obtained for the determination of their Mn and Fe concentrations levels, and identification of their mineral contents.

Table 2.2: Details of other geological materials sampled at the Kgwakgwe study area

No	Name of geological material	Number of samples obtained	Remarks
1.	Manganiferous shale	Five	Host rock of Mn oxide ore
2.	Ferruginous shale	Five	Principal source rock of Fe, and overlies the Manganiferous shale
3.	Mn oxide ore	Five	Principal source of Mn ions in soils
4.	Mn wad	Five	Source of Mn ions in soils
5.	Tectonised manganiferous chert breccia	Five	Source of Mn ions in soils

2.2.1.4 Coding of samples

Each sample was given a code, which facilitated its recognition during laboratory analyses and data interpretation. The details are reported in corresponding sections in the thesis.

2.3 LABORATORY ANALYSES

Laboratory analyses focused on soils and vegetation. The leaves of plants were analysed for their Mn and Fe contents. The type of analyses performed depended on the type of material (soil, plant or other geological material), the physical state of the sample, and the objective of the experiment in relation to Mn

contamination of the environment. The laboratory results are reported according to the analyses, which were performed: physico-chemical, mineralogical and chemical experiments. The physico-chemical tests were granulometric analyses, pH, EC and colour determination. The mineralogical tests were minerals identification by XRPD, minerals characterisation by SEM, EDX and optical microscopy. The chemical analyses were mainly carried out using the aas technique, and determination of total organic carbon. The cation exchange capacity (CEC), exchangeable bases (Na, K, Ca and Mg) and the percent base satuaration were determined, as well as the amount of Cl, SO_4 and CO_3 present in the soil samples. Phosphorus test was also performed on some of the samples.

The physico-chemical tests were performed only on the soil samples. The mineralogical tests were carried out only on the soil samples. However, the XRPD analysis was done for both the soil samples and the samples of the other geological materials. Chemical analyses for Mn and Fe concentrations were performed on all samples of soils and leaves of plants, whereas TOC test was done only on the soil samples.

The analyses performed are grouped into four categories and these were as follows:

1. Physico-chemical analyses
2. Mineralogical analyses

3. Chemical analyses

4. Remote sensing and geographical information systems

The various tests under the four major categories of analyses are given in the corresponding sections below.

2.3.1 Physico-chemical analyses

Granulometric analyses [which was mainly particle size distribution (PSD)], soil moisture, hydrogen ion concentration (pH), electrical conductivity (EC), and colour of bulk soil samples were determined. Details of the physico-chemical tests performed on the studied samples are described below.

2.3.1.1 Granulometric analyses

The particle size (PS) and particle size distribution (PSD) of soil samples were carried out employing both a mechanical shaker and a 1993 model Shimadzu SA-CP4 particle size analyser (PSA). The soil samples were granulometrically characterised based on the principle of Stoke's law of sedimentation of individual spherical particles falling freely at a steady velocity under the influence of gravity, resisted only by the viscous drag of the medium (Gaspe *et al.,* 1994), expressed in equation 2.1 as:

$$V = [2r^2(d_p-d_w)g]/9\eta \qquad (2.1)$$

where V = rate of settling of particles ($cm.s^{-1}$)

r = radius of particles (cm)

d_p = density of particle ($g.cm^{-3}$)

d_w = density of fluid (water) ($g.cm^{-3}$)

η = poise ($g.cm^{-1}\ s^{-1}$)

g = acceleration due to gravity ($981cm.s^{-2}$).

The mechanical/electrical shaker was set at 60 strokes per minute (spm) for effective shaking, and the sieves consisted of the particle size ranges in μm: 500 and 53 according to USDA (1996) specifications. The < 53 μm size fraction of soil samples were analysed using the 1993 model Shimadzu SA-CP4 automatic particle size analyser (PSA). The analyser was set at 240 revolutions per minute (rpm) for effective segregation of particles, and the < 4 μm size fraction was determined.

2.3.1.2 pH determination

Van Reeuwijk (1993) and Barnard, Buys, Coetzee, Du Preez, Meyer, Van der Merwe, Van Vuuren and Volschenk (1990) describe the method for pH analysis of soil samples. Finely ground or pulverised soil samples were used for pH determination. If the soil samples were not hard, an agate mortar and pestle was used for grinding, and where the clay sample was hard, a sieb mill was used to pulverise the sample (Van Reeuwijk, 1993). Two and a half grams aliquots of 10 g of sample were placed in three centrifuge tubes and suspended in 25 mL of distilled H_2O. After shaking on a horizontal shaker for about 30 minutes, the tubes were centrifuged for five minutes. The pH of the supernatant of the

samples was measured using a Jenway 3020 pH meter available in the Geology Department, University of Botswana. Average values on three analyses were calculated and recorded for each sample analysed. The temperature of the samples at the time of analyses was recorded in order to control the pH values due to temperature fluctuations.

2.3.1.3 Electrical conductivity determination

Finely ground or pulverised soil samples, as explained in 2.3.1.2 above, were used for EC determination. Sample preparation as explained by Barnard *et al.* (1990), Okalebo, Gathua and Woomer (1993), and Reeuwijk (1993), was similar to that of pH analyses mentioned in section 2.3.1.2. The EC of the supernatant of the samples was analysed with a Jenway 4020 EC meter available in the Geology Department, University of Botswana. Average values on three analyses were calculated and recorded for each sample analysed. The temperature of the samples at the time of analyses was recorded in order to control the EC values due to temperature fluctuations.

2.3.1.4 Colour determination

In this study, soil samples for colour determination were exposed to air for 24 hours. Clayey aggregates of soil samples were separated using a mortar and pestle to single particles. With a spatula, the samples were mounted on white cardboard sheets provided by the Munsell Color Company Inc., MD 21218, USA. The colour descriptions, which comprised the hue, value/chroma and colour of

the mounted samples, were obtained by visually comparing them to those of standard soils recorded in the Munsell soil color book (1995).

2.3.2 Mineralogical analyses

Mineral identification and characterisation studies were conducted using X-ray powder diffraction (XRPD) and scanning electron microscopy (SEM), and Optical Microscopy (OM) techniques.

2.3.2.1 X-ray powder diffraction (XRPD) technique

Whole and clay fraction soil samples were analysed by XRPD for their minerals content as described in Ekosse *et. al*. (2003). The XRPD technique was used to provide information on the mineral composition of the soil samples. In XRPD, diffraction peaks occur when the path of the diffracted X-rays is equal to an integer multiple of the path difference expressed by Bragg's equation which is given by

$$n\lambda = 2d\sin\theta \qquad (2.2)$$

where n is an integer, λ is the wavelength, d is the interatomic spacing, and θ is the diffraction angle.

In this study, a Philips PW 3710 XRPD system, available at the XRD Unit of the University of Botswana, operated at 40kV and 45 mA, having a Cu-K_α radiation and a graphite monochromator. A PW 1877 Automated Powder Diffraction, X'PERT Data Collector software package was employed to capture raw data, and

a Philips X'PERT Graphics & Identify software package was used for qualitative identification of the minerals from both the data and patterns obtained by scanning at a speed of $1^{o}2\theta$ / min. Samples were scanned from $2^{o}2\theta$ to 40^{o} 2θ and their diffractograms recorded. The interpreted results were compared with data and patterns available in the Mineral Powder Diffraction File, data book and the search manual issued by the International Center for Powder Diffraction Data (ICDD), in 1986 for confirmation.

The clay fraction of the soil samples for minerals identification were obtained based on the principle of sedimentation according to Stoke's law (Gaspe *et. al*., 1994). The clay fractions of soil samples were mixed with a few drops of epoxy glue to control particle orientation, and allowed to dry overnight in an oven. The dried samples were gently crushed in an agate mortar to a fine texture. The powder samples were mounted on the sample holder with very little pressure, using a blade to minimise preferred orientation of the kaolinite particles (Hughes and Brown, 1979), and later scanned in the XRPD.

2.3.2.2 Scanning electron microscopy (SEM) technique

Mineralogical characterisation centred on morphology and orientation of particles of whole and clay fraction of soil samples. The powdered samples were placed on a 3 mm pin type stub with a carbon tab on. The stubs for Energy Dispersive Analysis (EDS) were given a thin C-cat in a SPI carbon coater to improve conductivity. The analysis was done on an EDAX system equipped with a Super

Ultra Thin Window (SUTW). The samples were examined in a Philips XL30 Environmental Scanning Electron Microscope (ESEM) in Low Vacuum mode (LVM) at the Electron Microscopy Unit of the University of Botswana to prevent possible morphological changes in the particles due to dehydration in the vacuum. Afterwards the samples were gold (Au) coated in an SPI sputter coater and viewed in High Vacuum mode (HVM). The results were also compared with the Low vacuum mode images to ensure that the shapes of the plates were not deformed due to dehydration in the high vacuum. Since there were no significant differences either mode could be used.

The environmental scanning electron microscopy with X-ray dispersive spectrometry (ESEM-EDX) aided in the microchemical characterisation of the minerals. Microchemical analyses were performed using an energy dispersive X-ray spectrometer attached to an ESEM (ESEM-EDAX). The EDS analysis was done in low vacuum mode (LVM) taking the beam scattering into consideration during the tests. The stubs were coated with a thin Carbon layer and examined in high vacuum as well. Significant changes in the results between the different vacuum operational modes could not be established.

2.3.2.3 Optical microscopy technique

The optical microscopy (OM) technique was used in identifying coarse-grained components contained in the soil samples. A Leitz Ortholux II Pol-BK petrographic microscope was used for descriptive analyses of non-clay fractions

of the samples. The non-clay size fractions of samples were mounted on the petrographic microscope from which grains were identified and described in terms of hardness, cleavage, fracture, colour, streak, lustre and crystal appearance.

2.3.3 Chemical analyses

Chemical analyses performed in this study were determination of Mn and Fe concentrations in soils and plants using atomic absorption spectrometry (AAS) technique, and organic carbon using a Carbon/Hydrogen/Moisture determinator. The details of both techniques are explained in sections 2.3.3.1 and 2.3.3.2 below.

2.3.3.1 Atomic absorption spectrometry (AAS) technique

The determination of Fe and Mn concentrations after acid digestion of samples was performed on a Varian Spectra AA-220 FS atomic absorption spectrometer (Varian, Australia) equipped with deuterium background correction. The operational parameters are provided in Table 2.3 below. Ultra pure water used for the analysis was obtained by passing tap water through a reverse osmosis system Milli-Q water system, Millipore. Nitric, perchloric and hydrochloric acids used in the digestion process were of spectral purity (Fluka, Switzerland). 1000 mg/L Fe and Mn stock standards were purchased from SAACHEM, South Africa.

Table 2.3: Operational parameters set for the determination of manganese and iron in soils and leaves of plants from the Kgwakgwe area

Parameter	Fe	Mn
Wavelength (nm)	248.3	279.5
Lamp current (mA)	5.0	5.0
Slit width (nm)	0.2	0.2
Fuel composition	air-acetylene	air-acetylene

The procedure for sample digestion is as reported by Jones and Case (1990) and Page, Miller and Keeney (1982). About two to three grams of soil or plant sample was weighed and dried at 110 ^{0}C in an Ecotherm^{e} oven manufactured by Labotec Pty, South Africa, for four hours. The dry samples were manually ground using an agate pestle and mortar and then sieved through a stainless steel sieve with mesh aperture of 63 μm. 0.50 g of each sample was weighed into 250 mL pyrex conical flasks using an analytical balance. Ten millilitres of a 3:1 mixture of concentrated nitric acid (70 wt %) and perchloric acid (70 wt %) were added and then gently heated on a hot plate, with swirling to incipient dryness indicated by the production of dense white fumes of perchloric acid. It was then cooled to room temperature after which 10 mL of 0.5 M hydrochloric acid was added to dissolve the residues. The dissolved residues were filtered through a 0.45 μm cellulose nitrate filter membrane. The filtrate was quantitatively transferred into

50 mL volumetric flasks and made to the mark with ultra pure water. Iron and manganese were determined using flame atomic absorption spectrophotometry (FAAS) at 248.3 and 279.5 nm wavelength respectively.

The data obtained with the Varian SpectrAA 220 FS AAS interfaced to Pentium 4 PC (Veriton 7500, Vic, Australia) was manipulated by the software, SpectrAA CFR (2001). The latter used the equation by Jones and Case (1990) to calculate concentrations of metal in µg /g of soil or plant sample, on entering the parameters; *final volume* after dilution, *dilution factor* and *mass of* the digested sample.

$$Conc.\,in\ \mu g/g = \frac{AAS\,\text{instrument reading x final Volume}\,(50\,\text{mL})\,\text{x dilution factor}}{\text{Mass of soil or plant}\,(0.5\,\text{g})} \qquad (2.3)$$

The concentration (µg /g) values are accompanied by the errors expressed as standard deviation (SD) automatically generated by the software. In order to calculate the percent relative standard deviation (% RSD), the mean (X) and SD values were entered in equation (2.4) using Microsoft Excel.

$$\%\text{RSD} = \frac{\text{SD}}{\text{X}}\,\text{x}\,100 \qquad (2.4)$$

2.3.3.2 Cation exchange capacity and exchangeable bases

The exchangeable bases analysed are K, Na, Ca and Mg. The method used for the determination of the exchangeable bases in the soil samples have been described in detail in Barnard *et. al*. (1990), Okalebo *et. al*. (1993, and Van

Reeuwijk (1993). The procedure is briefly summarised. Five grams of dry soil sample was weighed into a clean plastic bottle with stopper. Into the 5 g of soil sample was added 100 ml of IM ammonium acetate solution having a pH of 7.The contents were shaken for 30 minutes and later filtered through a Whatman No. 42 filter paper. This extract was used for K, Na, Ca and Mg determinations.

For the determination of Na, K and Ca, 5 ml of the extract was used whereas for the determination of Mg, 3 ml of the extract was used. For the analyses of K, Na and Ca, the soil extract solution was diluted ten times. For the analyses of Mg, the soil extract was diluted seventeen times. Exchangeable cations were determined in the laboratory by flame photometry for K and Na, and by atomic absorption spectrophotometry (AAS) for Ca and Mg. The atomic absorption spectrophotometer was for measurements, as explained in section 3.2.3.1.

The CEC determination was done immediately after that of exchangeable bases, using the same sample and tube which was used for the analyses of exchangeable bases. After percolation with ammonium acetate, 250 ml beaker was placed under the tube. From a 200 ml volumetric flask which was filled almost to mark with sodium acetate, 25 ml of it was added to the tube and then the flask was inverted in the tube. The outlet was adjusted for to allow 200ml to percolate within four hours. The percolate was discarded and beakers placed under the tubes, and the walls of the tubes were rinsed with 15 ml of 80 % ethanol. From 100 ml of volumetric flask which was filled to mark with 80 %

ethanol, 25 m was added to the tube and the tube inverted. Percolation was adjusted to have 100 ml in two hours. The walls of the tubes were once more rinsed with 80 % ethanol. Outlet was rinsed and 100 ml volumetric flask placed there. From the 100 ml volumetric flask filled with 1 M ammonium acetate, 25 ml of it was added to the tube, making sure that entrapped air bubbles were removed, and the flask inverted in the tube. The flask was adjusted to enable percolation to last four hours. The collecting volumetric flask was filled to mark with 1 M ammonium acetate, and homogenised. The percolate was used to determine the CEC by measuring the Na.

The base saturation percent was calculated by dividing the sum of the exchangeable bases to the CEC and and multiplying by 100 to convert to percent.

2.3.3.3 Phosphorus determination

The Olsen method was used in the determination of soil phosphorus on randomly selected soil samples from both the study area and the control site. This method was chosen because of its suitability over a wide range of soil types and pH values (Okalebo *et. al*., 1993). The procedure is reported in Barnard *et. al*. (1990), Okalebo *et. al*. (1993, and Van Reeuwijk (1993).

Two point five grams of dry soil was weighed into 150 ml polythene shaking bottle. Into it was added 50 ml of Olsen extracting solution which consisted of 0.5

M $NaHCO_3$ at pH 8.5. This was mounted on a mechanical-electric shaker and allowed to shake for 30 minutes. After this the suspension was filtered through the Whatman No. 42, 44 and 542 filter paper.

Ten milliliters of each P standard solution was pipetted into 10 mls of the each of the filtrates and two reagent blanks into 50 mls volumetric flasks. Five milliliters of 0.8 H_3BO_4 was added to each flask. Beginning with the standards and the blanks, 10 mls of ascorbic acid reagent was added to each of the flasks, and made to mark using distilled H_2O. The contents were stoppered and allowed to shake for one hour, after which the absorbance was measured at a wavelength setting of 800 nm. The phosphorus values were obtained from the standard P curve, and corrections were made for the reagent blank P concentration.

2.3.3.4 Determination of chloride and sulphate

The Metrohm 761 Compact IC Ion Chromatograph was used to determine the chloride, sulphate and phosphate present in the soil samples. Carbonate content in the soil samples was determined using a different method. The 761 Compact IC comprises a low-pulsation dual-piston pump, pulsation dampner, electromagnetic injection valve, two channel peristaltic pump, conductivity detector, eluent organiser as well as a data recording and processing module. All the components that come into contact with the eluent and sample are metal-free. The procedure used has been adapted from Harris (1999), Jackson (2000), Park *et. al*. (2002) and Metrohm News (2004),

Five grams of the dried soil samples was weighed accurately into a clean, dry beaker before dispersion with 50 mls of deionised H_2O. This was followed by the addition of 10 mls of conc HNO_3. Another 50 mls of deionised H_2O was added before the beaker was covered with a watch glass and gently boiled for 5 minutes. The solution was then allowed to cool before being filtered through a Whatman 52 filter paper.

The filtered solution was diluted 1:50 with deionised H_2O before being placed on the sample carousel of the Metrohm 788 IC Filtration Sample Processor where it was injected into the Metrohm 761 Compact IC through a 0.2 mm membrane. The response for the peaks was recorded using a mobile phase eluent of sodium carbonate/sodium bicarbonate with the Metrosep A SUPP 5 analytical column. The calculation was carried out automatically using integration software IC Net 2.1 against a previously prepared calibration plot. Because there are no external displays or switches on the instrument, all the hardware is fully controlled via a single RS232 connection between the IC and the PC. This outstanding temperature stability reduces interference and allows exact conductivity measurements. The detector is the heart of every ion chromatograph. The Metrohm detector's temperature varies by less than 0.01°C and can be optimally adapted to the ambient conditions.

2.3.3.5 Carbonate determination

The Eijkelkamp calcimeter designed to handle five samples at a time was used to determine the carbonate content in the soil samples. All the analyses were

operated in an almost similar condition with temperature variation not exceeding 4 ^{o}C. The calcimeter method applied was that described in Eijkelkamp (2003), for the determination of the amount of carbonate in soil. One gram of dry soil was accurately weighed and transferred into the 100ml round flask. Two to 3 ml of HCl was poured into the small weighing bottle. With the artery forceps the weighing bottle was lowered into the flask taking care that no acid made contact with the soil. The flask was attached to the Calcimeter ensuring an airtight seal (in some cases, when it was necessary, greasing was done using Vaseline), again being careful that the acid had no contact with the soil. The tap was opened and adjusted by raising / lowering the tube with no scale until the tube with scale read 0.0 – the tubes should have water at the same level. At this stage the tap was closed.

The flask was now tilted for the acid to make contact with the soil and by swirling. The tube with no scale was raised / lowered so that the water levels were again equal (this puts the gas inside the other tube at atmospheric pressure). The volume was read directly from the other tube. In cases whereby the volume began to diminish, there was a leak and the experiment had to be repeated.

Calibration was carried out prior to measurements. The procedure was similar to the one as above, but this time using the anhydrous Sodium Carbonate rather than soil. Calibration usually varies slightly according to local atmospheric pressure and temperature conditions, but 0.1 gm of Sodium Carbonate should

give about 21 ml of CO_2. A calibration curve was constructed by varying the amount of Sodium Carbonate. Calculations were done as follows:

$$\% \text{ Carbonate} = \frac{(66 * Vs)}{(W * Vc)}$$

where Vs = Volume of CO_2 produced by soil

W = weight of soil

Vc= Calibration volume of Na_2CO_3 (calculated as ml CO_2 produced by 1 gm of Na_2CO_3)

2.3.3.6 Organic carbon determination

Soil samples were analysed quantitatively for their total organic carbon (TOC) contents using a LECO RC-412 multiphase Carbon/Hydrogen/Moisture Determinator. The principle is based on converting all C to CO_2 in an oxidising analytical atmosphere. The organic form of C produces both H_2O and CO_2, which enables TOC to be measured from observable H_2O peaks. The quantitative analysis program was set for the time and temperature required, which is thirty minutes at 125 ^oC, after qualitative tests were conducted to obtain the ranges.

2.3.4 Remote Sensing and Geographical Information Systems

2.3.4.1 Image description.

A Quick bird 2.4 – 2.8 m resolution with zero cloud cover multispectral standard imagery was obtained from DigitalGlobe Satellite Imagery of MAPS Geosystems,

United Arab Emirates. The Quick bird imagery is a multispectral image covering four bands within the range 450-900 nm (Table 2.4). Basically it covers the visible (blue, green and red) to near infrared bands. Band widths are similar to Landast TM band width and listed in Table 2.4.

Table 2.4: Band widths and names of multi spectral image of study area

Band no	**Band width (nm)**	**Band name**
1	450-520	Blue
2	520-600	Green
3	630-690	Red
4	760-900	NIR

High-resolution imagery data was used due to the detailed nature of the work. The Quickbird MSS was opted for as opposed to standard Landsat due to its resolution. The MSS has a higher resolution of 2.4 m so it can be used for detailed analysis, as opposed to the 30 m resolution of Landsat. Data was collected at the end of March just off peak of the wet season so as to reduce impact of cloud cover.

2.3.4.2 Software packages

Three main software packages were used for classification and processing of the data and these were Integrated Land and Water Information System (ILWIS), Geosoft Oasis Montaj^{TM}, and ArcGIS. The software used for processing the

satellite image is ILWIS version 3.0 released May 2001. The ILWIS is a PC-based GIS and remote sensing package. The International Institute for Aerospace Survey and Earth Sciences (ITC) in the Netherlands developed it. Development of the software started in 1984 and its main emphasis then was for use in land use zoning and watershed management studies. The ILWIS software has been commercialised since early nineties and is used extensively as a tool for training, research and advisory services all over the world. Presently over 500 ILWIS systems are in use in more than 100 countries. The ILWIS 2.0 was the first windows version released in April 1996. In May 2001, the ILWIS 3.0 was released in May 2001 and has a completely modernised user-interface, and is fully compatible with Windows 95, 98, NT4 and 2000

The Geosoft Oasis Montaj™ offers an integrated environment for earth science data processing and analysis. Geosoft's software and services are based on the Oasis Montaj™ spatial data interface — a powerful spatial data technology developed for the earth science community. Geosoft provides a variety of systems that address specific applications in environmental investigations, exploration geochemistry, exploration geophysics, drillhole geology and other areas. The product enables productive use of spatial data for essential decision-making. The systems consist of menus and corresponding Geosoft executables that run on the Oasis Montaj core platform.

ArcGIS was used to process mineralogical data. The data was imported into Arc Gis as a DB IV file so as to create point symbol mineral distribution maps.

The main aim of .the distribution maps was to use GIS so as to show location and mineral abundance. Gradational symbols were used so as to portray the difference in mineral abundance. Each mineral group was plotted in one or two maps and the relations in mineral distribution were analysed.

2.3.4.3 Creating the Maps

The data obtained through field mapping and laboratory tests were coded, processed and analysed both qualitatively and quantitatively. The satellite image of the area was rectified and processed using different image processing software packages. Classification exercise was carried out on the MSS image using the ILWIS software. Contrast stretching, image filtering, false colour composite, normalised difference vegetation index (NDVI) maps and multi band statistics were performed and the results and interpretation are given in chapters three and four. The software packages aided in the application of suitable indices such as NDVI in characterising vegetation cover of the study area.

For the handling of physico-chemical, mineralogical and chemical data, gridded maps were made as the base map. Gridding is an interpolative method that is used to create a two dimensional surface of a distribution of point data. Point interpolation is performed on randomly distributed point values to create a raster map in which each pixel has a value calculated on the input point values. The result is an equally spaced “grid” of values in a specified co-ordinate system. It is often used to display geochemical data in environmental studies and mineral

exploration. Statistical analysis was also done in Oasis Montaj and a histogram was plotted on the map.

The data was imported and then gridded in Oasis Montaj (version 4.2). Element data was received in excel spreadsheet format. The spreadsheet was used in Oasis motanj to create gridded maps. The excel files were first saved as text format and then the text files were imported into Oasis. Minimum curvature gridding was then performed for each element and the data was also contoured to create contour maps that overlay on the grid. Minimum curvature is a numerical gridding technique for random data. Different cell sizes were experimented with so as to create the best grid and a grid cell size of 15 m worked best for the soil samples that were taken at 100m intervals and a grid cell size of 25 m was efficient for the leaf samples which were taken at 200m intervals. Gridded maps were made as the base map. Statistical analysis was also done in Oasis and a histogram was plotted on the map.

Image enhancement techniques contrast stretching and image filtering were applied to data to improve visual interpretation. Contrast linear stretching was performed so as to make the important features more interpretable/visible to the human eye by providing maximum contrast and hence improve the visible contrast of the images. Contrast stretching increases the range of brightness values by stretching out original pixel values over a wider range for the purpose

of enhancing visibility of the features in the image. This application does not alter the pixel values; it is purely for display purposes.

Spatial frequency filter was used to emphasise or suppress image data of various spatial frequencies. There is a speckled effect in the image especially with the infrared band. The images were filtered with a low pass filter to reduce the speckle effect. A 3x3 low pass filter was applied to smoothen the image and reduce the noise created by the speckles. Each pixel is multiplied by the corresponding coefficient in the filter. For the 3x3 filter, a convolution is carried out such that the resulting values are summed and the resulting values replace the original value of the central pixel. The resulting filtered image is smoother than the original image.

CHAPTER THREE

RESULTS

3.1 FIELDWORK

The results obtained during the fieldwork period are reported in sections 3.1.1 and 3.1.2; these thus include general field observations and sampling methods.

3.1.1 General field observations

The general field observations of the exposed outcrops and mine workings, soils and vegetation are reported below.

3.1.1.1 Exposed outcrops and mine workings

At the study site, the Mn oxides orebodies and the kaolin occurrences are both hosted by the Kgwakgwe Shale. From field observations, the foot walls of the deposits are not exposed. However, Aldiss *et. al*.(1989), estimated the thickness of the host rock to be between 10 m and 20 m. The lowest portion of the exposed outcrops begins with Mn oxides ore of about 10 cm to 20 cm thick, and is overlain by laminated kaolins ranging in thickness from 1 cm to 3 cm. The fine grained greyish white laminated kaolins are succeeded by very black Mn oxides orebodies having a thickness of between 25 cm and approximately 50 cm. The Mn oxide orebodies are succeeded by kaolins having a thickness of between 15 cm and 40 cm. The kaolins are overlain by Mn oxide ore ranging from 50 cm to 2 m in thickness.

The Mn oxide ore is succeeded by the manganiferous shale which is characterised by chocolate brown lumps, pillows and lenses that are interbedded with very thin layering of greyish white kaolins. The manganiferous shale is in turn overlain by three to four layers of kaolins occurring as lenses, pockets and veins equally interbedded with Mn oxide ore. These kaolin layers are further succeeded by Mn oxide ore.

The manganiferous shale is succeeded by the ferruginous shale, and the later begins with a 15 cm thick thin orange yellow Fe layer, most probably goethite, and varicoloured ochres alternating with thin layers of Mn oxides. The goethite layer is overlain by ferruginous shale of between 20 cm and 30 cm thick, which is in turn succeeded by a layer of goethite that is about 20 cm thick. In the south eastern flank of the Kgwakgwe Hill, the ferruginous layer extends vertically to about 2 m thick and there consists of goethitic ochres, already reported by Ekosse and Modisi (1999).

The upper part of the ferruginous shale, which is between 1 m and 1.5 m thick succeeds the goethite layer. This part of the outcrops consists of fragments of large angular opaque and whitish chert breccia with a high degree of silicification. Loose lumps of chert breccia, which are about 1 m thick, cap the outcrops.

Thirty mine workings were identified from where in the past Mn ore was mined. The mine workings were hosted in the manganiferous shale, although a few were

spotted in the ferruginous shale. Some of the mine workings created large caves as high as four metres, with diameter extending to 10 m. At some of the slopes of sites of mine workings, grass has been planted to control erosion and reinforce soil stability.

Neither exposed outcrops nor mine workings were present at the control site. The terrain is flat.

3.1.1.2 Soils

The topography of the study area had a direct influence on soil thickness. At the flanks of the Kgwakgwe and Mothlatsa Hills (Figure 3.1), the soils are thin to very thin barely attaining 10 cm. At the valleys and plains of the study area, soil thickness was more than 50 cm. At the control site, the soil thickness was more than that of the study area attaining a minimum of 70 cm.

The colour of the soils was predominantly dark brown and reddish brown to light brown to dark reddish grey. From the mine workings, located in the southern part of the study area, the soils were dark coloured, and the colour became lighter as one moved away from the workings. It was visibly remarked that the darker colours imparted on the soils of the area were as a result of the Mn oxide ore particles from the mine mixing up with the soils.

In the northern part of the study area where no mine workings are located, the soils were yellowish red to light brown. White speckles of agglomerated clayey material were also visible but sparsely scattered in the study area. At the control site, the soils were slightly light yellowish red and no black particles were noticed

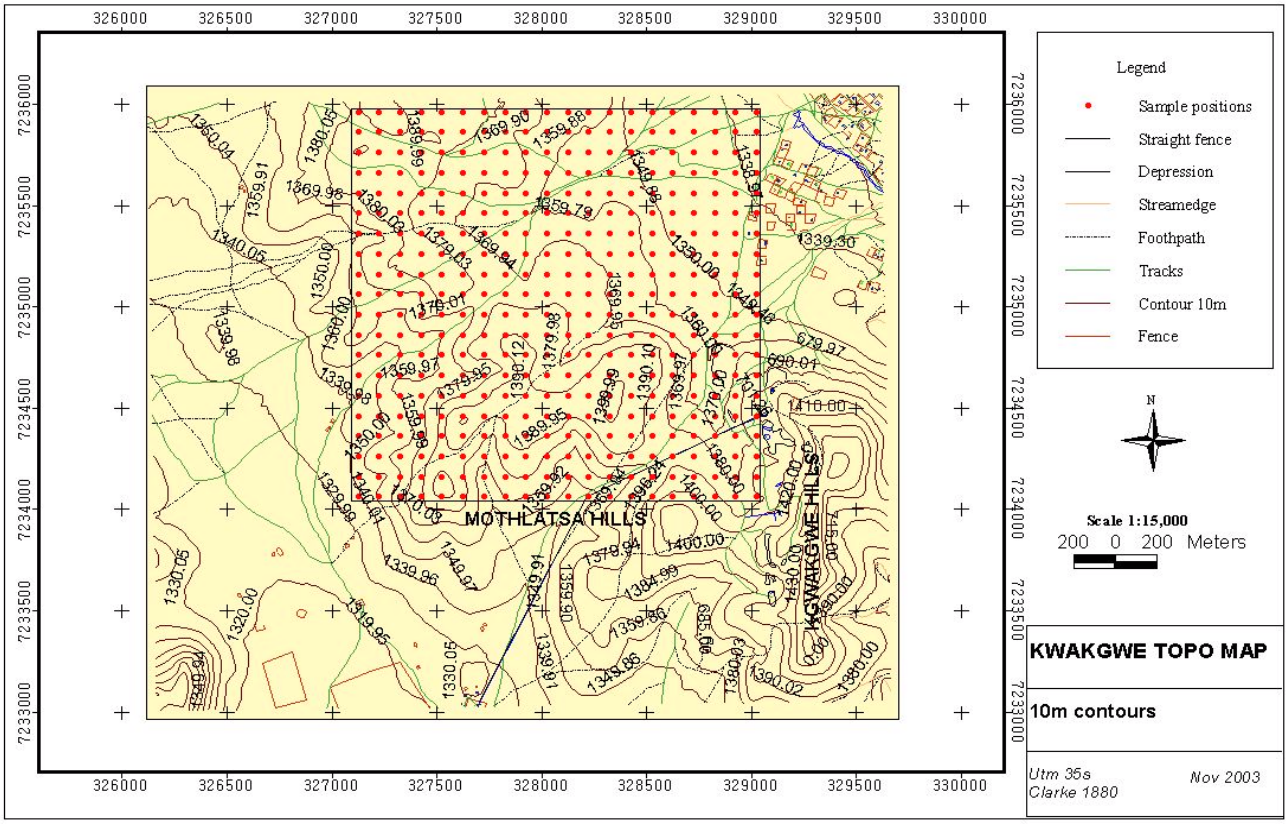

Figure 3.1: Topographic map of the study area with soil sample points superimposed

3.1.1.3 Vegetation

It was observed that the plant leaves changed in colour from light reddish yellow around the mine workings area to green in the valleys and close to settlements. Leaves of plants located at the periphery were more colour affected than others. The peripheral leaves were the first to alter in colour. Where discoloration of

leaves occurred, it was noticed that the young leaves started out as green but changed progressively in colour to light reddish yellow and eventually to golden yellow.

In areas where Mn oxide ore occurred and/or was mined, either there was no vegetation cover observed or the area was covered with sparse vegetation. In these mine working areas, the plants were stunted and conspicuously shorter than their distant neighbours within the study area and the control site. Mature leaves of plants in areas of darkly coloured soils were between 2 cm and 2.5 cm in length compared to areas where soils were light brown to yellow in colour with plants having fresh broad leaves exhibiting full growths both in colour (green) and length (6 cm to 7 cm).

3.1.2 Sampling

3.1.2.1 Soil samples

Four hundred soil samples were obtained from the study site and nine soil samples from the control site. Sampling points were easily accessible through footpaths and tracks. Moreover low vegetation density in the study area made accessibility easier. No problems were encountered in obtaining the soil samples.

3.1.2.2 Vegetation samples

Vegetation samples consisted of leaves. Two hundred vegetation set samples were obtained from the study site and four vegetation set samples from the

control site. Sampling points for leaves of plants were quite accessible through footpaths and tracks. The vegetation sample sets were obtained at alternate soil sample points. Some of the bushes were thorny, making it a bit difficult to pluck the leaves from plants.

3.1.2.3 Other materials sampled

Five other types of geological materials were samples and these were the manganiferous shale, ferruginous shale, manganese oxides ore, manganese wad and tectonised manganiferous chert breccia. The manganiferous shale is the host rock for the Mn minerals. There were five samples obtained from each of the five types of geological materials.

Sampling of the geological materials was done from exposed outcrops containing them. The outcrops were easily accessible. Both the manganiferous shale and the ferruginous shale occurred in outcrops of which the former was stratigraphically an older stratum located at the bottom of the ferruginous shale. In this regard samples of the manganiferous shale and ferruginous shale were obtained from the same outcrops but at different strata. The Mn oxide ore were samples from the host rock where Mn mineralisation was evident. The manganese wad is a localised occurrence in the southwestern part of the study area, and it was only there that the wad samples were collected.

3.1.3 Meteorological parameters

Temperatures during sampling period ranged from 18 ^{o}C to 24 ^{o}C, with an average of 21 ^{o}C. Lower temperatures were obtained in the mornings and evenings whereas higher temperatures were recorded during the day. In the mornings and evenings during the sampling period, there was gentle breeze blowing in the northeast – southwest direction. The skies were generally clear with close to zero cloud cover. During the sampling period, there were no rains.

3.1.4 Coding of samples

In the field the study area was divided into four blocks (A, B, C and D) of 1 km^2 per block. One hundred samples were obtained from each block. Samples were coded from one to 400 for ease of reference. Table and maps showing details of sample points have already been presented in Table 2.1 and Figures 2.1 and 2.2.

3.2 LABORATORY ANALYSES

3.2.1 Physico-chemical analyses

3.2.1.1 Granulometric analyses

Based on the classification scheme of particle sizes for the United States Department of Agriculture (USDA), soil particles could be considered according to their euhedral spherical diameter (esd) to be clay, silt or sand. Soil particles that are < 4 μm esd are classified as clay, soil particles that are > 4 μm esd ≤ 53 μm esd are taken to be silt, and the soil particles having an esd > 53 μm esd $\leq$

500 μm are considered to be sand. However, soil particles > 250 μm esd are usually quartz grains and could be discarded because they do not affect the chemistry of the surface environment as explained by Kralik (1999) and Gaspe, Messer and Young (1994).

The statistical data which included the mean, standard error, median, mode, standard deviation, sample variance, Kurtosis, skewness minimum and maximum particle sizes, the sum and count for the particle size analyses of soil samples for both < 53 μm and < 4 μm fractions is given in Table 3.1.

Table 3.1: Summary statistics for particle size analyses of samples from the study site

Parameter	**< *53* μ m**	**< *4* μ m**
Mean	64.32	5.23
Standard Error	0.94	0.19
Median	69.75	4.43
Mode	45.25	3.99
Standard Deviation	18.87	3.71
Sample Variance	355.94	13.78
Kurtosis	-0.75	13.35
Skewness	-0.52	3.03
Range (minimum – maximum)	11.05 - 109.80	0.30 - 30.58
Sum	25728.95	2092.62
Count	400.00	400.00

The results of the particle size distribution of soil samples of the study area and the control site of this research project are given in Tables 3.2 (Appendix B) and 3.3 respectively. Average trend of distribution of particles in the study area revealed clay size fraction to be between 1.4 wt % and 12.7 wt %, and for the silt portion to be 31 wt % and 87.9 wt %. The wt % of the clay size fraction of the dark coloured soils located close to mine workings was lower than that of soils located away from the mine workings.

Soils close to the small streams and valleys were more clayey than those thin soils on hill caps, hill sides and mine working environments. At these sites which are located close the streams, leaching of ions for clay mineral formation could occur. The more clayey samples were less silty compared to the less clayey samples. Trends in sandiness of soil samples were consistent with trends for clay and silt fractions of the soil samples.

Table 3.3: Particle size distribution of soil samples from the control site

Sample code and size fraction	% Fraction	Sample code and size fraction	% Fraction	Sample code and size fraction	% Fraction	Sample code and size fraction	% Fraction
C1 500 μm	60.17	C2 500 μm	12.64	C3 500 μm	45.04	C4 500 μm	12.90
< 53 μm	33.85	< 53 μm	80.80	< 53 μm	46.48	< 53 μm	81.00
< 4 μm	5.57	< 4 μm	6.53	< 4 μm	8.45	< 4 μm	5.02
C5 500 μm	38.50	C6 500 μm	14.04	C7 500 μm	68.40	C8 500 μm	14.52
< 53 μm	61.53	< 53 μm	76.54	< 53 μm	27.16	< 53 μm	81.17
< 4 μm	3.35	< 4 μm	9.05	< 4 μm	4.39	< 4 μm	4.27
C9 500 μm	32.62						
< 53 μm	61.36						
< 4 μm	5.29						

Average trend of distribution of particles in the control site revealed clay size fraction to be between 4.27 wt % and 9.05 wt %, and for the silt portion to be 27.16 wt % and 81.27 wt %. These values obtained for soil samples within the control site were close to the average values obtained for clay and silt fractions of the soil samples obtained within the study area.

3.2.1.2 pH determination

For the soil samples, values of mean, standard error, median, mode, standard deviation, sample variance, Kurtosis, skewness, range, minimum and maximum values, sum and count for pH and EC are reported in Table 3.4.

Table 3.4: Statistical data of pH and electrical conductivity (EC) values for soils of the study area

Variable	pH	EC
Mean	4.68	115.99
Standard Error	0.03	0.49
Median	4.64	117.9
Mode	4.71	119.5
Standard Deviation	0.67	9.73
Sample Variance	0.45	94.66
Kurtosis	0.40	27.63
Skewness	0.41	-5.05
Range	4.34	74.4
Minimum	2.92	49.1
Maximum	7.26	123.5
Sum	1872.4	46395.7
Count	400	400

Table 3.5 (Appendix B) and Table 3.6 below consist of the results of analyses for soil pH and EC of samples from the study area and the control site respectively. Soil pH values obtained for samples from the study area ranged from 2.92 to 7.26, with a mean of 4.64. The results depicted a strongly acidic to slightly acidic environment. The pH values for soil samples from the control site ranged from 4.27 to 4.99 (Table 3.4). These values obtained for soil samples from the control site are close to the mean pH value of the samples from the study area.

Table 3.6: The pH and electrical conductivity values of samples from the control site

Sample Number	pH	EC
Control 1	4.99	101.5
Control 2	4.35	105.4
Control 3	4.38	106.2
Control 4	4.77	106.6
Control 5	4.61	100.9
Control 6	5.46	102.7
Control 7	4.27	105.2
Control 8	4.46	104.5
Control 9	4.4	104.1

3.2.1.3 Electrical conductivity determination

The results of EC analyses for soil samples from the study area and the control site values are given in Tables 3.5 and 3.6 respectively. Soil EC values obtained for samples from the study area ranged from 49.1 μScm^{-1} to 123.5 μScm^{-1} with a mean of 115.98 μScm^{-1}. The results depicted a relatively low EC environment. The EC values for soil samples from the control site ranged from 100.9 μScm^{-1} to 106.6 μScm^{-1} (Table 3.5). These values obtained for soil samples from the

control site (Table 3.6) are slightly lower than the mean EC value of the samples from the study area.

3.2.1.4 Colour determination

The value/chroma, hue and colour of soils of samples obtained from the study area were varied in their colour distribution pattern as reflected in the results in Table 3.7 (Appendix B).

Eleven different colours as classified in the Munsell Soil Colour Book (1992) were observed and these were yellowish red, red, dark red, brown, dark reddish brown, strong brown, dark reddish grey, very dark grey, and light brown. At the control site, only one colour was observed for the nine samples, and it was yellowish red.

3.2.2 Mineralogical analyses

Mineralogical tests conducted included identification by XRPD of mineral phases present in soil samples and other geological materials, characterisation of soil samples by electron microscopy and optical microscopy. The results are reported in corresponding sections below.

3.2.2.1 X-Ray Powder Diffraction technique

A summary of minerals contained in soil samples identified by XRPD is given in Table 3.8. Typical x-ray diffractograms of the < 53 μm fraction and the < 4 μm

fraction of soil samples from the study site and the < 53 μm fraction of soil sample from the control site are presented in Figures 3.2, 3.3 and 3.4 respectively. Results of the minerals identified by XRPD for the < 53 μm fraction of the soil samples, the other geological materials and the < 4 μm fraction of soil samples are reported in Tables 3.9 (Appendix B), 3.10 and 3.11(Appendix B) respectively.

The minerals contained in soil samples identified by XRPD included the Fe rich minerals (hematite and goethite), Mn rich minerals (bixbyite, braunite, ramsdellite, pyrolusite and cryptomelane), feldspars (microcline and sanidine) and the clay minerals (muscovite, illite and kaolinite) (Table 3.8). The Mn rich minerals, Fe rich minerals and the feldspars were contained in the < 53 μm fraction of the soil samples. Quartz (SiO_2) was present in the < 53 μm fraction of all the soil samples of the study site, the control area and the other geological materials, which were samples and analysed. It is therefore not reflected in Tables 3.8, 3.9 and 3.11 for soil samples as well as in Table 3.10, which shows the mineral contents of the other geological materials. The < 4 μm fraction of the soil samples mineralogically consisted of the clay minerals (Table 3.11). At the control site, only quartz and hematite were identified in the < 53 μm fraction of the soil samples, and the < 4 μm fraction of the soil samples consisted mainly of kaolinite with traces of quartz.

Table 3.8: Summary results of minerals identified in soil samples by XRPD

Mineral Group	Mineral	Chemical formula	Trace	Minor	Major	Total
Fe minerals	Haematite	Fe_2O_3	63	12	122	197
	Goethite	$Fe^{+3}O(OH)$	76	31	7	114
Mn minerals	Bixbyte	Mn_2O_3	45	33	1	79
	Braunite	$Mn^{+2}Mn_6^{+3}SiO_{12}$	45	33	77	155
	Ramsdellite	MnO_2	48	20	5	73
	Pyrolusite	MnO_2	30	15	2	47
	Cryptomelane	$K_{2-x}Mn_8O_{16}$	21	6	79	106
Feldspars	Microcline	$KAlSi_3O_8$	91	21	9	121
	Sanidine	$K(Si_3Al)O_8$	116	36	1	153
Clays	Muscovite	$KAl_2Si_3AlO_{10}(OH)_2$	65	36	1	102
	Illite	$KAl_2Si_3AlO_{10}(OH)_2$	94	15	117	226
	Kaolinite	$Al_2Si_2O_5(OH)_4$	63	35	70	168

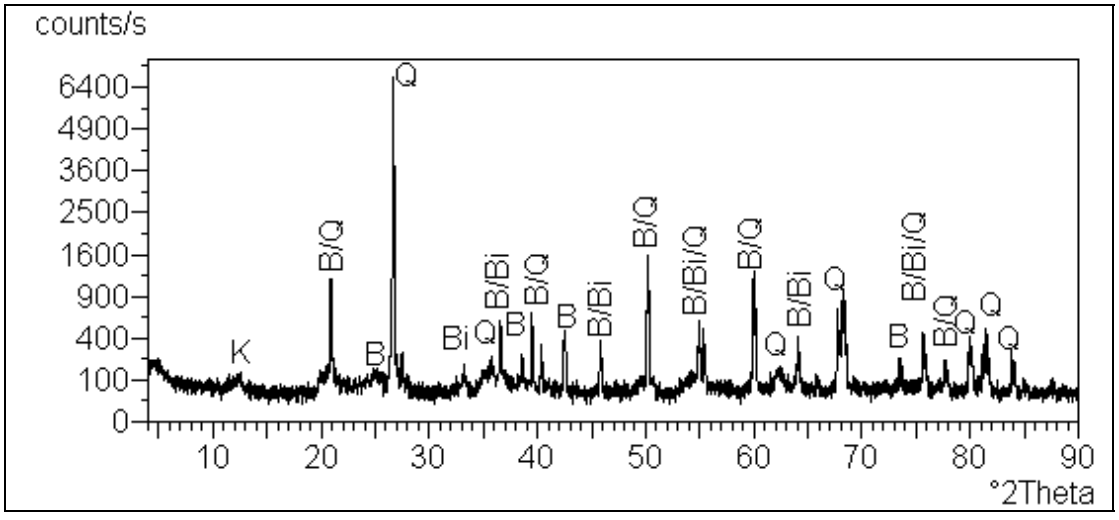

Figure 3.2: X-ray powder diffractogram of < 53 μm fraction of representative soil sample from the study area (K is kaolinte; B is braunite; and Bi is bixbyite)

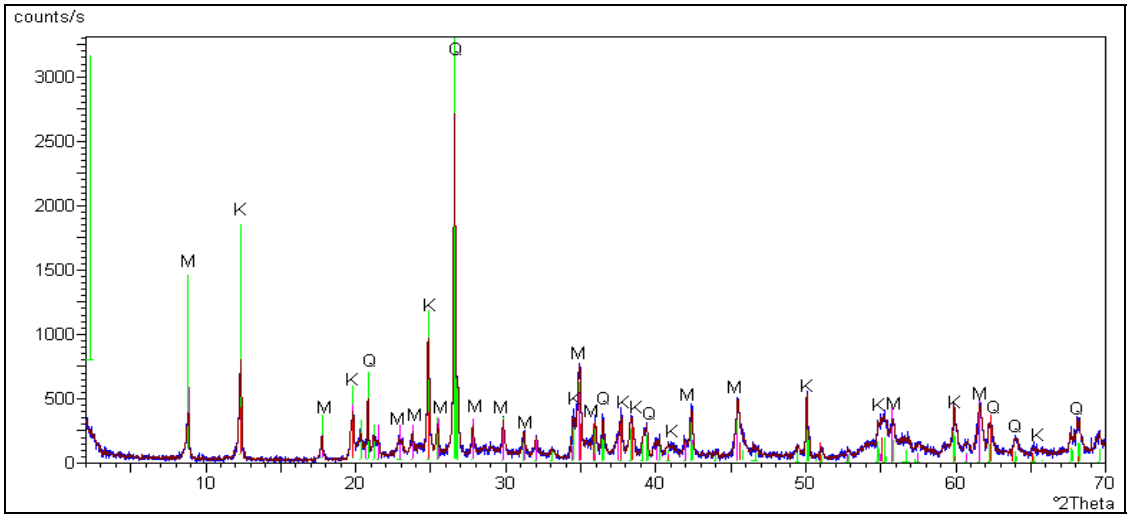

Figure 3.3: X-ray powder diffractogram of < 4 μm fraction of representative soil sample from the study area (M is muscovite; K is kaolinite; and Q is quartz).

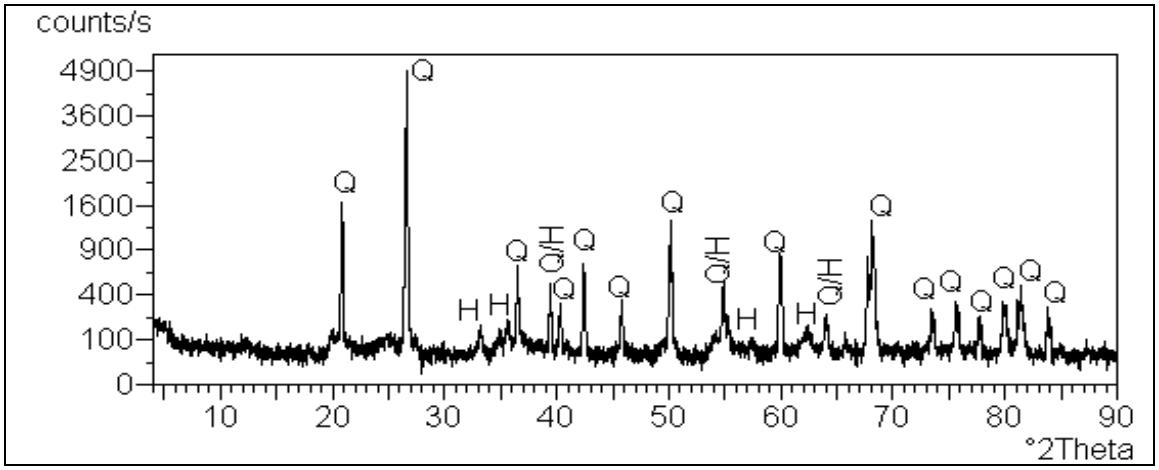

Figure 3.4: X-ray powder diffractogram of < 53 μm fraction of representative soil sample from the control site (Q is quartz; and H is haematite)

Table 3.10: Mineralogy of other geological materials sampled at the Kgwakgwe study area as determined by X-ray diffraction

No	Name of material	Sample number	Minerals identified by XRPD
1	Manganiferous shale	A	Quartz, cryptomelane, microcline, goethite, kaolinite
		B	Quartz, cryptomelane, bixbyite, pyrolusite, microcline, kaolinite
		C	Quartz, cryptomelane, ramsdellite, bixbyite, microcline, muscovite kaolinite
		D	Quartz, cryptomelane, pyrolusite, microcline, goethite, kaolinite
		E	Quartz, cryptomelane, microcline, goethite, kaolinite
2.	Ferruginous shale	F	Quartz, hematite, goethite, kaolinite, illite
		G	Quartz, haematite, goethite, microcline, illite
		H	Quartz, haematite, goethite, kaolinite,
		I	Quartz, haematite, kaolinite, illite
		J	Quartz, haematite, goethite, kaolinite, illite
3.	Mn oxide ore	K	Quartz, cryptomelane, bixbyite
		L	Quartz, cryptomelane, bixbyite, pyrolusite
		M	Quartz, cryptomelane, bixbyite, pyrolusite, braunite
		N	Quartz, ramsdellite, bixbyite, pyrolusite, braunite
		O	Quartz, cryptomelane, bixbyite, pyrolusite, microcline
4.	Mn wad	P	Quartz, cryptomelane, goethite
		Q	Quartz, cryptomelane, bixbyite, goethite
		R	Quartz, pyrolusite, bixbyite, goethite
		S	Quartz, cryptomelane, bixbyite, goethite
		T	Quartz, cryptomelane, bixbyite, goethite
5.	Tectonised manganiferous chert breccia	U	Quartz, cryptomelane, braunite
		V	Quartz, braunite
		W	Quartz, cryptomelane, braunite
		X	Quartz, cryptomelane ramsdellite
		Y	Quartz, cryptomelane, braunite

3.2.2.2 Scanning electron microscopy technique

The photomicrographs of goethite, kaolinite and Mn oxide minerals contained in soil samples from the study area are presented in Figures 3.5, 3.6 and 3.7 respectively. These photomicrographs were compared with those in published literature (Bailey, 1980; Butuzova, Drits, Morozov and Gorschkov, 1990;

Cairncross, Beukes and Gutzmer, 1997; Taylor, 1987) and the particle morphologies were found to be similar.

Goethite particles were found interbedded with either kaolinite (Figure 3.5), and/or Mn oxide particles. The average size of the goethite particles as revealed in the photomicrographs was 1 μm by 1.25 μm. Most of the observed goethite particles occur as microcrystals elongated along the “b” axis. The EDX results showed concentration levels of mainly Fe and in wt % concentrations reaching 30 wt % in some of the samples, Mn, K, Al, Si and O. The presence of these elements is indicative of possibly goethite and/or hematite, kaolinite and Mn oxide minerals.

The morphology of the fraction of soil samples reveals irregular platelets, well developed and irregular flakes, and booklets of kaolinite as indicated in Figure 3.6. The morphological features of some of the kaolinite particles observed indicate good crystallinity and high porosity. Pseudo hexagonal kaolinite platelets with angular edges were evident in some of the observed samples. Clusters of these crystals lie in an ordered direction and the EDX results indicated concentration levels of Al and Si in an almost equal intensity, and O in slightly less than half of the intensity of the former two elements.

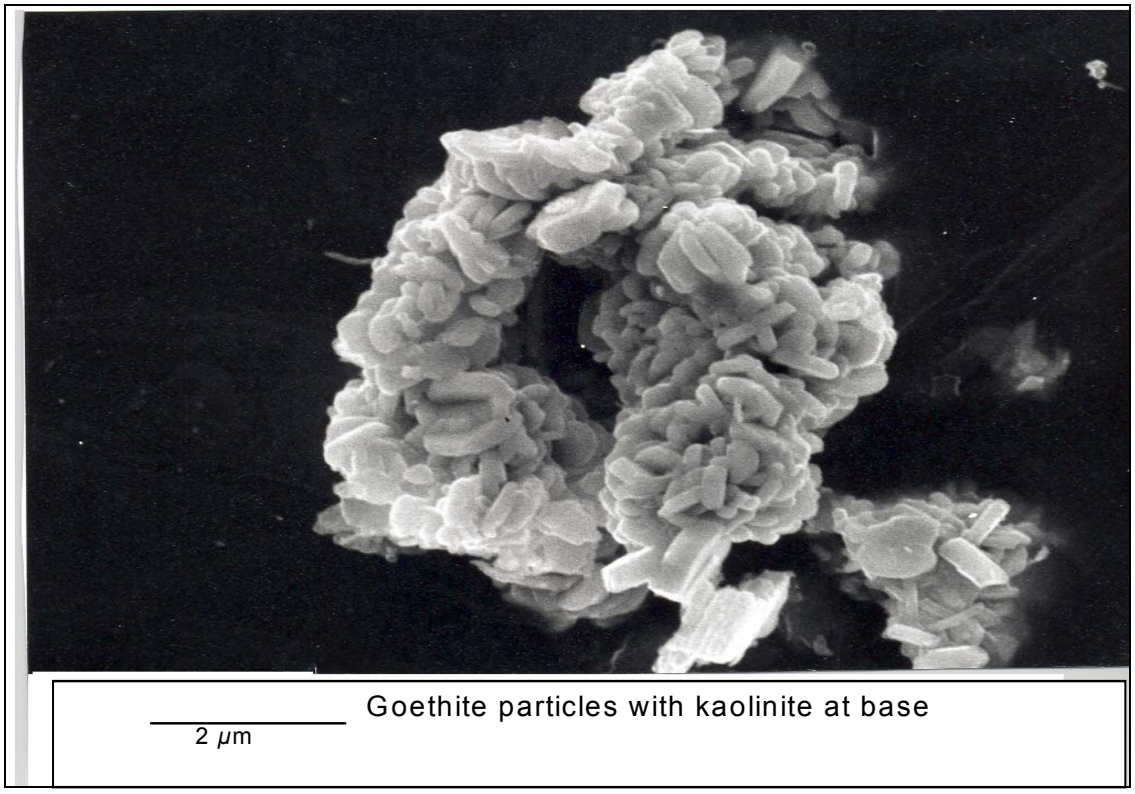

Figure 3.5: Scanning electron photomicrograph of representative < 4 μm fraction of the soil sample from the study site depicting goethite interbedded with kaolinite

It was also observed for the kaolinite particles that some were ragged edged and flaky, with swirl texture, coupled with some reasonable rounding at the edges. With these kaolin particles, the elements detected by EDX included Fe, Mn, K together with Al, Si and O. The presence of these elements is indicative of either goethite or hematite, and Mn oxide minerals forming thin coatings on kaolinite crystal surfaces.

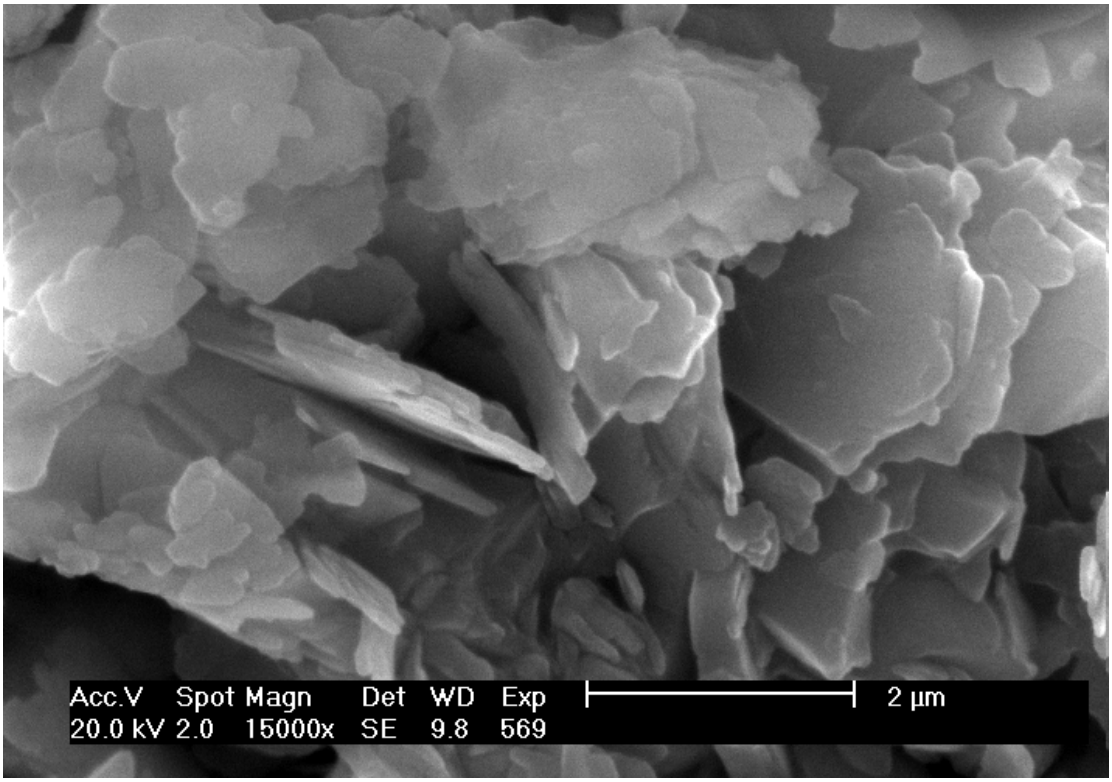

Figure 3.6: Scanning electron photomicrograph of representative < 4 μm fraction of the soil sample from the study site revealing thin pseudo hexagonal booklet of kaolinite

There were charging effects by the Mn minerals, making it difficult to observe morphological structures properly. Particles reflected a coarse surface with no clear distinct morphology. However, the elements which were detected by EDX for this photomicrograph (Figure 3.7) included mainly Mn with concentration levels attaining 27 wt %, Fe 12 wt % together with Al, Si and O in less wt %ages. The presence of these elements is indicative of principally Mn oxide minerals, and Fe oxide minerals as well as kaolinite crystals.

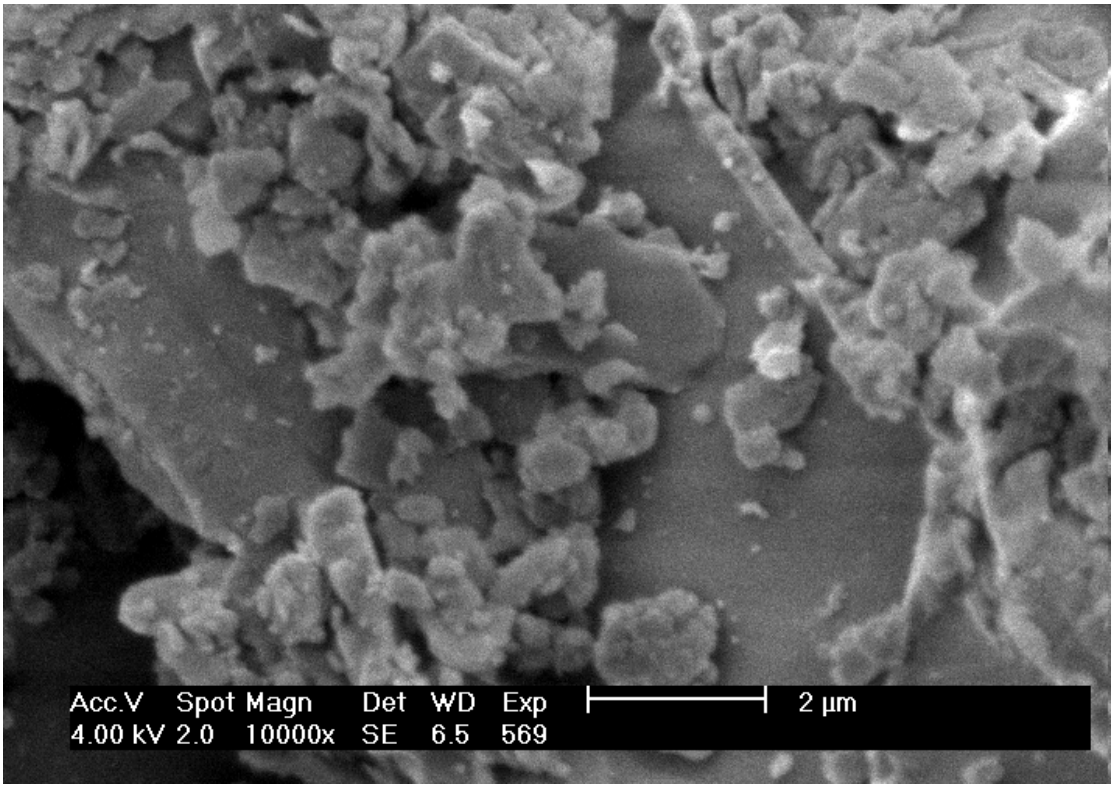

Figure 3.7: Scanning electron photomicrograph of representative < 4 μm fraction of the soil sample from the study site revealing Mn oxide particles

3.2.2.3 Optical microscopy technique

In optical microscopy, only the < 53 μm fraction of soil samples were studied. The magnification used was 20X/0.40. The < 4 μm fraction of the soil samples could not be characterised by optical microscopy because the particles were too small to be individually distinct at this magnification of the microscope. Particle morphology at this size fraction has been described in section 3.2.2.2 above. The hardness, cleavage, fracture, colour and streak were properties used to characterise the different minerals contained in the samples, which were observed at this magnification of the microscope.

Quartz grains were identified in all the samples, although the grains were of different colours ranging from white, milky, colourless, pink, yellowish white, light purple to dark brown. On the Mohr scale of hardness, the quartz grains measured seven. The quartz grains had no cleavage, maintained a white streak and vitreous lustre. Moreover, the quartz grains were poorly sorted, and were subangular at sampling points close to the mine workings and were dark coloured. Further away from the mine workings and exposed outcrops, the quartz grains became light coloured, and the grains sorted, semi rounded to round.

Both microcline and sanidine at the study area had a hardness of six. Microcline had distinct cleavage, and a conchoidal to uneven fracture. Sanidine showed a distinct close to 90^{o} cleavage with disordered structure. The microcline grains were stained darkish blue, to black whereas sanidine particles were pink to yellowish red. These observed colours were possibly due to adhesion of Mn and Fe ions on their surfaces. These particles also had a vitreous lustre. The hardness of hematite grains was 6 and that of goethite grains 5.5. Hematite grains were fragile with no observed cleavage, and were opaque with a metallic lustre, and dark red streak. Goethite grains were soft, silky yellow lustre, having distinct cleavage and a greasy feel, with brownish yellow streak.

Bixbyite crystals were cubic in appearance, whereas pyrolusite crystals were prismatic. Both bixbyite and pyrolusite crystals had a hardness of 6.5. Bixbyite

manifested no distinct cleavage and had an uneven fracture. The cleavage of pyrolusite was poor. Both bixbyite and pyrolusite crystals were opaque with metallic to submetalic lustre. The streak of bixbyite was black and that of pyrolusite was bluish black.

The colour of cryptomelane was greyish black, dark brown, brown to greyish white that of braunite was black to greyish black and that of ramsdellite brownish black. Cryptomelane had an earthy lustre, and maintained a hardness of 6 with a brownish black streak. The hardness of observed braunite was 6.5, and it had a brownish back grey streak. Ramsdellite crystals had a hardness of 3, with a grey streak.

3.2.3 Chemical analyses

Chemical analyses were carried out with the FAAS, ion chromatograph and the calcimeter. Phosphorus was determined using the Olsen method and the TOC measured with the Carbon/Hydrogen/Moisture Determinator. Results of the chemical analyses for Fe and Mn concentration values in soils and leaves and of the TOC from both the study site and the control area are reported in Tables 3.12 and 3.13, and Tables 3.14 and 3.15 (Appendix B). The metallic concentration values were converted to corresponding oxides.

3.2.3.1 Atomic absorption spectrometry technique

A summary statistics of the results of analyses of Fe and Mn assays of soil and leaf samples from the study area is given in Table 3.12. Both $\mu g\ g^{-1}$ and ppm are

used interchangeably in the thesis. The range of concentration levels of Fe in soils was from 1116 μg g^{-1} to 870766 μg g^{-1} with a mean of 17593 μg g^{-1} and for Mn in soils was 35 μg g^{-1} to 24907 μg g^{-1} with a mean of 1088 μg g^{-1}. For the leaves, range of concentration levels of Fe contained in them was from 101.2 μg g^{-1} to 3758 μg g^{-1} with a mean of 637 μg g^{-1} and for Mn in leaves was from 26.2 μg g^{-1} to 3611.5 μg g^{-1} with a mean of 598.4 μg g^{-1}. The standard deviation and threshold values of the analysed assays are also reported in Table 3.12. For the soil samples, values of median, mode, sample variance, Kurtosis, skewness, sum and count for Fe and Mn concentrations as well as TOC are also given in Table 3.13. Tables 3.14 and 3.15 (Appendix B) depict the concentration values of Fe and Mn in the soils and leaves from the study area and Tables 3.16 and 3.17 give the concentration levels of Mn and Fe in soils and leaves from the control area.

Table 3:12: Statistics of iron and manganese assays of soil and leaf samples from the study area (Note: LN = log normal, N = normal)

Element	**Fe ppm soils**	**Mn ppm soils**	**Fe ppm leaves**	**Mn ppm leaves**
No. of samples	400	400	200	200
Freq.dist	LN	LN	N	N
Range	1116-870766	35-24907	101.2-3758	26.2-3611.5
Mean	17593	1088	637.0	598.4
Std Deviation	47950	2620	513.8	511.5
Threshold	22500	3000	950	1200

Table 3.13: Statistical data of manganese and iron concentrations in soils and leaves of the study area

Parameters	Soils Fe, conc. (μg /g)	Soils Mn, conc. (μg /g)	Total organic carbon (TOC) (wt %)	Leaves Fe, conc. (μg /g)	Leaves Mn, conc. (μg /g)
Mean	17593.52	1088.57	1.90	67.07	598.38
Standard Error	2397.55	131.03	0.07	36.33	36.17
Median	14026.31	295.14	1.535	502.99	455.75
Mode	21256.5	3038.51	0	197.99	232.90
Standard deviation	47950.98	2620.49	1.41	513.84	511.47
Sample Variance	2299296921	6866982	1.989005	264028.09	261602.50
Kurtosis	263.91	41.93	0.49	8.79	9.69
Skewness	15.62	5.95	0.97	2.57	2.61
Range	869649.41	24871.72	7.91	3656.82	3585.30
Minimum	1116.59	35.84	0	101.27	26.20
Maximum	870766	24907.56	7.91	3758.09	3611.50
Sum	7037406.42	435429.80	761.95	127413.24	119675.40
Count	400	400	400	200	200

Table 3.16: Concentration levels of iron, manganese and total organic carbon in soils obtained from the control area

Sample Number	Fe, conc. (μg g^{-1})	%rsd	s.d	Mn, conc. (μg g^{-1})	%rsd	s.d	TOC (wt %)
Control 1	7415.98	2.7	200.23	763.39	1.8	13.74	4.07
Control 2	2547.42	3.4	86.61	69.34	1.6	144.30	4.10
Control 3	4884.91	2.9	141.67	240.08	1.0	2.40	4.72
Control 4	7887.87	2.0	157.75	107.12	1.4	1.49	4.34
Control 5	2541.49	3.3	86.59	69.34	1.6	144.28	4.10
Control 6	3281.71	3.4	111.58	241.08	1.1	2.41	4.69
Control 7	7687.87	1.9	148.75	100.12	1.3	1.41	4.54
Control 8	2546.42	3.4	86.51	62.34	1.4	137.30	4.86
Control 9	2551.49	3.4	86.61	69.34	1.6	144.29	4.71

As could be seen from Tables 3.14 to 3.17, the concentration levels of Mn and Fe in the control area were significantly lower than the mean concentration values of soils and leaves from the study site.

Table 3.17: Concentration levels of iron and manganese in leaves obtained from the control area

Sample Number	Fe, conc. (μg g^{-1})	%rsd	s.d	Mn, conc. (μg g^{-1})	%rsd	s.d
Control 2	296.43	2.2	148	324.5	1.3	4.22
Control 4	334.61	0.5	1.67	231.14	2.1	4.85
Control 6	444.89	2.6	11.57	232.9	2.8	6.52
Control 8	605.29	1.3	7.87	131.35	3.2	4.20

3.2.3.2 Exhangeable bases and cation exchange capacity

The mean, standard error, median, mode, standard deviation, sample variance, Kurtosis, skewness, range, minimum and maximum values, sum and count for Na, K, Ca and Mg which constitute the exchangeable bases as well as Cl, SO_4, CO_3 in soil samples are summarised in Table 3.18.

Table 3:18: Statistics of exchangeable bases and anions of soil samples from the study area

Parameter	*Cl*	*SO_4*	*CO_3*	*Na*	*K*	*Ca*	*Mg*
Mean	7.63	19.36	40.98	0.44	0.82	5.68	8.26
Standard Error	0.09	0.28	0.42	0.22	0.41	2.83	4.12
Median	7.5	18.1	41.3	0.2	0.3	2.6	4.2
Mode	7.8	15.1	35.1	0.2	0.3	2.9	4.3
Standard Deviation	1.88	5.60	8.44	4.44	8.15	56.77	82.51
Sample Variance	3.52	31.33	71.30	19.71	66.49	3222.65	6808.27
Kurtosis	0.34	3.71	1.63	400.41	400.11	400.10	400.17
Skewness	0.17	1.12	-0.72	20.00	19.99	19.99	19.99
Range	11.7	43.6	54	89	163.5	1138.7	1655.3
Minimum ($cmol_c kg^{-1}$)	0.2	2.1	5.1	0.1	0.1	0.3	0.3
Maximum ($cmol_c kg^{-1}$)	11.9	45.7	59.1	89.1	163.6	1139	1655.6
Sum	3014.8	7742.9	16390.9	178.2	327.2	2278	3311.2
Count	395	400	400	401	401	401	401

The values obtained for Na, K, Ca and Mg concentrations in the soil samples from the study area and the control site are given in Table 3.19 and Table 3.20 respectively. The values for Na concentration in the soil samples from the study area ranged from 0.1 $cmol_c kg^{-1}$ to 89.1 $cmol_c kg^{-1}$, with a mean of 0.44 $cmol_c kg^{-1}$, and for the soil samples from the control site, they were from 1.2 $cmol_c kg^{-1}$ to 1.5 $cmol_c kg^{-1}$. As reflected in Table 3.19, the values for K concentration in the soil samples from the study area ranged from 0.1 $cmol_c kg^{-1}$ to 163.6.1 $cmol_c kg^{-1}$, with a mean of 0.82 $cmol_c kg^{-1}$, and for the soil samples from the control site (Table 3.20), they were from 1.6 $cmol_c kg^{-1}$ to 2.3 $cmol_c kg^{-1}$.

The values for Ca concentration in the soil samples from the study area, as reported in Table 3.19 (Appendix B), ranged from 0.3 $cmol_c kg^{-1}$ to 1139 $cmol_c kg^{-1}$, with a mean of 5.68 $cmol_c kg^{-1}$, and for the soil samples from the control site (Table 3.20), they were from 3.0 $cmol_c kg^{-1}$ to 4.9 $cmol_c kg^{-1}$. As further reflected in Table 3.19, the values for Mg concentration in the soil samples from the study area ranged from 0.3 $cmol_c kg^{-1}$ to 1655.3 $cmol_c kg^{-1}$, with a mean of 8.26 $cmol_c kg^{-1}$, and for the soil samples from the control site (Table 3.20), the values were from 9.0 $cmol_c kg^{-1}$ to 9.9 $cmol_c kg^{-1}$. The ranges reported for exchangeable bases in the soil samples may appear high for these parameters. However, it can be deducted from the mean values that there are few samples with high concentrations. These few samples are reflected as outliers. The few outliers do not affect the overall spatial distribution of the exchangeable bases in the area as can be depicted from the maps in the next chapter.

Table 3.20: Concentration levels of exchangeable bases in soil samples obtained from the control area

Sample code	Na $cmol_c kg^{-1}$	K $cmol_c kg^{-1}$	Ca $cmol_c kg^{-1}$	Mg $cmol_c kg^{-1}$	Sample code	Na $cmol_c kg^{-1}$	K $cmol_c kg^{-1}$	Ca $cmol_c kg^{-1}$	Mg $cmol_c kg^{-1}$
Control 1	1.5	1.9	4.6	9.3	Control 6	1.4	2.3	3.9	9.1
Control 2	1.2	2.0	4.9	9.7	Control 7	1.3	2.2	3.6	9.0
Control 3	1.4	2.2	4.3	9.9	Control 8	1.2	2.1	3.0	9.3
Control 4	1.3	2.1	4.8	9.7	Contol 9	1.2	2.0	4.1	9.0
Control 5	1.5	1.6	4.2	9.1					

The values for CEC and percent base saturation for the soil samples from both the study area and the control site are presented in Table 3.21 and Table 3.22 respectively. The CEC values in the soil samples from the study area, as reported in Table 3.21, ranged from 1.1 $cmol_c kg^{-1}$ to 29.2 $cmol_c kg^{-1}$, with a mean of 8.2 $cmol_c kg^{-1}$, and for the soil samples from the control site (Table 3.22), they were from 15.9 $cmol_c kg^{-1}$ to 21.2 $cmol_c kg^{-1}$. As further reflected in Table 3.23 (Appendix B), the values for percent base saturation in the soil samples from the study area ranged from 33.77% to 100 % with a mean of 82.10 % $cmol_c kg^{-1}$, and for the soil samples from the control site (Table 3.24), the values were from 81.60 % to 98.89 %.

Table 3.22: Cation exchange capacity of soil samples from the control area

Sample code	**CEC ($cmol_c kg^{-1}$)**	**Sample code**	**CEC ($cmol_c kg^{-1}$)**
Control 1	21.2	Control 6	17.3
Control 2	18.5	Control 7	16.4
Control 3	19.1	Control 8	15.9
Control 4	18.1	Control 9	16.7
Control 5	16.7		

Table 3.24: Percent base saturation of soil samples from the control area

Sample code	%	Sample code	%
Control 1	81.60	Control 6	96.53
Control 2	96.22	Control 7	98.17
Control 3	93.19	Control 8	98.11
Control 4	98.89	Control 9	97.60
Control 5	98.20		

Similarly for percent base saturation as for exchangeable bases, the ranges reported in the soil samples have excluded a few samples with high values. These few samples are reflected as outliers. The few outliers do not affect the overall spatial distribution of the exchangeable bases in the area as can be depicted from the maps in the next chapter.

3.2.3.3 Phosphorus determination

Phosphorus concentrations in 36 randomly chosen soil samples from the study area and two samples from the control site were determined and the results are reported in Table 3.25. This purpose of this test was to have an idea of the available phosphorus in the soils. Values obtained for P_2O_5 in soil samples from the study area were from 0.51 $mgkg^{-1}$ to 6.02 $mgkg^{-1}$and for soil samples from the control site were 3.77 $mgkg^{-1}$and 3.83 $mgkg^{-1}$.

Table 3.25: Phosphorus concentrations in randomly chosen soil samples from the study area and the control area

Sample No	P(mgkg^{-1})	P_2O_5 (mgkg^{-1})	Sample No	P(mgkg^{-1})	P_2O_5 (mgkg^{-1})
A2-2	2.61	6.02	C4-10	0.41	0.96
A 5-2	0.69	1.60	C-54	0.80	1.85
C1-6	1.86	4.31	C5-8	0.30	0.70
C1-9	0.38	0.87	C5-10	0.26	0.59
C2-1	2.44	5.65	C6-3	0.23	0.53
C2-2	1.44	3.33	C6-6	0.94	2.16
C2-6	1.34	3.09	C6-7	0.33	0.75
C2-8	0.70	1.62	C7-3	0.84	1.94
C2-9	0.22	0.51	C7-5	2.12	4.89
C2-10	2.26	5.22	C7-8	0.43	0.99
C3-1	1.66	3.84	C8-4	0.80	1.84
C3-6	1.38	3.18	C8-7	0.35	0.81
C3-8	2.32	5.36	C9-1	1.53	3.54
C3-9	3.39	7.83	C9-9	1.04	2.41
C3-10	0.41	0.96	C9-10	1.44	3.33
C4-9	0.30	0.69	C10-7	1.07	2.48
Control 1	1.63	3.77	Control 6	1.66	3.83

3.2.3.4 Determination of chloride, sulphate and carbonate

The values obtained for Cl, SO_4 and CO_3 concentrations in the soil samples from the study area and the control site are given in Table 3.26 (Appendix B) and Table 3.27 respectively. The values for Cl concentration in the soil samples from the study area ranged from 0.2 mgkg^{-1} to 11.9 mgkg^{-1}, with a mean of 7.63 mgkg^{-1}, and for the soil samples from the control site, they were from 6.3 mgkg^{-1} to 8.3 mgkg^{-1}. As reflected in Table 3.26, the values for SO_4 concentration in the soil samples from the study area ranged from 2.1 mgkg^{-1} to 47.5 mgkg^{-1}, with a mean of19.36 mgkg^{-1}, and for the soil samples from the control site (Table 3.27), they were from 12.3 mgkg^{-1} to 19.4 mgkg^{-1}.

The values for CO_3 concentration (measured in terms of $CaCO_3$ equivalent) in the soil samples from the study area, as further reported in Table 3.26, ranged

from 5.1 gkg^{-1} to 59.1 gkg^{-1}, with a mean of 40.98 gkg^{-1}. For the soil samples from the control site (Table 3.27), the CO_3 concentration (measured in terms of $CaCO_3$ equivalent) values obtained were from 22.9 gkg^{-1} to 34.1 gkg^{-1}.

Table 3.27: Chloride, sulphate and carbonate concentrations in soil samples from the control area

Sample code	Cl^- ($mgkg^{-1}$)	SO_4^{-2} ($mgkg^{-1}$)	CO_3^{-2} ($CaCO_3$ equiv) gkg^{-1}	Sample code	Cl^- ($mgkg^{-1}$)	SO_4^{-2} ($mgkg^{-1}$)	CO_3^{-2} ($CaCO_3$ equiv) gkg^{-1}
Control 1	7.2	12.3	34.1	Control 6	7.7	19.1	24.1
Control 2	6.3	15.1	29.3	Control 7	8.3	18.1	25.3
Control 3	7.8	17.3	24.4	Control 8	7.7	19.1	23.7
Control 4	7.6	18.9	28.6	Control 9	7.8	19.4	22.9
Control 5	8.1	18.7	28.8				

3.2.3.5 Total organic carbon

Values obtained for TOC in soil samples from both the study site and the control area ranged from 0 wt % to 7.91 wt %, with a mean of 1.90 wt %. The median for TOC in the soil samples was 1.54 wt % and the mode was 0 wt %. At the control area, the TOC in the soil samples ranged from 4.07 wt % to 4.86 wt % (Table 3.16). The TOC values obtained for soil samples at the control site were significantly higher than the mean TOC value for soil samples from the study site.

CHAPTER FOUR

INTERPRETATION AND DISCUSSIONS

4.1 FIELDWORK AND IMAGE ANALYSES

4.1.1 Topographic analyses

The topography of the study area is revealed by the topographical contour map superimposed on the satellite image in Figure 4.1 and the 10 m contour topographic map in Figure 4.2. In the southeast, south and southwestern corners of the satellite image are the Kgwakgwe Hills, the Motlhatsa Hills (Figure 4.2) and the Ditshaba Hills of which only a portion is reflected in Figure 4.2. The Mn oxide deposits are hosted only in the Kgwakgwe Hills.

The three hills gently slope to a close to flat terrain having an altitude of between 1399 m to 1349 m, and a topographic gradient of 0.025. In this close to flat terrain are settlements located mainly in the northeast, a few scattered huts in the north, and the cemetery in the northwest. Other indications of anthropogenic activities include visible tracks and footpaths (Figure 4.2).

Some streams flow in the eastern part, at the foot of the Kgwakgwe Hills. Meteoritic fluids percolating uphill in the Mn oxides outcrops could interact with the oxides through dissolution. The Mn enriched fluids flow downslope and eventually because of saturation with Mn ions, neomineralisation of Mn rich minerals occur. Also, aeolian transportation of Mn rich dust from exposed

outcrops could lead to deposition of Mn particles in the close to flat terrain. Topography thus has an influence on Mn and Fe contamination of soils at the study area.

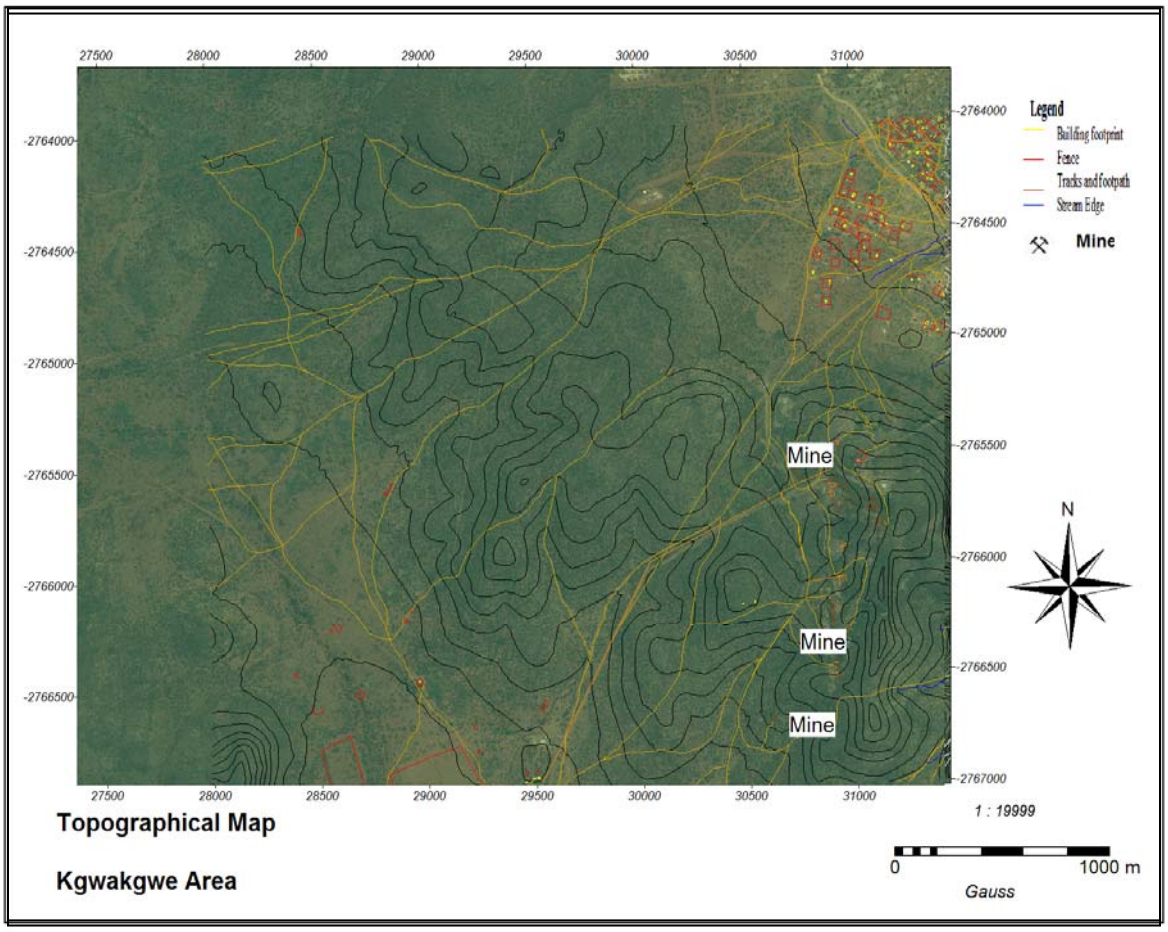

Figure 4.1: Topographical map superimposed on satellite image of the study area

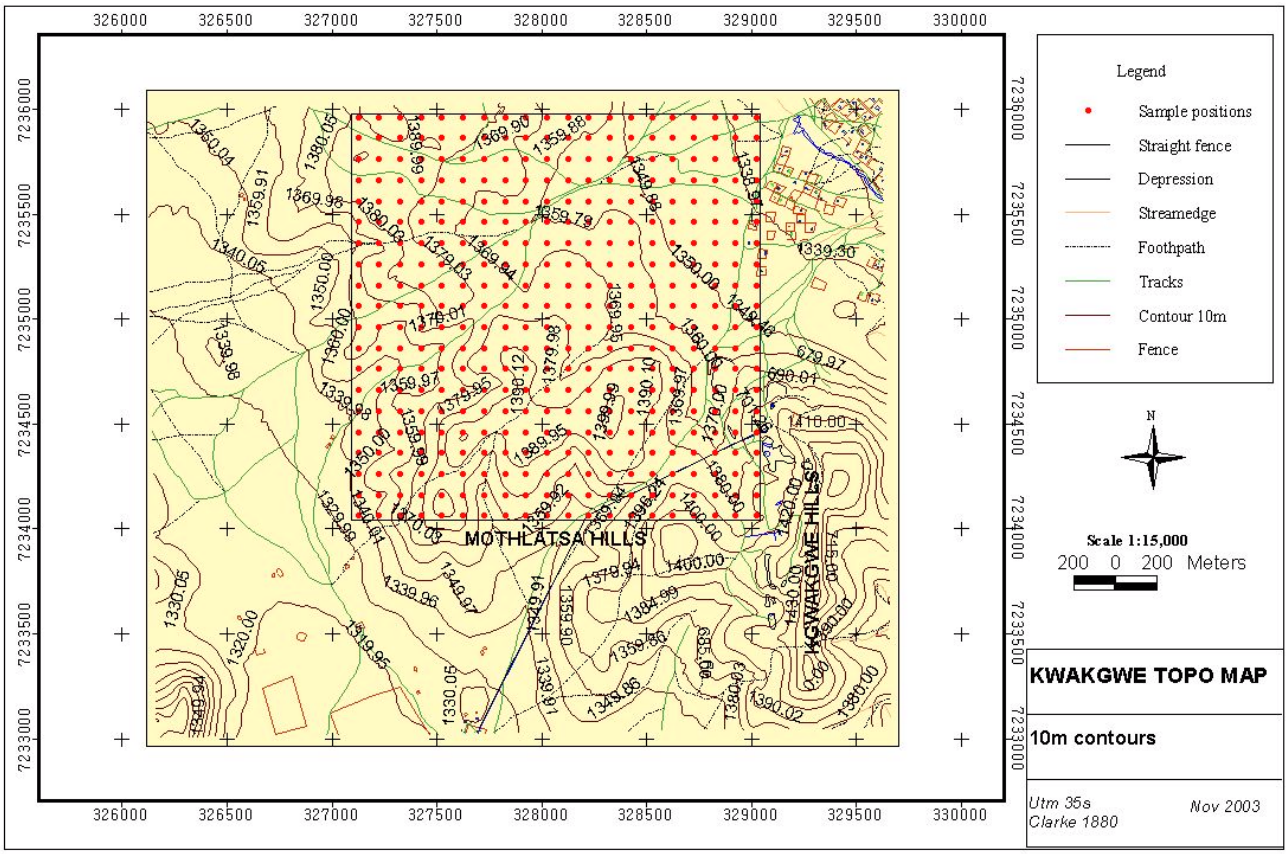

Figure 4.2: Ten metre contour map of the study area revealing the Kgwakgwe and Mothlatsa Hills, and the close to flat terrain sampled

4.1.2 False Colour Composite Data

The different bands in image data are useful for specific discrimination of features on the earth surface (Principles of Remote Sensing, 2000). The reflectance characteristics of vegetation for example differ considerably from that of other earth features such as soils, sand, rocks and clean water. This therefore makes the distinction between these features better in some wave bands than in others. Vegetated areas have high reflection in the near infrared and low reflectance in the visible range (Skidmore, 2002).

In this study, false colour composites were derived from a combination of three bands with one colour being allocated for each band (Table 4.1). The 4, 3, 2 combination was selected because; band 2 is the red chlorophyll absorption band and hence is one of the important bands for vegetation discrimination, band 3 is useful for discriminating between many plant species and it emphasizes soil/geological boundaries as well. Band 4 is responsive to the amount of vegetation biomass present in the image and it is useful for crop identification (Principles of Geographic Information System, 2000).

Table 4.1: Interpretation of colours in false composite maps

No.	Colour	Description
1.	White	Roads, houses and sunlit or highly illuminated areas of he image
2.	Blue	Houses with clear roof tops showing, water tanks
3.	Green	Bare ground, roads, fields and quarry sites
4.	Red	Vegetation, trees
5.	Black	Rock outcrop, Hills and shadows

In the false colour composite as explained by Goodchild (1992) and Skidmore (2002), red depicts for areas with high vegetation reflectance. Different shades of red will imply different forms of vegetation reflectance ranging from very dry grasses, sparse to dense vegetation. White or light tones represent areas of

exposed soil, roads and bare areas. Clear white normally represents cloud cover. Dark colour or black may refer to rock outcrop, hills and shadows (Botswana Range Inventory Monitoring Project, 2001). Blue may indicate water, urban areas or quarry/ mine pits. Intermediate categories may exist indicating mixtures of two or more land cover/ use types. Geometric layout of fields is visible in the image and fenced areas are clearly visible as the fence line can easily be identified. Vegetation appears red and water appears in navy or black, recently ploughed agricultural areas appear in black and fallow fields appear in green (Figure 4.3).

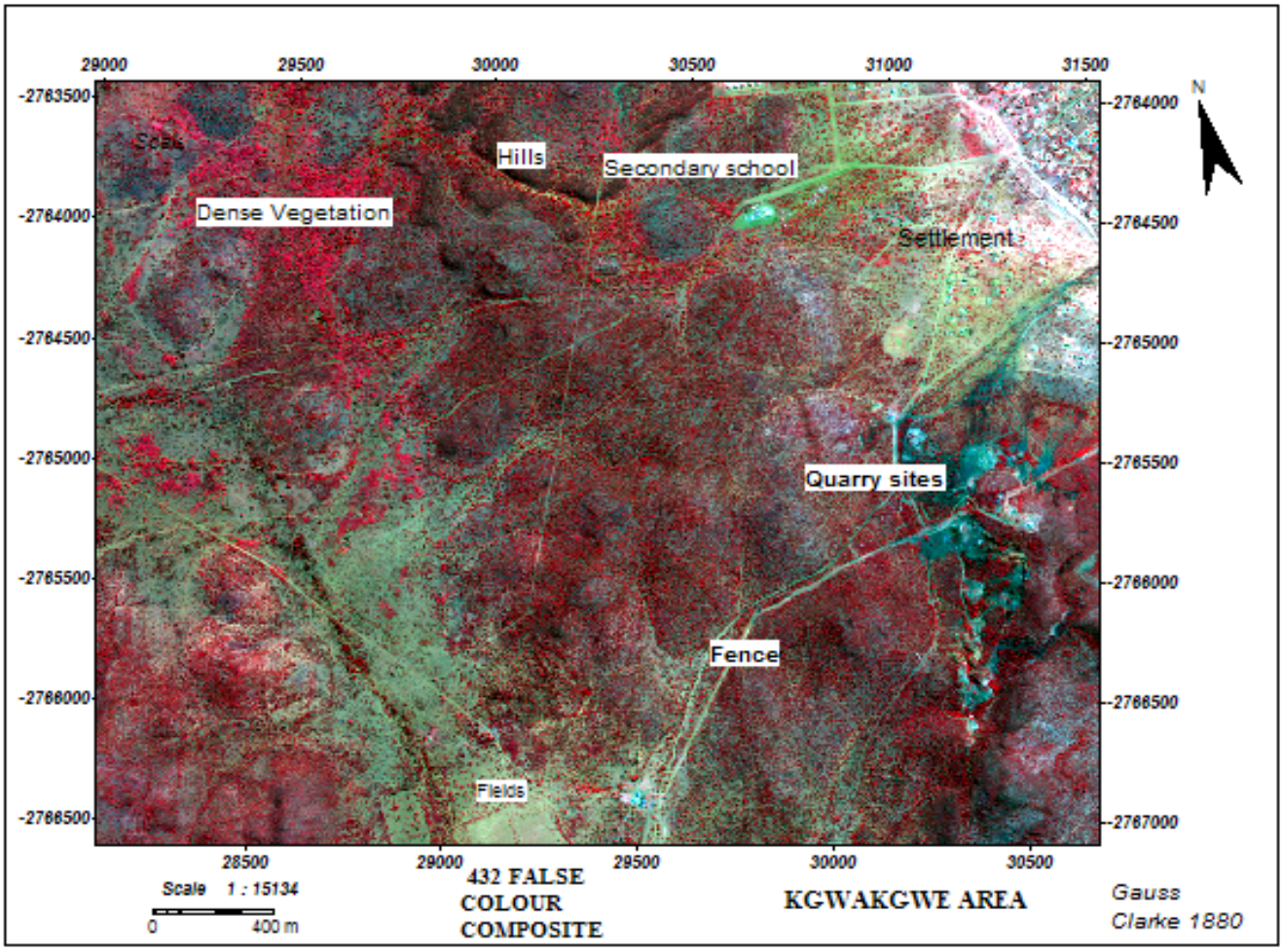

Figure 4.3: False colour composite map of the study area

In the false colour composite map of the study area shown in Figure 4.3, fields, fence, settlement, quarry sites, school, hills and vegetation have been indicated. In the map, white reflects secondary roads and sunlit areas; blue indicates huts and houses with clear roof tops showing, and the water tanks; green shows bare ground, roads, fields and the Mn quarries; red portrays vegetation including the shrubs and trees; and black is indicative of the rock outcrops which consisted of the ferruginous sandstone of the Waterberg Group, manganiferous and ferruginous shales and mudstones, and quartzite of the Transvaal Supergroup, and rhyolite of the Lobatse Volcanic Group, and as well as shadows. These geological formations have been identified and described in section 1.3.2 of this thesis and discussed concisely by Carney *et al.,* (1994); Ekosse and Modisi (1999); Ekosse and Vink (2001); SACS, (1980); Tombale, (1986); and Vink and Ekosse (1998).

4.1.3 Normalised difference vegetation index (NDVI) data

The near-infrared/red band ratio known as the Normalised Difference Vegetation Index (NDVI) is used for indicating vegetation (ILWIS 3.0 Academic, 2002; Principles of Remote Sensing, 2000). The NDVI is a ratio based index that assumes equal vegetation (isovegetation) lines converge at origin and that all bare soil in an image will form a line in spectral space known as the soil. This soil line is a hypothetical line in spectral space and is considered to be of zero vegetation. Green vegetation yields high values for the ratio whilst in contrast water yields negative values and bare soils give near zero values (Botswana

Range Inventory Monitoring Project, 2001). The NDVI works best at 30 % vegetation cover or more (Principles of Remote Sensing, 2000; ERDAS IMAGINE, 1992) was used to do the overlays. The study area definitely has more vegetation cover than that and hence it is still within the limits of applying NDVI efficiently. NDVI also compensates for changes in illumination conditions, surface slope and aspect. The NDVI is calculated as follows in equation 4.1 below:

$$NDVI = \frac{\text{Infrared} - \text{red}}{\text{Infrared} + \text{red}} = \frac{\text{band4} - \text{band3}}{\text{band4} + \text{band3}} \quad (4.1)$$

where NDVI values range from –1 to 1(Principles of Remote Sensing, 2000).

This equation can further be expressed as:

$$NDVI = \frac{NIR - R}{NIR + R}$$

Where NIR = Near infra red and R = Red.

The vegetation index values from the image of the study area shown in Figure 4.4 range from –0.2 to 0.3. Quarry sites, roads, houses and bare ground have the lowest values of around less than zero, fields, cleared areas have values around zero. Trees around homesteads, sparse vegetation shows values around 0.1 whilst dense vegetation shows the highest values between 0.2 - 0.3.

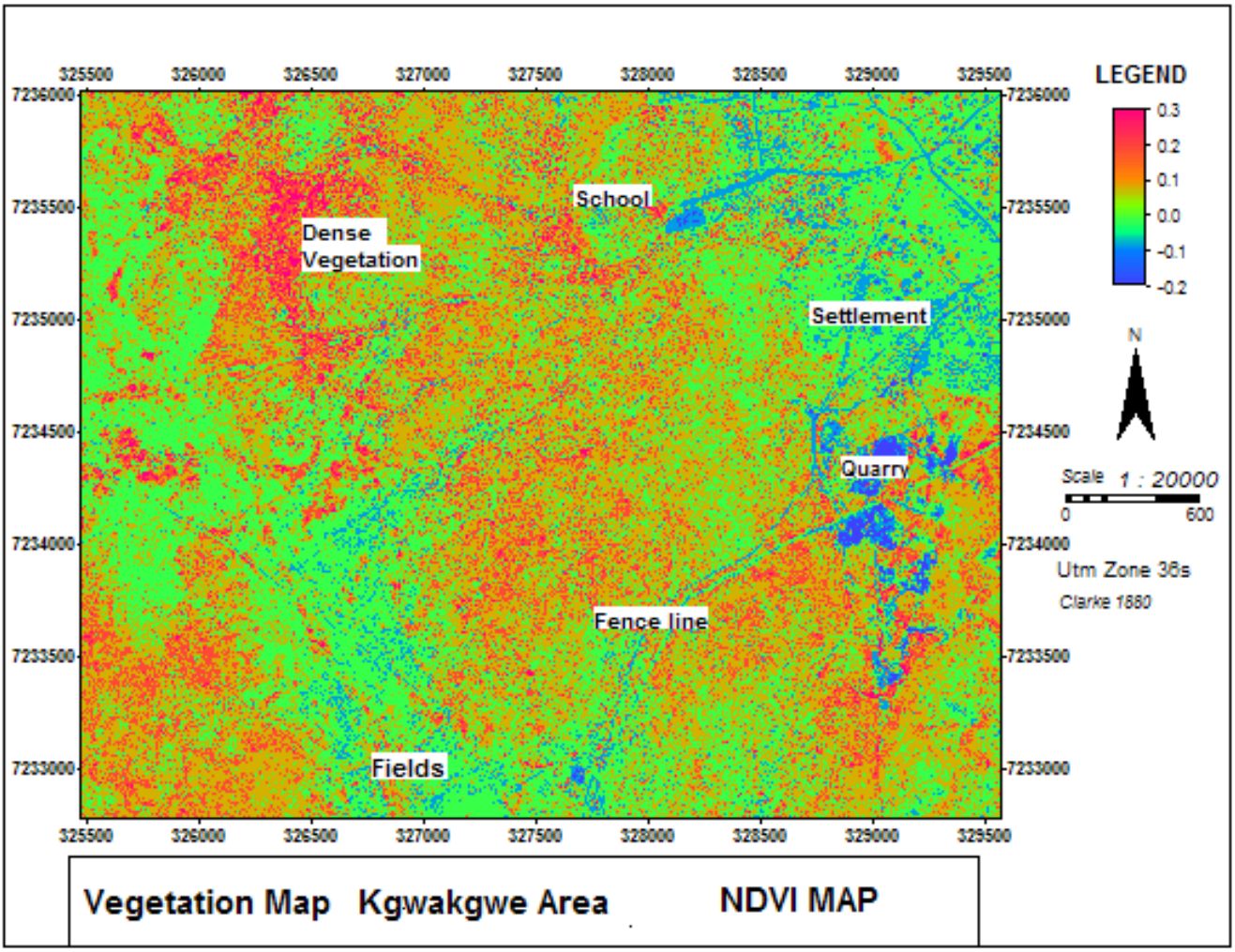

Figure 4.4: Normalised difference vegetation index map of the study area

Difference in brightness values in the image may have been caused by topographic conditions, shadows or changes in sunlit illumination angles and intensity. These conditions could hamper the ability to identify surface material in a satellite image. A ratio transformation of image data was used to reduce the effect of these environmental conditions. Ratio images were also used for discriminating subtle differences in spectral variations and to eliminate albedo effects and shadows. Vegetated areas have a high reflection in the near infrared

and a low reflection in the visible range of the spectrum. Clouds and water on the other hand have larger visual than near infrared reflectance. Rocks and bare soils have similar reflectance in both spectral regions (Ringrose and Matheson, 1991).

Multi band statistics was performed to find the difference between all pixel values and the mean values for each channel i.e. channel variability. Correlation between two or more channels is shown by covariance statistics. A correlation matrix was used to evaluate the degree of correlation between individual bands and is as shown in Table 4.2 below.

Table 4.2: Correlation between bands

Band no	**1**	**2**	**3**	**4**
1	**1.00**	0.95	0.88	0.38
2	0.95	**1.00**	0.94	0.50
3	0.88	0.94	**1.00**	0.40
4	0.38	0.50	0.40	**1.00**

The matrix normally has values ranging from –1 to 1, indicating a strong negative correlation to a strong positive correlation respectively. Each band has a 1.00 correlation with itself as expected otherwise the higher the correlation it implies that there is redundancy in the data as information is being repeated across the two bands. If the value is zero, then there is either no correlation or the

correlation is weak. Large positive values are indicative of strong positive correlation, and large negative vales reflect strong negative correlation. Band 1and Band 2, Band 1 and Band 3, and Band 2 and Band 3, show the highest correlation.

The NIR (Band 4) and visible bands have the lowest correlation in the order; Band 4 and Band 1, Band 4 and Band 3, Band 4 and Band 2 respectively. The NR shows a highest correlation of 0.5 to band 2 in the visible range. Band combinations with lowest in other words showing more information correlation were bands 4,1,3.

4.2 PHYSICO-CHEMISTRY OF THE STUDY AREA

4.2.1 Soil particle size

Three particle size fractions were classified in this study and these were as follows: > 53 μm, 53 μm – 4 μm, and < 4 μm. The > 53 μm fraction particle size of soil consists mainly of quartz and does not affect the chemistry of surface environments (Kralik, 1999). In this regard, this size fraction is not discussed, except where necessary. In the 53 μm – 4 μm fraction, the frequencies of number of samples with their different wt %ages is presented in Figure 4.5. The particle size distribution (PSD) of the soil samples revealed the 53 μm – 4 μm fraction to be in the range of 11.05 wt % to close to 100 wt %. The 53 μm – 4 μm fraction of the soil samples reflected a negatively skewed trimodal distribution. Soil samples in which 85 wt % of the particles were 53 μm – 4 μm had the

highest number of samples and there were 73 samples (Figure 4.5). As reflected in Figure 4.5, close to 50 soil samples had < 50 wt % of the particles to be 53 μm – 4 μm, and about 30 soil samples had > 90 wt % of the particles to be 53 μm – 4 μm.

Three populations could be deducted from the histogram showing the wt % of the < 53 μm fraction of the soil samples (Figure 4.5). This implies that there must be three areas of dominant concentration in the two maps (Figures 4.6 and 4.7), and these were colour reflected as bluish, reddish and yellowish colours, and a minor phase of greenish coloration. Very close to the hills and mine workings of the study area, there were more particles that were coarse sandy (> 53 μm in particle size), and this is reflected with the blue to light blue colours in the contoured and non contoured maps of Figures 4.6 and 4.7. Moreover, there was noticeable red to reddish brown colours in both maps depicting particle size distribution of the < 53 μm fraction of soils. These maps indicated that there were much more finer particles in the northern part of the study area which is further away from the hills and mine workings than the southern part. However, with the contouring as reflected in Figure 4.7, the distinct wt % of the classes of soil samples as distributed within the study area becomes more visible. Forty different wt % classes are presented for the < 53 μm fraction of the soil samples indicating their spatial distribution. The < 53 μm fraction of the soil particles were classified from 31.0 wt % to > 87.9 wt % (Figures 4.6 and 4.7).

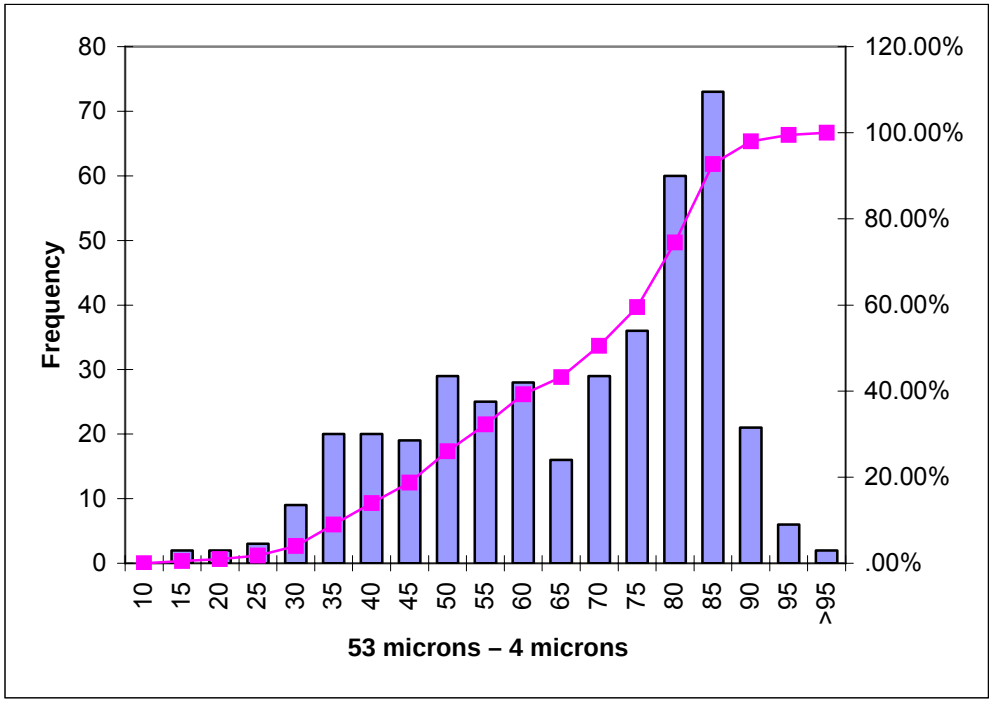

Figure 4.5: Particle size distribution of the 53 μm – 4 μm fraction of soil samples from the study area

In the < 4 μm fraction which is considered as the clay fraction of the soil samples, the frequencies of number of samples with their different wt %ages is presented in Figure 4.8. The particle size distribution for the clay fraction ranged from 0.3 wt % to 30 wt %. The distribution is normal and is positively skewed. Soil samples in which 4 wt % of the particles were < 4 μm had the highest number of samples and there were 160 samples (Figure 4.8). As reflected in Figure 4.8, close to 50 soil samples had < 10 wt % of the particles to be < 4 μm.

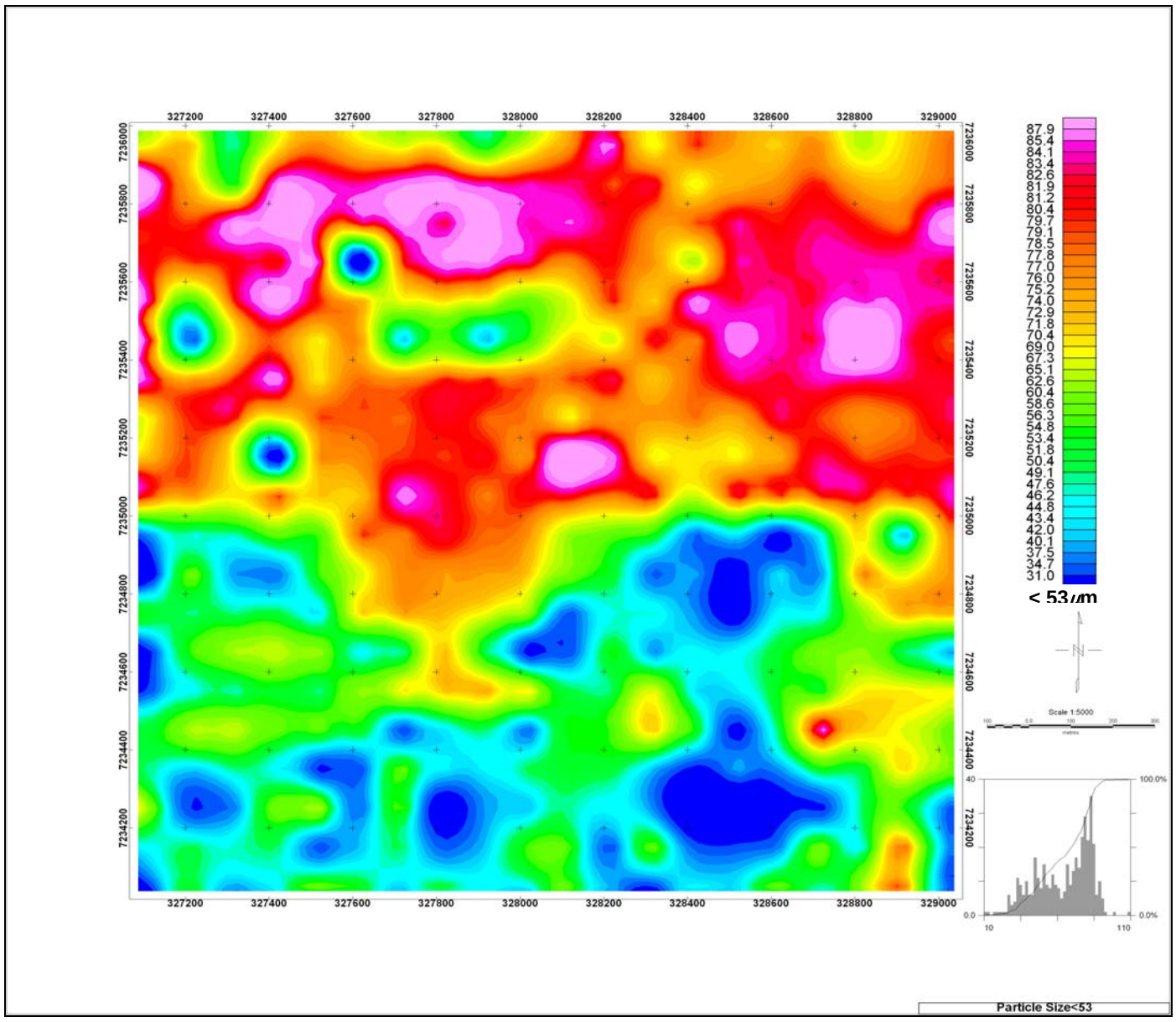

Figure 4.6: Non contoured particle size distribution map of the 53 μm – 4 μm fraction of soil samples from the study area

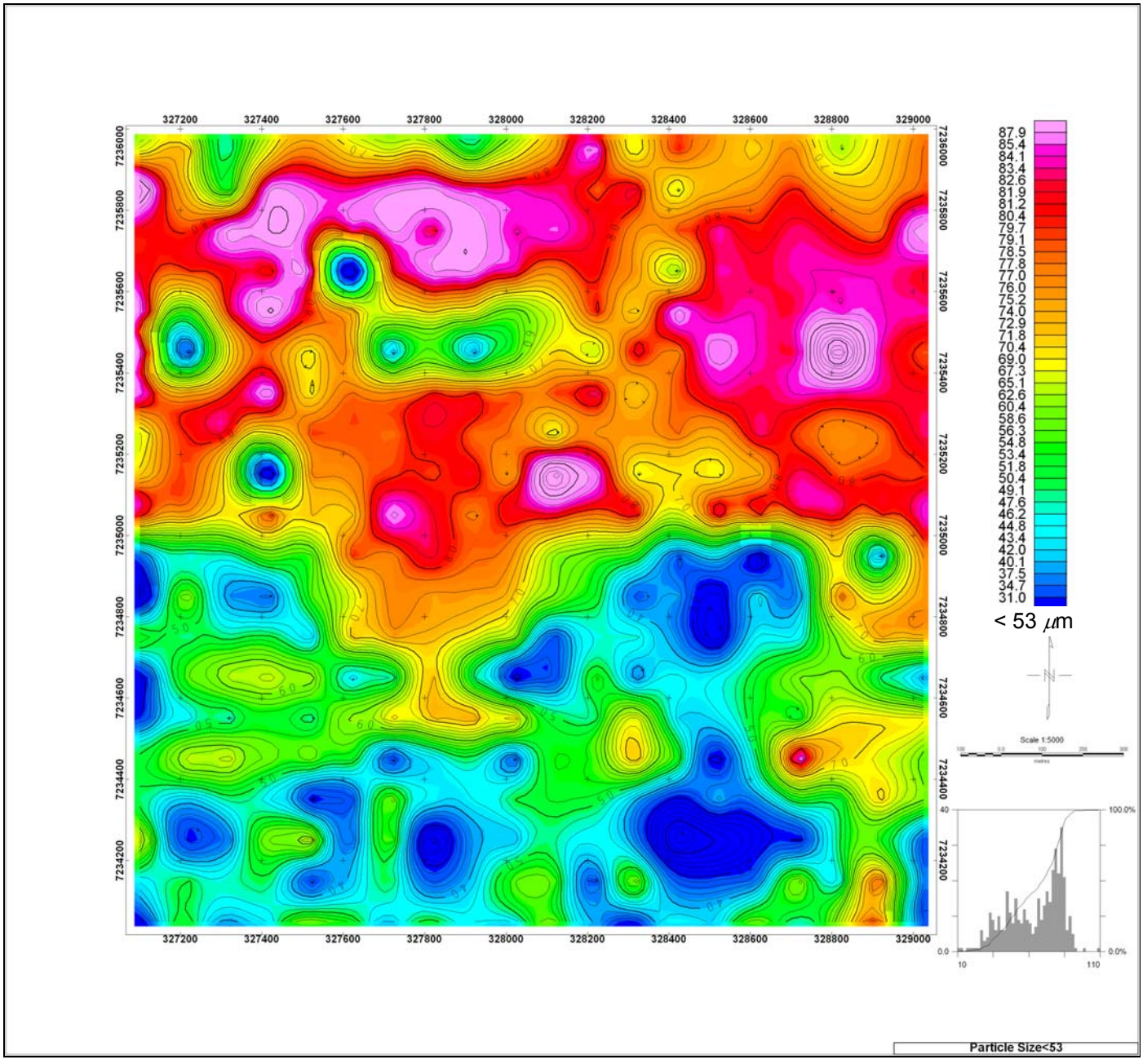

Figure 4.7: Contoured particle size distribution map of the 53 μm – 4 μm fraction of soil samples from the study area

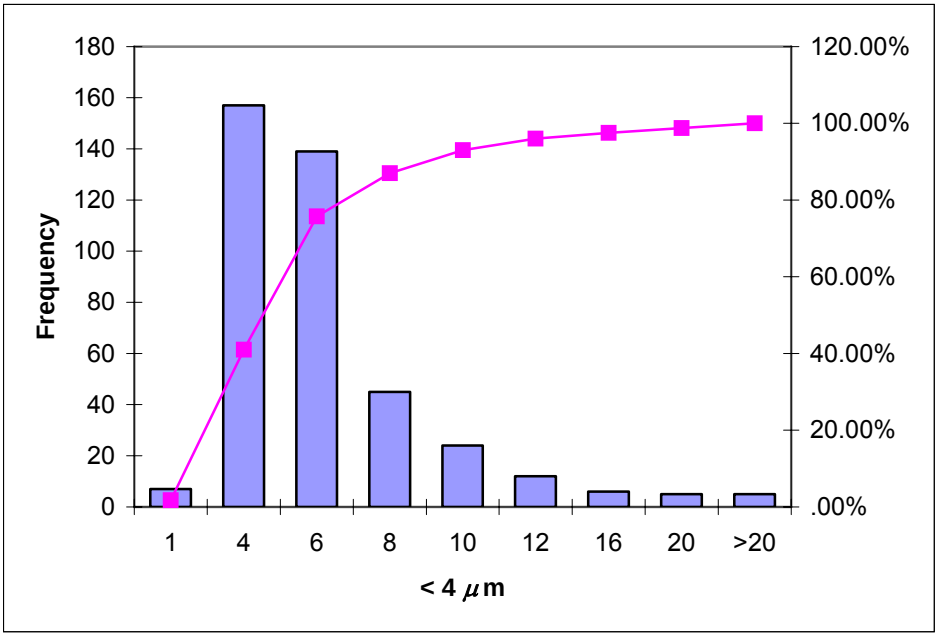

Figure 4.8: Particle size distribution of the < 4 μm fraction of soil samples from the study area

Several populations could be deducted from the histogram depicting the wt % of the clay fraction contained in the soil samples (Figure 4.8). This indicates that the wt % distribution of the clay fraction was not spatially distinct in the contoured and non contoured maps presented in Figures 4.9 and 4.10 compared to the < 53 μm fraction of soil samples. Forty different wt % classes are presented for the < 4 μm fraction of the soil samples indicating their spatial distribution. The colours reflected as bluish, reddish and yellowish colours, and a minor phase of greenish coloration were spatially inter mingled. The < 4 μm fraction of the soil particles were classified from 1.4 wt % to > 12.7 wt % with colour gradation changing from blue for the less clayey soils progressively to green, yellow,

brown, red and pink for the most clayey soils in the study site (Figures 4.9 and 4.10).

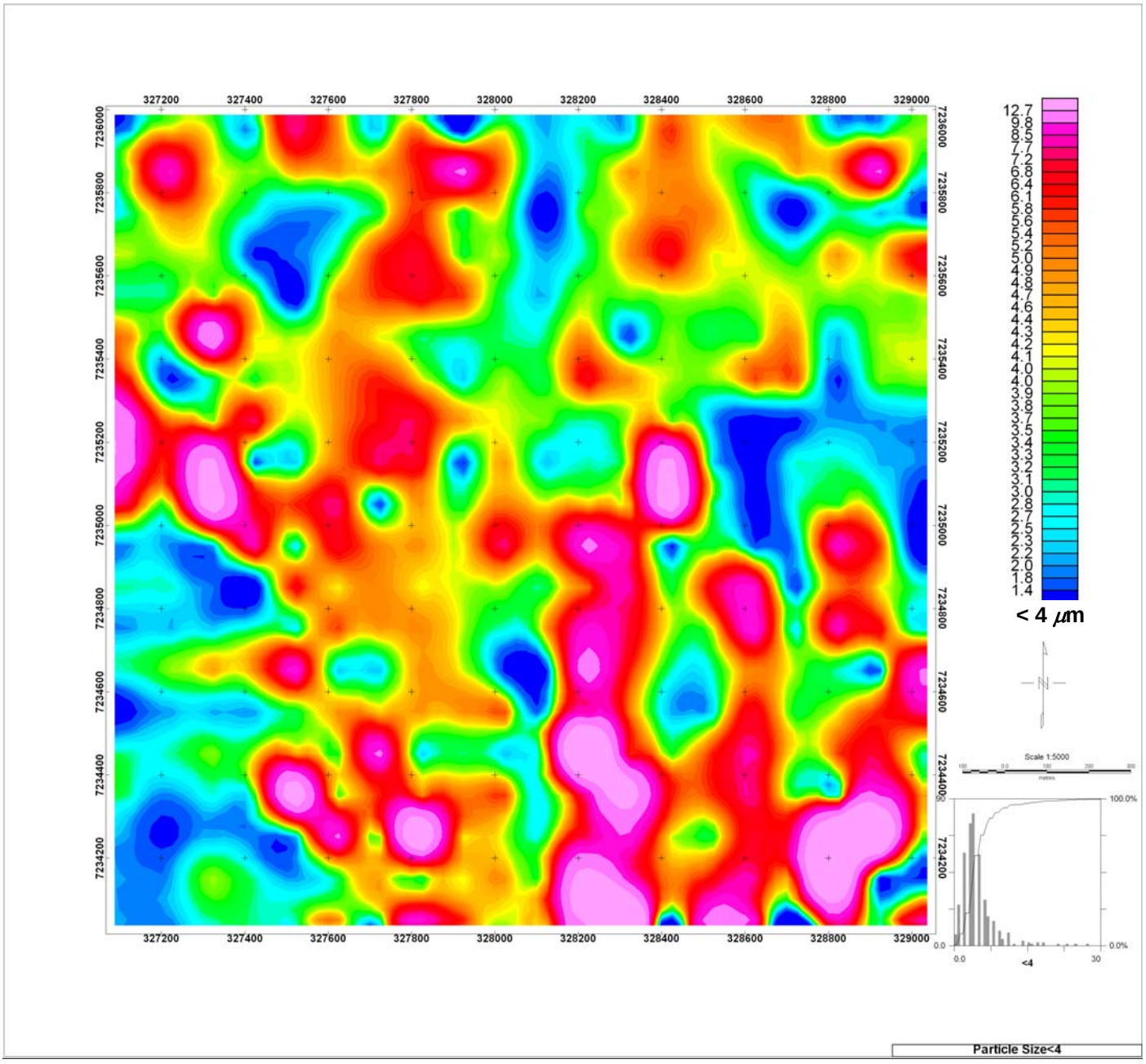

Figure 4.9: Non contoured map of the particle size distribution of the < 4 μm fraction of soil samples from the study area

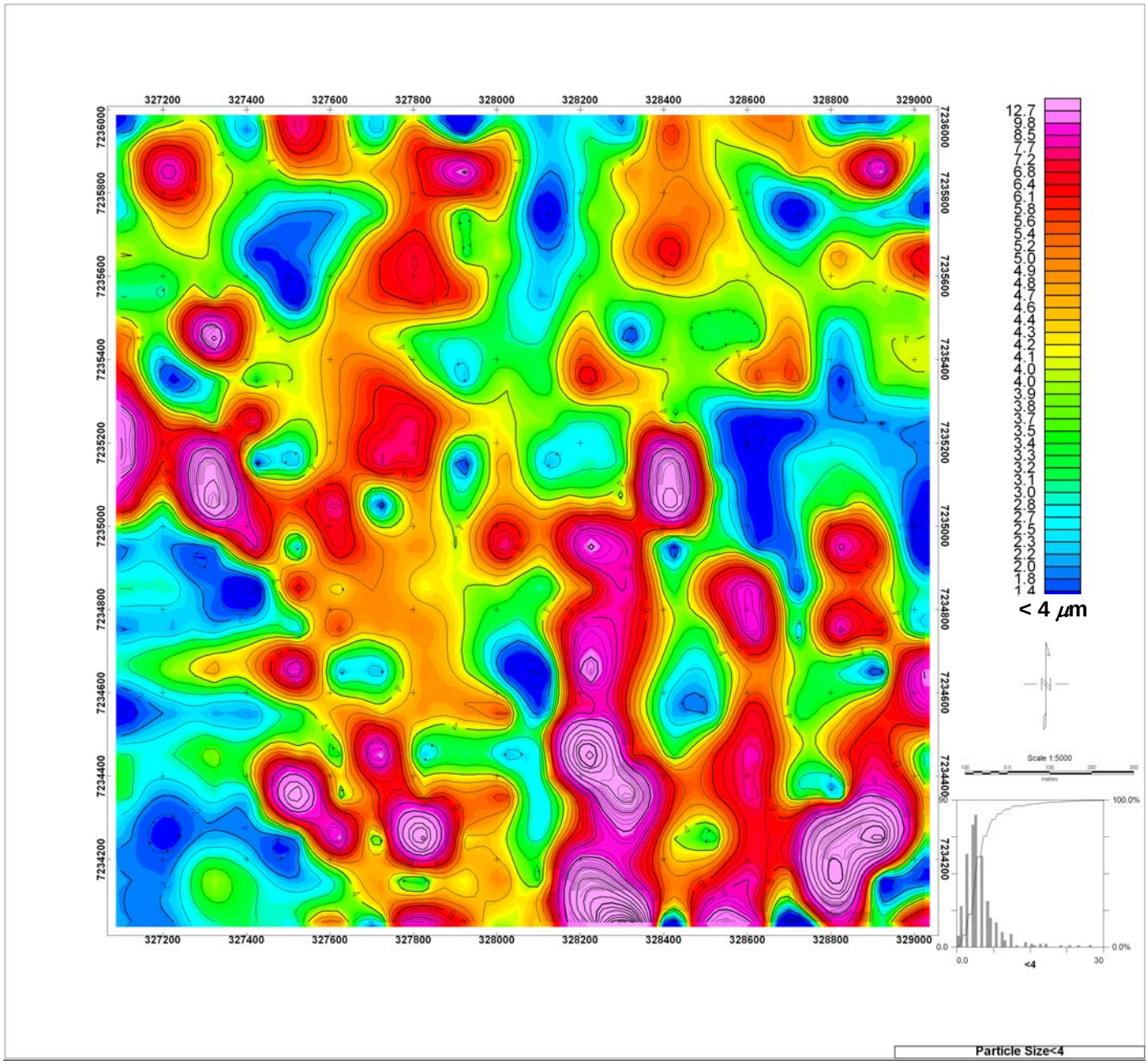

Figure 4.10: Contoured map of the particle size distribution of the < 4 μm fraction of soil samples from the study area

Particle size has a direct bearing on pollution. It is one of the major factors controlling both air pollution and the rate of chemical weathering. Manganese has been identified to be one of the constituents present in the atmosphere as particulate air matter (PAM) (International Program on Chemical Safety, 1981). About 80 % of Mn in PAM is < 5 μm in size and are of respirable range. In this regard, the PSD of the soils in the study area, having up to 13 wt % which is < 4 μm, favours the airborne distribution of Mn particles.

The smaller the particles, the higher the ratio of the surface area to the volume. Smaller particles easily get eroded compared to larger ones. However, there are other factors such as climate (water and temperature), time (duration) and parent material which influence the rate of physical and chemical weathering such as particle size reduction and release of ions.

The particle size distribution observed at the Kgwakgwe Mn oxide mine environment created equal opportunity for ions of heavy metals and especially those of Fe and Mn to migrate and adhere to the < 4 μm fraction of soil (clay fraction); thereby promoting soil contamination trends. Distance of source of contaminant may have played an important role in determining quantitative aspects of the contamination of the soils by Fe and Mn ions.

4.2.2 Soil pH

The pH values ranged from 2.92 to 7.26 and are plotted in the histogram as shown in Figure 4.11. The values are distributed in a staggered plot with pH of 3, 4, 5, 6 and 7. The pH 5 is the most dominant one showing in 233 samples, followed by pH 6 with about 100 samples.

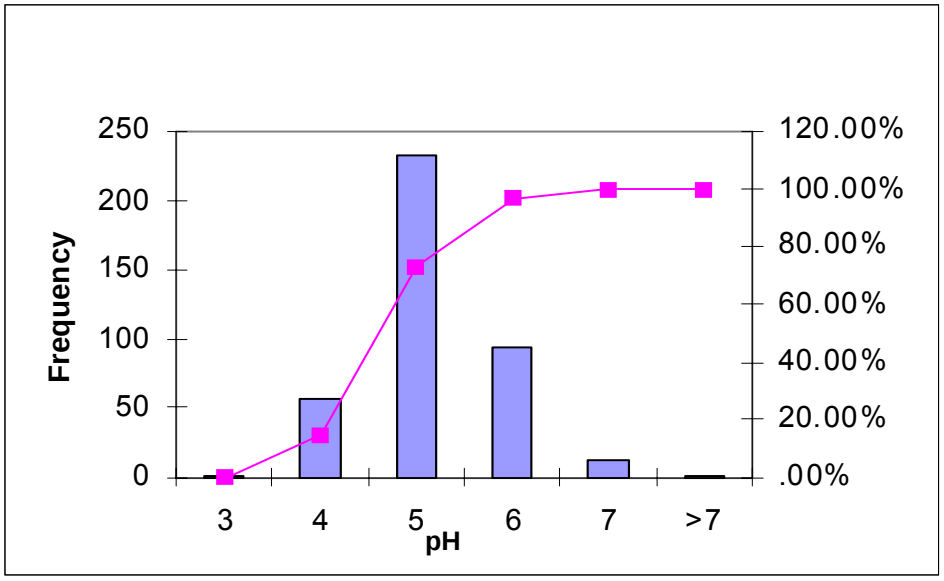

Figure 4.11: The pH values of soil samples from the study area

The colours reflected in the maps presented in Figures 4.12 and 4.13 as bluish, greenish, yellowish, brownish and reddish colour shades were spatially inter mingled and depicted prograded pH values. Colour gradation in the non contoured and contoured maps (Figures 4.12 and 4.13), is reflected from blue for

the low soil pH values progressively to green, yellow, brown, red and pink for the high soil pH values in the study site.

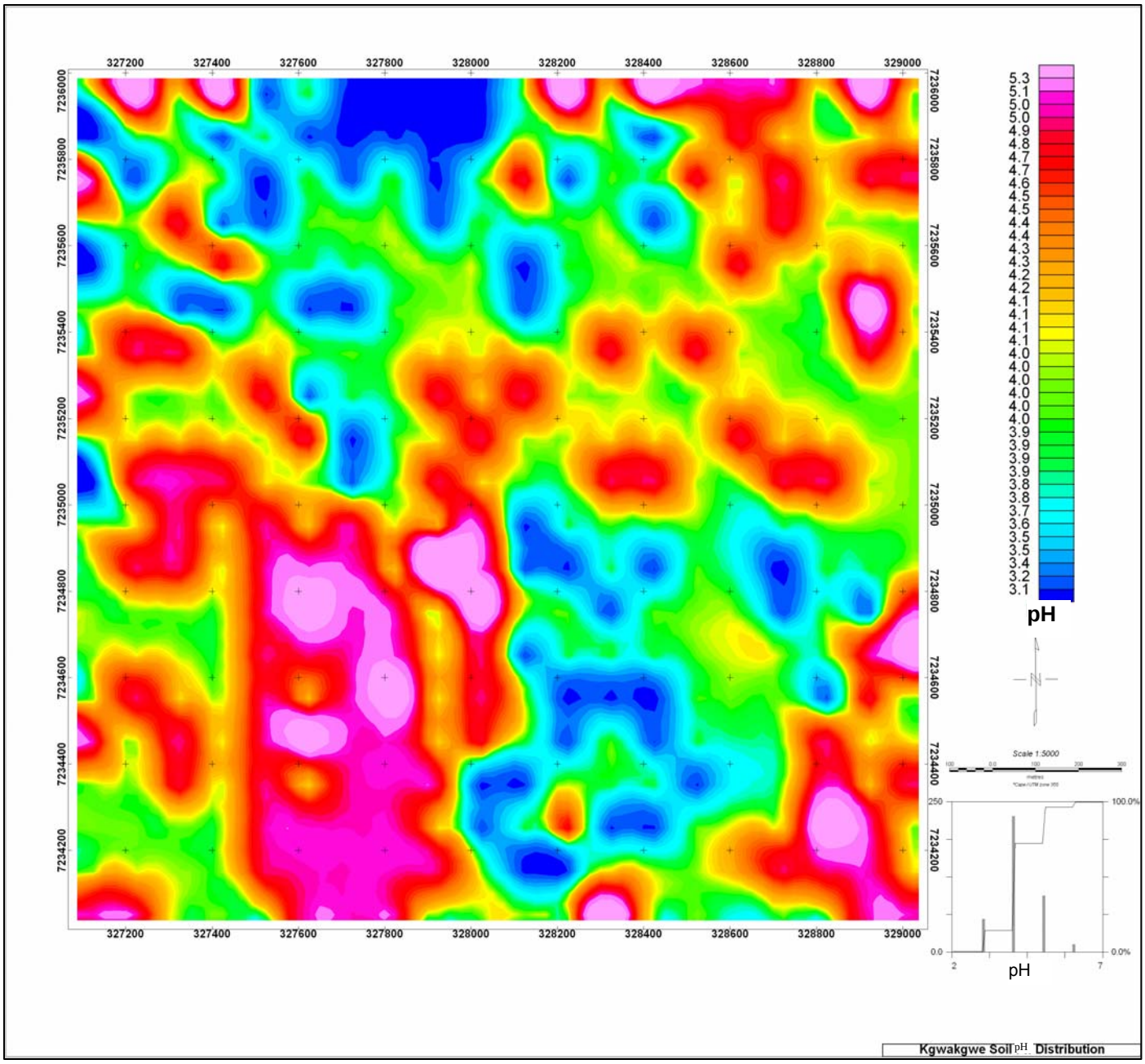

Figure 4.12: Non contoured map of spatial distribution of the soil pH in the study area

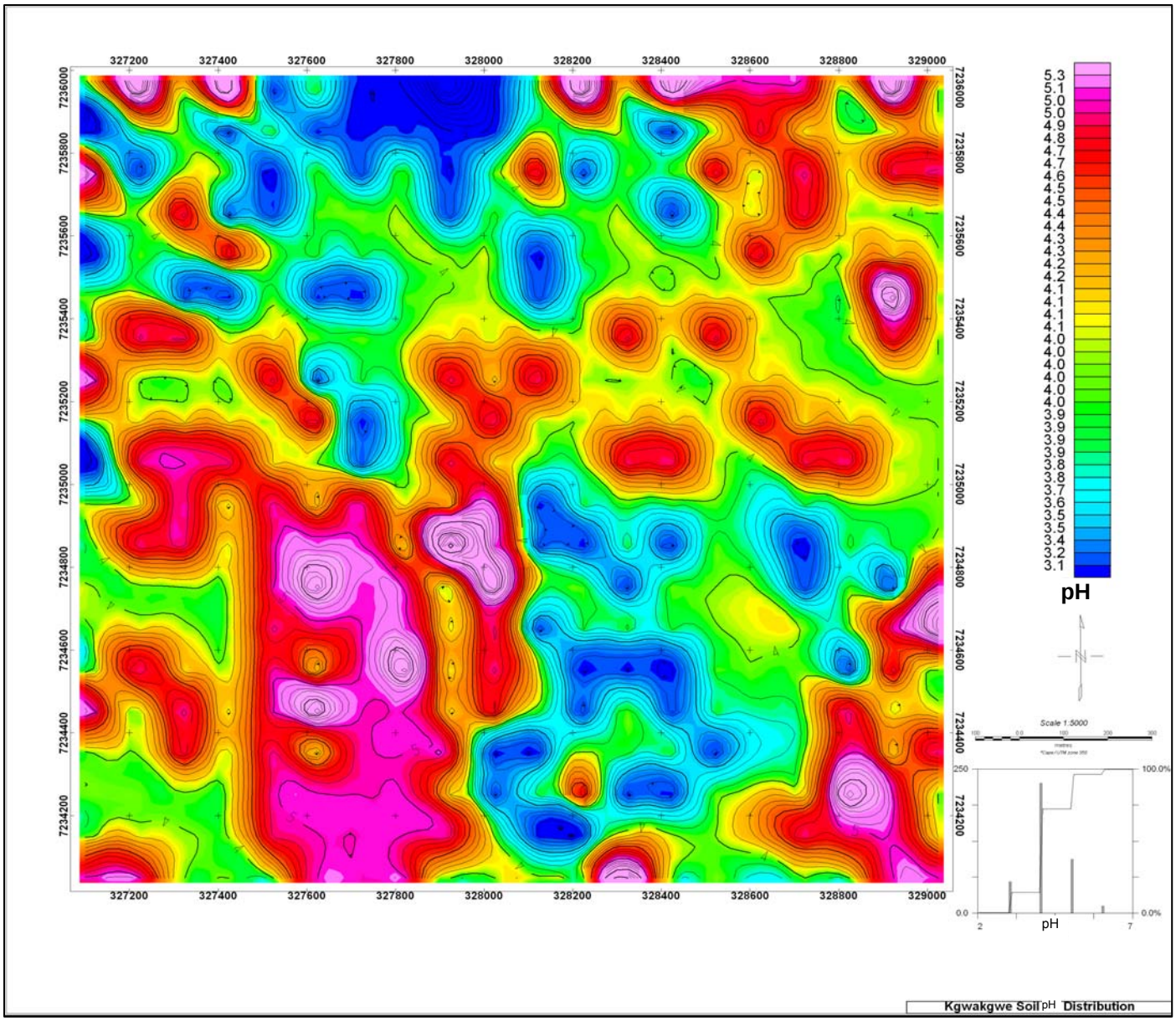

Figure 4.13: Contoured map of spatial distribution of the soil pH in the study area

The medium to high pH values were prominent in the southwestern part of the study area to the west of the mine workings whereas the low to medium pH values were observed in soil samples located further away from the mine

workings as depicted on the non contoured and contoured maps in Figures 4.12 and 4.13 respectively. However low to medium pH values were also observed at sites considered to be more affected with Mn contamination. Low pH values at these sites could be attributed to their closeness to the mine workings and areas of topographic lows.

According to Bowles *et. al.* (1992), very high concentrations of Fe and Mn ions increase soil acidity in the environment and there is the tendency of acid expansion due to probable depletion of the neutralising capacity of the soils (Shaw *et. al*., 1998). Eventually soil pH could drop as the surrounding soil acidity increases within the environment. According to Fouche (1979), acid cations such as $Fe(OH)^{+2}$ form complexes with organic materials. The high acidity in mining environments could influence the leaching of Ca and Mg ions caused by Fe/Mn replacement from the mine workings and Mn oxides ore bodies to the soils as illustrated in equation 4.2 below.

$$\begin{bmatrix} -Ca \\ \\ -Mg \end{bmatrix} + Fe^{++} \\ Mn^{++} \rightarrow \begin{bmatrix} -Fe \\ \\ -Mn \end{bmatrix} + Ca, Mg \downarrow \text{Leached}$$

4.2.3 Electrical conductivity of soil

The EC values obtained were significantly low and ranged from 49.1 μScm^{-1} to 123.5 μScm^{-1}as shown in the histogram in Figure 4.14. There are about 300

samples in the 120 μScm^{-1} range. These samples are distributed in the mine working areas and the western side of the study area. The colours reflected in the maps presented in Figures 4.15 and 4.16 as bluish, greenish, yellowish, brownish and reddish colour shades were unevenly spatially distributed and depicted prograded EC values. Colour gradation in the non contoured and contoured maps (Figures 4.15 and 4.16), is reflected from blue for the low soil EC values progressively to green, yellow, brown, red and pink for the high soil EC values in the study site.

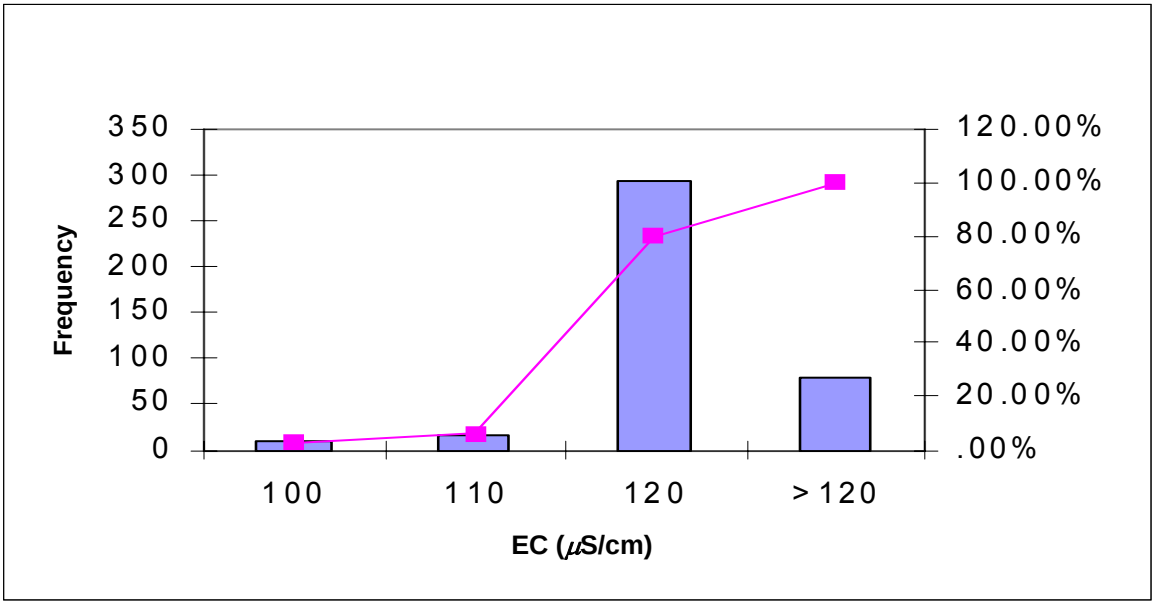

Figure 4.14: The electrical conductivity values of soil samples from the study area

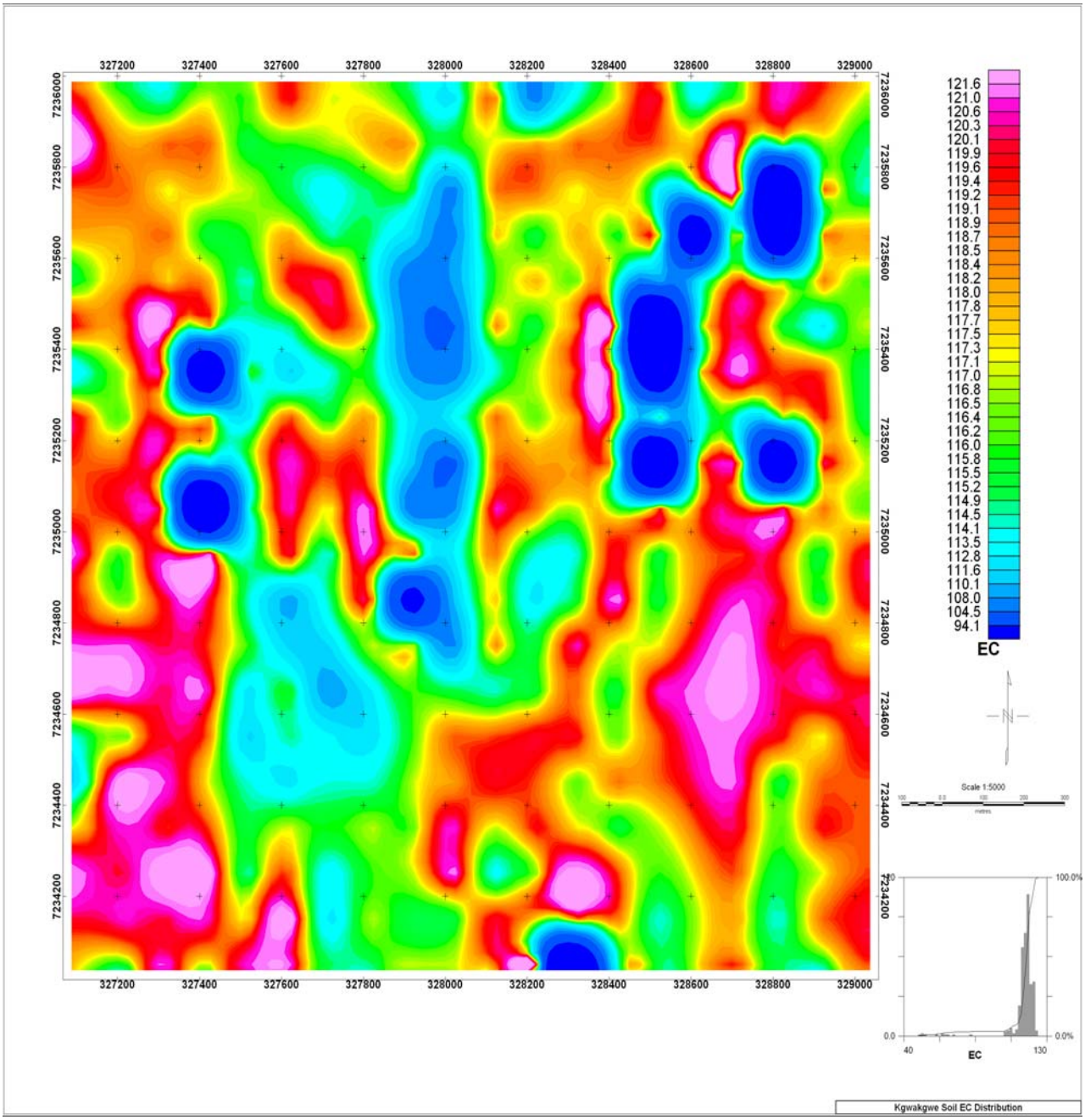

Figure 4.15: Non contoured map of spatial distribution of the electrical conductivity of soils in the study area

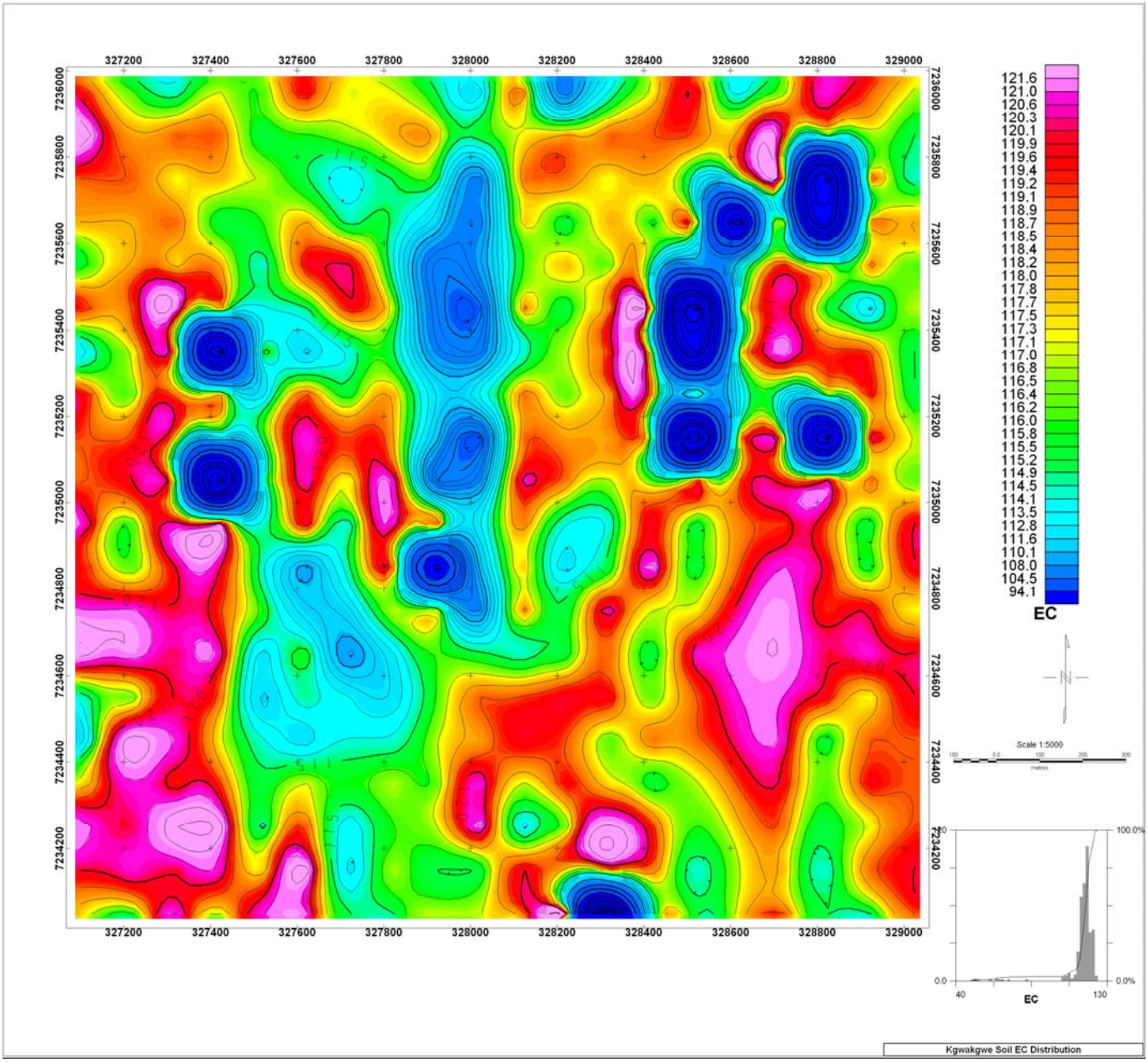

Figure 4.16: Contoured map of spatial distribution of the electrical conductivity of soils in the study area

The scatter plot of pH and EC values presented in Figure 4.17 depicts an *s* shape with two distinct populations. It further reveals that the high EC is

displayed by the higher pH samples. The higher the pH, the higher the EC and vice versa. There is a correlation factor of 0.62 between pH and EC. Acid soils had EC values at 120 μScm^{-1}. Results from the determination of the anions in the soils indicated the presence of SO_4^{2-}, CO_3^{2-}, Cl^-, and PO_4^{2}. Dissolved salts of SO_4^{2-}, CO_3^{2-}, Cl^-, and PO_4^{2-}, which may be present in solution, could be contributory to the EC status of soils and particularly the clay fraction (Ashton *et. al*., 2001;Murray, 1986; Weaver, 1989).

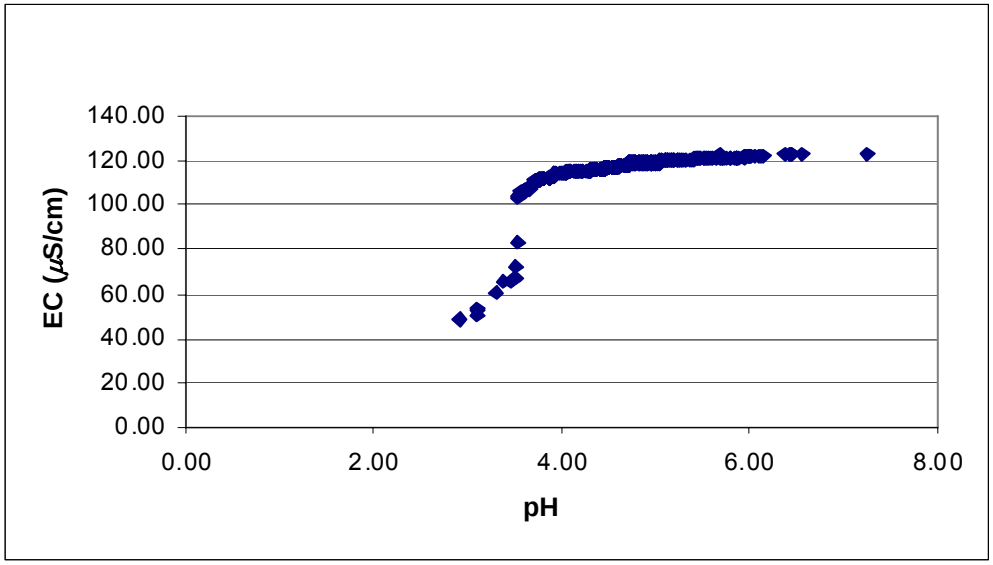

Figure 4.17: Scatter plot of pH versus electrical conductivity of soil samples from the study site

The ions of Mn, Fe and other metals present could constitute the anionic portion of the salts. Because of increase in soil salinity, the clay size fraction of soils easily gets flocculated. Soils close to the small streams in the study area were observed to be clogged. A similar phenomenon has also been reported by

Ashton *et. al*. (2001), of the soils along the Middle and Great Lebata rivers where increasing soil salinity has exacerbated the dispersive characteristics of its soils.

Increase in soil salinity could also be responsible for reduced crop yield due to decreased rates of photosynthesis. According to Ashton *et. al*. (2001), osmotic effects on soil fluids resulting from increasing soil salinity alters the Na: a K ratio which is essential for nutrient transformation processes. Examples within the southern Africa region where increased soil salinity due to mining activities has affected crop yield include middle reaches of the Olifants River downstream of the Witbank and Highveld coalfields, and the middle reaches of the Crocodile River downstream of the Thabazimbi Fe ore mines in South Africa (Ashton *et. al*., 2001).

4.2.4 Soil Colour

Soil colour data was recorded for each sample. A total of 11 colours was observed in this study based on interpretations in the Munsell Soil Colour Book (1992). The colours are yellowish red, red, dark red, brown, reddish brown, dark reddish brown, strong brown, dark reddish grey, very dark grey and light brown. The colours were each given a code and a number. Numbers 1-11 was entered for the soil colours. The number was used to grid the point map in Arcview. The gridded map was then sliced into 11 equal intervals and later colour coded (Figure 4.18).

Colour variation is an influence of changes in mineral and chemical compositions of the soil (Tan, 1996). The colour causing metals held within the structural octahedral sites of the clay size fraction and particularly the clay minerals contained in the soils affect the observed colour of soils (Dixon, 1989). Consequently clay minerals with a lot of octahedral sites taken over by metals such as Fe and Mn contain less structural water (Fellman, 1996), and hence will impart their colours in the soils. The soil colour at Kgwakgwe varied depending on the concentrations of Mn and Fe in the soils, and reflects their contents, which is, contained in the Mn and Fe minerals present in the soils (Ekosse and Modisi, 1999; Nkoma and Ekosse, 1999).

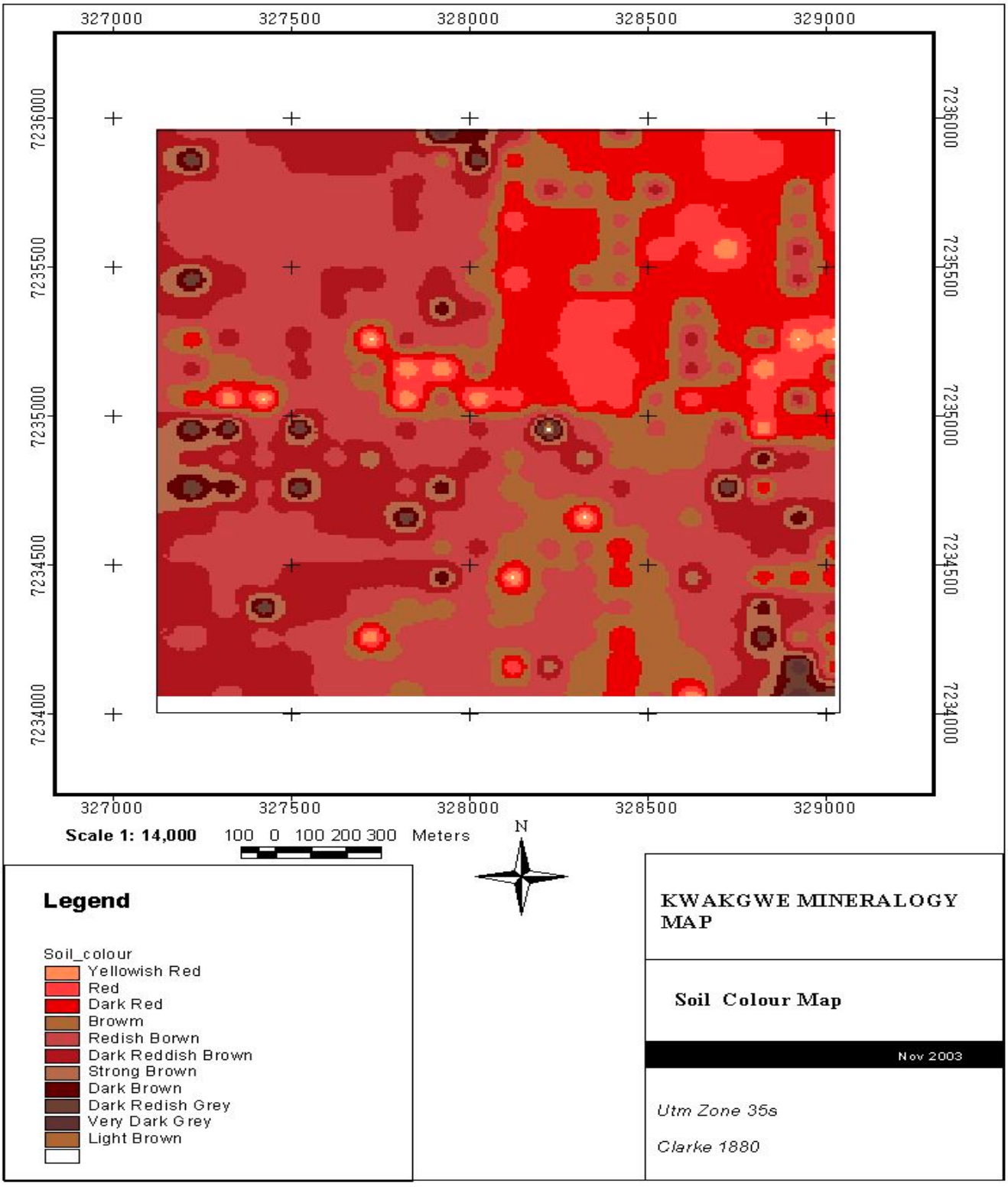

Figure 4.18: Map of spatial distribution of the colour of soils in the study area

4.3 MINERALOGY OF THE STUDY AREA

The results of mineral analyses obtained by XRPD were analysed and plotted into mineral distribution maps. In order to plot the mineral distribution maps, the data was imported into Arc GIS as a DB IV file so as to create point symbol mineral distribution maps. The main aim of .the distribution maps was to use GIS to show location and mineral abundance. Gradational symbols were used to portray the difference in mineral abundance. Each mineral group was plotted in one or two maps and the relations in mineral distribution were analysed. The mineralisation is in distinct zones that are clearly visible on the different maps.

Gridding was used to translate point data into a surface. The value attribute data was interpolated using inverse distance weighting so as to create a surface map for the mineralogy. Inverse distance weighted determines cell values using a linearly weighted combination of a set of sample points. The interpolation was carried out using 8 nearest neighbours to the sample point. The mineral abundances were given quantitative measure (numbers). Values put into the database are; None = 0,Trace = 1,Minor = 2 and Major = 3. The database was then imported into Arcview and gridded maps were made the. These maps were then reclassified into zones of equal area so as to give an output indicating the presence of the minerals. The gridded maps clearly show the mineral zoning and hallows that are found in the area. It is very good for target identification.

Soil samples were mineralogically analysed by XRPD techniques and twelve minerals were identified. Figure 4.19 indicates the number of soil samples containing identified minerals from the study area. The identified minerals were analysed to determine the trace, minor and major distributions of the minerals and the results are reported in Figure 4.20.

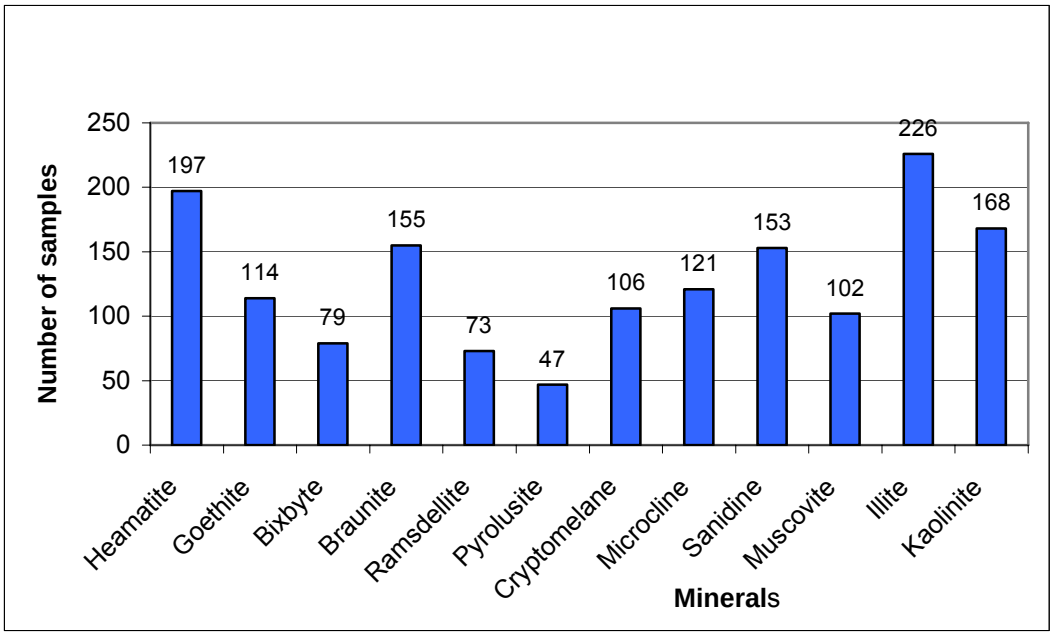

Figure 4.19: Number of samples containing identified minerals in the study area

It can be deducted from Figure 4.20 that illite is the most ubiquitous mineral followed by haematite and then kaolonite, braunite, and sanidine. The other three Mn minerals (pyrolusite, ramsdellite and bixbyte) have the lowest with pyrolusite being the least abundant mineral present in the soils of the study area.

Haematite, Braunite, Crytomelane, Illite and kaolinite occurred in major quantities. Both feldspars are present in mostly trace quantities; goethite, ramsdellite, pyrolusite and muscovite also occur as significant trace quantities. Illite and kaolinite are unique in the sense that they are present in almost equal major and trace quantities.

Haematite is the major iron mineral, braunite and cryptomelane are the major manganese minerals and bixbyte is mainly in minor quantities. Pyrolusite and Ransdellite are mostly trace. The feldspars are also in trace quantities with sanidine being the most predominant one. Illite and kaolinite are the most predominant clays whilst muscovite is mainly found in trace quantities (Figure 4.20).

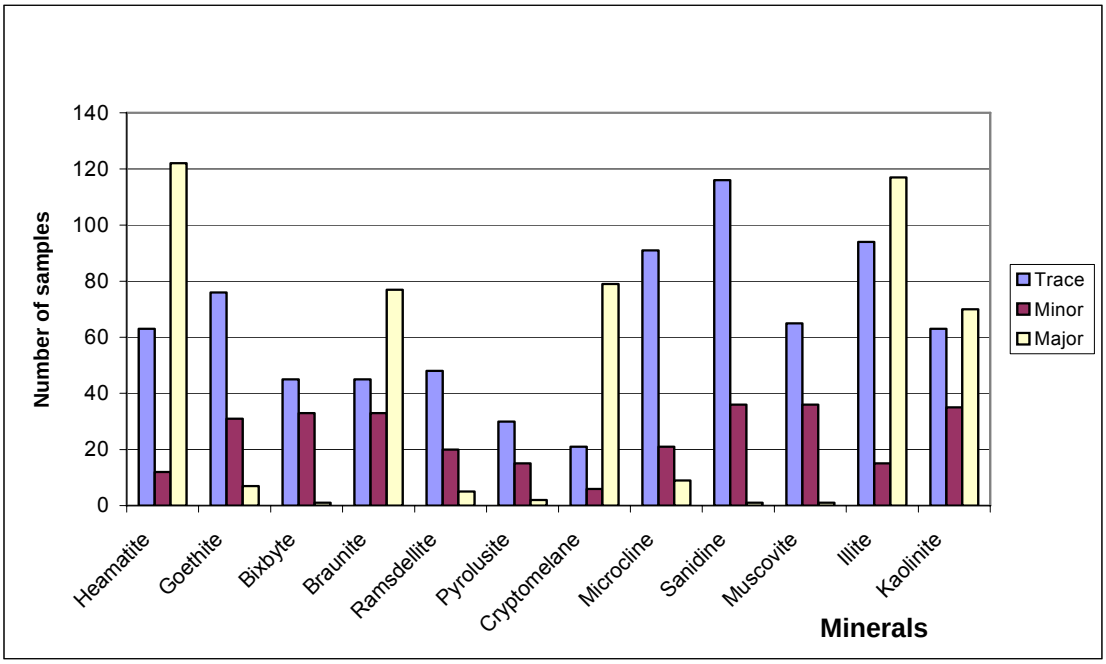

Figure 4.20: Distribution of trace, minor and major concentrations of identified minerals in soil samples from the study area

4.3.1 Distribution of cryptomelane and braunite

Cryptomelane and braunite are found in the two main E-W zone in the northern and central part of the study area as revealed in Figures 4.21 and 4.22 respectively. Traces of braunite are found in the southern part of the area. These two minerals are rarely found in the same sample irrespective of the fact they are in the same zone. Of the 155 samples with braunite only 12 samples overlap with cryptomelane (Figure 4.23). In the gridded maps the area where braunite is show as hallows in the cryptomelane map and vice versa; clearly showing how the minerals are scarcely found together (Figures 4.21 and 4.22).

4.3.2 Distribution of ramsdellite, bixbyte and pyrolusite

Ramsdellite, bixbyite and pyrolusite were plotted individually and the maps are presented in Figures 4.24, 4.25 and 4.26 respectively. Figure 4.27 shows the three minerals plotted together. They are mostly found in trace quantities and are distributed all over the map area. Bixbyite and pyrolusite are both contained in three samples. Whereas ramsdellite and pyrolusite have two samples where they overlap, ramsdellite and bixbyite overlap in eleven samples. Both ramsdelite and pyrolusite are scanty. The gridded maps show hallows that are edged in close to the few samples with pyrolusite scattered all over the study area. The southern part of the study area has these minerals in trace quantities. Minor ramsdellite distribution is found in the central and northern part of the study area. These three minerals are not zoned in the study area so they are found even in the zones where braunite and cryptomelane are not found.

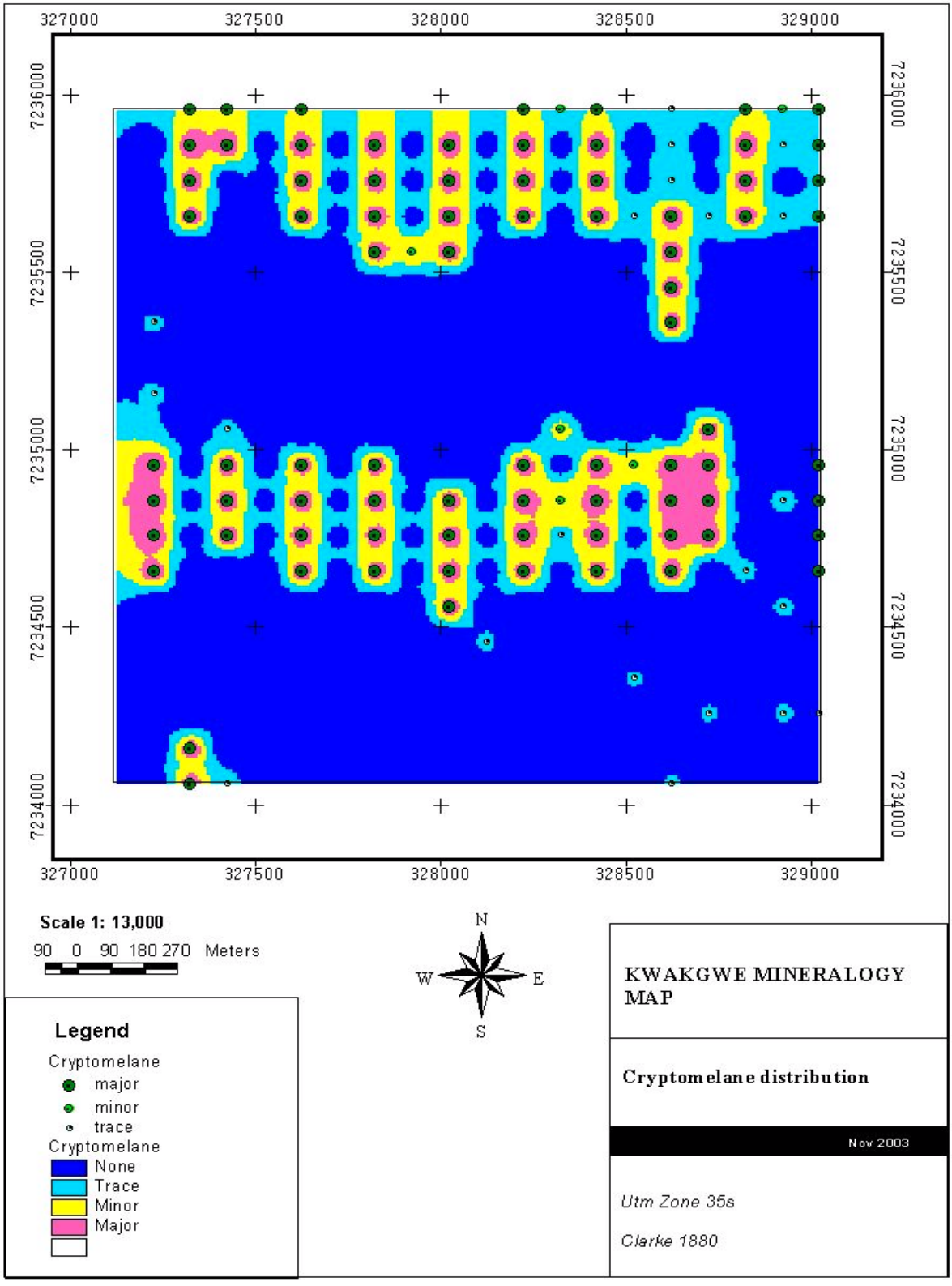

Figure 4.21: Map of cryptomelane distribution in the study area

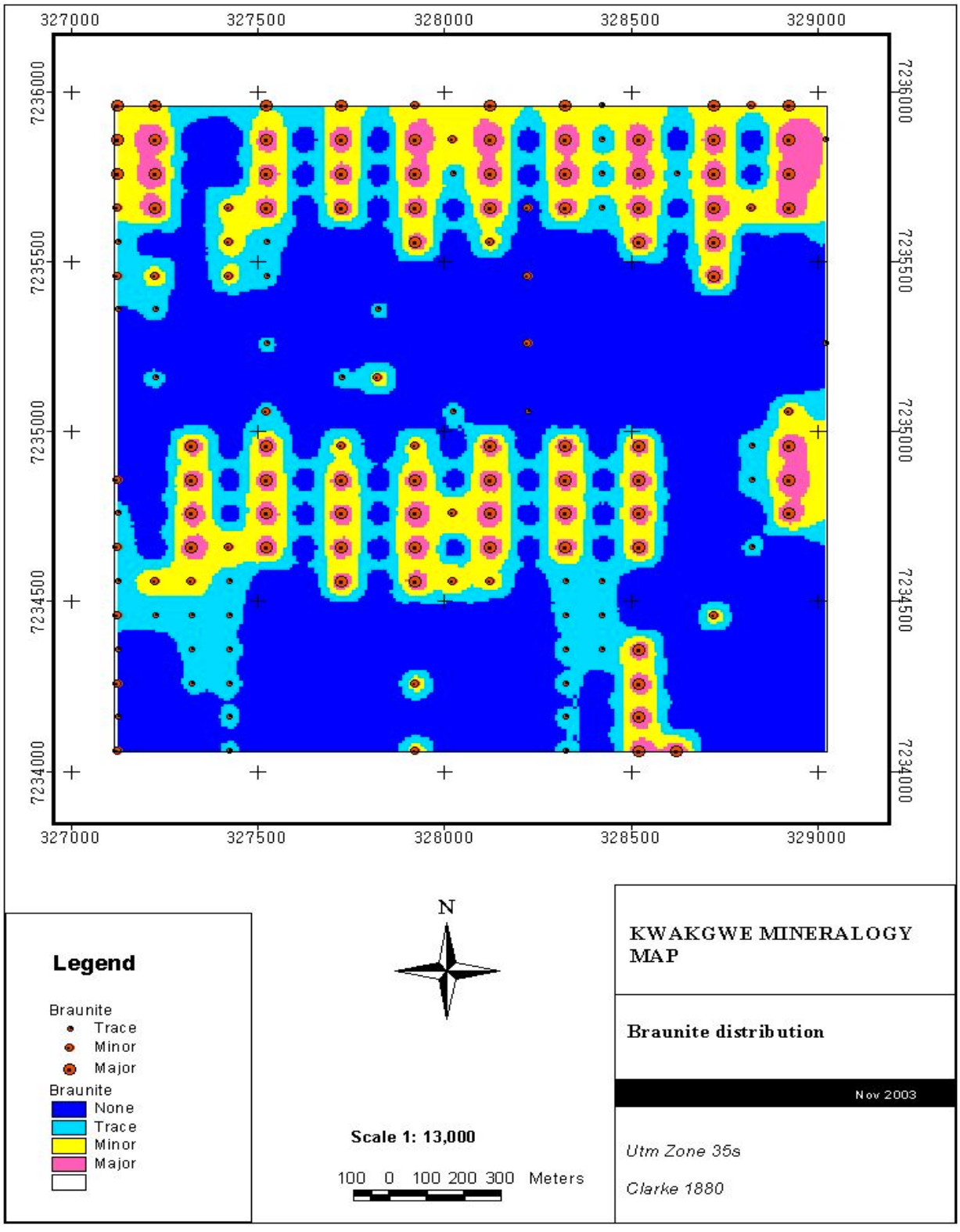

Figure 4.22: Map of braunite distribution in the study area

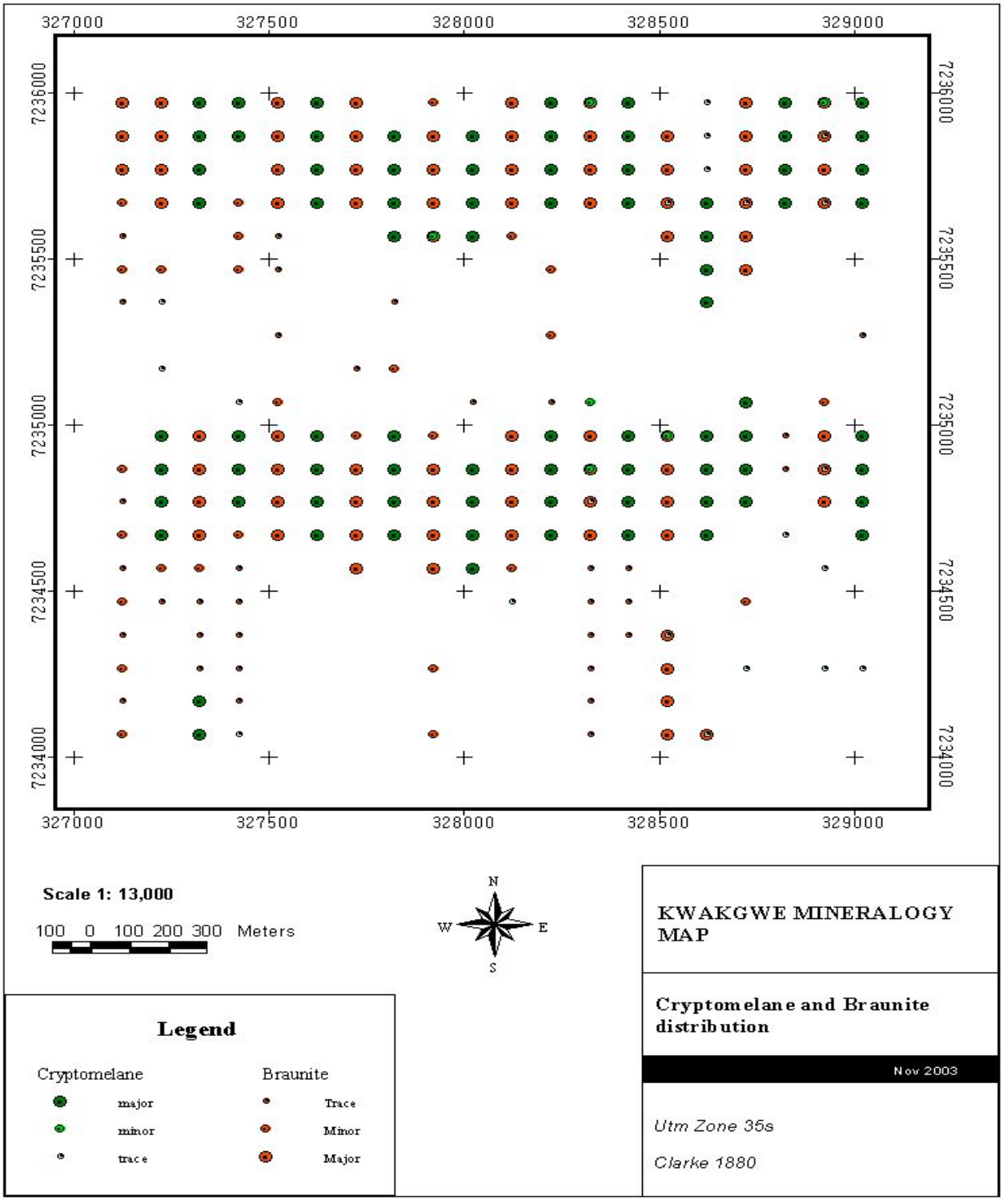

Figure 4.23: Map of cryptomelane and braunite distributions in the study area

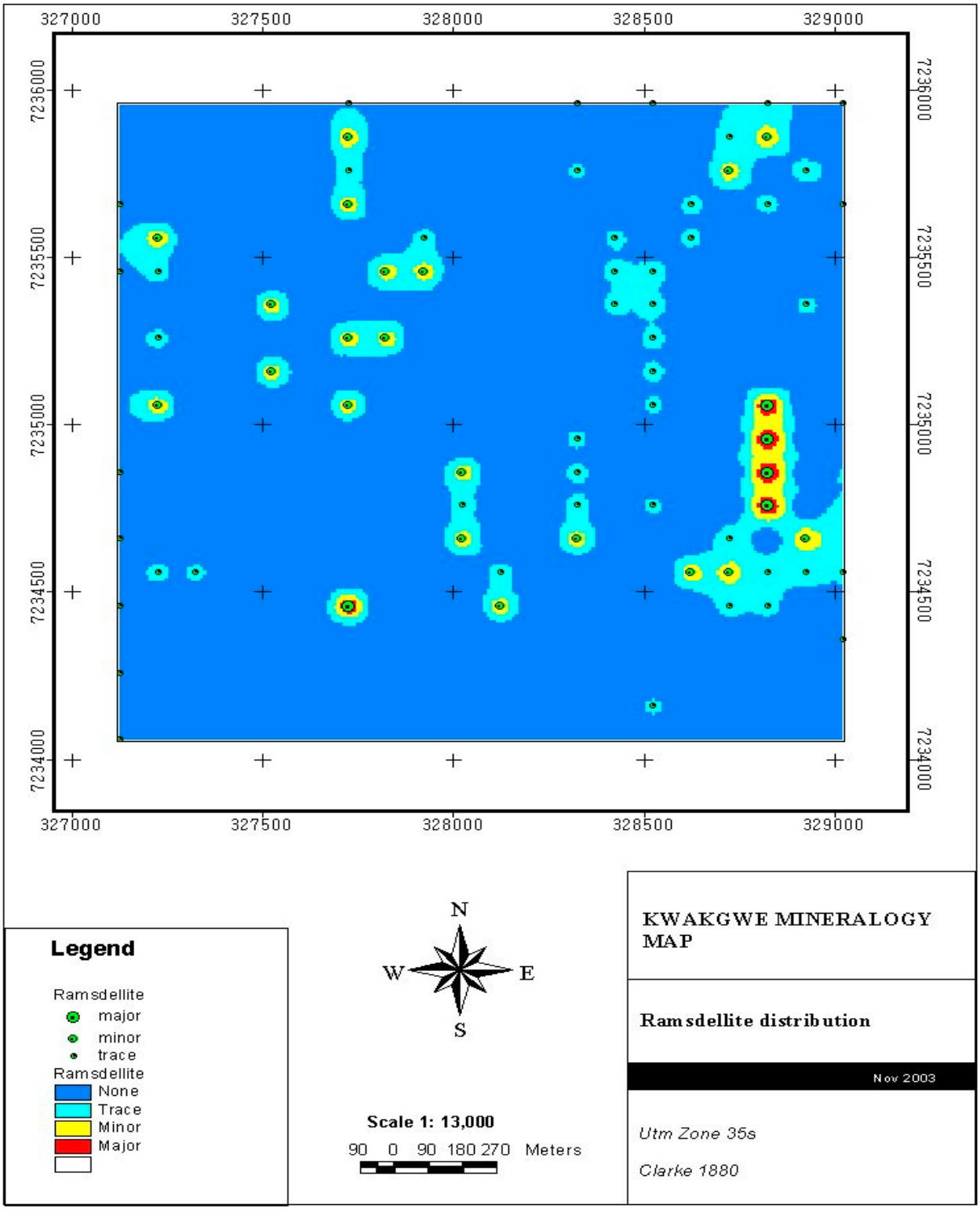

Figure 4.24: Map of ramsdellite distribution in the study area

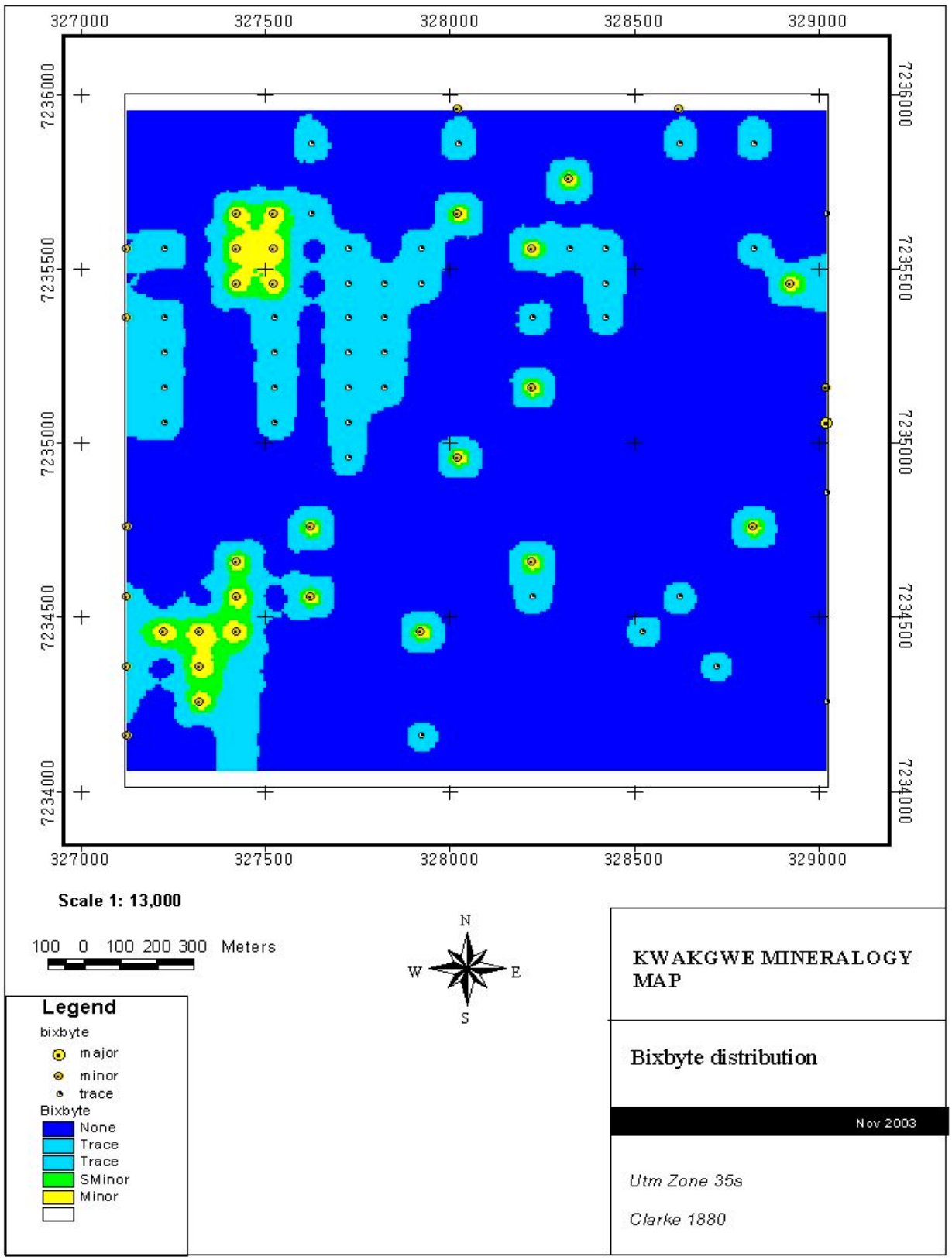

Figure 4.25: Map of bixbyite distribution in the study area

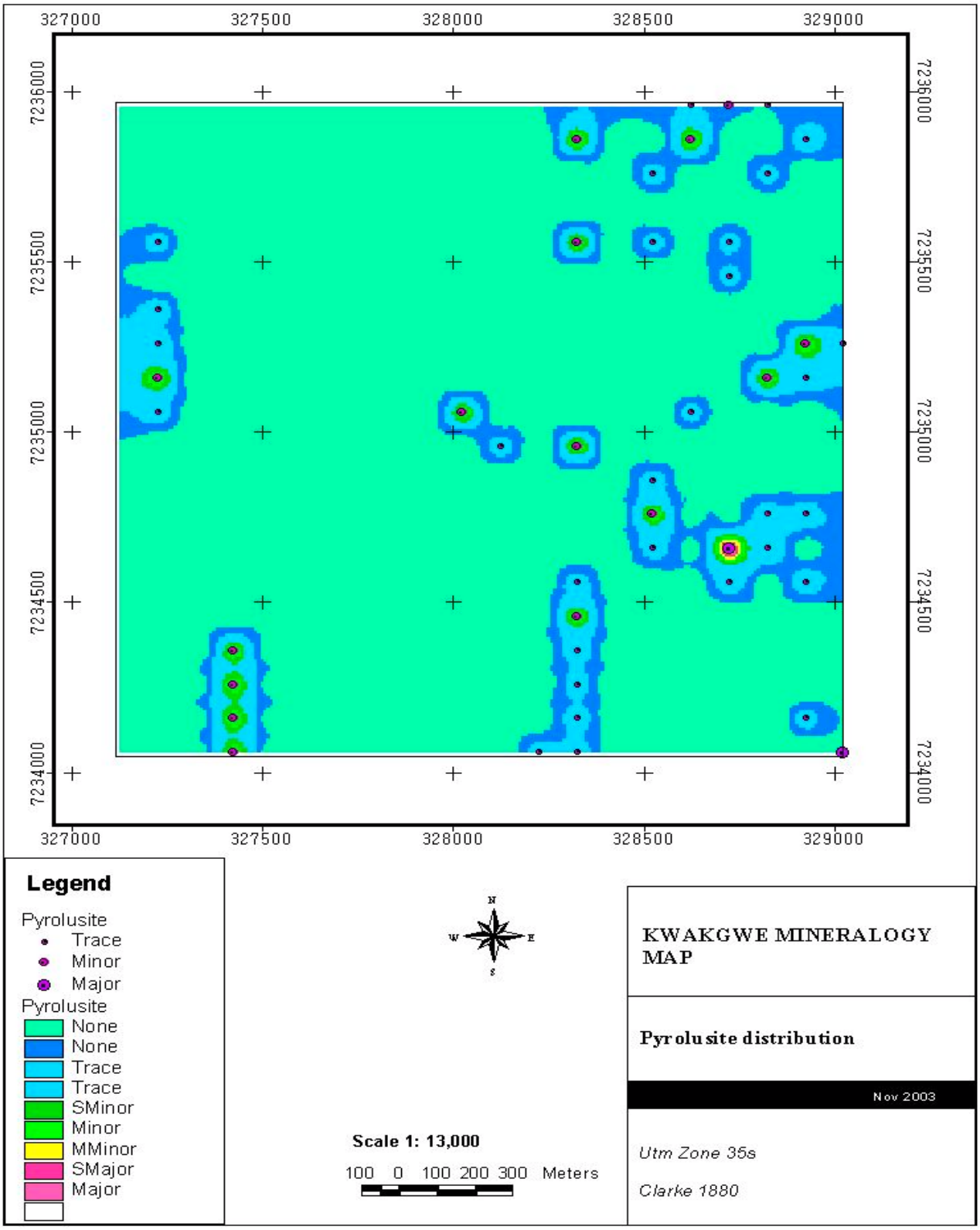

Figure 4.26: Map of pyrolusite distribution in the study area

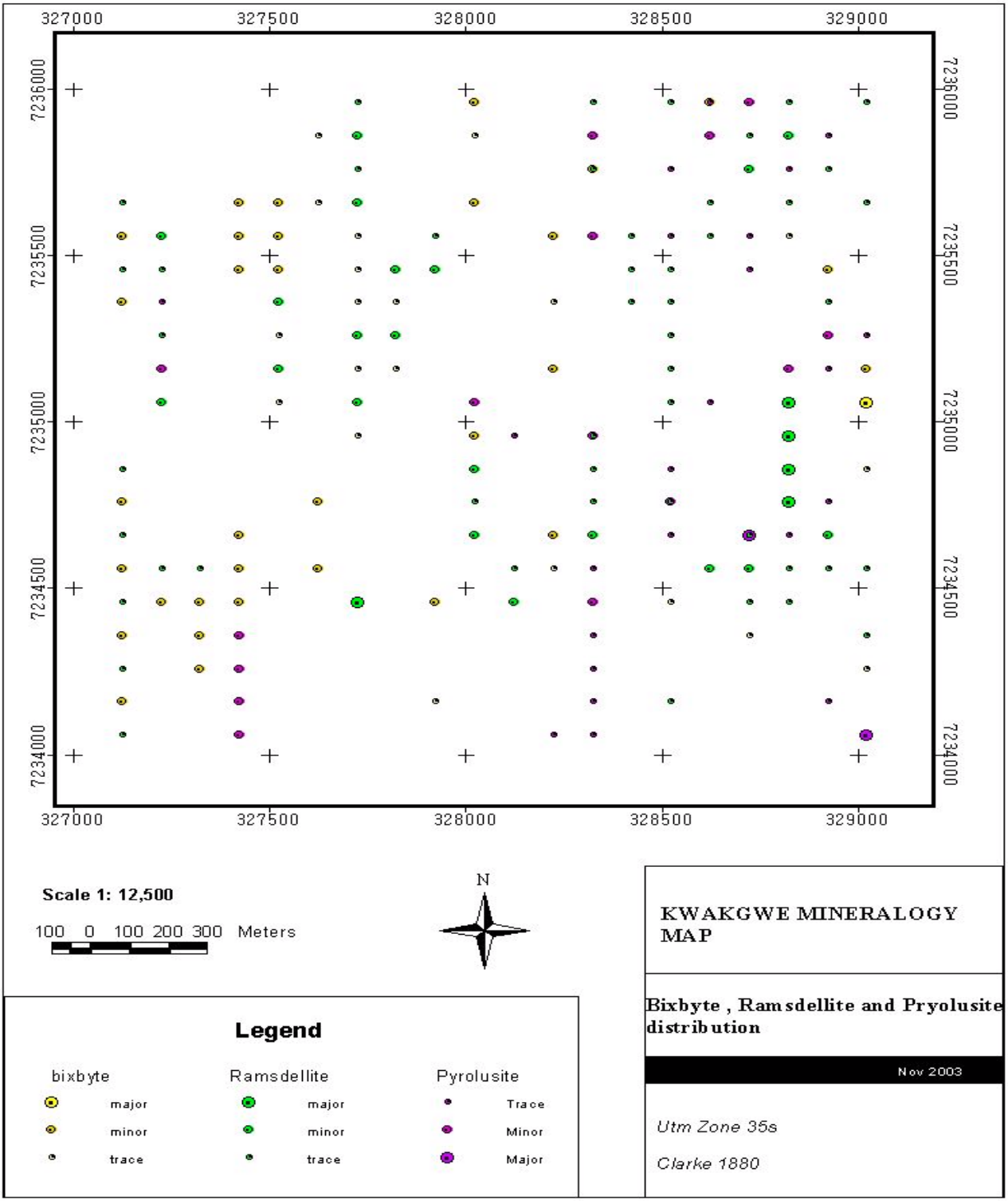

Figure 4.27: Map of ramsdellite, bixbyite and pyrolusite distributions in the study area

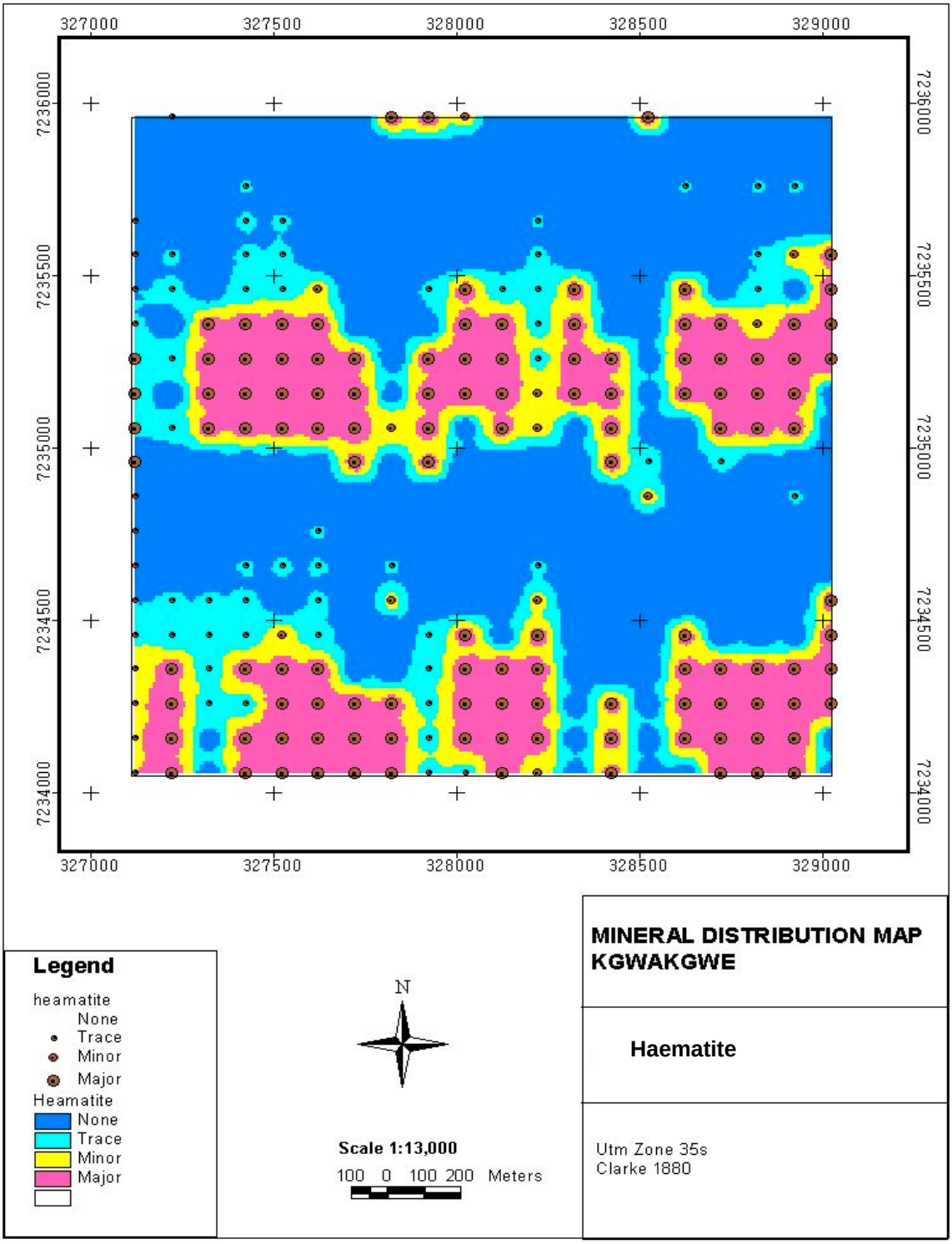

Figure 4.28: Map of haematite distribution in the study area

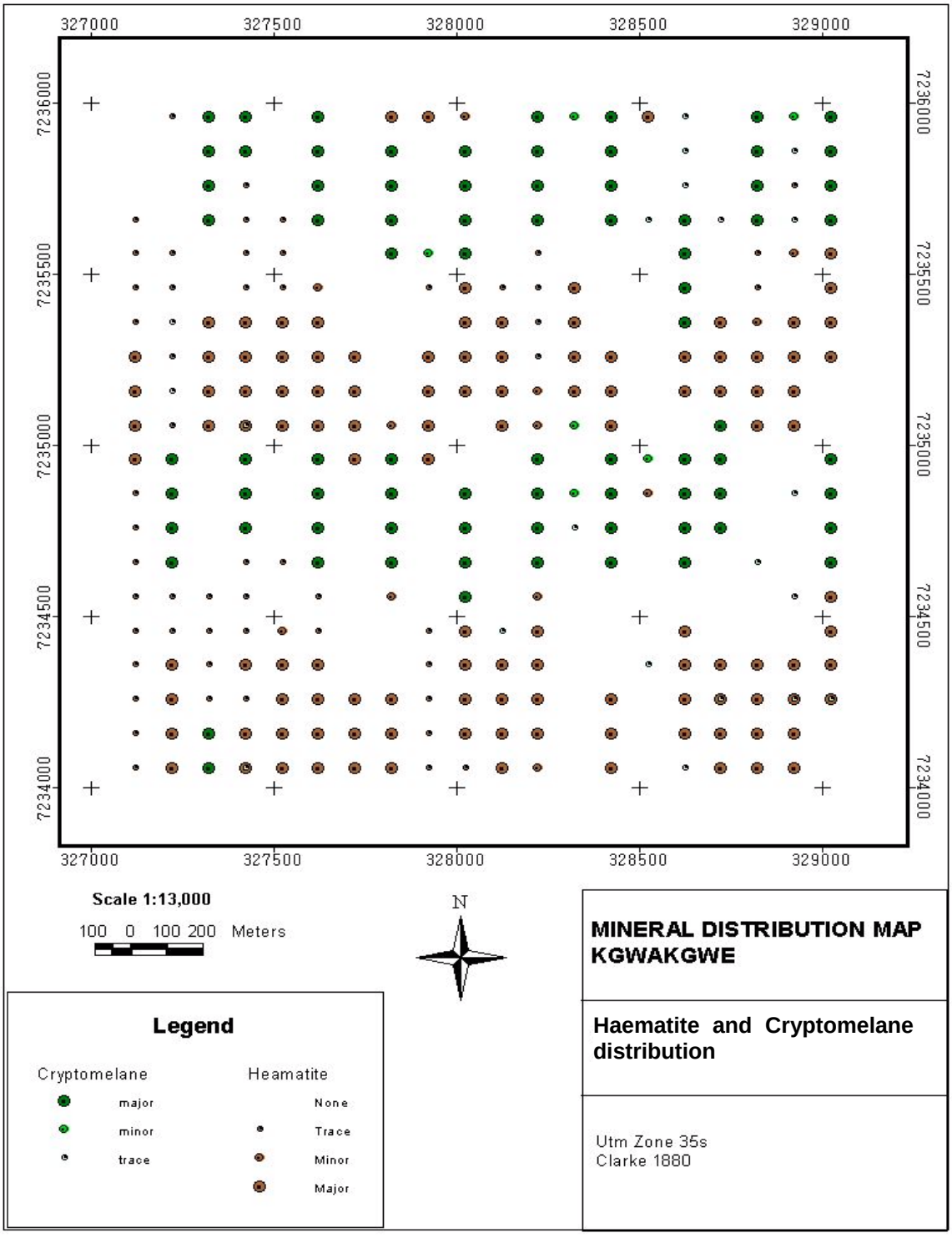

Figure 4.29: Map of haematite and cryptomelane distributions in the study area

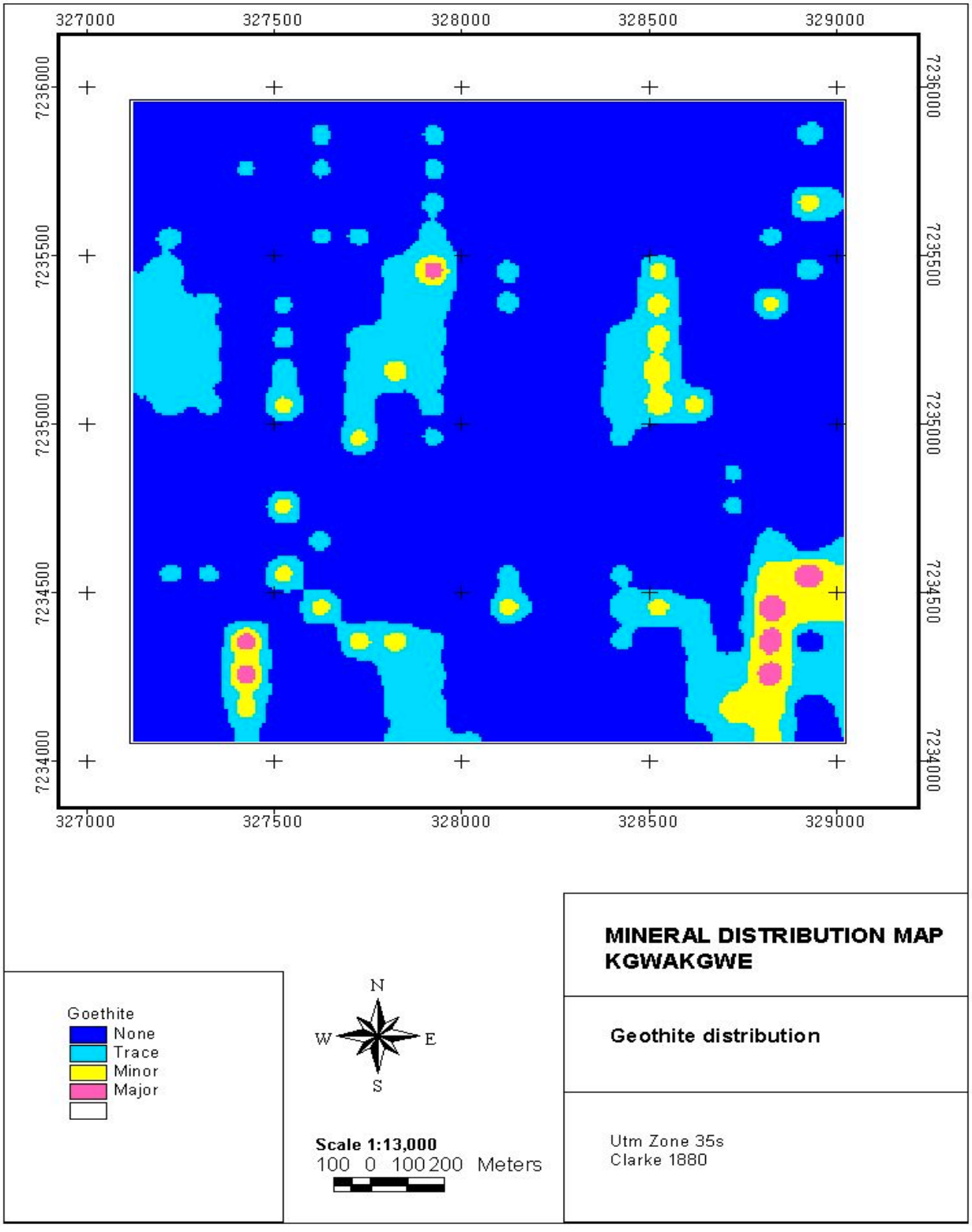

Figure 4.30: Map of goethite distribution in the study area

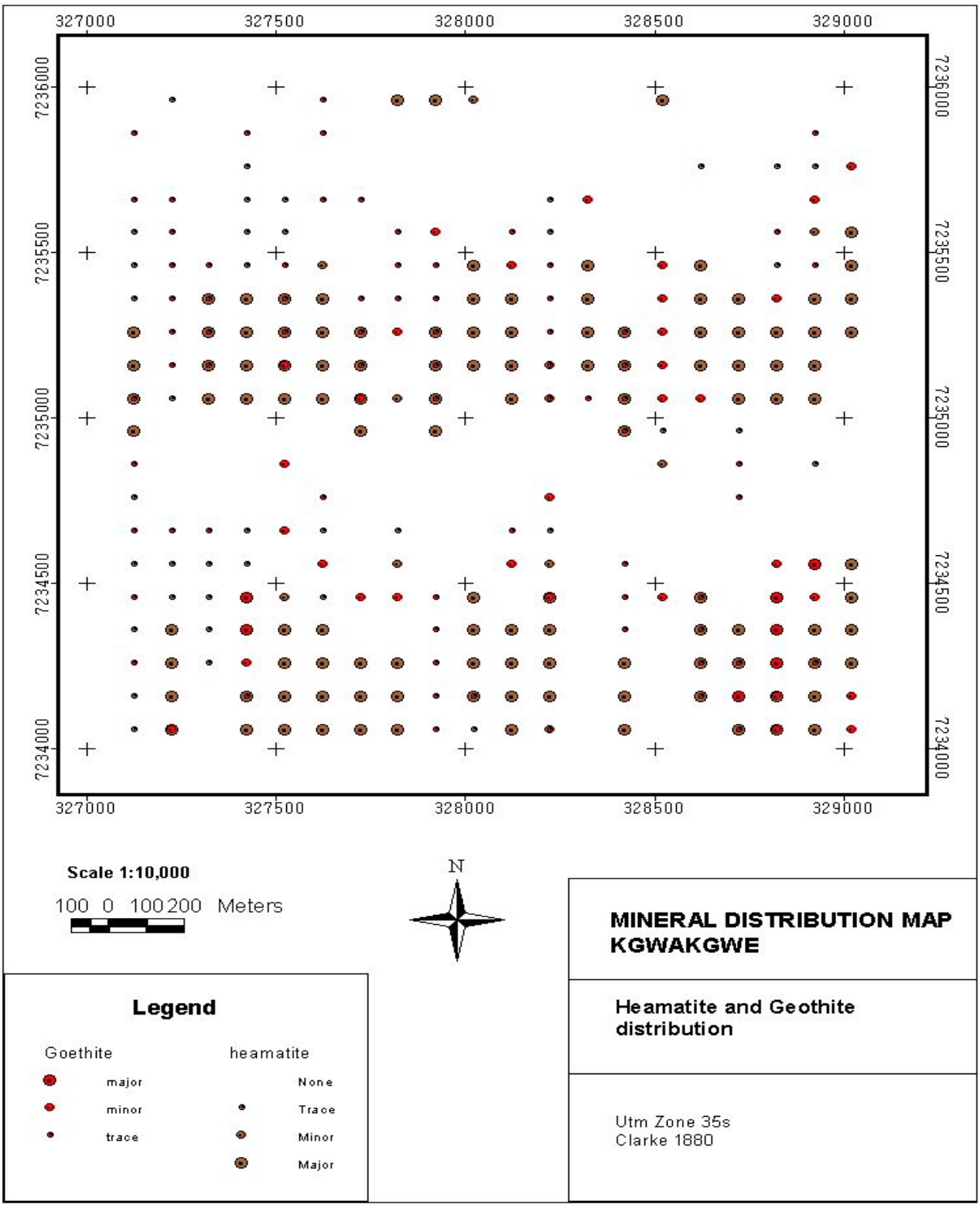

Figure 4.31: Map of haematite and goethite distributions in the study area

4.3.5 Distribution of sanidine and microcline

The feldspar minerals (sanidine and microcline) were plotted individually and the maps are presented in Figures 4.32 and 4.33 respectively. Figure 4.34 shows the two minerals plotted together. The feldspar minerals are present mostly in trace quantities. Sanidine is the most ubiquitous mineral in the study area though in trace quantities. Microcline occurrence in minor quantities is found in the western part of the study area. Microcline distribution is very similar to the distribution of bixbyte. Sanidine is almost evenly distributed in the study area. There are only 11 samples that contain both feldspars.

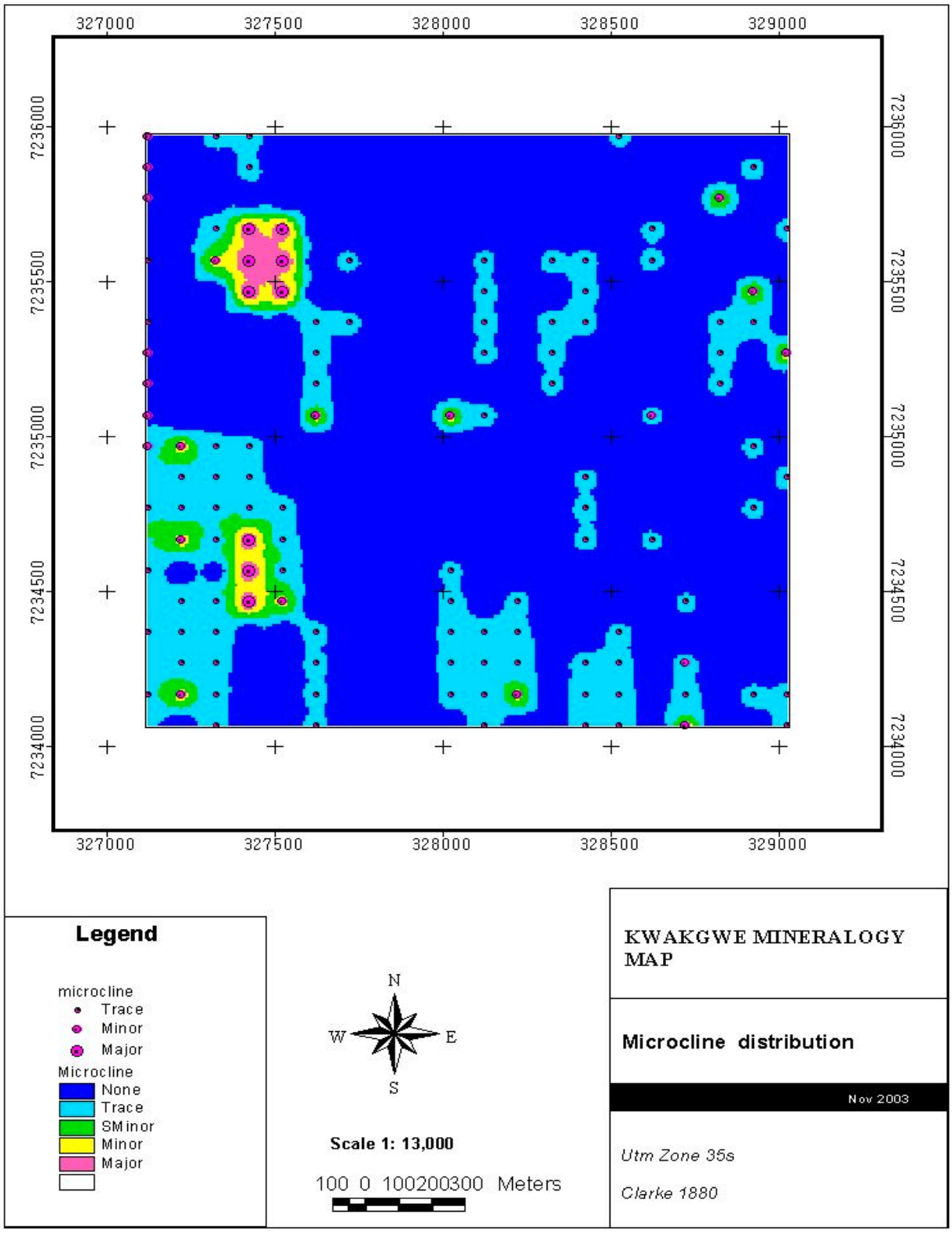

Figure 4.32: Map of microcline distribution in the study area

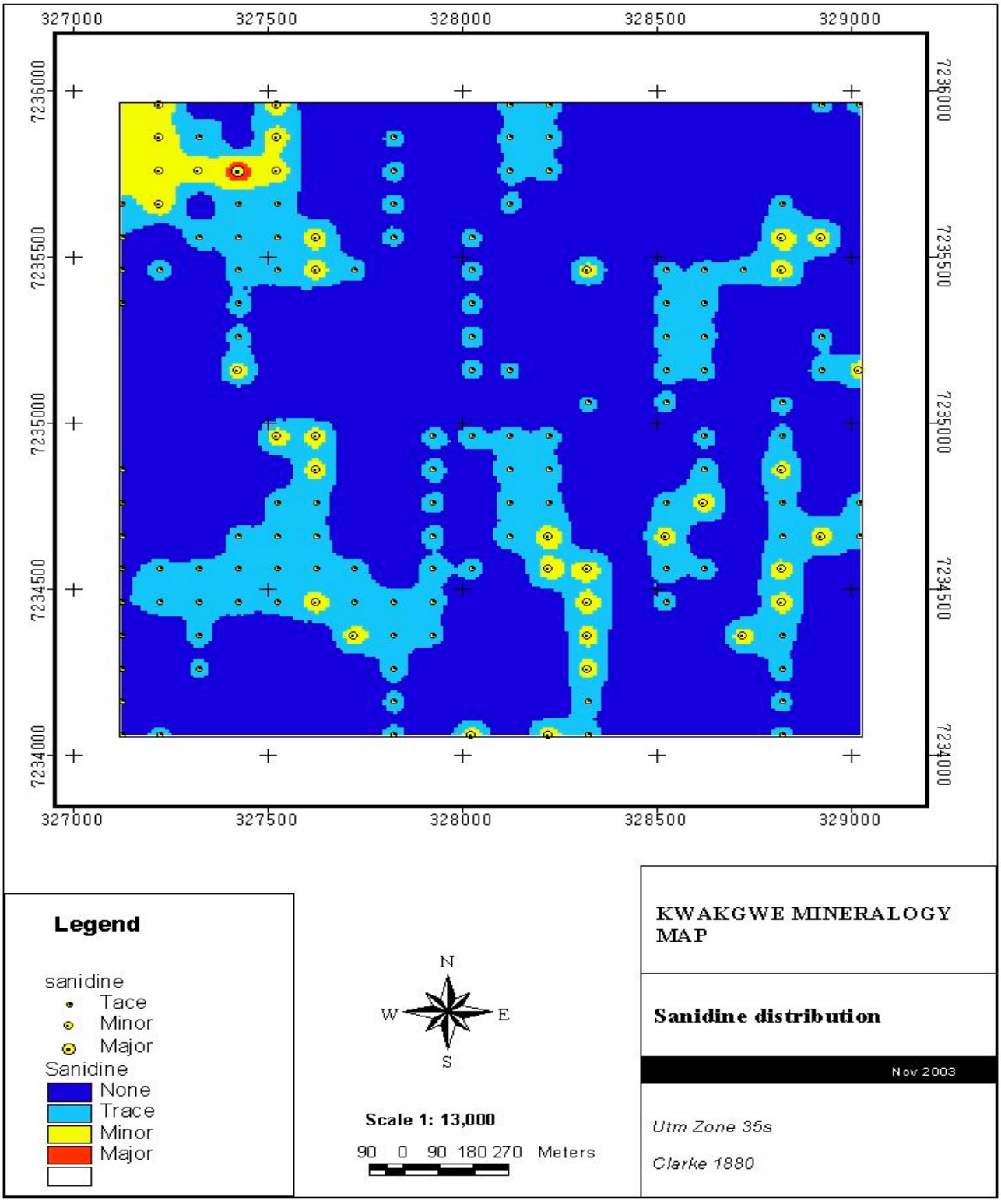

Figure 4.33: Map of sanidine distribution in the study area

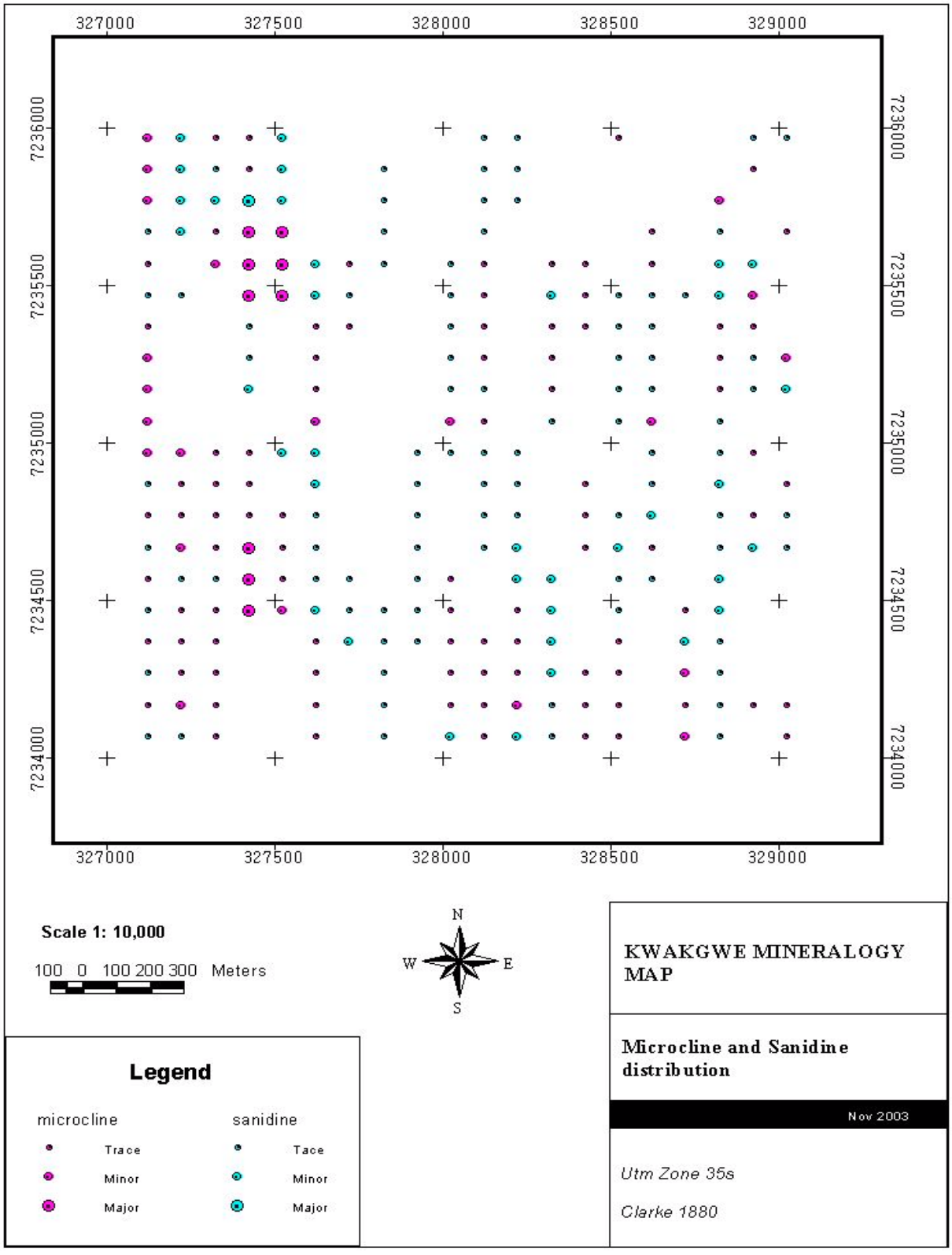

Figure 4.34: Map of sanidine and microcline distributions in the study area

4.3.6 Distribution of clay minerals

The clay minerals identified in the study area are kaolinite, illite and muscovite. Kaolinite, illite and muscovite were plotted individually and the maps are presented in Figures 4.35, 4.36 and 4.37 respectively. Figures 4.38 and 4.39 show kaolinite and illite; and illite, muscovite and kaolinite plotted together. Kaolinite and Illite occur in major quantities in the study area. They are also distributed in distinct E-W tending zones. Illite is found in the zones where there is Fe mineral occurrences, and these are in the central and southern parts of the study area. Kaolinite on the hand is found in the zones of some of the Mn minerals (specifically braunite and cryptomelane) and these are in the central and northern parts of the study area. Muscovite occurs mostly in trace quantities though there are zones in the western part of the study area where it occurs in minor quantities.

The spatial distribution of kaolinite as plotted in the gridded map (Figure 4.35) is very similar to the spatial distribution of the maps for cryptomelane and braunite (Figures 4.21 and 4.22). On the other hand, the spatial distribution of illite as shown in the gridded map (Figure 4.36) is very similar to the spatial distribution of haematite as indicated in the gridded map (Figure 4.28). These distribution patterns could be attributed to the concentrations of the elements and their mineral associations in the different zones of the study area.

Where kaolinite occurs in major quantities, cryptomelane coexists also occurring in major quantities. Furthermore, where kaolinite occurrence is in trace quantities, braunite coexists similarly occurring in trace quantities. In terms of clay minerals overlap, 12 samples were found to contain both kaolinite and illite, 21 samples contain both muscovite and kaolinite, and 12 samples have both muscovite and illite. At the study area, it is more common to find muscovite with kaolinite than to find it with illite.

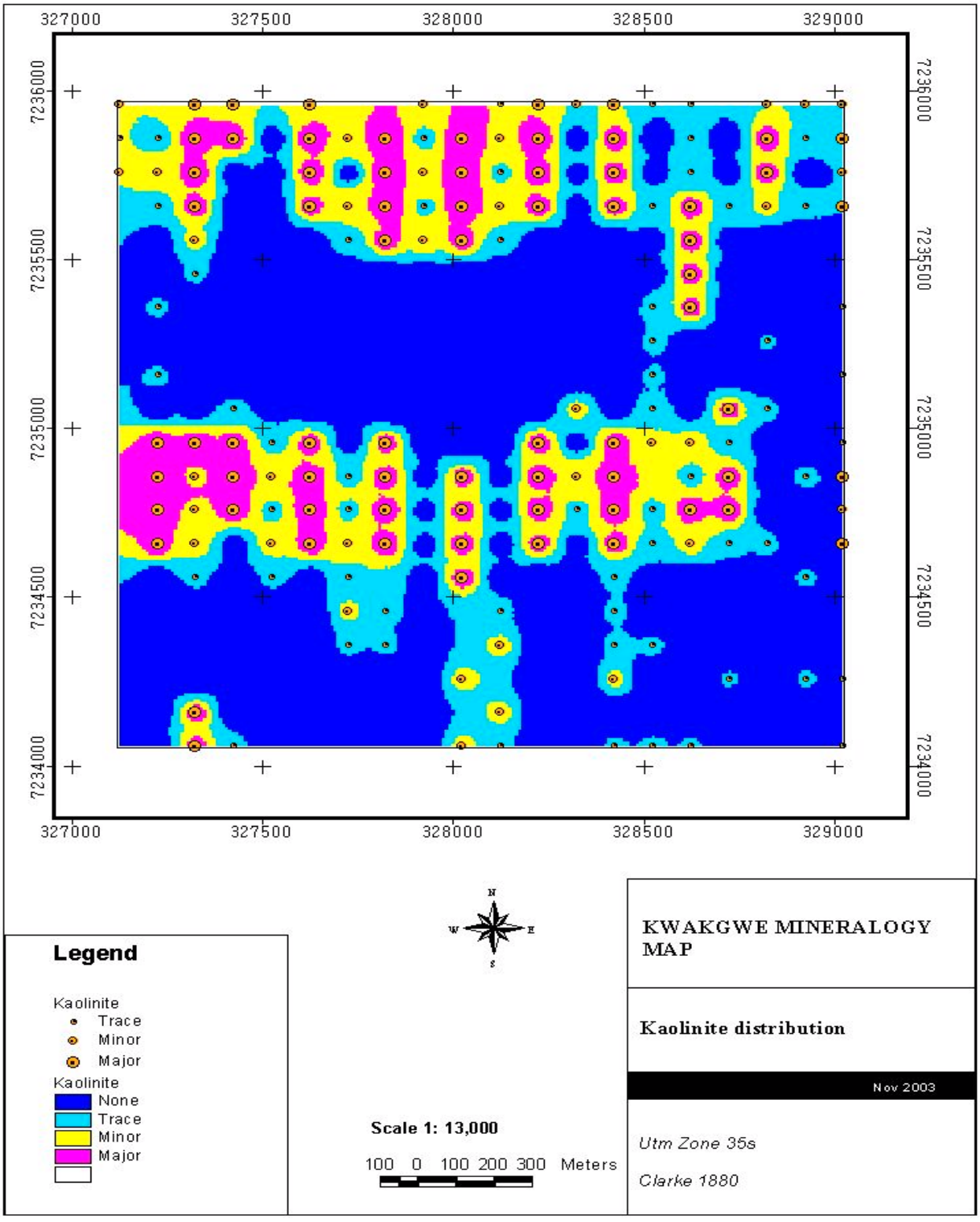

Figure 4.35: Map of kaolinite distribution in the study area

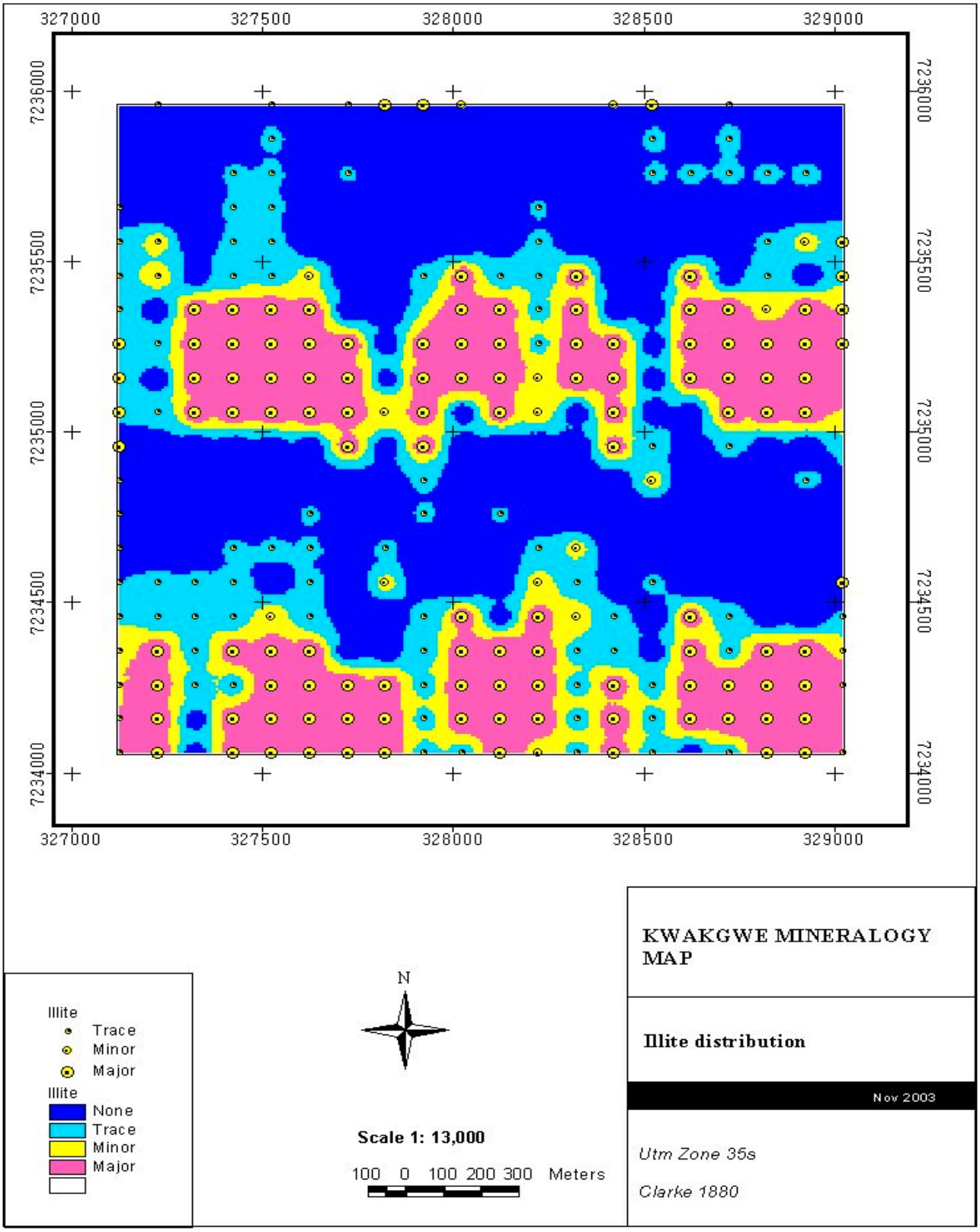

Figure 4.36: Map of illite distribution in the study area

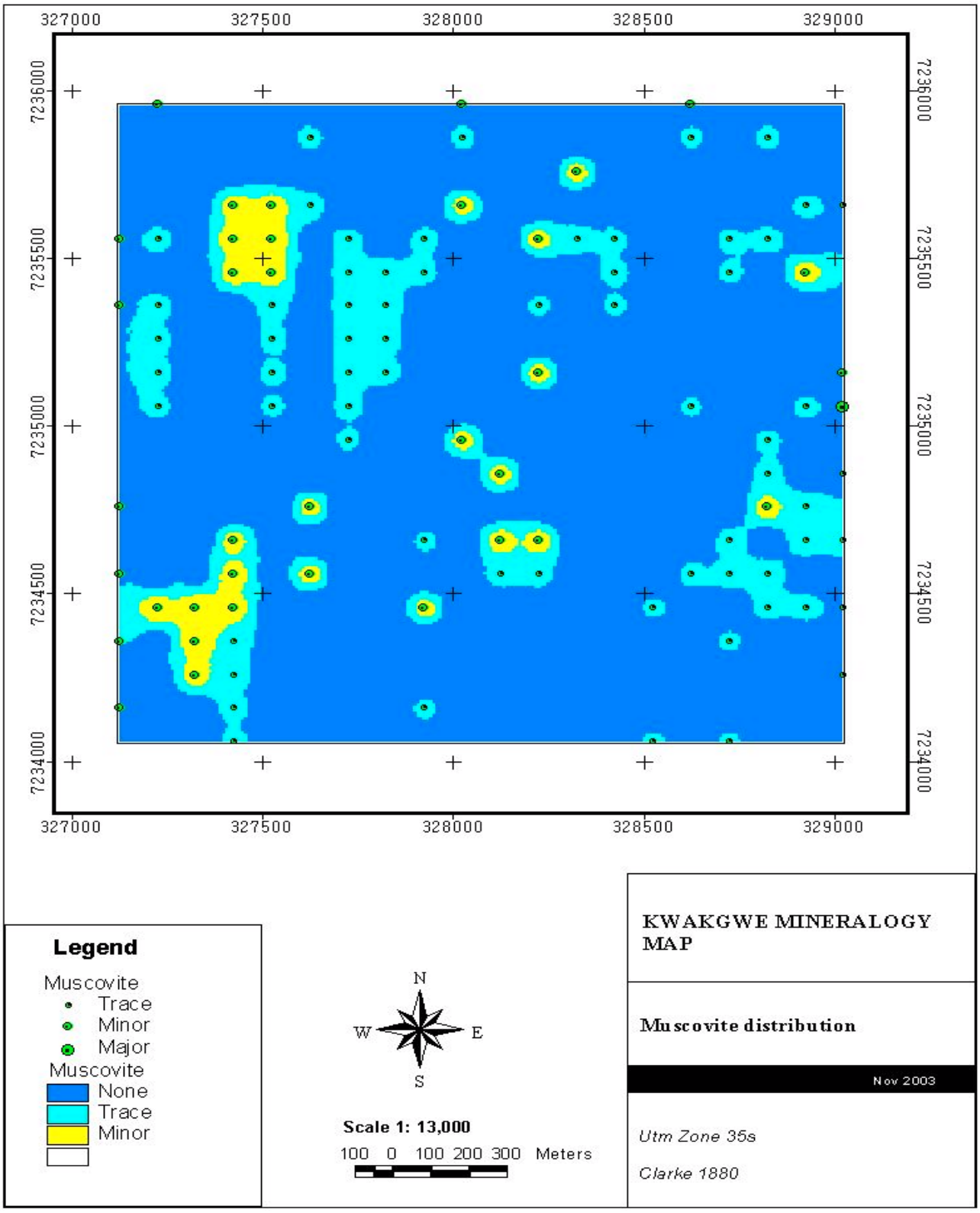

Figure 4.37: Map of muscovite distribution in the study area

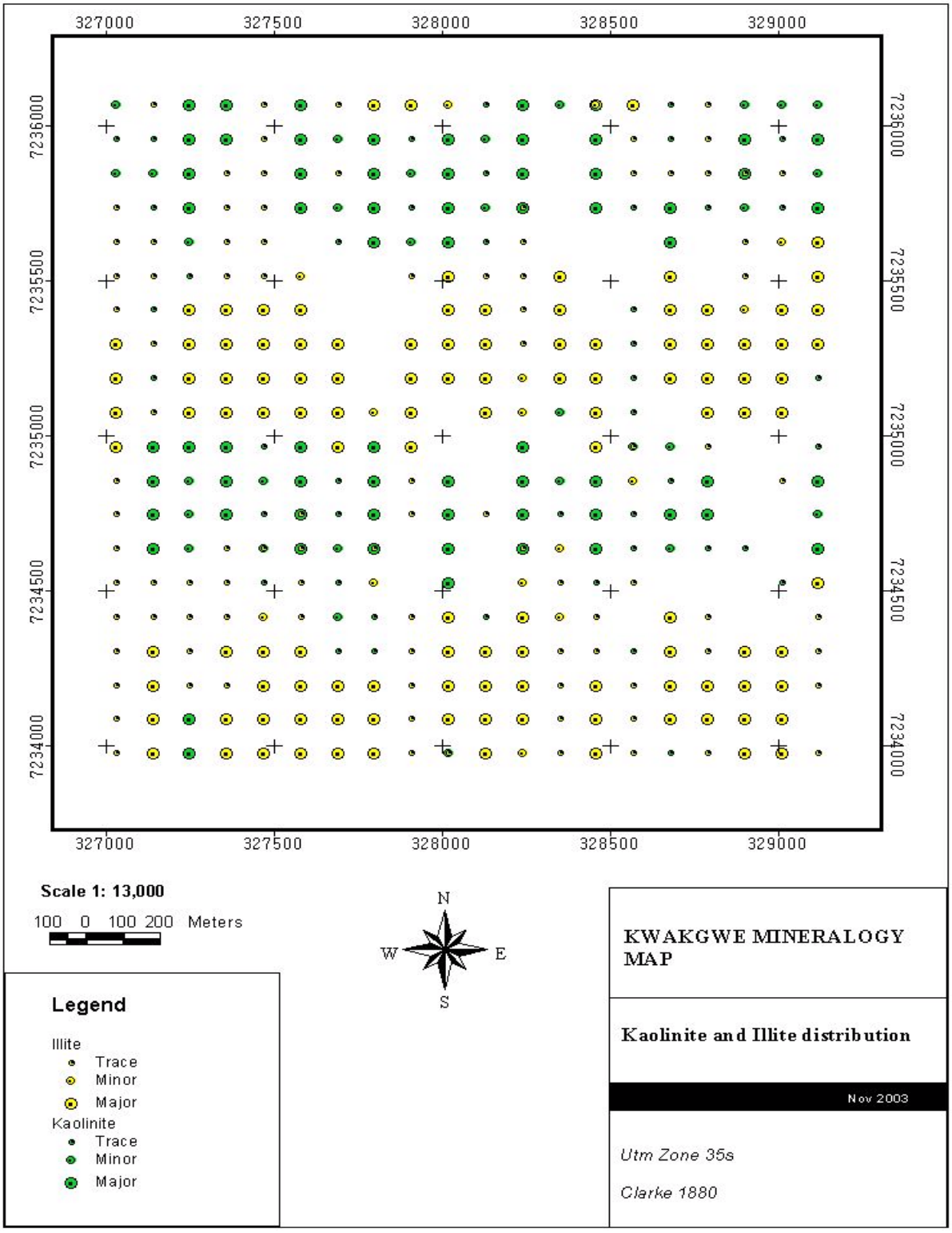

Figure 4.38: Map of kaolinite and illite distributions in the study area

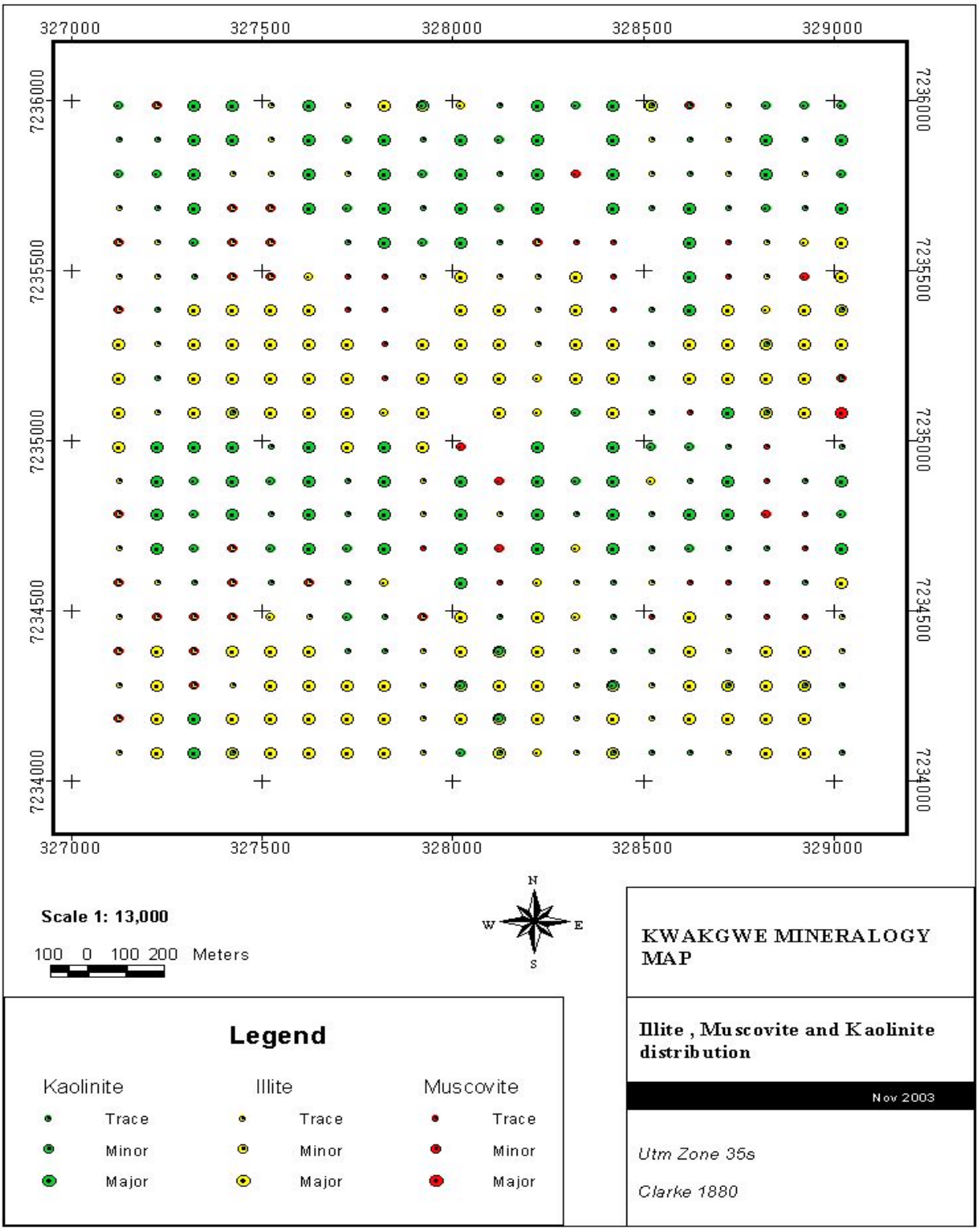

Figure 4.39: Map of illite, muscovite and kaolinite distributions in the study area

4.3.7 Mineralogy of the control site and other geological materials sampled

The results of XRPD analyses of other geological materials sampled at Kgwakgwe has been reported in Table 3.10. The manganiferous shale consisted of cryptomelane, ramsdellite, bixbyite and pyrolusite as well as quartz, kaolinite, goethite, microcline and illite. The major mineral phase is cryptomelane. There were neither Fe bearing and nor clay minerals present in the Mn oxide ore, and cryptomelane was the major mineral phase. Minor phases present in the Mn oxide ore included pyrolusite and bixbyite, and in trace quantities braunite, microcline and ramsdellite. Cryptomelane and bixbyite occurred in major phases, and pyrolusite and goethite were in minor quantities in the Mn wad. The tectonised manganiferous chert breccia was predominantly cryptomelane, although minor quantities of braunite and trace quantity of ramsdellite were also present. The ferruginous shale consisted mainly of haematite and goethite. Minor quantities of illite and kaolinite were also present. At the control site, soil samples consisted of quartz and haematite in major quantities, and kaolinite in minor quantity.

The mineral distribution pattern of the geological materials sampled and the soil samples from the control site revealed that the sources of the Mn bearing minerals in the soils are the manganiferous shale, the Mn oxide ore, the Mn wad and the tectonised manganiferous chert breccia. The haematite and goethite contained in the soils most possibly originated from the ferruginous shale, and to

a less extent goethite from the manganiferous shale. At the control site there were no Mn bearing minerals, and the haematite was possibly derived from the Fe rich country rocks dolerite and rhyolite.

Sediments containing exposed Mn particles eroded and were transported either by wind or water (meteoric fluids and streams) to contaminate surrounding soils especially those at the study area. Higher Fe concentration levels in soils was due to input from Fe particles which were associated with the ferruginous shale. Another form in which the Mn contaminated the soils could have been due to dissolution, saturation and neomineralisation (Ekosse and Modisi, 1999; Ekosse and Vink, 1998). Manganese and Fe ions dissolved from the Mn and Fe bearing rocks and migrated through different pathways southwards whereupon saturation, they became neomineralised thereby reconstituting the Mn and Fe bearing minerals in the soils.

4.3.8 Genesis and associations of minerals in the study area

Laznicka (1992) classifies the Kgwakgwe Mn oxide ore field to be predominantly detrital (terrigenous), and to have been deposited in a sedimentary environment of passive continental margin and/or epicontinental sea. Manganese mobility is intermediate between the relatively immobile Fe, Al, Ti and the more mobile Cu, Zn and Pb, and deposition of either Mn or kaolinite depends on which ions are in equilibrium with the fluids. Secondary Mn mineralisation could have resulted from the diagenesis of the manganiferous shale.

The protore rock that led to the formation of the kaolin and present Mn oxide ore could have been a manganiferous shale rich in rhodochrosite ($MnCO_3$) (Ekosse, 2001). Meteoric fluids reacted with the protore rock and Mn oxides were formed in a slightly acidic environment as represented in equation 4.3.

$$MnCO_3 + H_2O \rightarrow MnO + H_2CO_3 \quad (4.3)$$

Further oxidation of MnO led to the formation of the MnO_2 minerals. The feldspars from the feldspar rich rocks were altered to kaolinite in a very slightly acidic milieu as shown in equation 4.3.

$$2KAlSi_3O_8 + 3H_2CO_3 \rightarrow Al_2Si_2O_5(OH)_4 + 4SiO_2 + 3CO_2 + 2K(OH) \quad (4.3)$$

However with the introduction of K(OH) in the depository, the pH shifted from very slightly acidic to brackish conditions. The process of kaolinitisation may have been affected by high concentrations of K during diagenesis, especially close to the boundary between the rhyolite of the kanye Volcanic Formation and the Kgwakgwe Shale horizon. At times all the K contained in the feldspar was not leached out; thereby leading to the formation of illite.

Iron and Mn minerals are widely distributed in the kaolin and Mn oxide deposits. The possibility of Fe and Mn structural contamination of the clay minerals and especially kaolin cannot be ruled out. Kaolinite crystallinity of the Kgwakgwe kaolin is low (Ekosse, 2001), and this may be attributed to Fe^{3+} substituting for Al^{3+} in the octahedral sheet thereby reducing the degree of order (Mestdagh, Herbillion, Rodrique and Rouxhet, 1982).

The Mn mineralogy is dominated by tetravalent oxides of Mn such as cryptomelane. These Mn minerals are commonly associated with Fe oxides, mainly goethite, indicating incomplete separation of Mn from Fe during arid climate weathering of older manganiferous shales. Similar observations have been reported by Ostwald (1993). Thin sedimentary layering observed indicates that both Mn and kaolin was deposited in a quiet aquatic environment, with minor currents and not disturbed by bioturbation. According to Pettijohn (1975), the Mn oxides are compatible with suspension sedimentation in relatively deep and quiet environments. The presence of well defined laminations of Mn rich layers and kaolin are indicative of an undisturbed environment of deposition (Bosch *et. al*., 1993). In this vein, both the Mn oxide ore and the kaolin were deposited through suspension sedimentation.

The cyclic deposition and distribution of the Mn minerals, the kaolinite and illite in the basin were largely controlled by their specific hydraulic behaviour as explained by Taitel-Goldman *et. al.* (1995), and the water chemistry at the time of deposition (Parham, 1966). An explanation for a possible mechanism that led to the formation of clay minerals, Mn minerals, and Fe minerals has been postulated by Pracejus (1989), and could be used to explain such mineral associations at Kgwakgwe. Primary sediments rich in Mn oxides (manganiferous and ferruginous shales) were subjected to redox reactions resulting in the dissolution of elements such as K, Mn, Fe, Si and Al leading to precipitation of Mn – K oxide, Fe oxyhydroxide and kaolinite.

4.4 CHEMISTRY OF THE STUDY AREA

4.4.1 Soil chemistry

4.4.1.1 Total organic carbon in soils

The TOC values obtained were significantly low and ranged from 0 wt % and 7.91 wt % as shown in the histogram in Figure 4.40. The distribution in terms of wt % in the study area is positively skewed and the range between 0.5 wt % and 1 wt % with the highest number of samples (79 samples).

The colours reflected in the contoured and non contoured maps presented in Figures 4.41 and 4.42 as bluish, greenish, yellowish, brownish and reddish colour shades were unevenly spatially distributed and depicted prograded TOC values. Colour gradation in the non contoured and contoured maps (Figures 4.41 and 4.42), is reflected from blue for the low soil TOC values progressively to green, yellow, brown, red and pink for the high soil TOC values in the study site.

The TOC values for soil samples are high in the part west of Kgwakgwe Hills and in the central northern part of the study area. Otherwise the TOC values are generally low in the Kgwakgwe quarry sites and in the northeastern parts of the map area. High and low are used relatively in this context to distinguish the wt % of TOC in the soils in the study area; otherwise in general the TOC values are low.

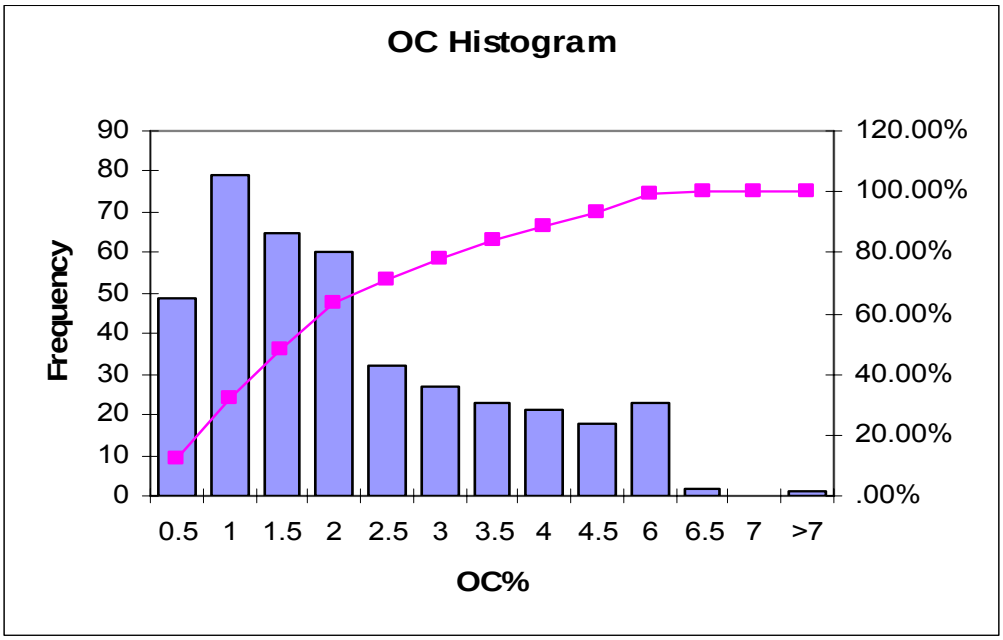

Figure 4.40: The total organic carbon values of soil samples from the study area

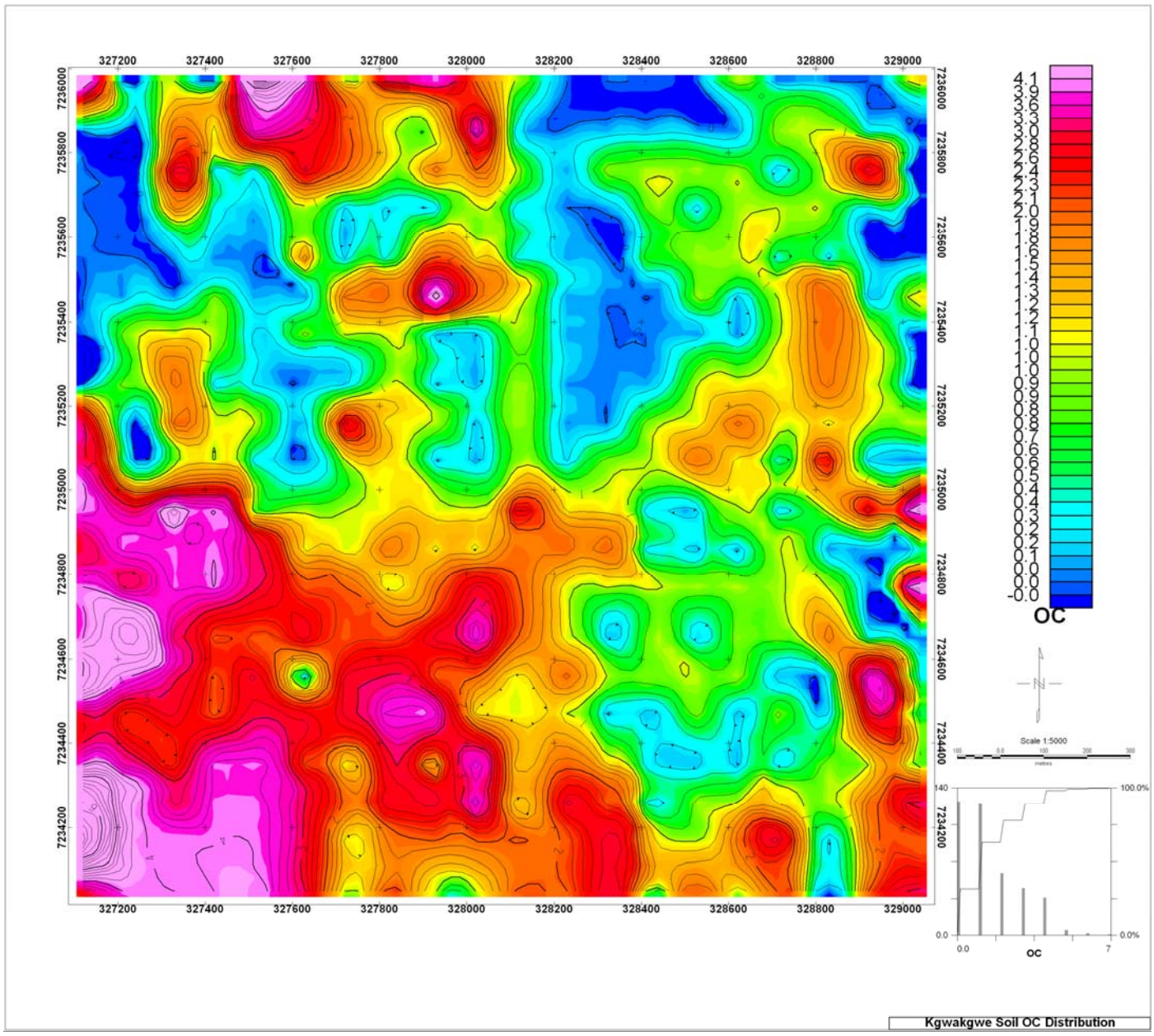

Figure 4.41: Contoured map of spatial distribution of the total organic carbon content in the soils of the study area

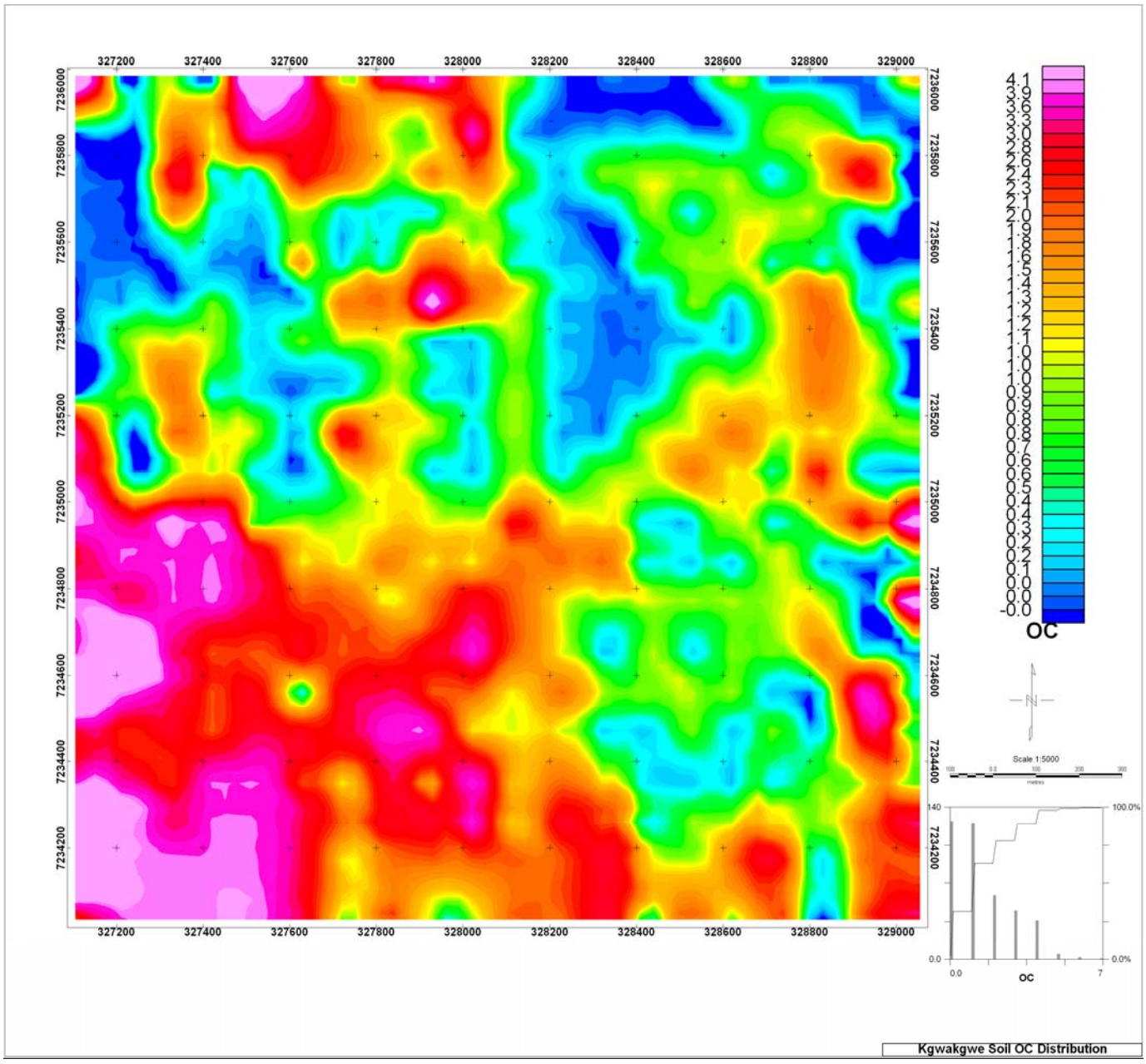

Figure 4.42: Non contoured map of spatial distribution of the total organic carbon content in the soils of the study area

4.4.1.2 Manganese concentration in soils

The Mn concentration levels in the soil samples obtained were significantly high and ranged from 56 μg g^{-1} and 6401 μg g^{-1} as shown in the histogram in Figure 4.43 and the non contoured and contoured maps in Figures 4.44 and 4.45 respectively. The Mn concentration levels in the soils depict as plotted in the histogram in Figure 4.43, a log normal distribution though it is positively skewed as described by Miller and Miller (1994), and it has one population. The data set does not distinguish different classes of Mn in soils. Threshold value is at 3000 whereby there are about 197 samples above this threshold value. The colours reflected in the contoured and non contoured maps presented in Figures 4.44 and 4.45 as bluish, greenish, yellowish, brownish and reddish colour shades were unevenly spatially distributed and depicted prograded Mn concentration levels. Colour gradation in the non contoured and contoured maps (Figures 4.44 and 4.45), is reflected from blue for the low Mn concentration level progressively to green, yellow, brown, red and pink for the high Mn concentration level in the study site.

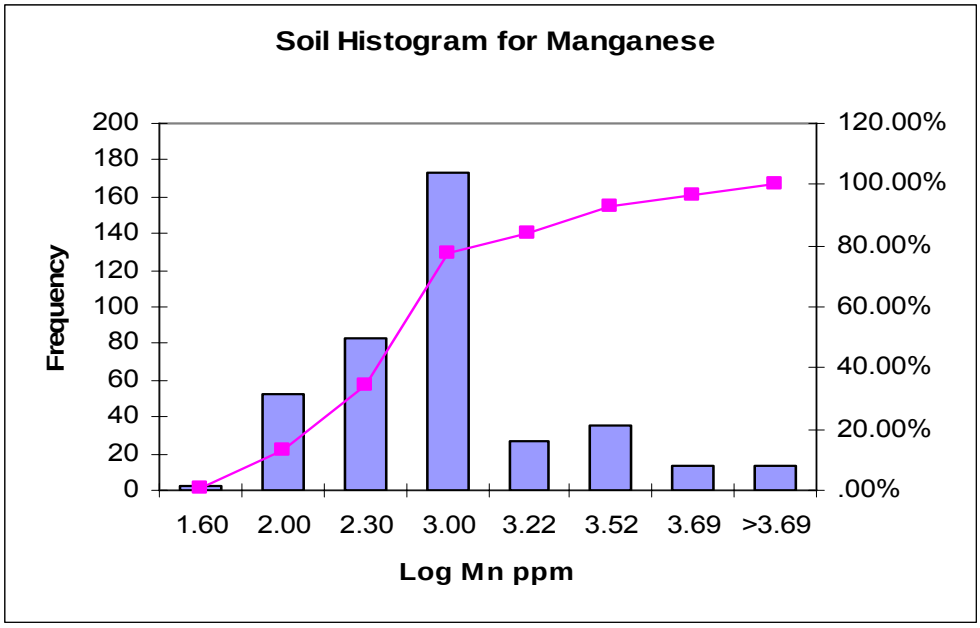

Figure 4.43: Manganese concentration values in soil samples from the study area

The high Mn concentration levels were prominent in the southwestern part of the study area to the west of the mine workings whereas the low to medium Mn concentration levels were observed in soil samples located further away from the mine workings as depicted on the non contoured and contoured maps in Figures 4.44 and 4.45 respectively. The high concentration levels of Mn at these sites could be attributed to their closeness to the mine workings and areas of topographic lows. Concentration levels of Mn decreased as one moved away from the mine workings, Mn orebodies and stockpiles.

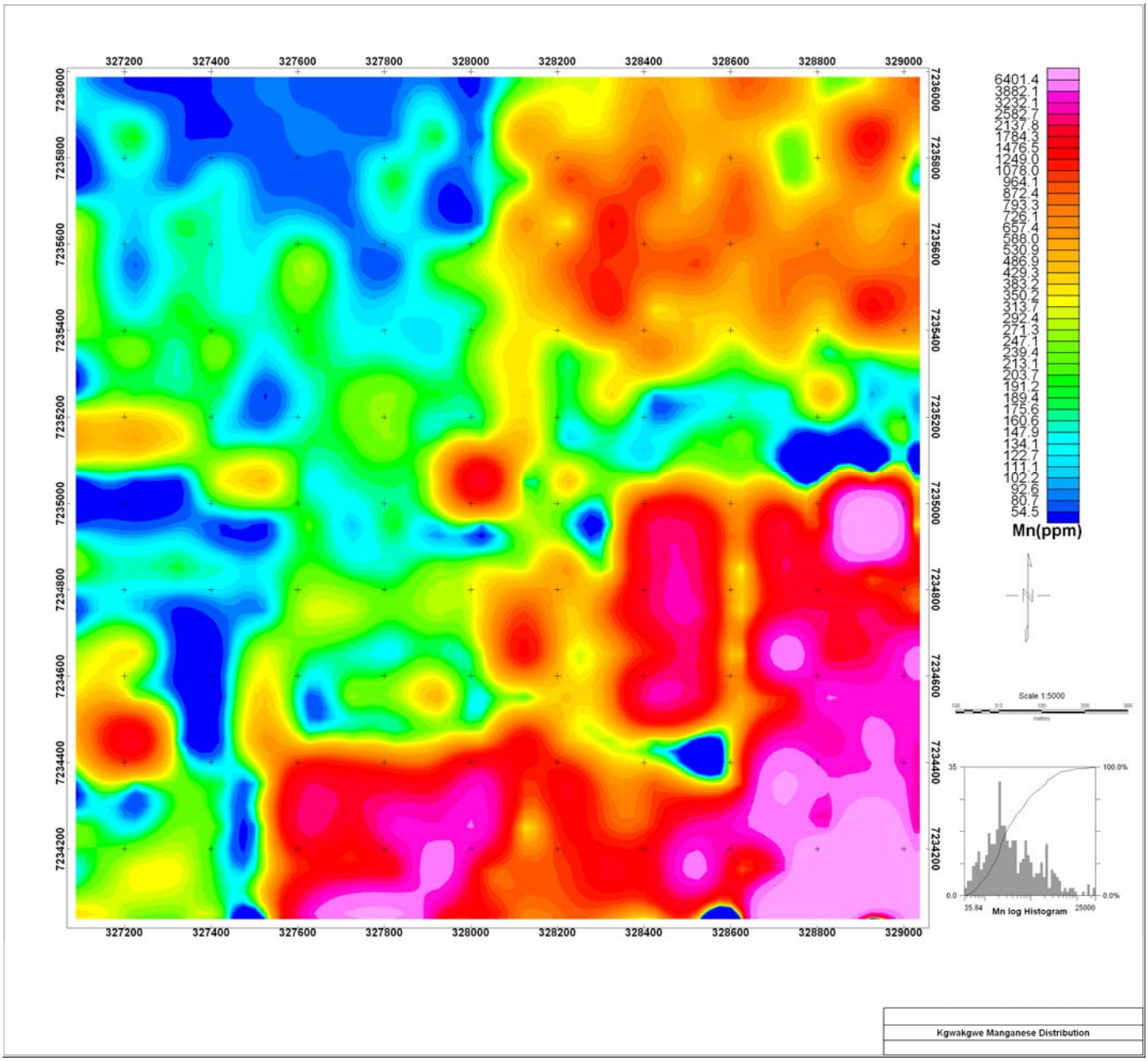

Figure 4.44: Non contoured map of spatial distribution of manganese concentrations in the soils of the study area

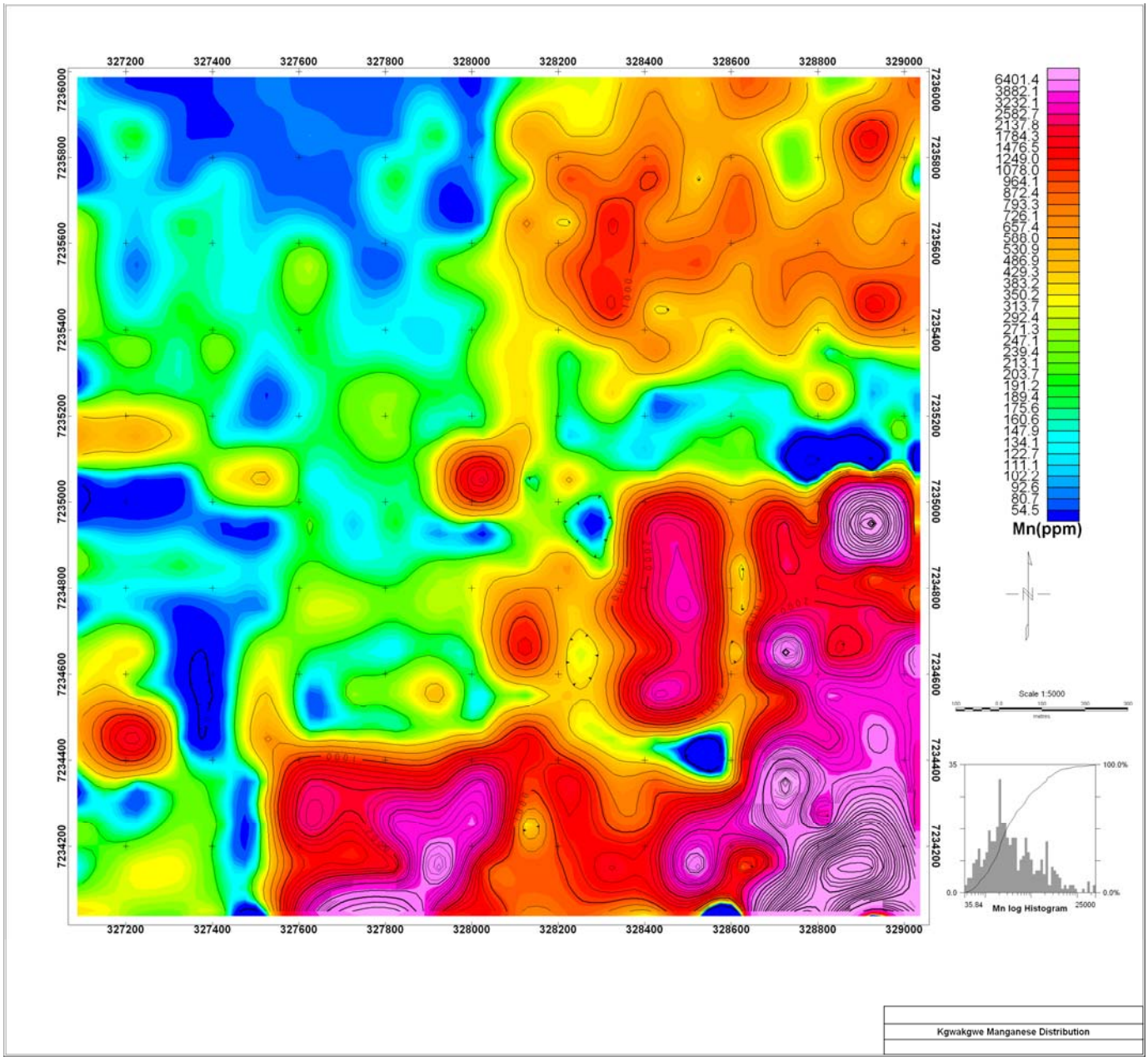

Figure 4.45: Contoured map of spatial distribution of manganese concentration in the soils of the study area

4.4.1.3 Iron concentration in soils

The Fe concentration levels in the soils samples obtained were high and ranged from 2361 μg g^{-1} to 45297 μg g^{-1} as shown in the histogram in Figure 4.46 and the non contoured and contoured maps in Figures 4.47 and 4.48 respectively. The Fe concentration levels in the soils is plotted in the histogram presented in Figure 4.46 a log normal distribution and it is polymodal in nature as it reveals at least three populations. Threshold is at 22500 whereby there are about 47 points above this threshold value. The colours reflected in the contoured and non contoured maps presented in Figures 4.47 and 4.48 as bluish, greenish, yellowish, brownish and reddish colour shades were unevenly spatially distributed and depicted prograded Fe concentration levels. Colour gradation in the non contoured and contoured maps (Figures 4.47 and 4.48), is reflected from blue for the low Fe concentration level progressively to green, yellow, brown, red and pink for the high Fe concentration level in the study site.

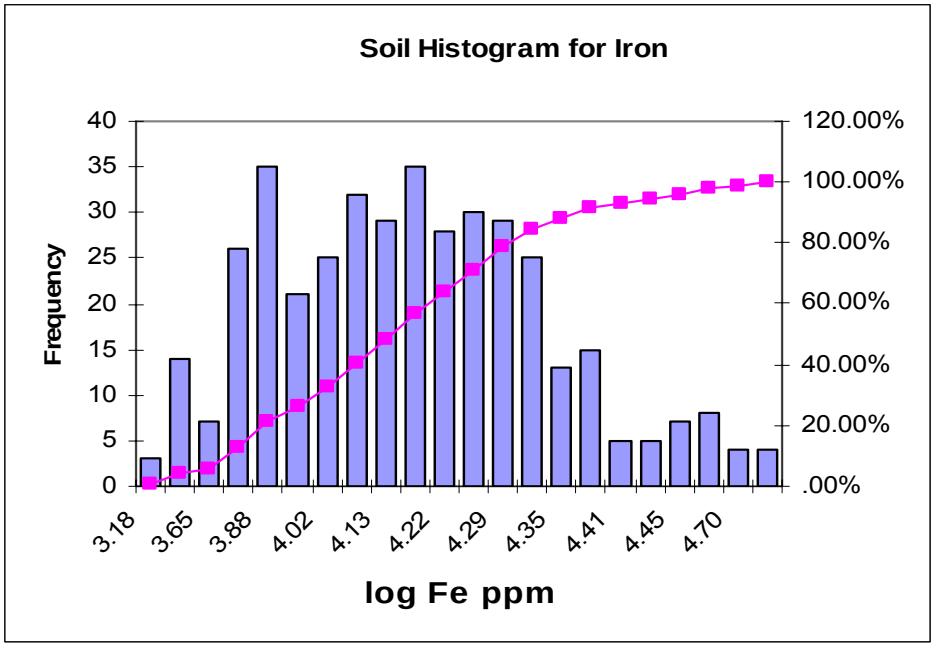

Figure 4.46: Iron concentration values in soil samples from the study area

The low Fe concentration levels were prominent in the southwestern part of the study area to the west of the mine workings whereas the medium to high Fe concentration levels were observed in soil samples located further away from the mine workings as depicted on the non contoured and contoured maps in Figures 4.47 and 4.48 respectively. The low concentration levels of Fe at the sites enriched with Mn could be attributed to the closeness of the mine workings and areas of topographic lows. Concentration levels of Fe significantly increased as one moved away from the mine workings, Mn orebodies and stockpiles.

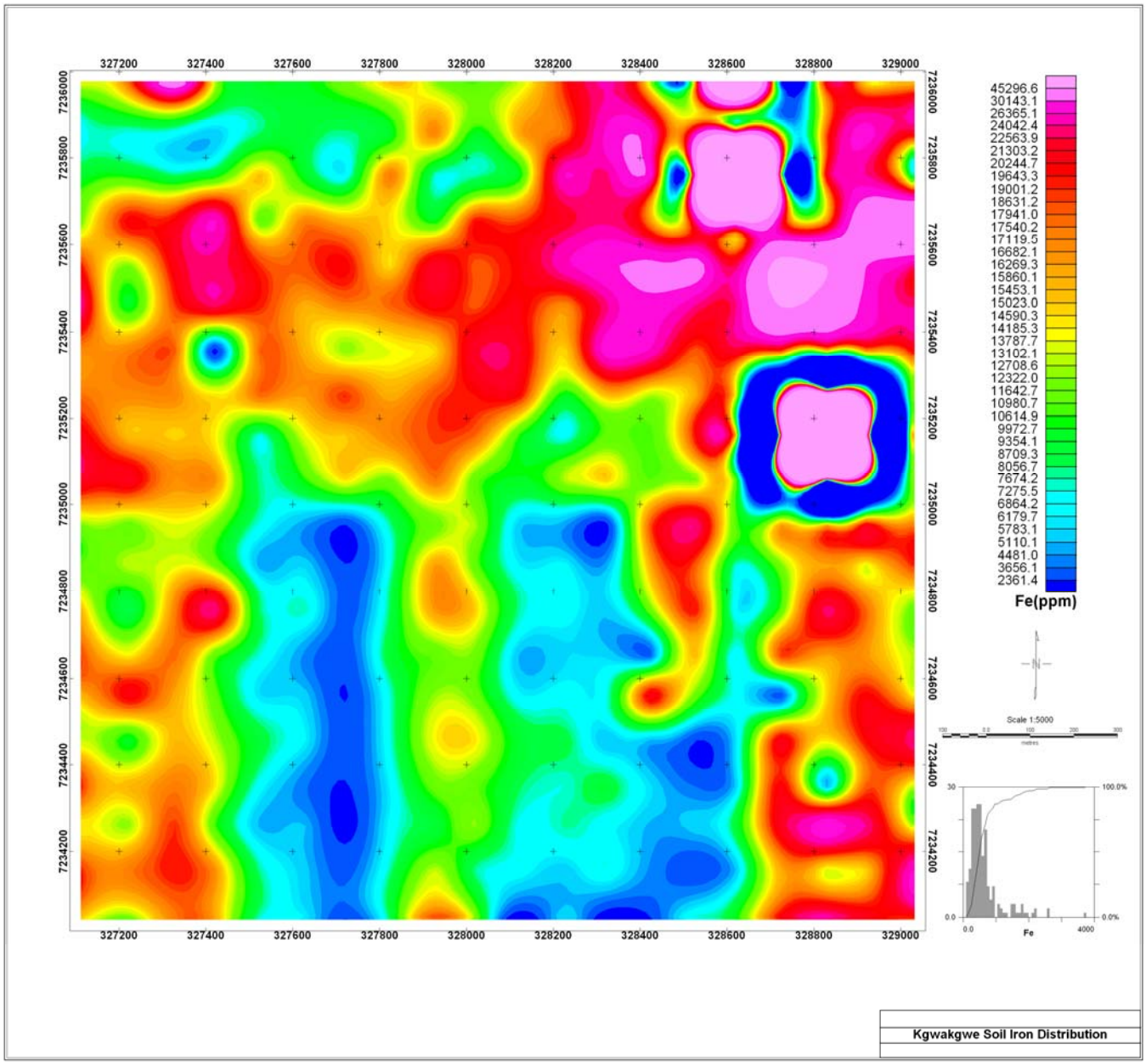

Figure 4.47: Non contoured map of spatial distribution of iron concentration in the soils of the study area

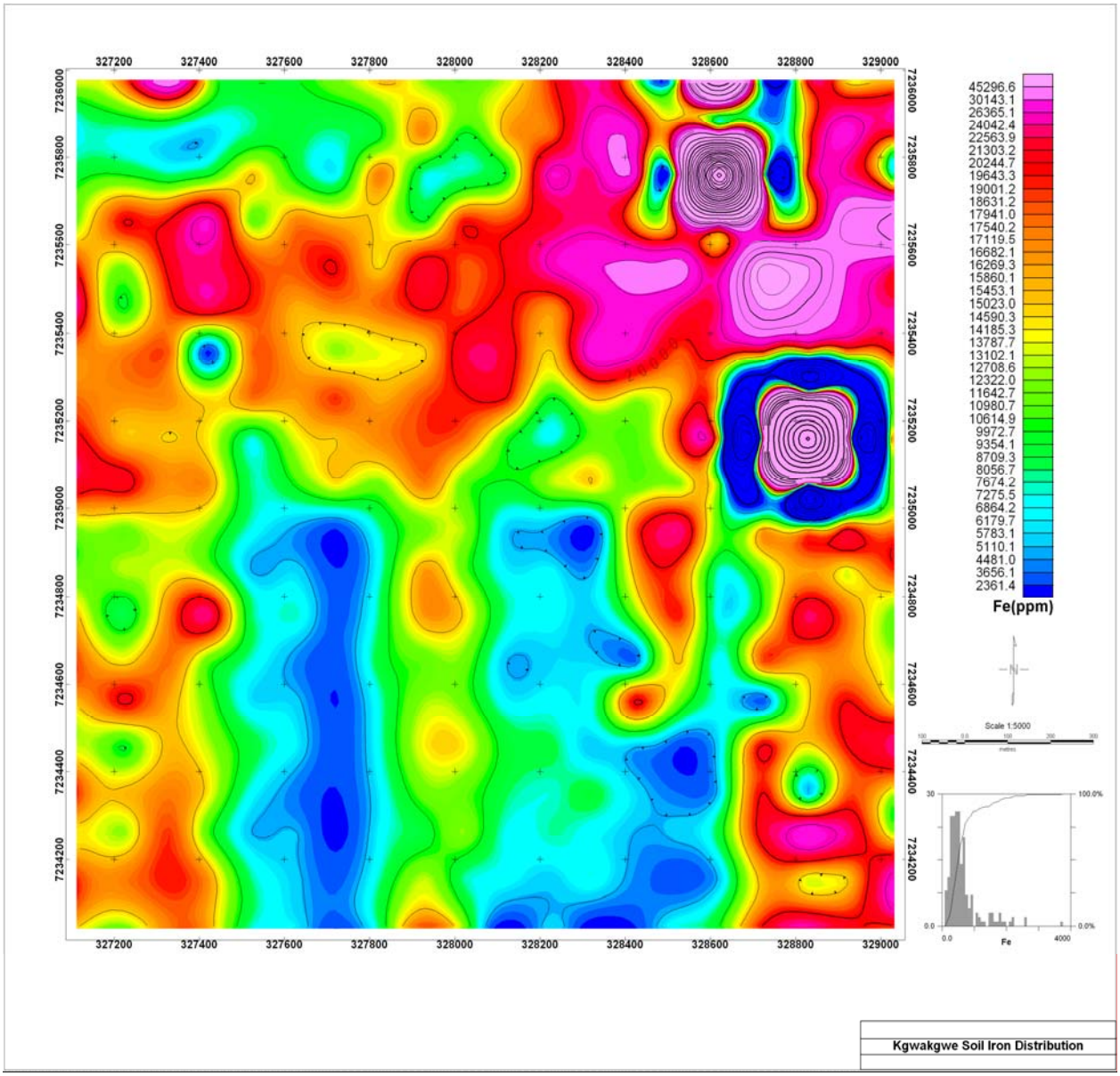

Figure 4.48: Contoured map of spatial distribution of iron concentration in the soils of the study area

4.4.1.4 Relationship between manganese and iron concentrations in soils

Though looking at the Fe and Mn histogram there is a certain small population that shows extremely high values almost like outliers in the graph (Figure 4.49). There is a high correlation of 0.70 between the Fe and the Mn. The anomalies of Fe and Mn were overlaid, and it was clear that these anomalies did not coincide (Figure 4.50).

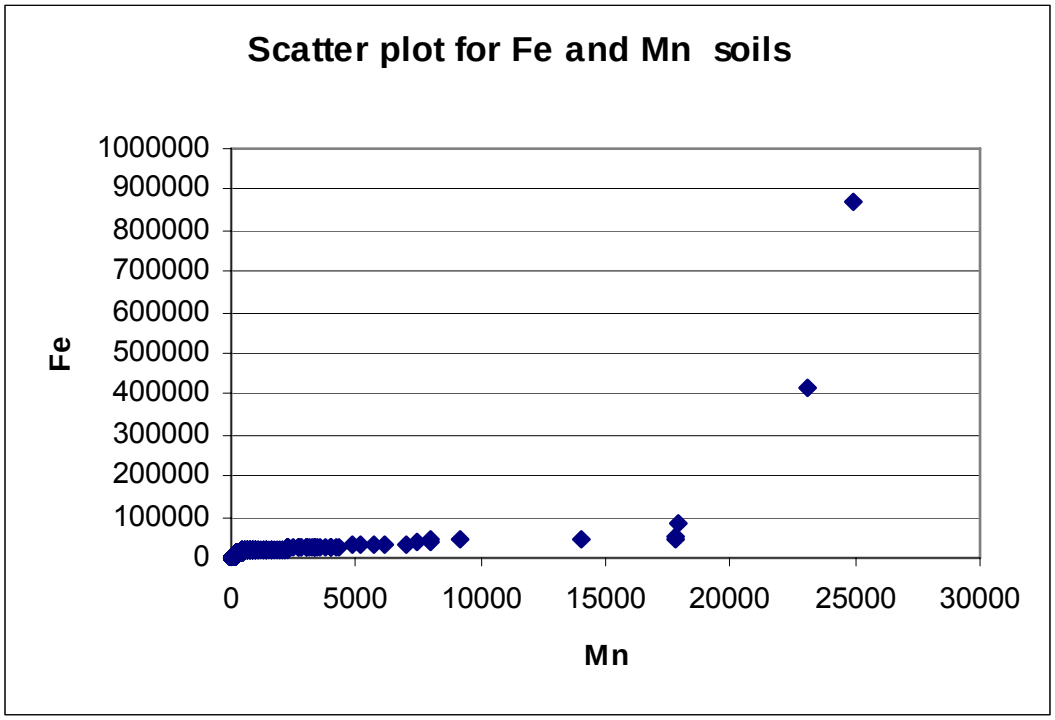

Figure 4.49: Scatter plot of manganese and iron concentration values in soil samples from the study area

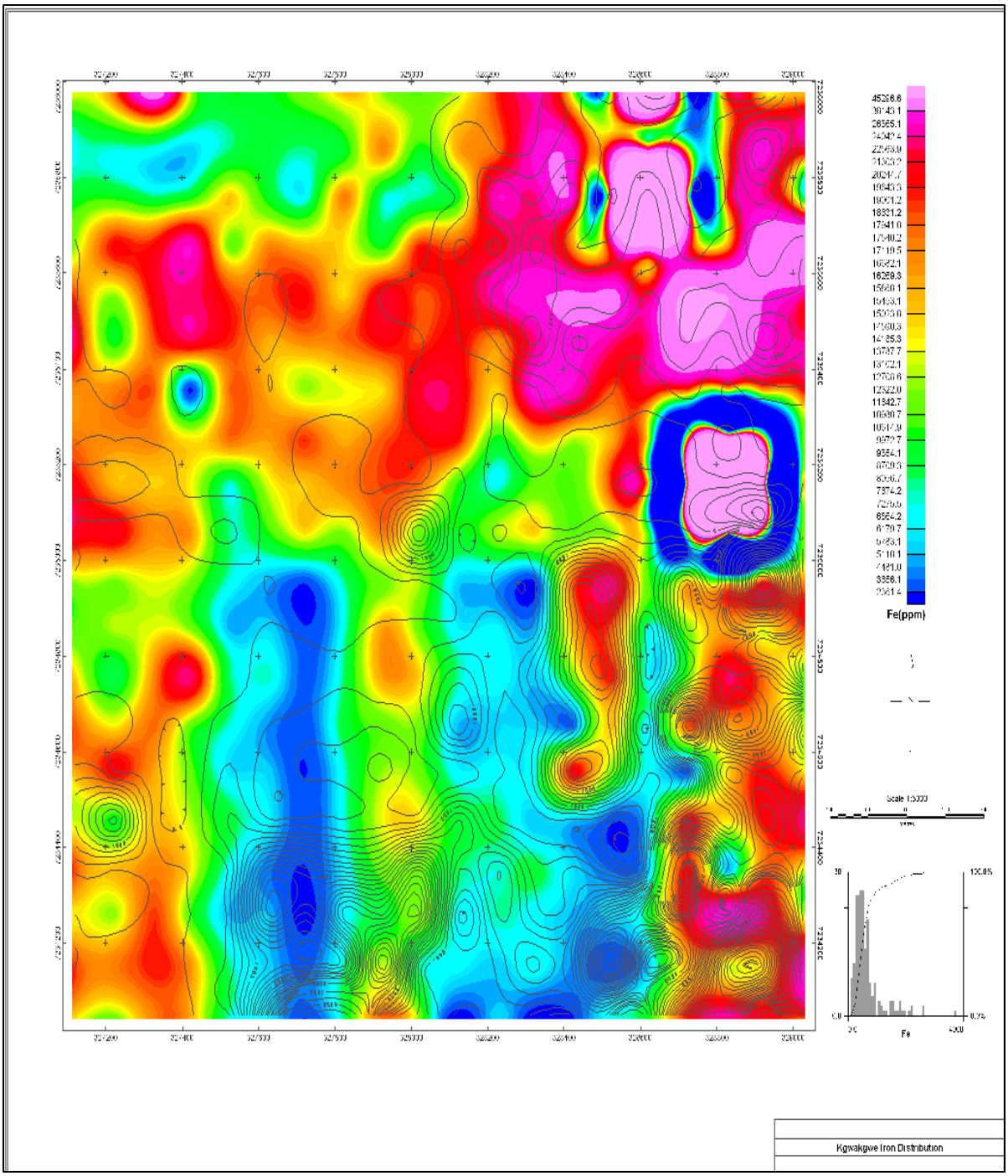

Figure 4.50: Contoured map of spatial distribution of iron concentration and manganese concentration overlay in the soils of the study area

Iron content in soils is low in the quarry sites (SW) and on the Kgwakgwe hills themselves. The anomalies are in the northeastern parts of the area. There is a big petal shaped anomaly that is surrounded by an immediate decrease of the iron. The southern part of the area has low iron content as opposed to the northern parts. Manganese on the other hand is very high around the quarry sites and on the Kgwakgwe hills. Manganese is generally low in the northern part of the area with the lowest points being in the northwestern parts of the map area. Also notable that it is not the whole of the southern part that shows Mn anomalies. The southwestern parts of the map have very low Mn concentrations. The anomalous Mn form pockets in the southeastern part of the map area. There is some inference that can be drawn between the geology and the Mn content with this data set.

4.4.1.5 Exchangeable bases and cation exchange capacity in soils

The Na concentration levels in the soil samples were low and ranged from 0.1 $cmol_c kg^{-1}$ to 89.1 $cmol_c kg^{-1}$, with a mean of 0.44 $cmol_c kg^{-1}$. The histogram in Figure 4.51 and the non contoured and contoured maps in Figures 4.52 and 4.53 depict the histographical and spatial distribution of Na within the study area.

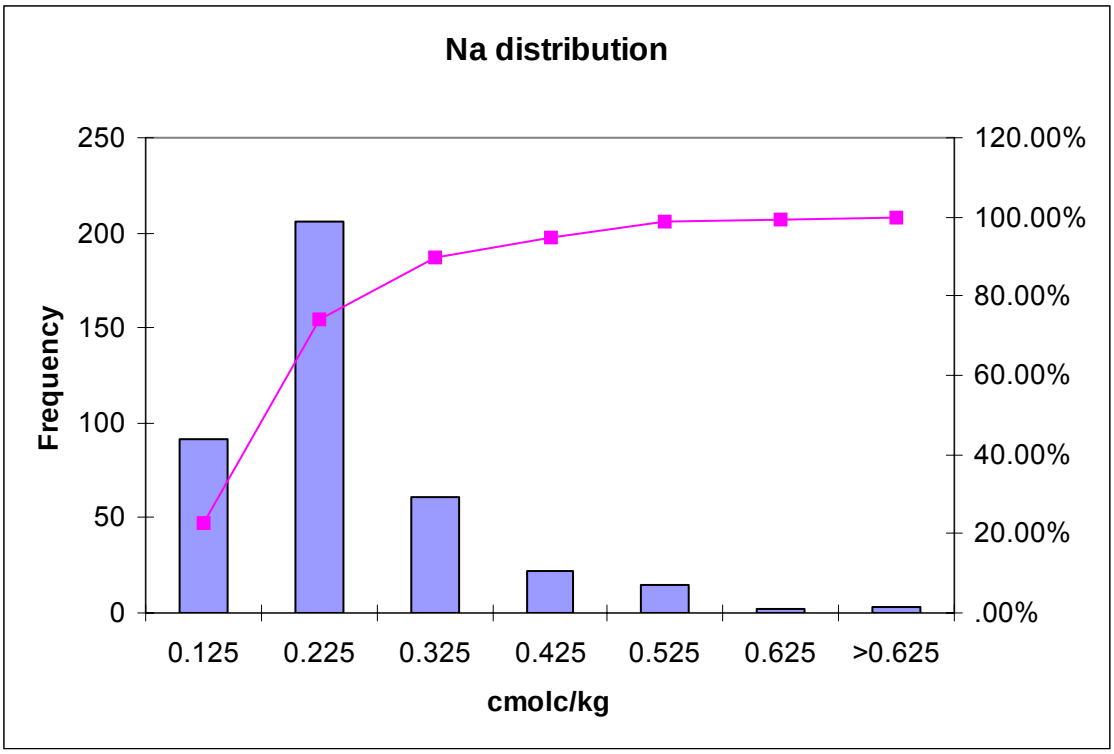

Figure 4.51: Sodium concentration values in the soil samples from the study area

Sodium shows a normal distribution with a range between 0.1 and 1.1.The data is positively skewed and the distribution staggered. More than half the samples have values >.20 for the Na element concentration in the soils, and only twenty samples display values more than 0.55

Sodium has a high correlation of 0.83 with potassium. Sodium is generally very low in the study area. Sodium hallows are found in the central part of the area and highs are found in the northern part and in the south eastern and south western part of the area as reflected in Figures 4.52 and 4.53 for the non contoured and contoured maps respectively.

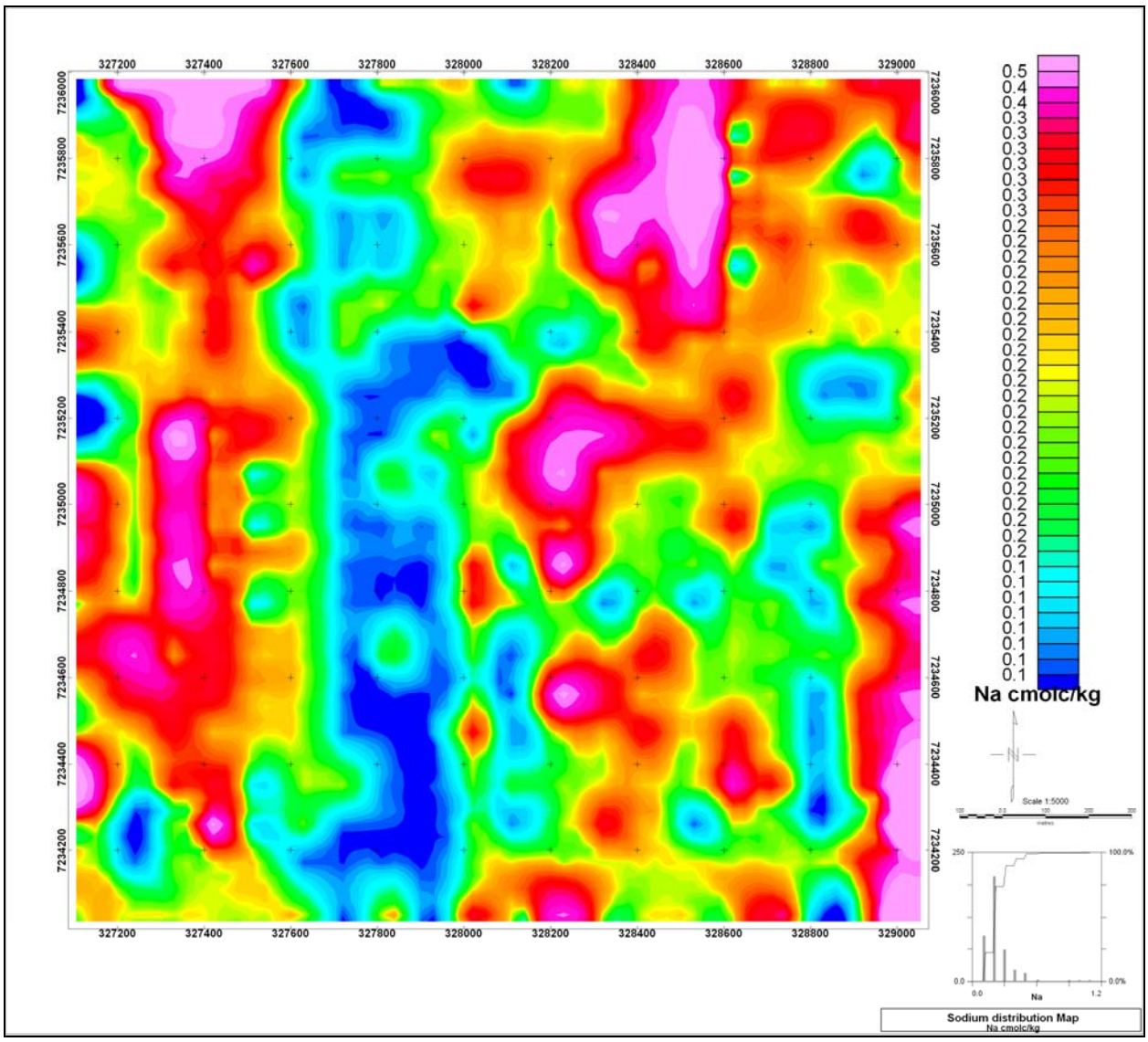

Figure 4.52: Non contoured map of spatial distribution of sodium concentration in the soils of the study area

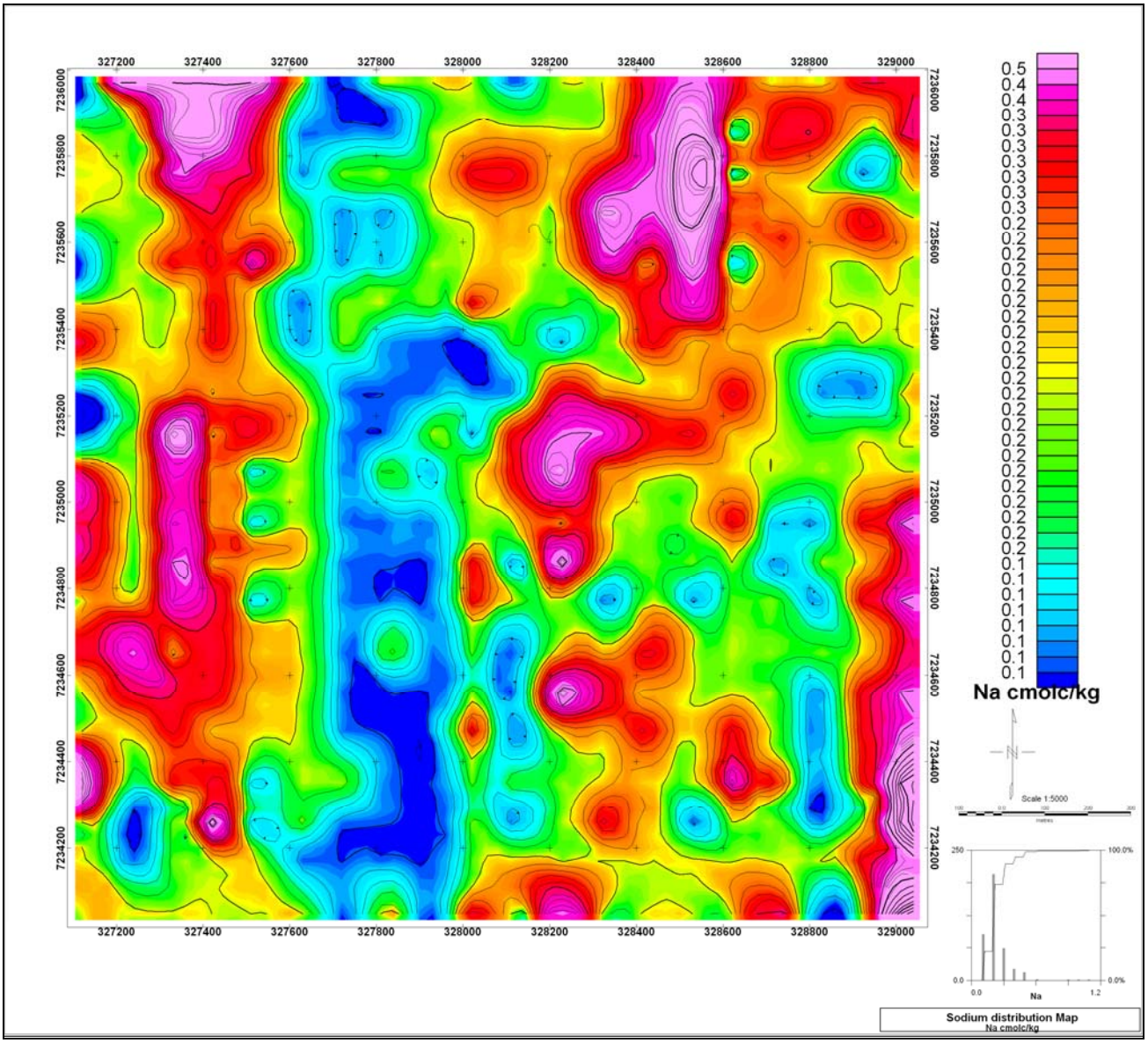

Figure 4.53: Contoured map of spatial distribution of sodium concentration in the soils of the study area

The K concentration levels in the soil samples ranged from 0.1 $cmol_c kg^{-1}$ to 163.6 $cmol_c kg^{-1}$, with a mean of 0.82 $cmol_c kg^{-1}$. The histogram in Figure 4.54 and the non contoured and contoured maps in Figures 4.55 and 4.56 depict the histographical and spatial distribution of K within the study area.

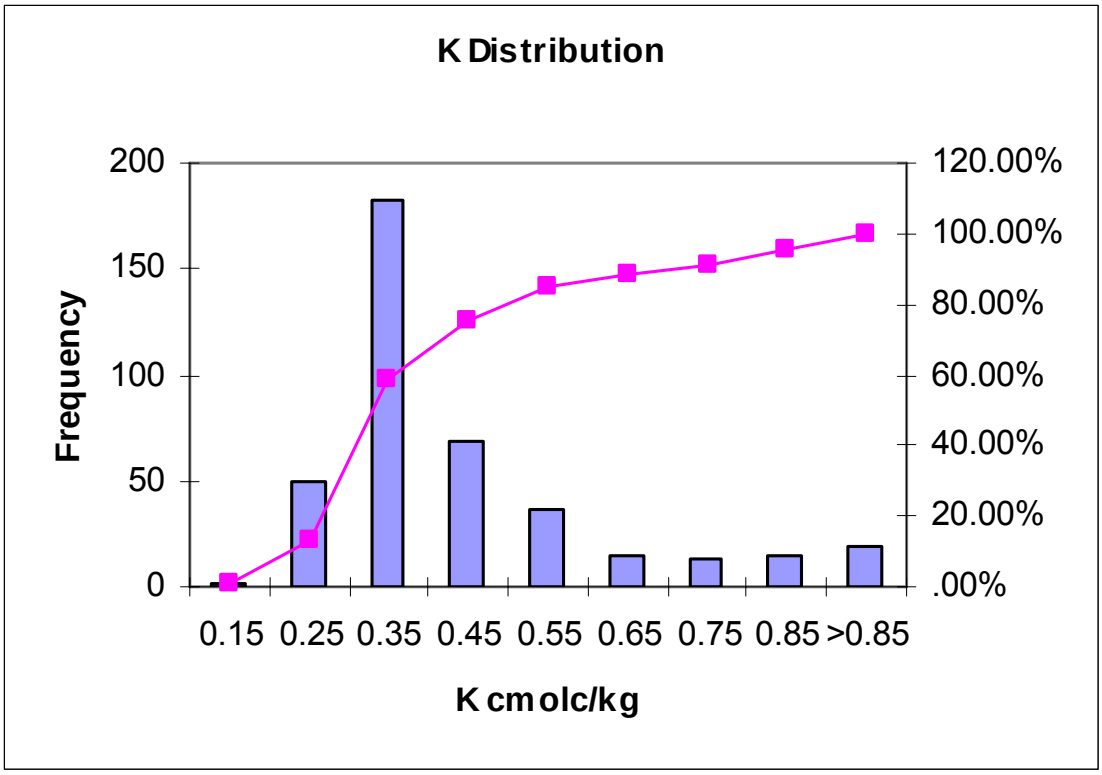

Figure 4.54: Potassium concentration values in the soil samples from the study area

The distribution of K is close to that of Na. One hundred and eighty three soil samples have the value 0.3. Only 19 samples have values above 0.85. Potassium distribution is very similar to the sodium distribution, low values are

found in the central part of the area and high values are found in the northern part and in the south eastern and south western part of the area (Figures 4.55 and 4.56). The anomalies in the south eastern part of the study area are highly pronounced. Soils from the manganese mine sites have low potassium and sodium.

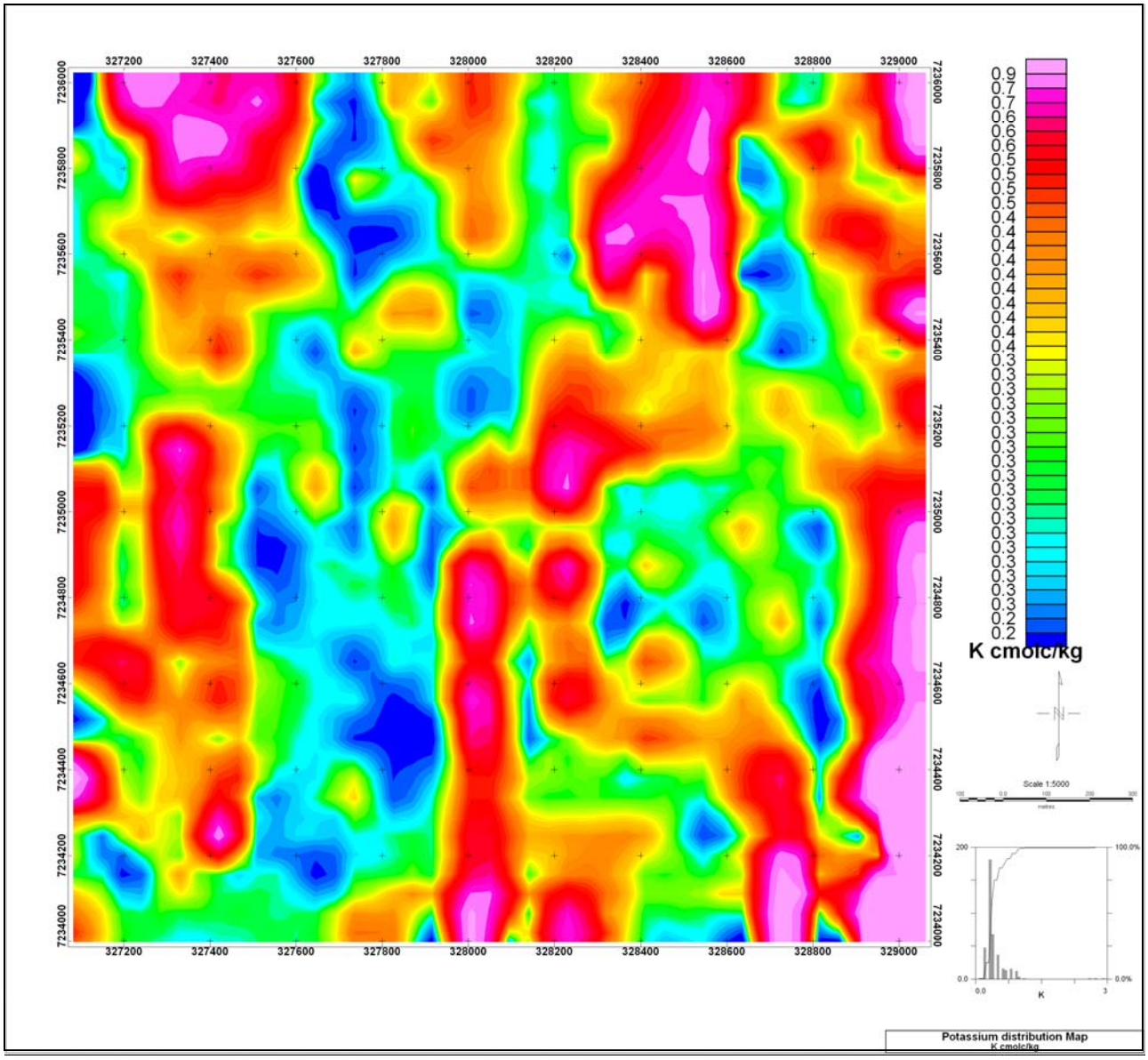

Figure 4.55: Non contoured map of spatial distribution of potassium concentration in the soils of the study area

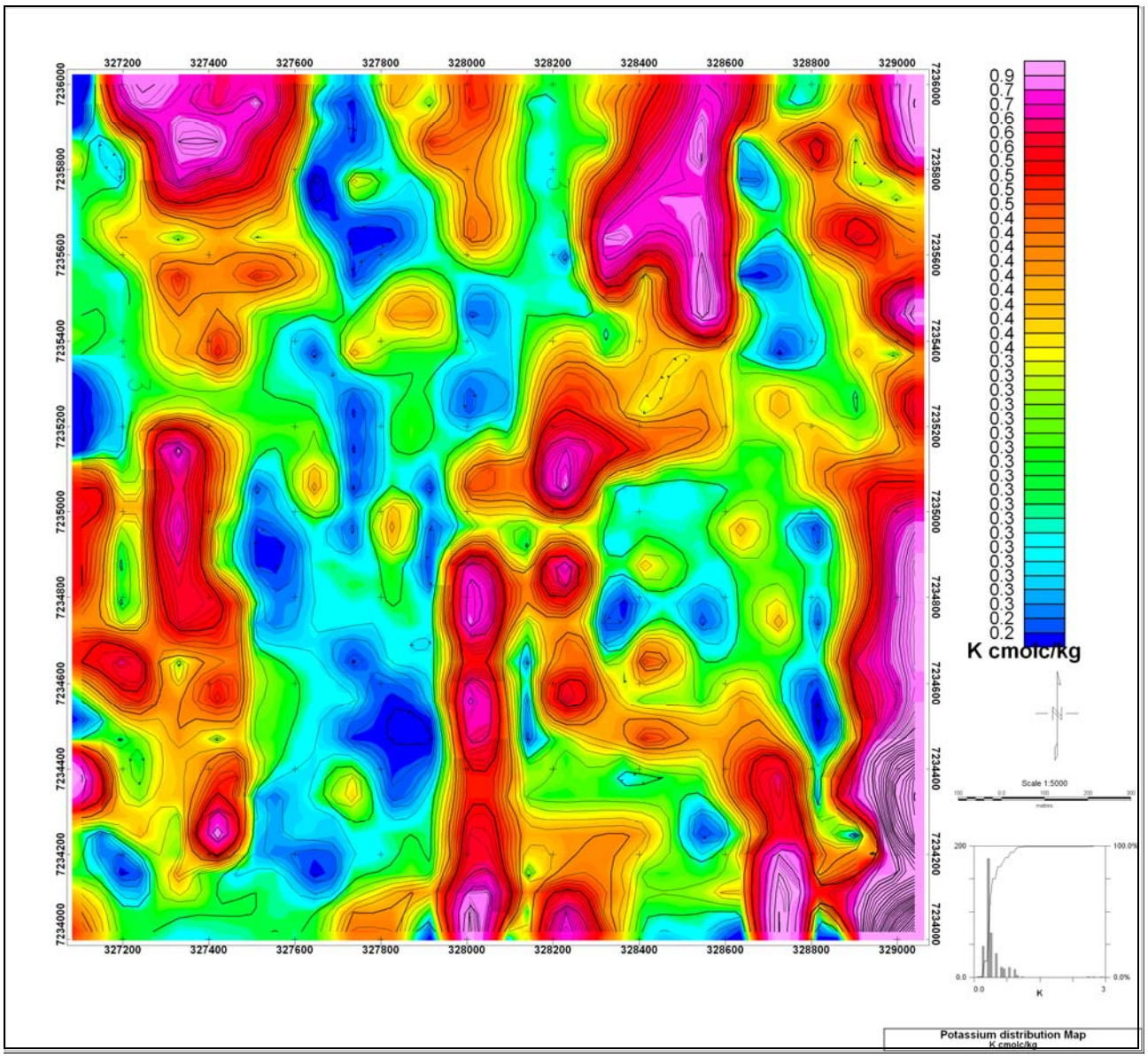

Figure 4.56: Contoured map of spatial distribution of potassium concentration in the soils of the study area

The Ca concentration levels in the soil samples ranged from 0.3 $cmol_cKg^{-1}$ to 1139 $cmol_cKg^{-1}$, with a mean of 5.68 $cmol_cKg^{-1}$. The histogram in Figure 4.57 and the non contoured and contoured maps in Figures 4.58 and 4.59 depict the histographical and spatial distribution of Ca within the study area.

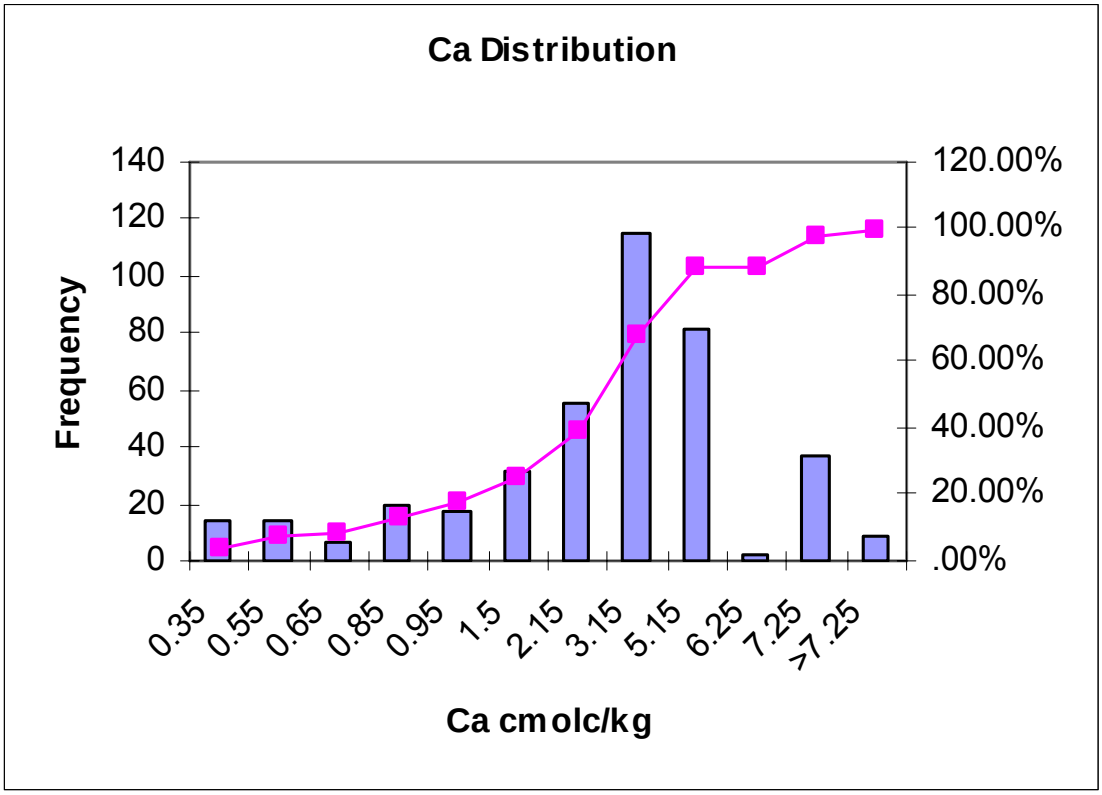

Figure 4.57: Calcium concentration values in the soil samples from the study area

Calcium is normally distributed with values ranging between 0.3 and 9.8. The distribution is negatively skewed. 115 samples have a concentration of 0.3 and there are only 9 samples with values above 7.25.The distribution has a mean value of 2.85.

Calcium has a high of 0.95 correlation with magnesium. A calcium hallow is found in the central part of the area and high values are found in the northern part and in the south eastern and south western part of the area as depicted in the non contoured and contoured maps presented as Figures 4.58 and 4.59.

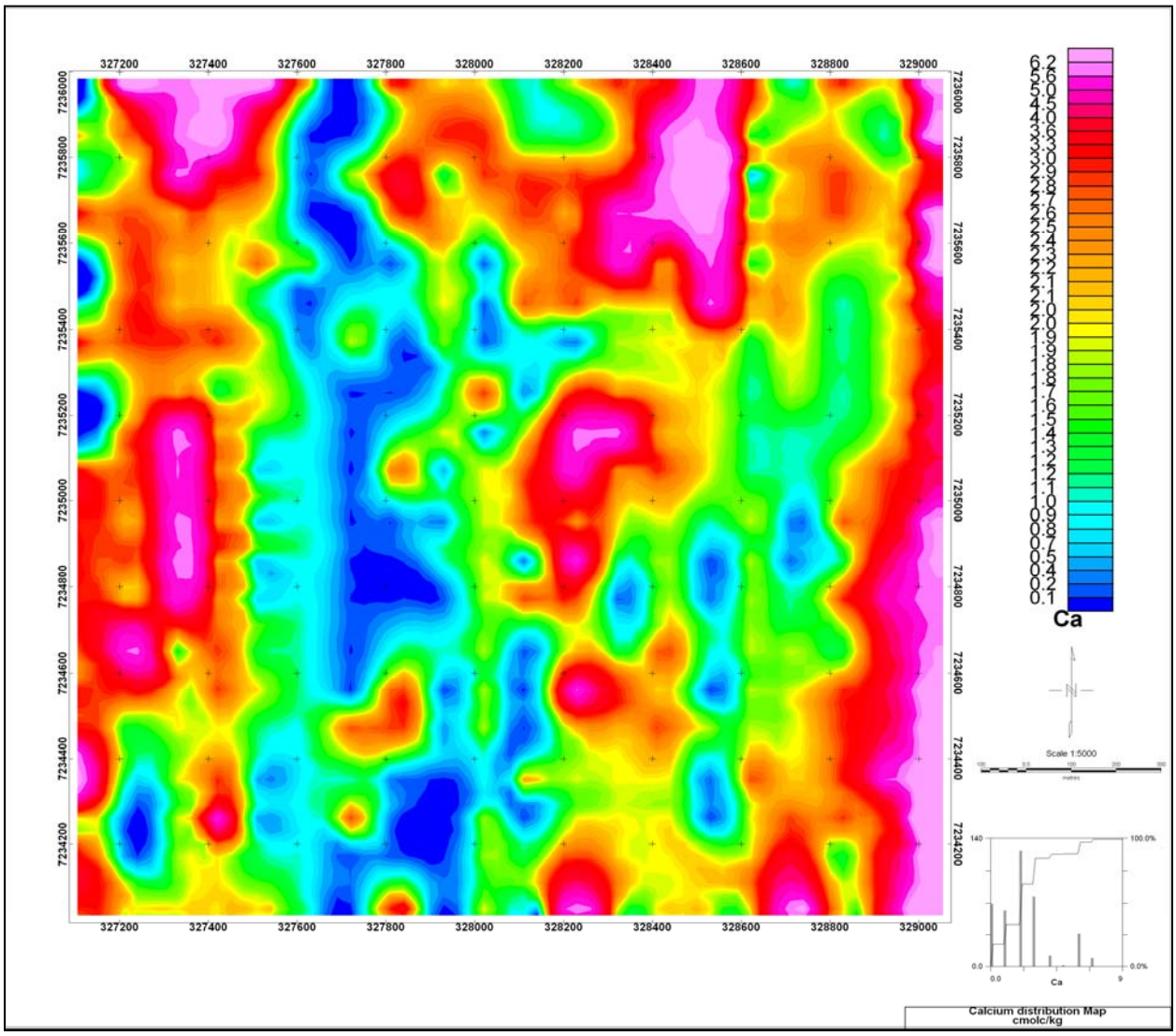

Figure 4.58: Non contoured map of spatial distribution of calcium concentration in the soils of the study area

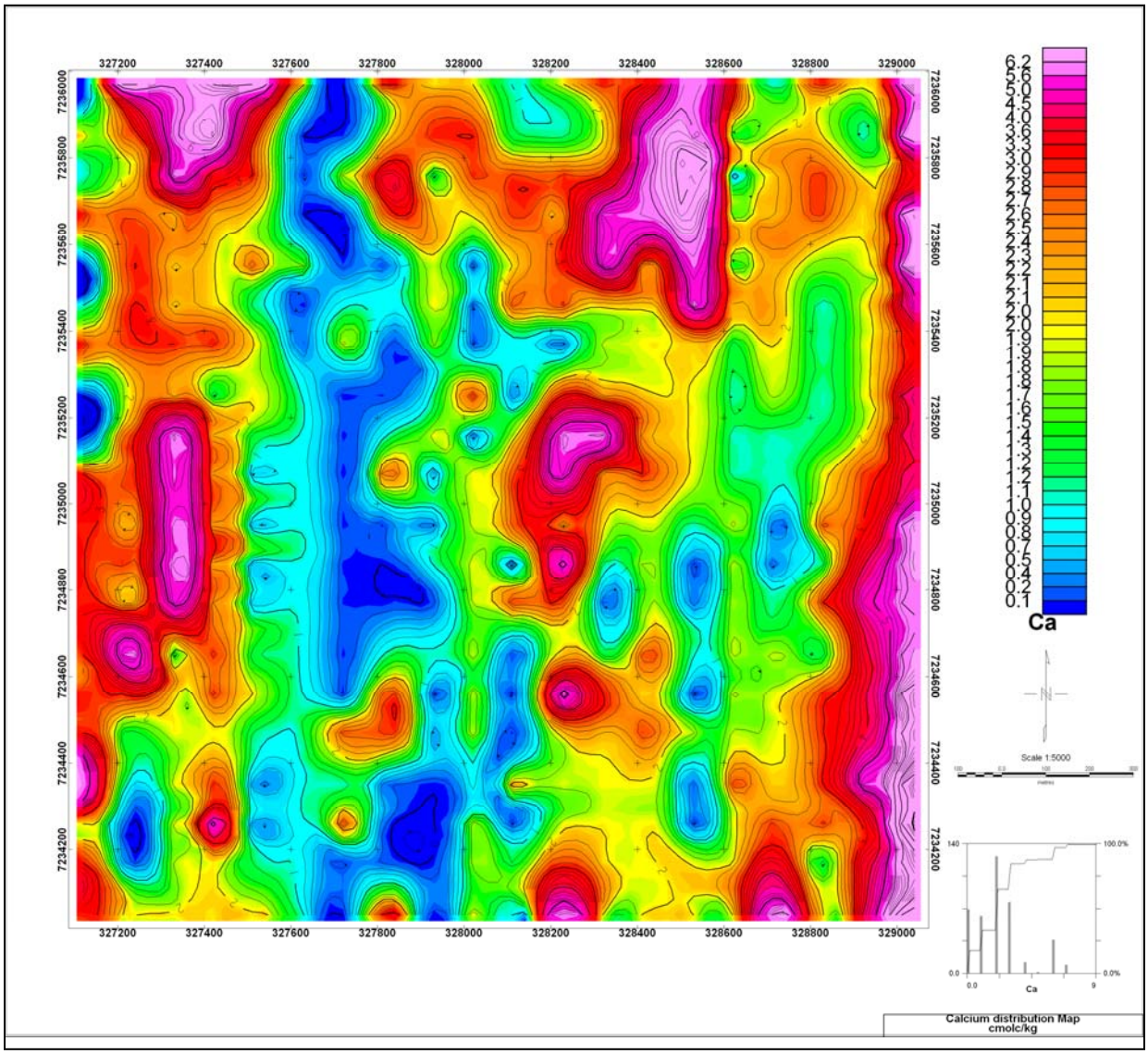

Figure 4.59: Contoured map of spatial distribution of calcium concentration in the soils of the study area

The Mg concentration levels in the soil samples ranged from 0.3 $cmol_cKg^{-1}$ to 1656.3 $cmol_cKg^{-1}$, with a mean of 8.26 $cmol_cKg^{-1}$. The histogram in Figure 4.60

and the non contoured and contoured maps in Figures 4.61 and 4.62 depict the histographical and spatial distribution of Mg within the study area.

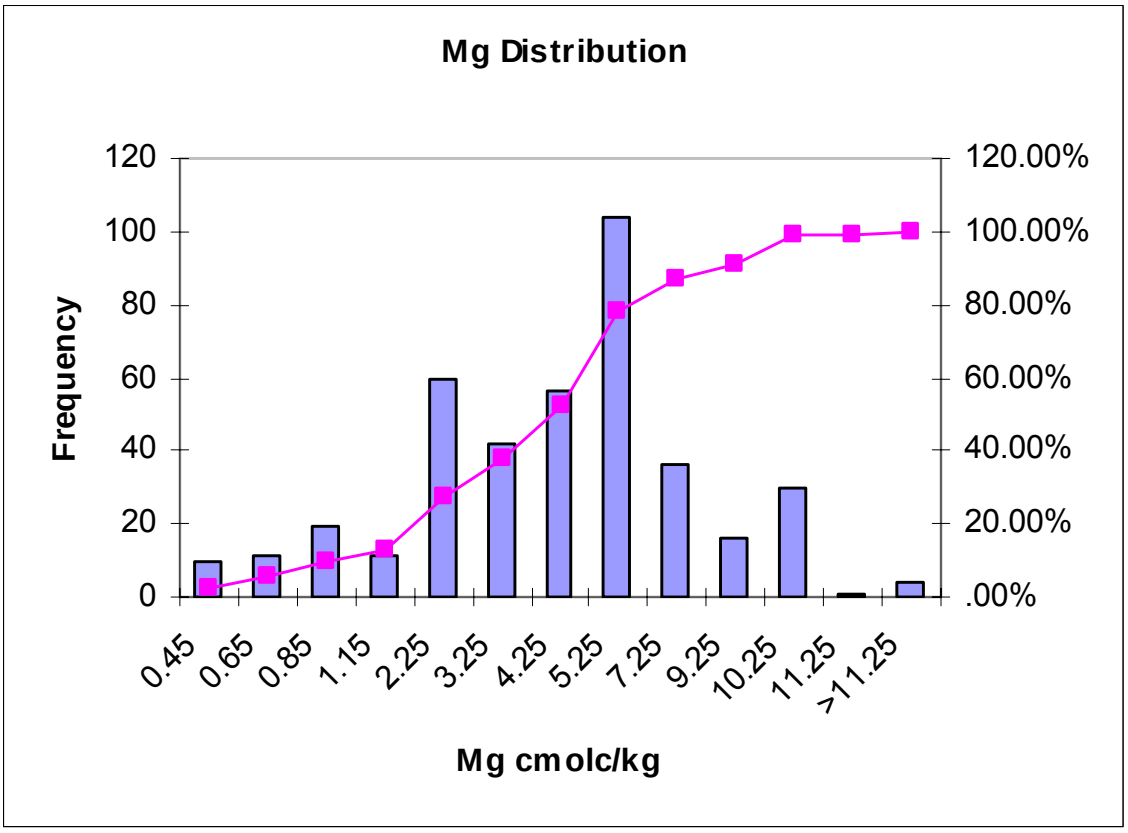

Figure 4.60: Magnesium concentration values in the soil samples from the study area

The graph for Mg shows a normal distribution and its bimodal in nature as it shows two populations. The distribution ranges between 0.3 and 12.3 with a mean of 4.11. Modal values are 2.25 and 5.25 are each with a number of 60 and 104 samples respectively.

A magnesium hallow is found in the central part of the area and high values are found in the northern part and in the south eastern and south western part of the area as depicted in the non contoured and contoured maps presented as Figures 4.61 and 4.62.

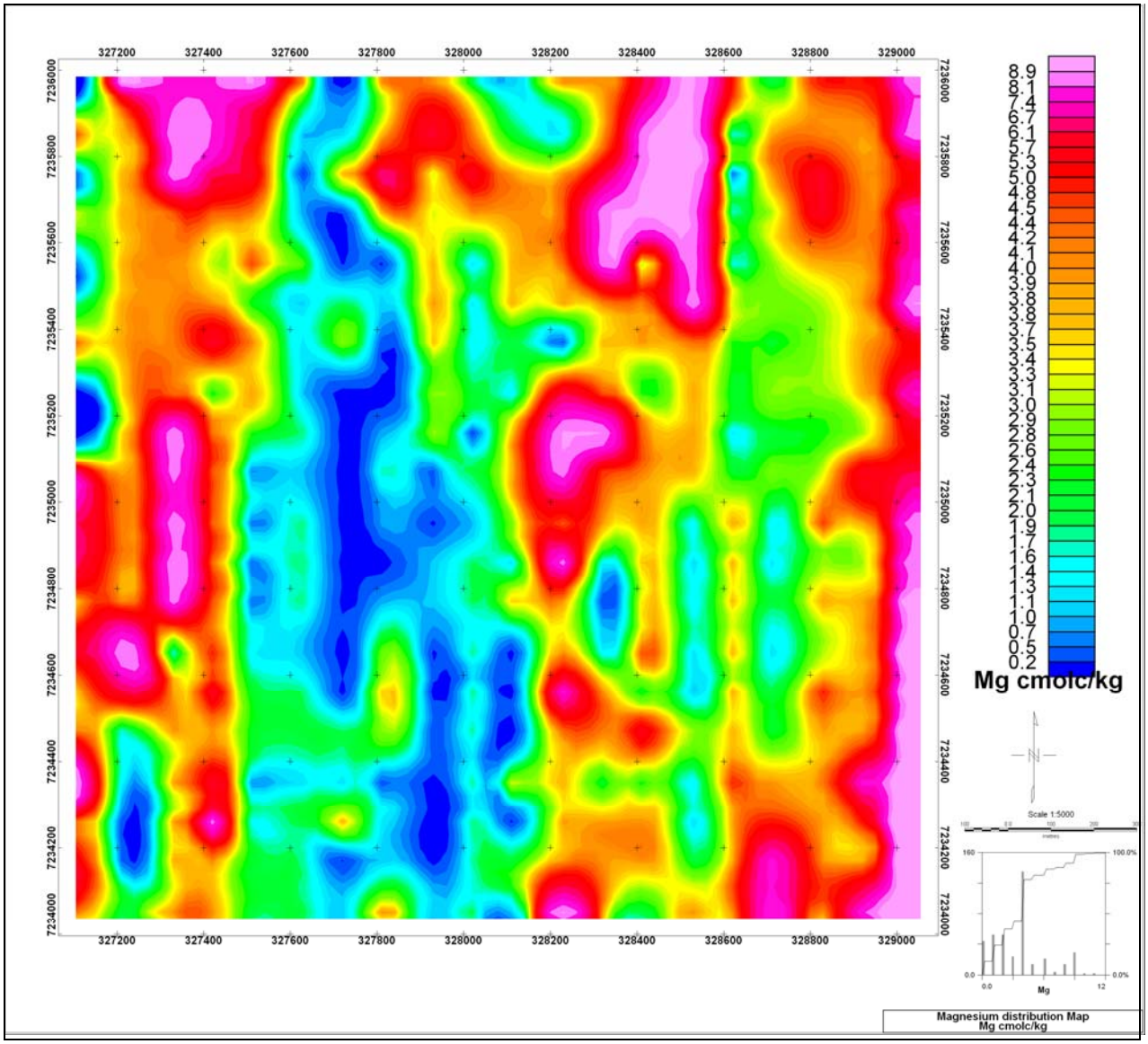

Figure 4.61: Non contoured map of spatial distribution of magnesium concentration in the soils of the study area

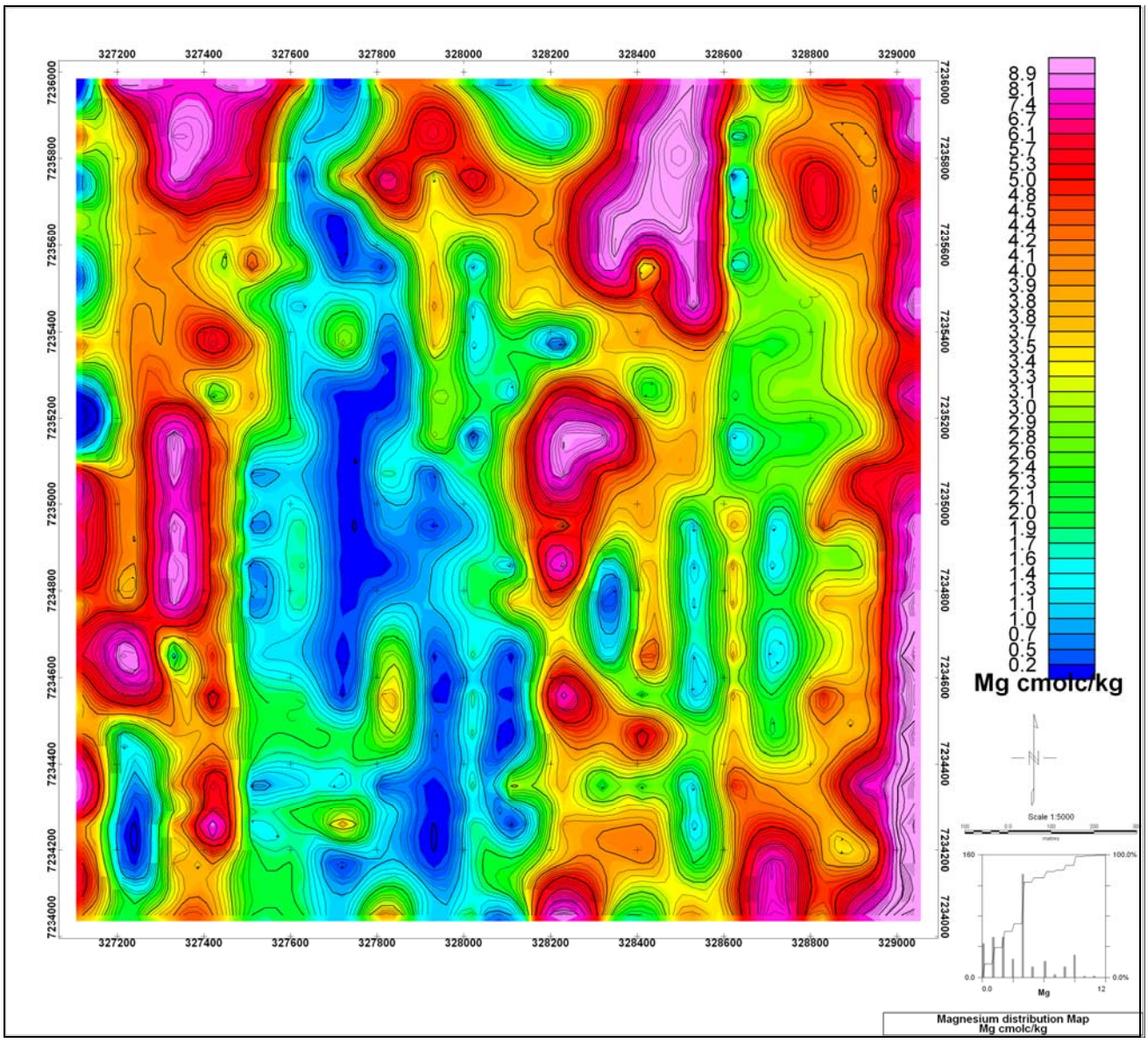

Figure 4.62: Contoured map of spatial distribution of magnesium concentration in the soils of the study area

The magnesium distribution is very similar to the calcium distribution. Mangnesium distribution being very similar to the calcium also has the same

general trend as K does. Furthermore, the concentration levels of bases are generally low in the ore bearing rocks.

The CEC values in the soil samples from the study area, as reported in Table 3.21, ranged from 1.1 $cmol_cKg^{-1}$ to 29.2 $cmol_cKg^{-1}$, with a mean of 8.2 $cmol_cKg^{-1}$. The histogram in Figure 4.63 and the non contoured and contoured maps in Figures 4.64 and 4.65 depict the histographical and spatial distribution of the CEC within the study area.

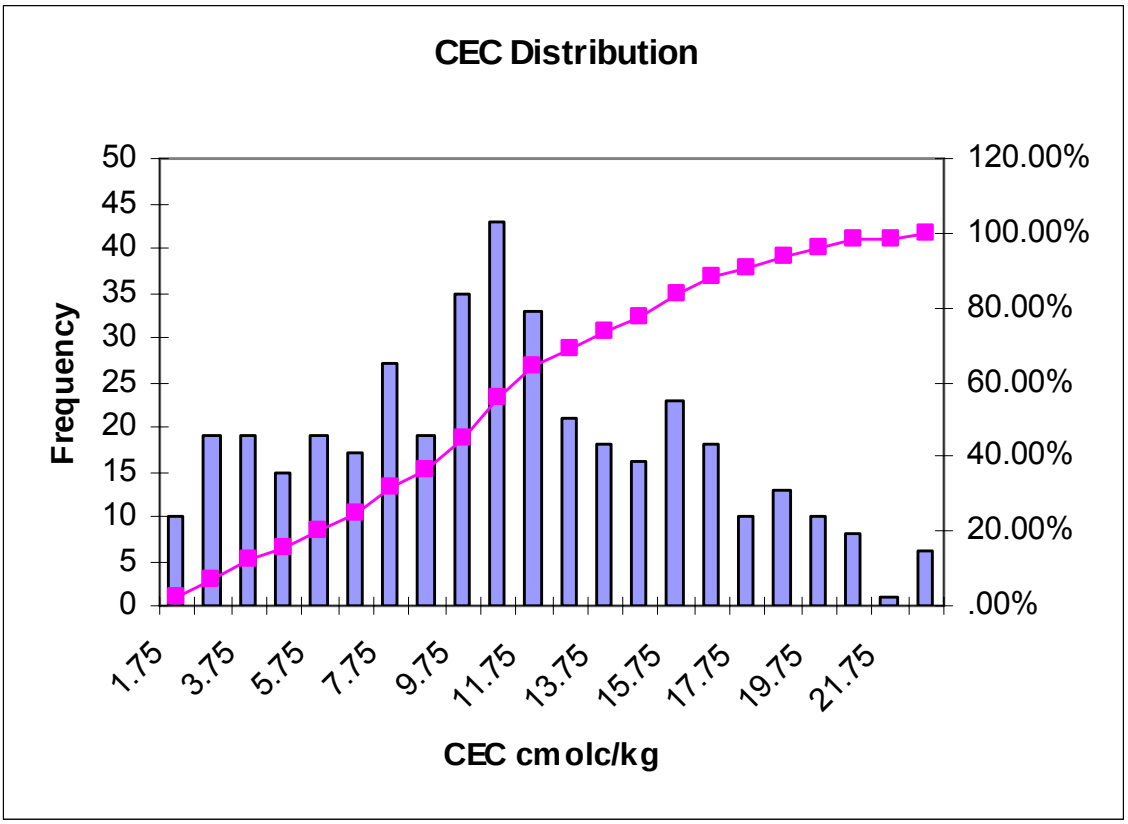

Figure 4.63: Cation exchange capacity values in the soil samples from the study area

The CEC shows a normal distribution and its polymodal in nature as it shows at least three populations.160 of the samples range between 7 and 13 and the mean is 10.49. Furthermore the CEC has a high correlation with calcium and magnesium (Table 4.3). As indicated in Table 4.3, these correlation values are 0.92 between CEC with magnesium, and 0.87 between CEC and calcium respectively. The CEC correlation with Na and K is also above 0.5. For Na, the CEC correlation is 0.74, and for K, it is 0.65.

Table 4.3: Correlation matrix of exchangeable bases and cation exchange capacity of soil samples from the study area

Parameter	Na	K	Ca	Mg	CEC
Na	1.00				
K	0.84	1.00			
Ca	0.81	0.72	1.00		
Mg	0.78	0.67	0.95	1.00	
CEC	0.74	0.65	0.87	0.92	1.00

The values of CEC form three almost continuous N-S anomaly zones in the western, eastern, and middle part of the study area. There is one N-S CEC hallow in the central part of the study area, in between two high zones as can be seen from the non contoured and contoured maps given in Figures 4.64 and 4.65 respectively.

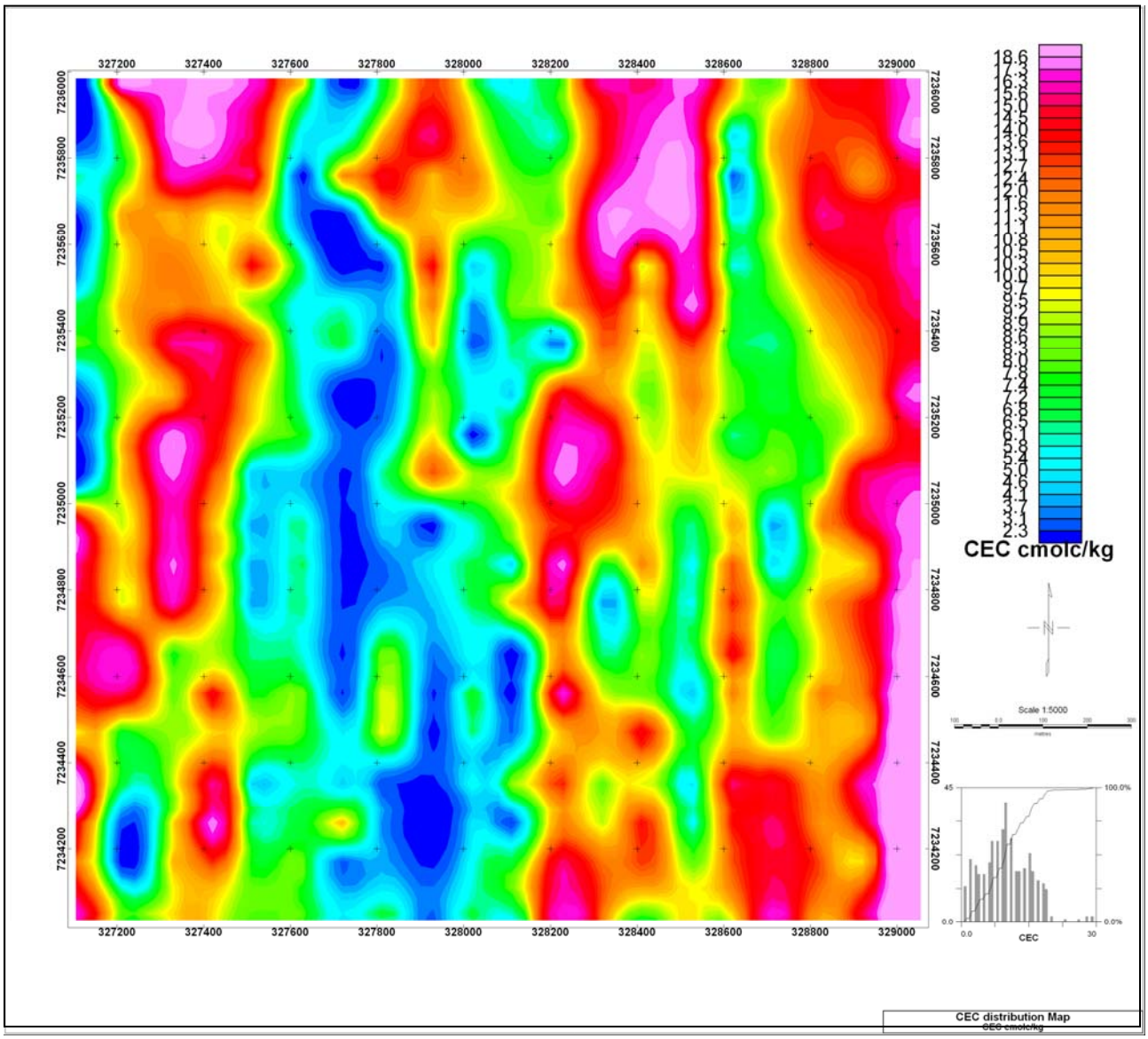

Figure 4.64: Non contoured map of spatial distribution of cation exchange capacity levels in the soils of the study area

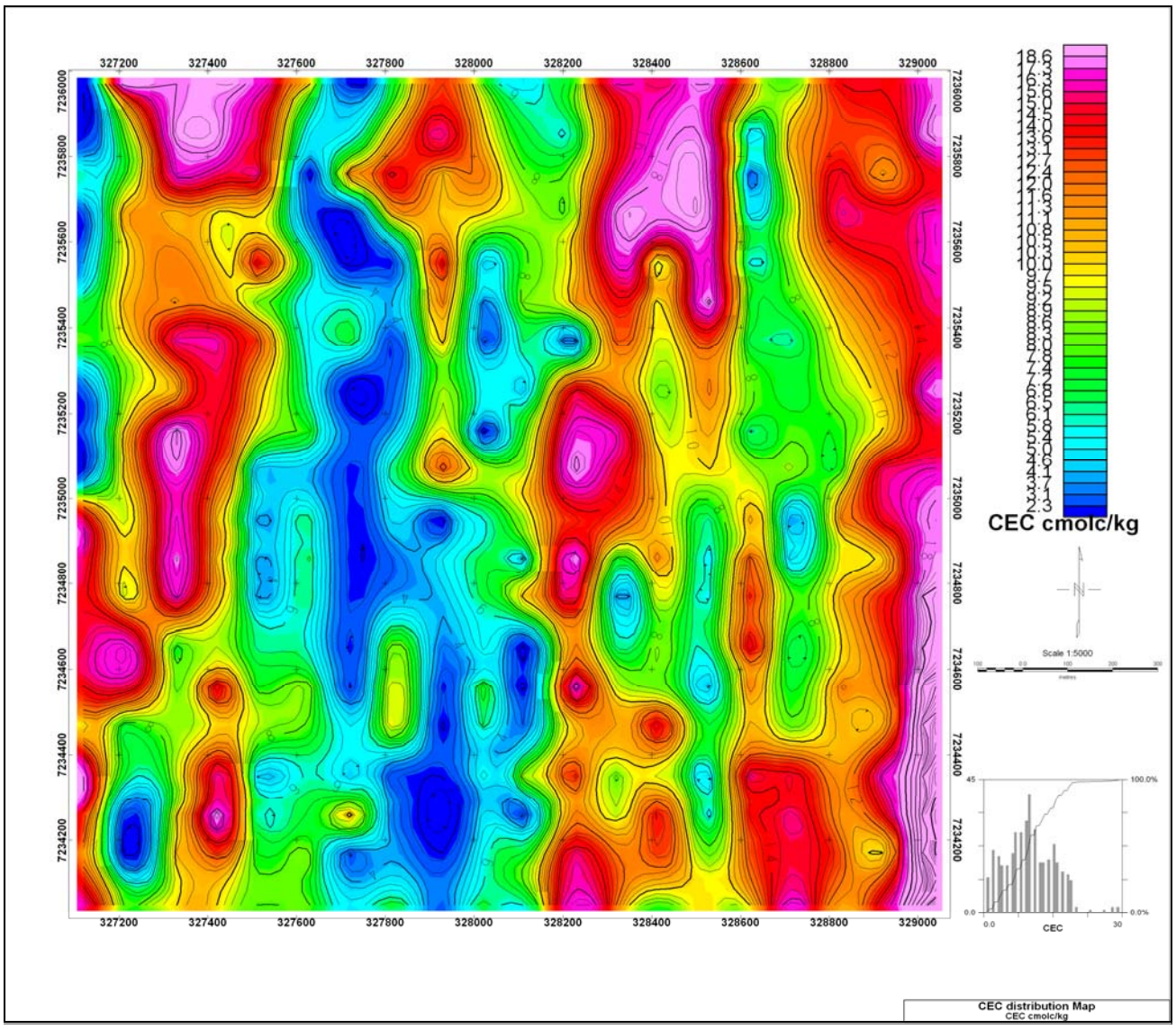

Figure 4.65: Contoured map of spatial distribution of cation exchange capacity levels in the soils of the study area

The exchangeable base saturation was calculated using the formula:

$$\text{Percent base saturation (\%)} = \frac{Na+K+Ca+Mg}{CEC}$$

Where Na = sodium; K = potassium; Ca = calcium; Mg = magnesium; CEC = cation exchange capacity. The non contoured and contoured maps for exchangeable base saturation were plotted and presented as Figures 4.66 and 4.67.

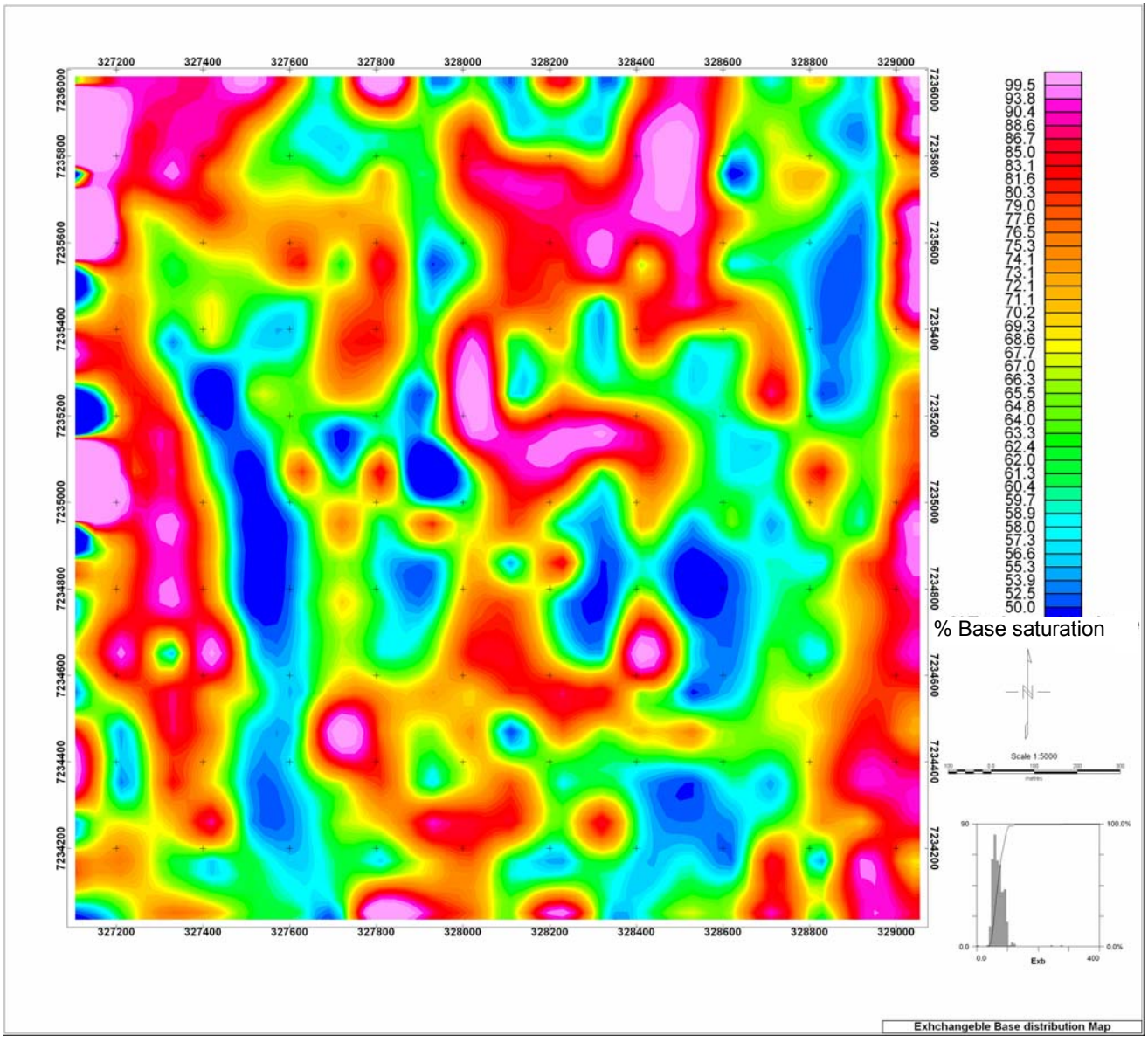

Figure 4.66: Non contoured map of spatial distribution of percent base saturation of the soils of the study area

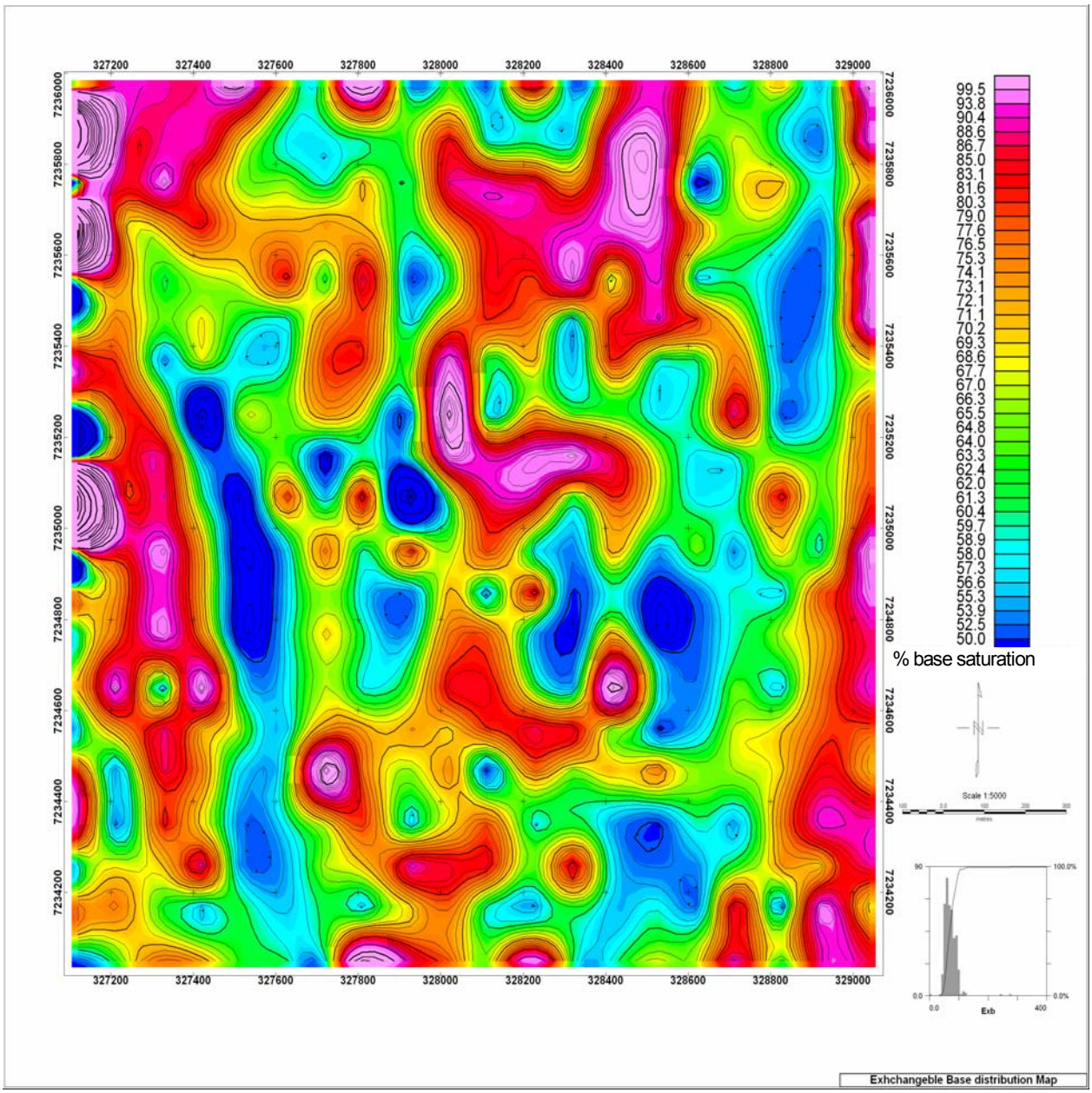

Figure 4.67: Contoured map of spatial distribution of percent base saturation of the soils of the study area

The distribution has pockets of high zones in the northern part and two high pockets in the southwestern and south eastern part of the area. There is one hallow of exchangeable iron bases around the mine site area.

4.4.1.6 Anions in soils

The chloride, sulphate and carbonate concentration values in the soil samples were determined as explained in Chapter Two and results reported in Chapter Three. A correlation matrix of the anions was plotted and is as shown in Table 4.4.

Table 4.4: Correlation matrix of chloride, sulphate and carbonate in soil samples from the study area

Parameter	Cl	SO_4	CO_3
Cl	1.00		
SO_4	0.98	1.00	
CO_3	0.77	0.76	1.00

The values for Cl concentration in the soil samples from the study area ranged from 0.2 $mgkg^{-1}$ to 11.9 $mgkg^{-1}$, with a mean of 7.63 $mgkg^{-1}$. The histogram in Figure 4.68 and the non contoured and contoured maps in Figures 4.69 and 4.70 depict the histographical and spatial distribution of the Cl concentration in the soils within the study area.

Chloride shows a normal staggered distribution that ranges between 0.2 and 11.9. The mean is 7.63 and the modal distribution is found between 6.25, 7.25 and 8.25 which have a frequency of 83, 89 and 90 respectively. Chloride has a very high correlation of 0.98 with sulfate and correlates with the carbonate at 0.77 (Table 4.4).This means that the distribution trends of the chloride, sulphate

and carbonate are very similar and this is evident in the corresponding gridded maps of each of the analysed anions.

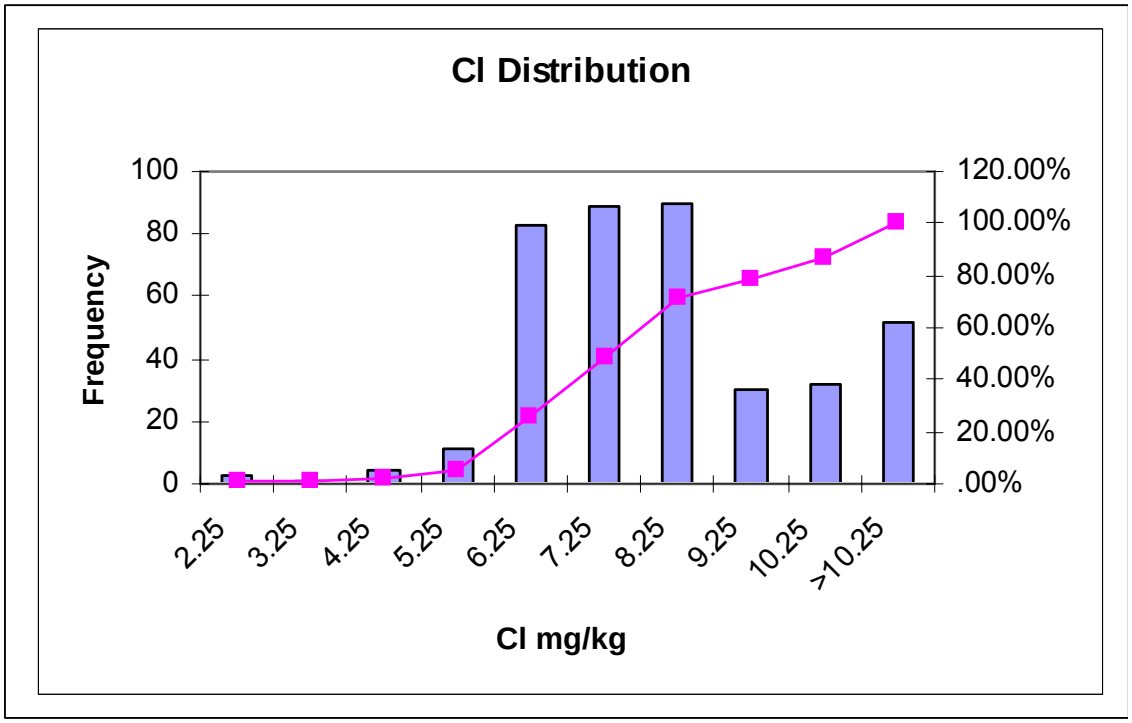

Figure 4.68: Chloride concentration values in the soil samples from the study area

From Figures 4.69 and 4.70 for non contoured and contoured maps of chloride distribution in the soil samples, it can be seen that chloride is generally low in the northern part of the study area except for two small pockets in the eastern and western corners. There is a chloride hallow in the north eastern part of the study area. High and anomalous values are found in the central southern part of the study area (Figures 4.69 and 4.70).

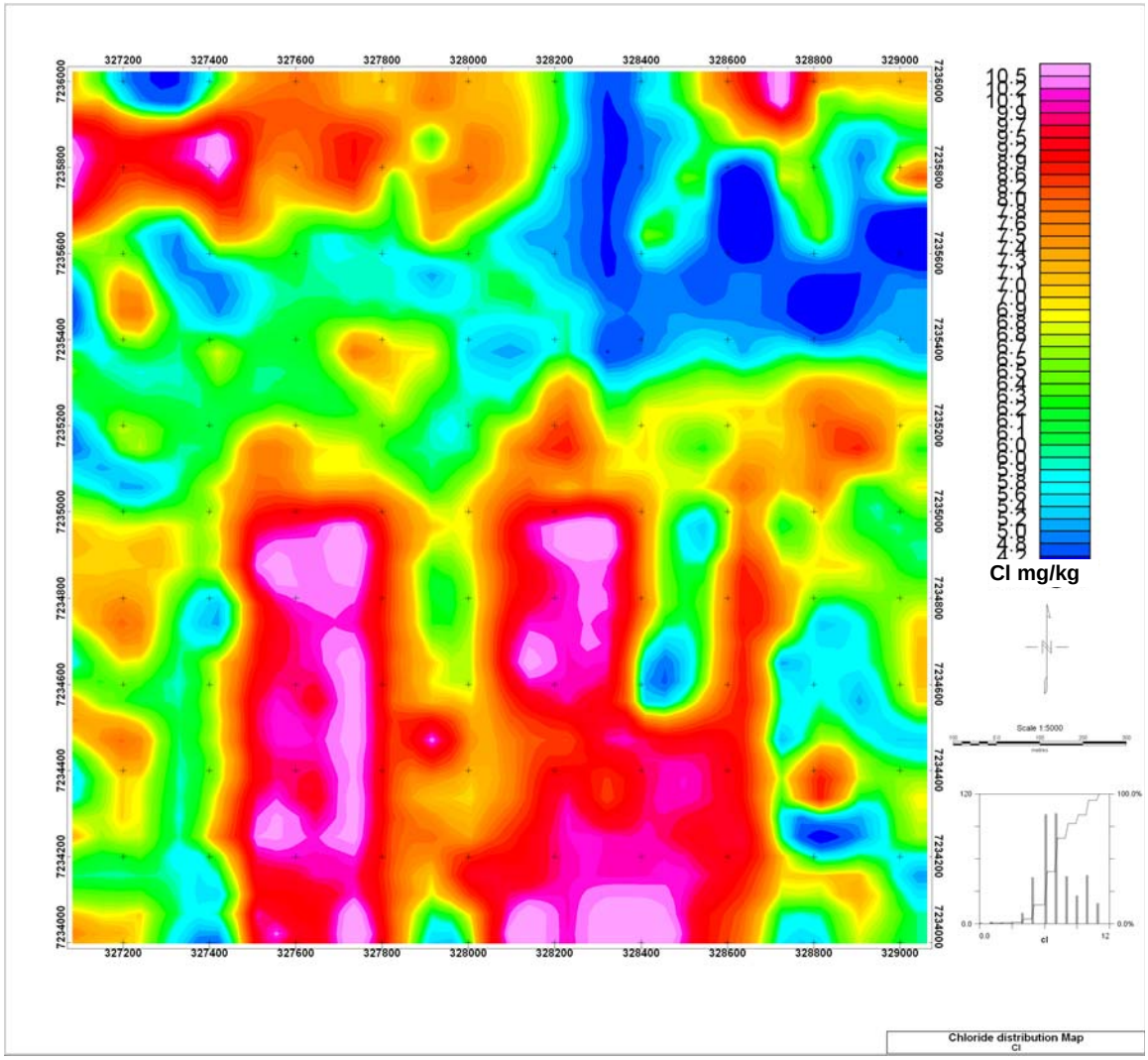

Figure 4.69: Non contoured map of spatial distribution of chloride concentration in soils of the study area

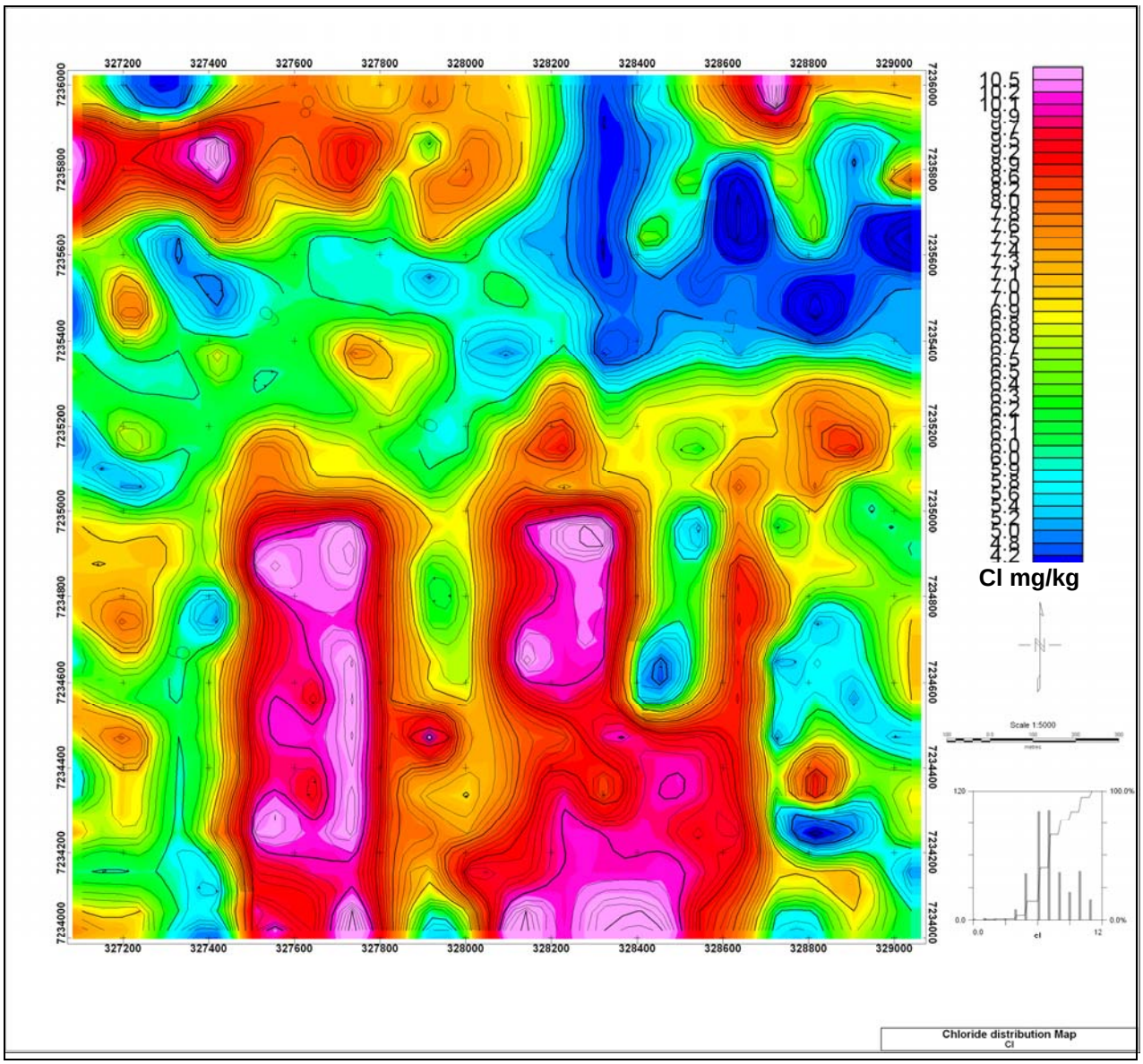

Figure 4.70: Contoured map of spatial distribution of chloride concentration in soils of the study area

As reflected in Table 3.26, the values for SO_4 concentration in the soil samples from the study area ranged from 2.1 mgL^{-1} to 47.5 mgL^{-1}, with a mean of 19.36 mgL^{-1}. The histogram in Figure 4.71 and the non contoured and contoured maps

in Figures 4.72 and 4.73 depict the histographical and spatial distribution of the SO_4 concentration in the soils within the study area.

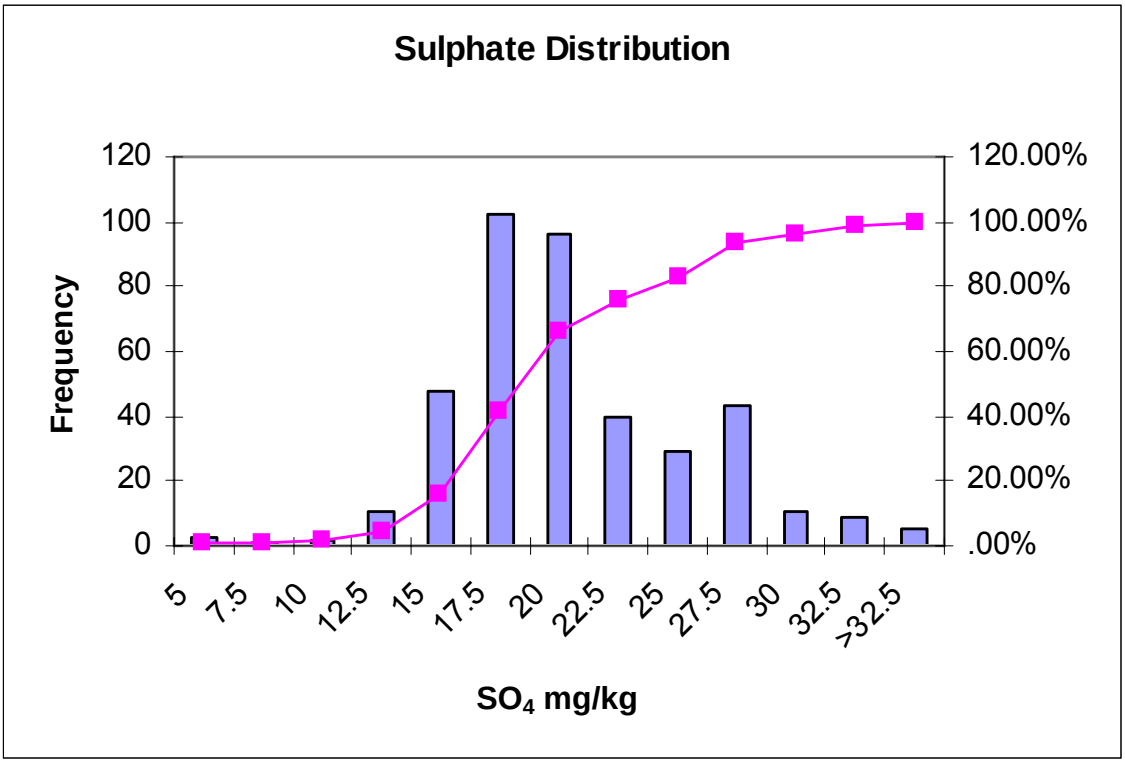

Figure 4.71: Sulphate concentration values in the soil samples from the study area

Sulphate has a normal distribution ranging between 2.1 and 43.6. The mean is 19.35 and 17.5 is the mode with 102 samples. Sulphate has a very high correlation of 0.98 with chloride and correlation of 0.755 with carbonate. Sulphate distribution is very similar to the chloride one. High and anomalous values are found in the central part of the study area as reflected in Figures 4.72 and 4.73

for the non contoured and contoured maps. There is a sulphate hallow in the north eastern part of the study area (Figures 4.72 and 4.73).

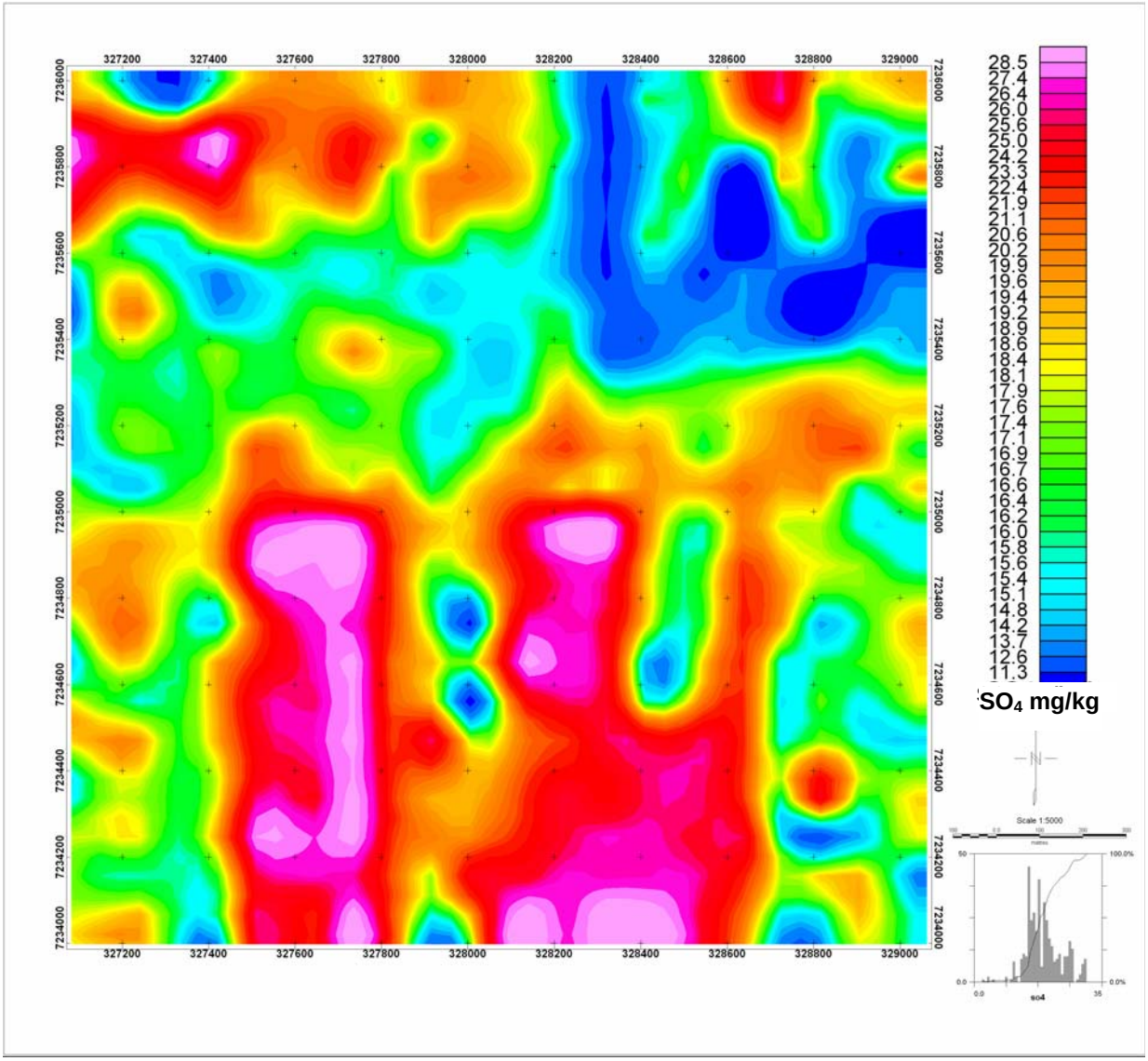

Figure 4.72: Non contoured map of spatial distribution of sulphate concentration in soils of the study area

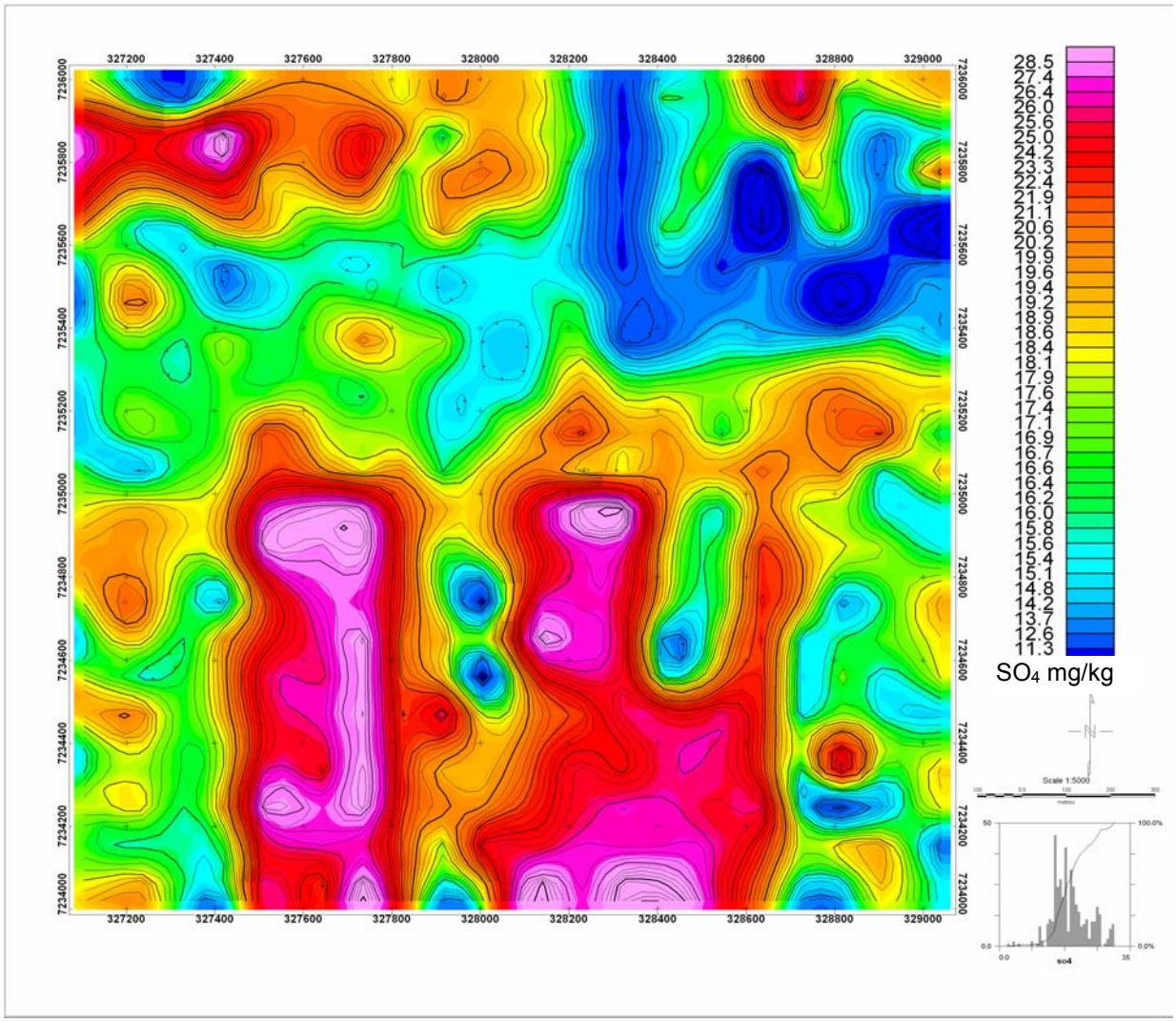

Figure 4.73: Contoured map of spatial distribution of sulphate concentration in soils of the study area

The values for CO_3 concentration (measured in terms of $CaCO_3$ equivalent) in the soil samples from the study area, as reported in Table 3.26, ranged from 5.1 gkg^{-1} to 59.1 gkg^{-1}, with a mean of 40.98 gkg^{-1}. The histogram in Figure 4.74 and the non contoured and contoured maps in Figures 4.75 and 4.76 depict the histographical and spatial distribution of the CO_3 concentration in the soils within the study area.

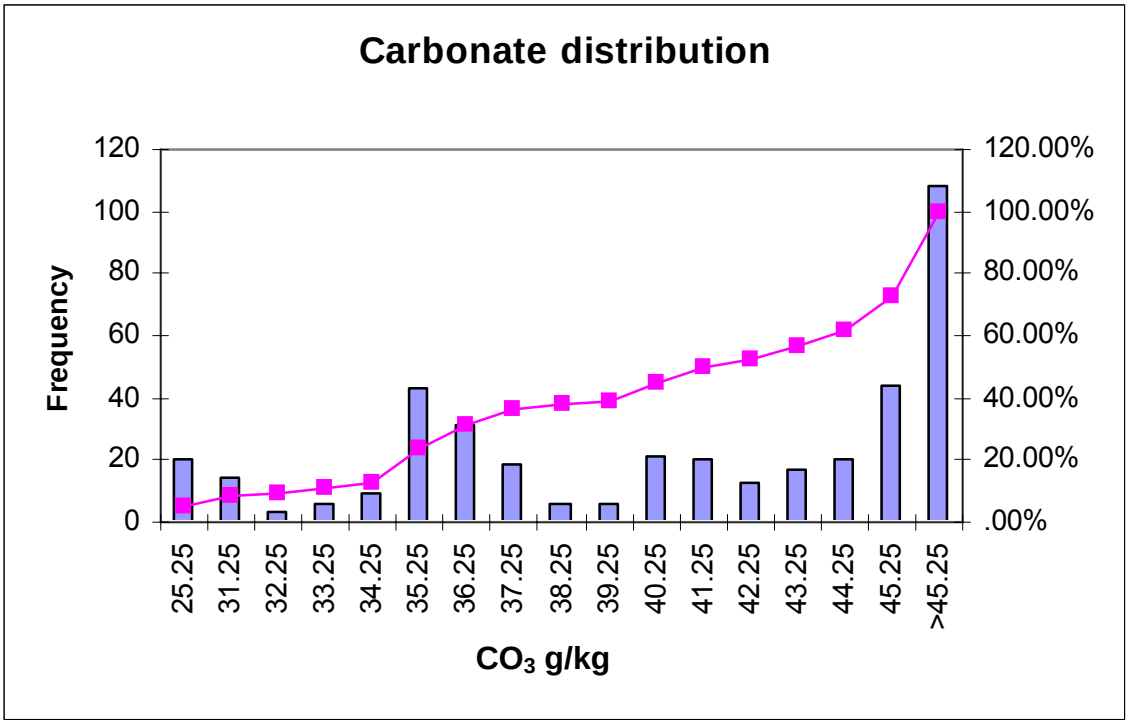

Figure 4.74: Carbonate concentration values in the soil samples from the study area

It can be deducted from the non contoured and contoured maps presented in Figures 4.75 and 4.76 that carbonate has a negatively skewed normal distribution. The distribution ranges between 5.1 and 59.1. Most of the values fall between 22 and 59. Carbonate has a similar correlation of 0.77 and 0.755 with chloride and sulphate (Table 4.4).

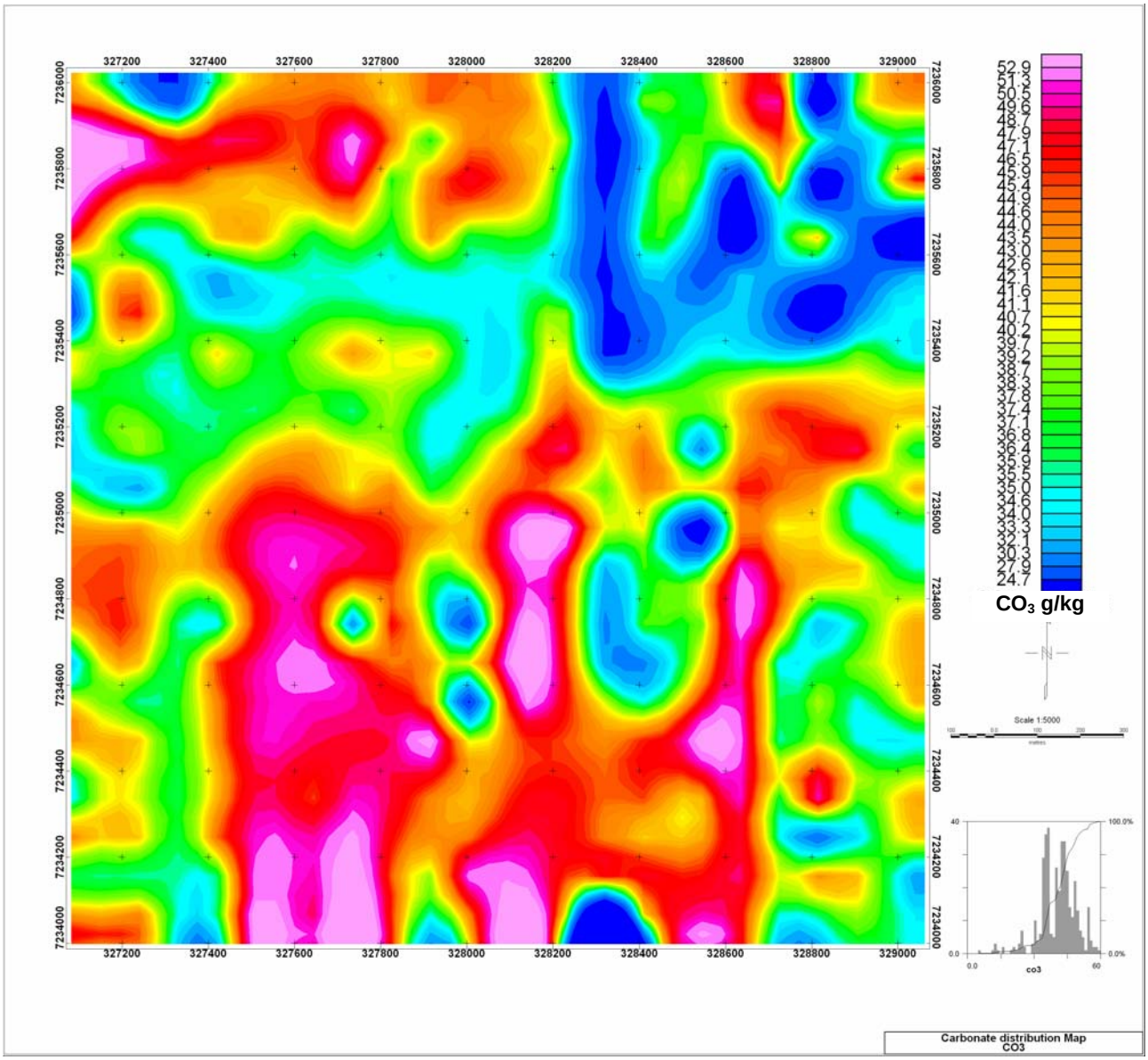

Figure 4.75: Non contoured map of spatial distribution of carbonate concentration in soils of the study area

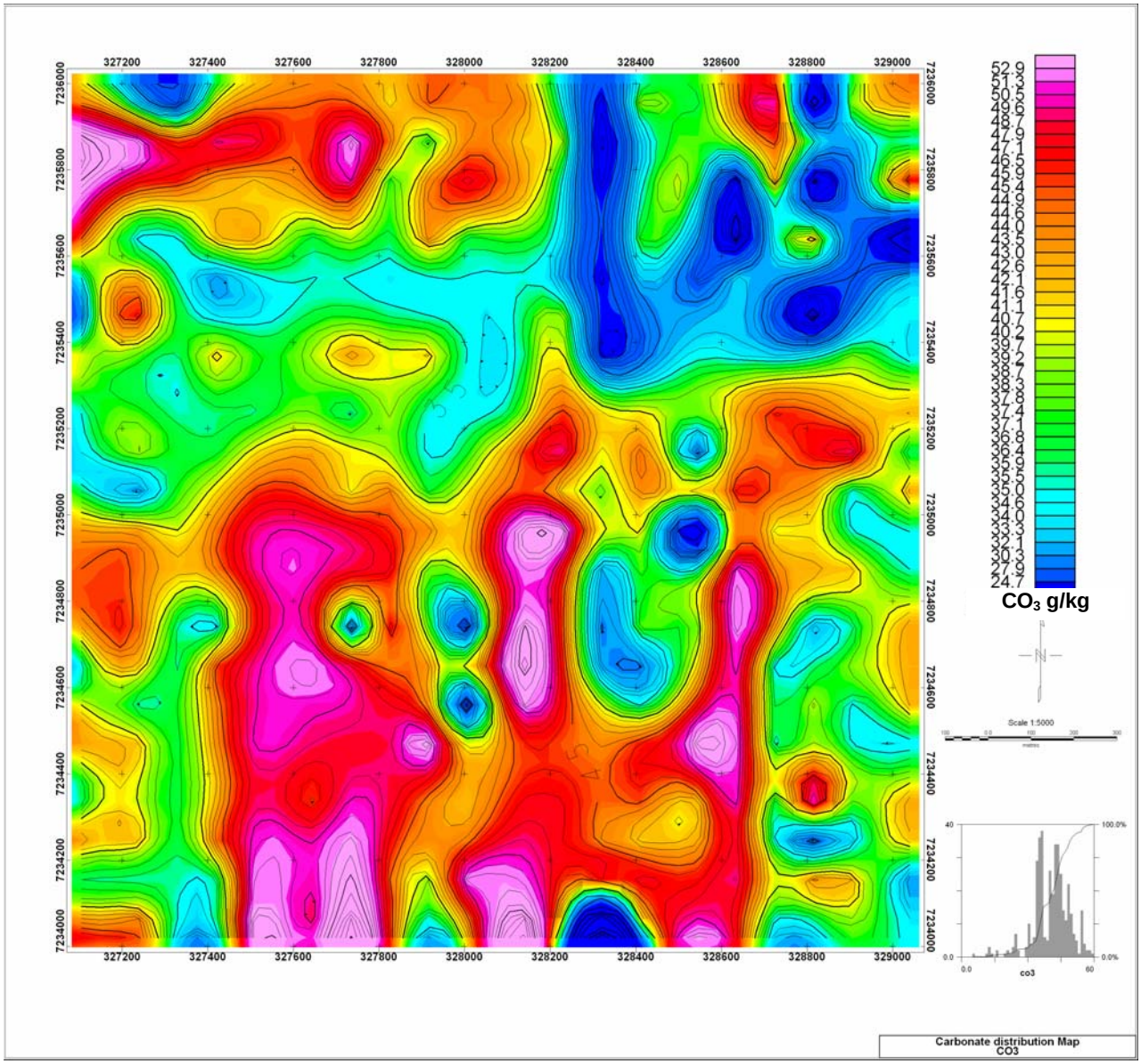

Figure 4.76: Contoured map of spatial distribution of carbonate concentration in soils of the study area

The carbonate distribution displays high and anomalous values in the central part of the study area. The northern part of the area generally has low values and there is a carbonate hallow in the northeastern part of the study area (Figure 4.75 and 4.76). Generally where the cations display high values the anions are low and vice versa.

4.4.2 Vegetation chemistry

4.4.2.1 Manganese concentration in leaves

The Mn concentration levels in the samples of leaves obtained were significantly high and ranged from 26 μg g^{-1} to 3611 μg g^{-1} as shown in the histogram in Figure 4.77 and the non contoured and contoured maps in Figures 4.78 and 4.79 respectively. The Mn concentration levels in the leaves depict as plotted in the histogram in Figure 4.77, a log normal distribution though it is positively skewed as described by Miller and Miller (1994), The threshold was at 1100 with 20 samples above the threshold value and with a few outliers as well as one population. The colours reflected in the contoured and non contoured maps presented in Figures 4.78 and 4.79 as bluish, greenish, yellowish, brownish and reddish colour shades were unevenly spatially distributed and depicted prograded Mn concentration levels. Colour gradation in the non contoured and contoured maps (Figures 4.78 and 4.79), is reflected from blue for the low Mn

concentration level progressively to green, yellow, brown, red and pink for the high Mn concentration level in the study site.

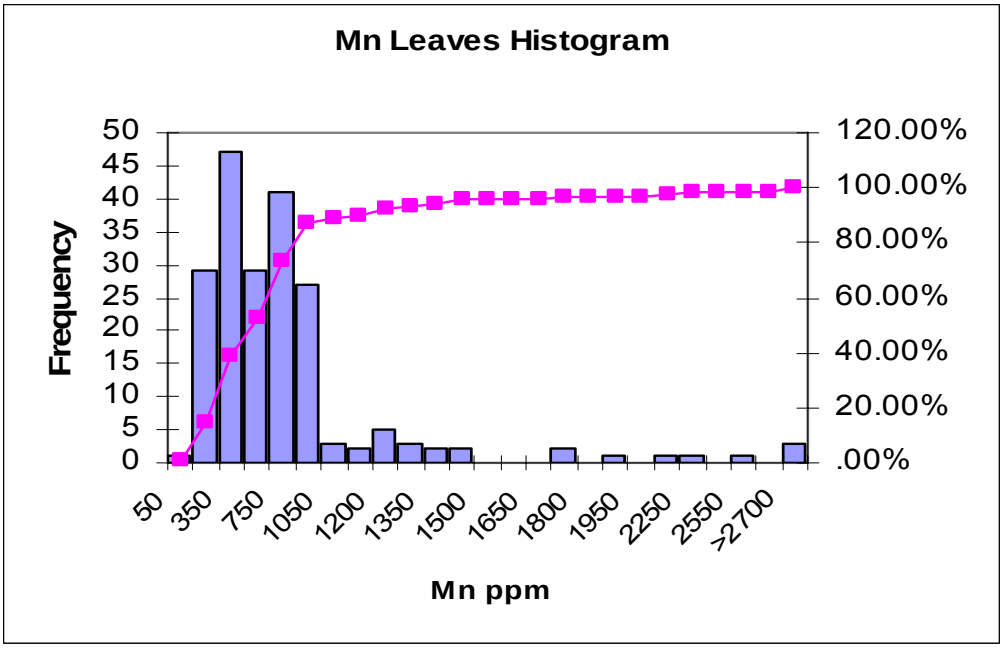

Figure 4.77: Scatter plot of manganese concentration values in samples of leaves from the study area

An attempt was made to correlate the Mn concentration levels between the leaves and the soils in the study area. The correlation matrix is presented in Table 4.5. There is a positive correlation of 0.11 between manganese in the soil and in the leaves.

Table 4.5: Correlation matrix of iron between leaves and soil from the study area

Parameter	Mn soil	Mn leaves
Mn in soil	1.00	

Mn in leaves	0.11	1.00

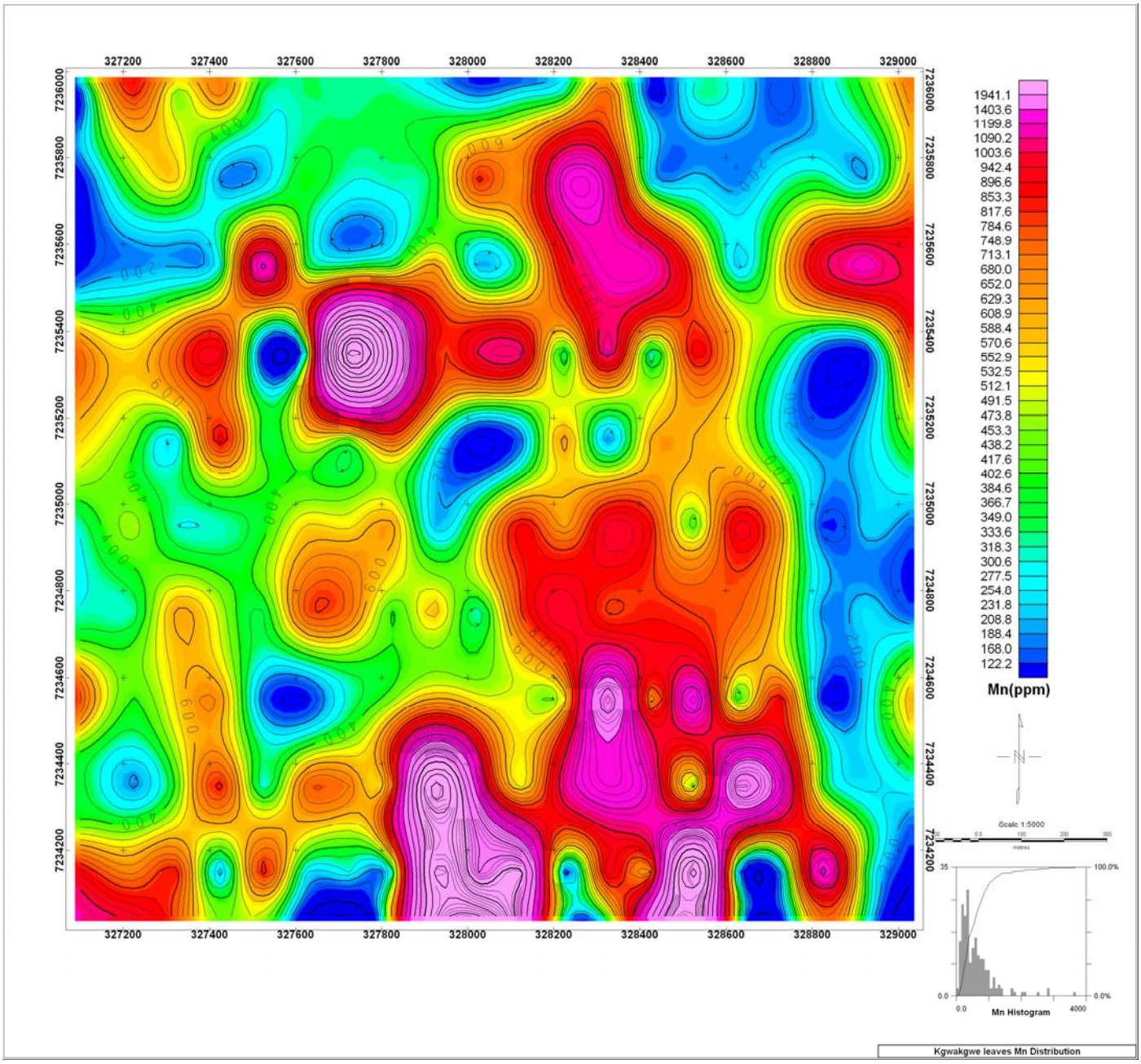

Figure 4.78: Contoured map of spatial distribution of manganese concentration in the leaves of plants from the study area

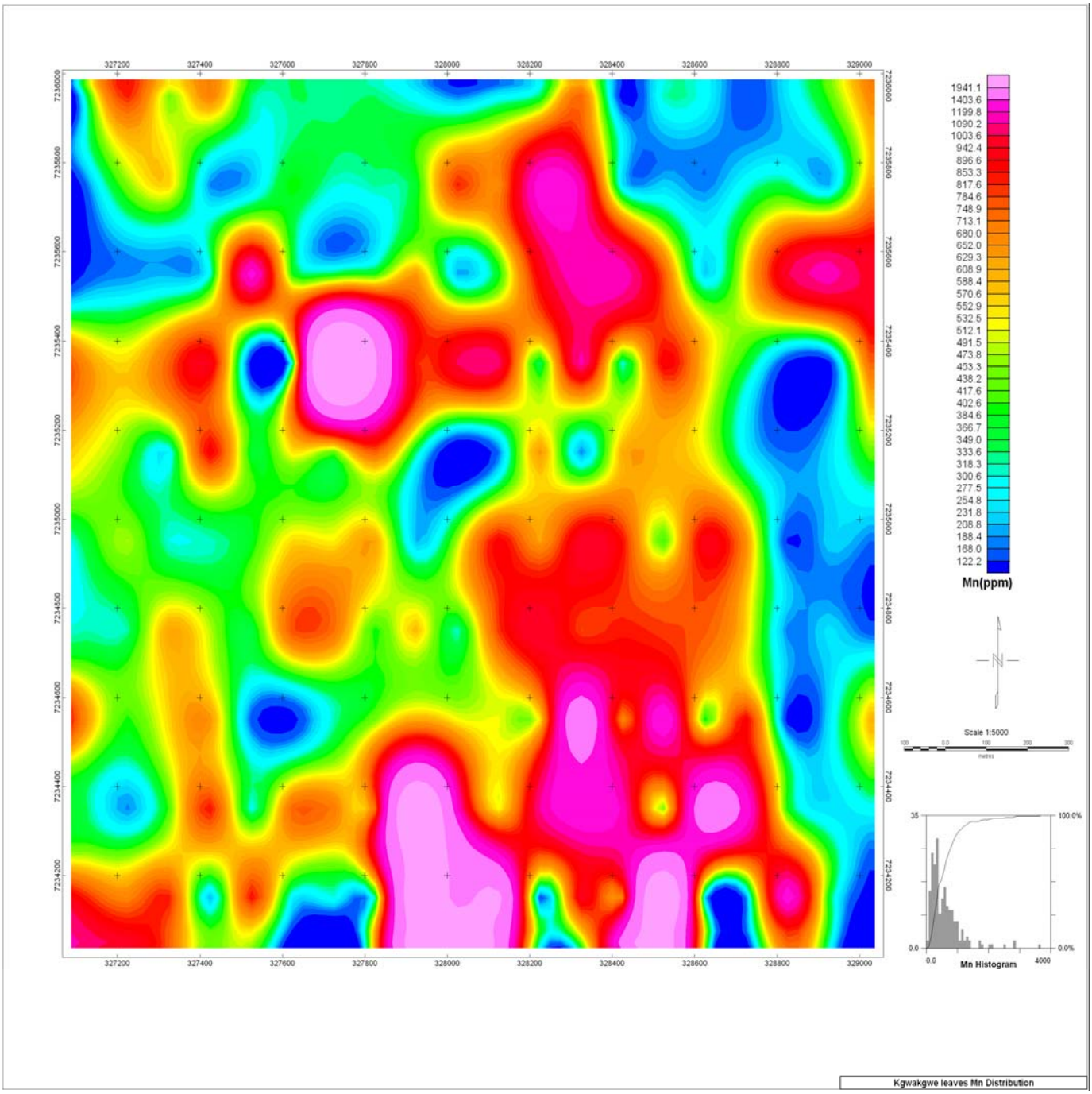
327200
327400
327600
327800
328000
328200
328400
328600
328800
329000
7236000
7235800
7235600
7235400
7235200
7235000
7234800
7234600
7234400
7234200
1941.1
1403.6
1199.8
1090.2
1003.6
942.4
896.6
853.3
817.6
784.6
748.9
713.1
680.0
652.0
629.3
608.9
588.4
570.6
552.9
532.5
512.1
491.5
473.8
453.3
438.2
417.6
402.6
384.6
366.7
349.0
333.6
318.3
300.6
277.5
254.8
231.8
208.8
188.4
168.0
122.2
Mn(ppm)
Scale 1:5000
metres
35
100.0%
0.0
0.0%
0.0
4000
Mn Histogram
Kgwakgwe leaves Mn Distribution

Figure 4.79: Non contoured map of spatial distribution of manganese concentration in the leaves of plants from the study area

The high Mn concentration levels in samples of leaves were prominent in the southwestern part of the study area to the west of the mine workings whereas the low to medium Mn concentration levels were observed in samples located further away from the mine workings as depicted on the non contoured and contoured maps in Figures 4.78 and 4.79 respectively. The high concentration levels of Mn in the leaves at these sites could be attributed to their closeness to the mine workings and areas of topographic lows. Concentration levels of Mn decreased directly with increase in distance from the mine workings, Mn orebodies and stockpiles.

4.4.2.2 Iron concentration in leaves

The Fe concentration levels in the samples of leaves obtained were significantly high and ranged from 171 μg g^{-1} to 1742 μg g^{-1} as shown in the histogram in Figure 4.80 and the non contoured and contoured maps in Figures 4.81 and 4.82 respectively. The Fe concentration levels in the leaves shows as plotted in the histogram presented in Figure 4.80. The Fe in the leaves displays a unimodal normal with a skewness of 2.57. The distribution has a threshold around 950 whereby there were 25 samples above the threshold level. The colours reflected in the contoured and non contoured maps presented in Figures 4.81 and 4.82 as

bluish, greenish, yellowish, brownish and reddish colour shades were unevenly spatially distributed and depicted prograded Fe concentration levels. Colour gradation in the non contoured and contoured maps (Figures 4.81 and 4.82), is reflected from blue for the low Fe concentration level progressively to green, yellow, brown, red and pink for the high Fe concentration level in the study site.

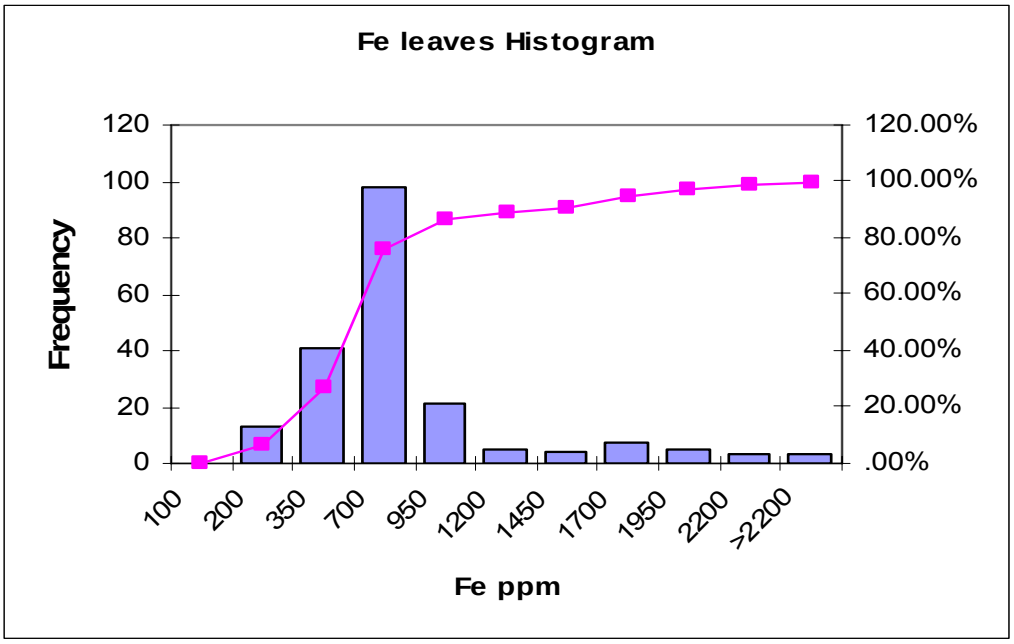

Figure 4.80: Iron concentration values in samples of leaves of plants from the study area

An attempt was made to correlate the Fe concentration levels between the leaves and the soils. The correlation matrix is presented in Table 4.6. There is a negative correlation between the iron in the soil and in the leaves.

Table 4.6: Correlation matrix between leaves and soil samples from the study area

Parameter	Fe soil	Fe leaves
Fe in soil	1.00	
Fe in leaves	-0.02	1.00

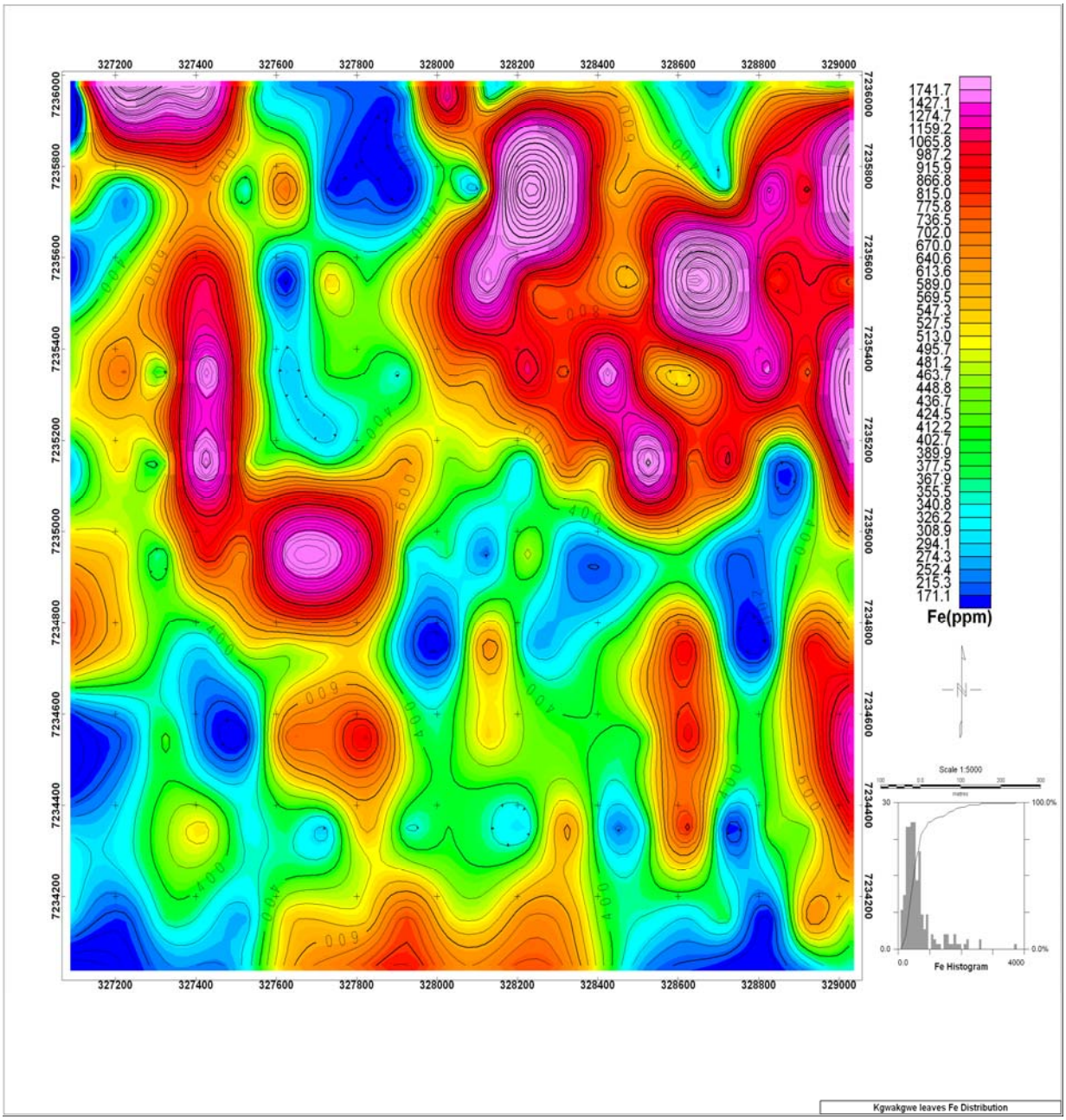

Figure 4.81: Contoured map of spatial distribution of iron concentration in the leaves of plants from the study area

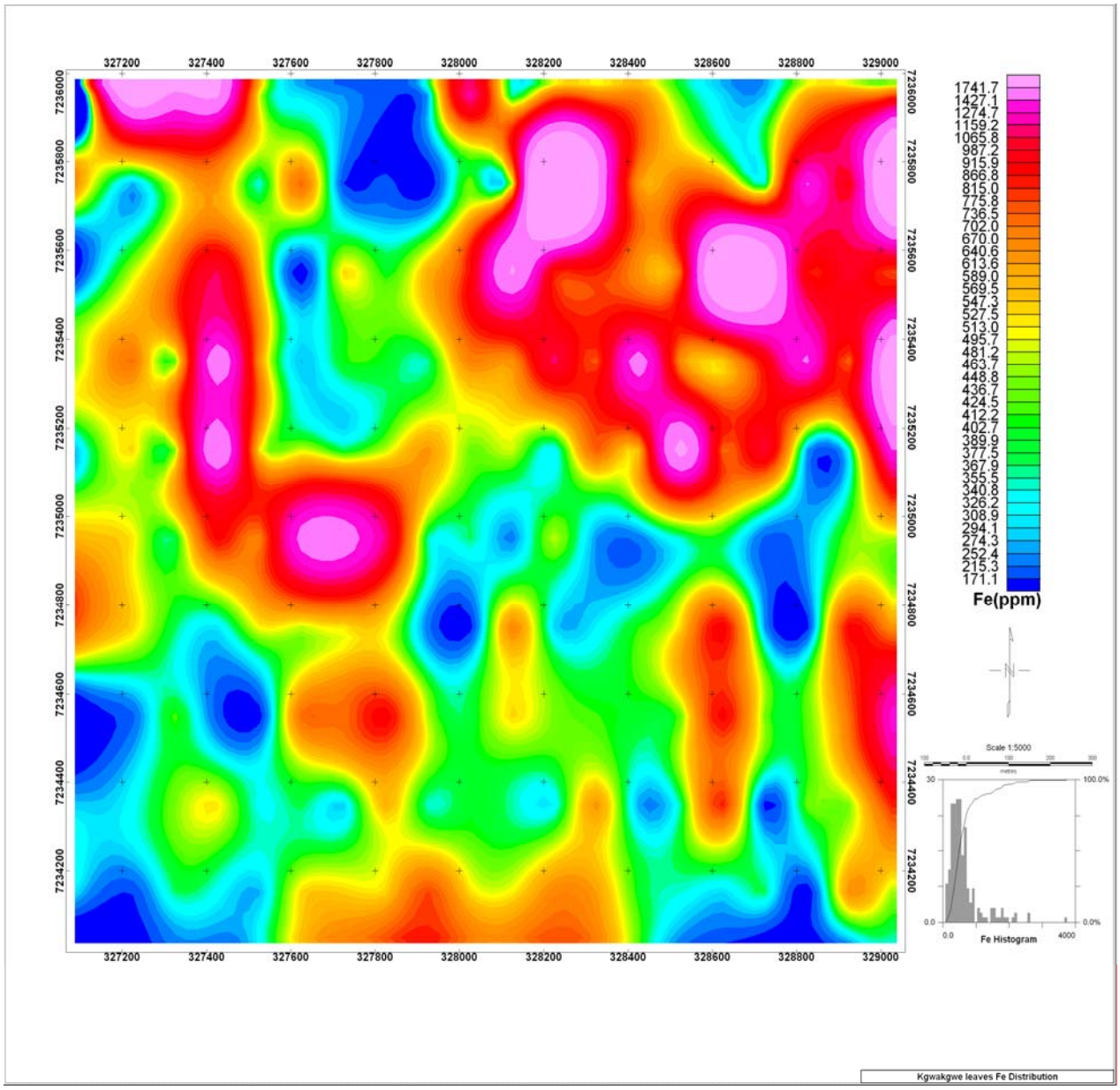

Figure 4.82: Non contoured map of spatial distribution of iron concentration in the leaves of plants from the study area

The low Fe concentration levels in leaves were prominent in the southwestern part of the study area to the west of the mine workings whereas the medium to high Fe concentration levels were observed in samples of leaves located further away from the mine workings as depicted on the non contoured and contoured maps in Figures 4.81 and 4.82 respectively. The low concentration levels of Fe in leaves at the sites enriched with Mn could similarly be attributed to the closeness of the mine workings and areas of topographic lows. Concentration levels of Fe significantly increased as one moved away from the mine workings, Mn orebodies and stockpiles.

4.4.2.3 Relationship between manganese and iron concentrations in leaves

Assay data was plotted and histograms of the two elements were made and are reflected in Figure 4.83. There is a strong correlation factor of 0.98 between the Iron and Manganese. Even the range of the data between the two elements is very close.

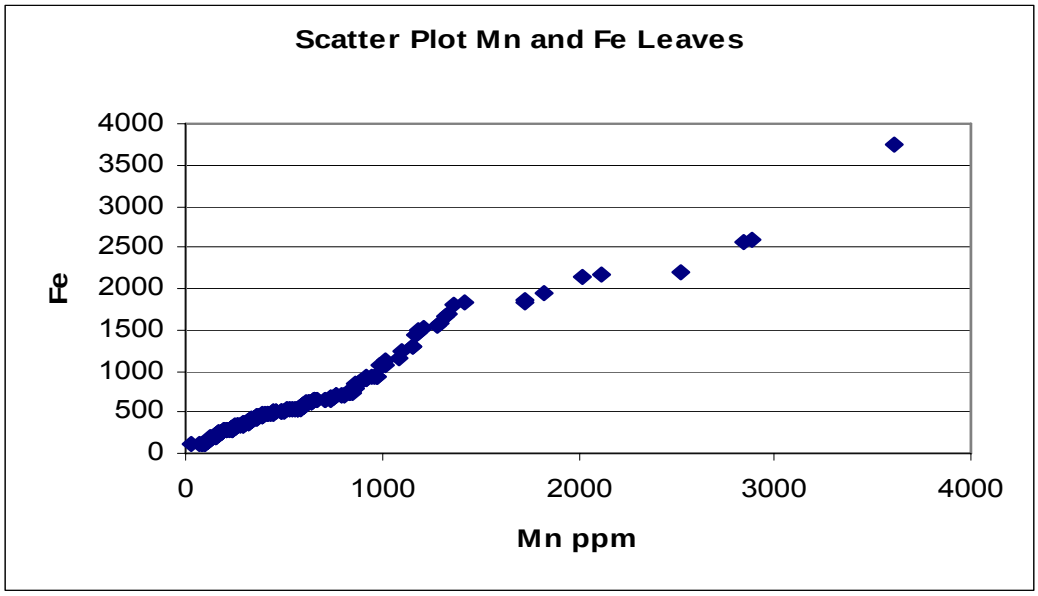

Figure 4.83: Scatter plot of manganese and iron concentration values in samples of leaves from the study area

Iron content in leaves is low in the quarry sites (SW) and on the Kgwakgwe hills. The anomalies are in the north eastern parts of the study area. There is equally a big petal shaped anomaly that is surrounded by an immediate decrease of the iron. The southern part of the area, which is close to the Mn, mines, has low iron content as opposed to the northern parts (Figure 4.84). The Mn content in leaves on the other hand is very high around the quarry sites and on the Kgwakgwe hills. Manganese is generally low in the northern part of the area with the lowest points being in the north western parts of the map area. The south western parts of the study area have very low Mn concentrations. The anomalous Mn form pockets in the south eastern part of the map area (Figure 4.84).

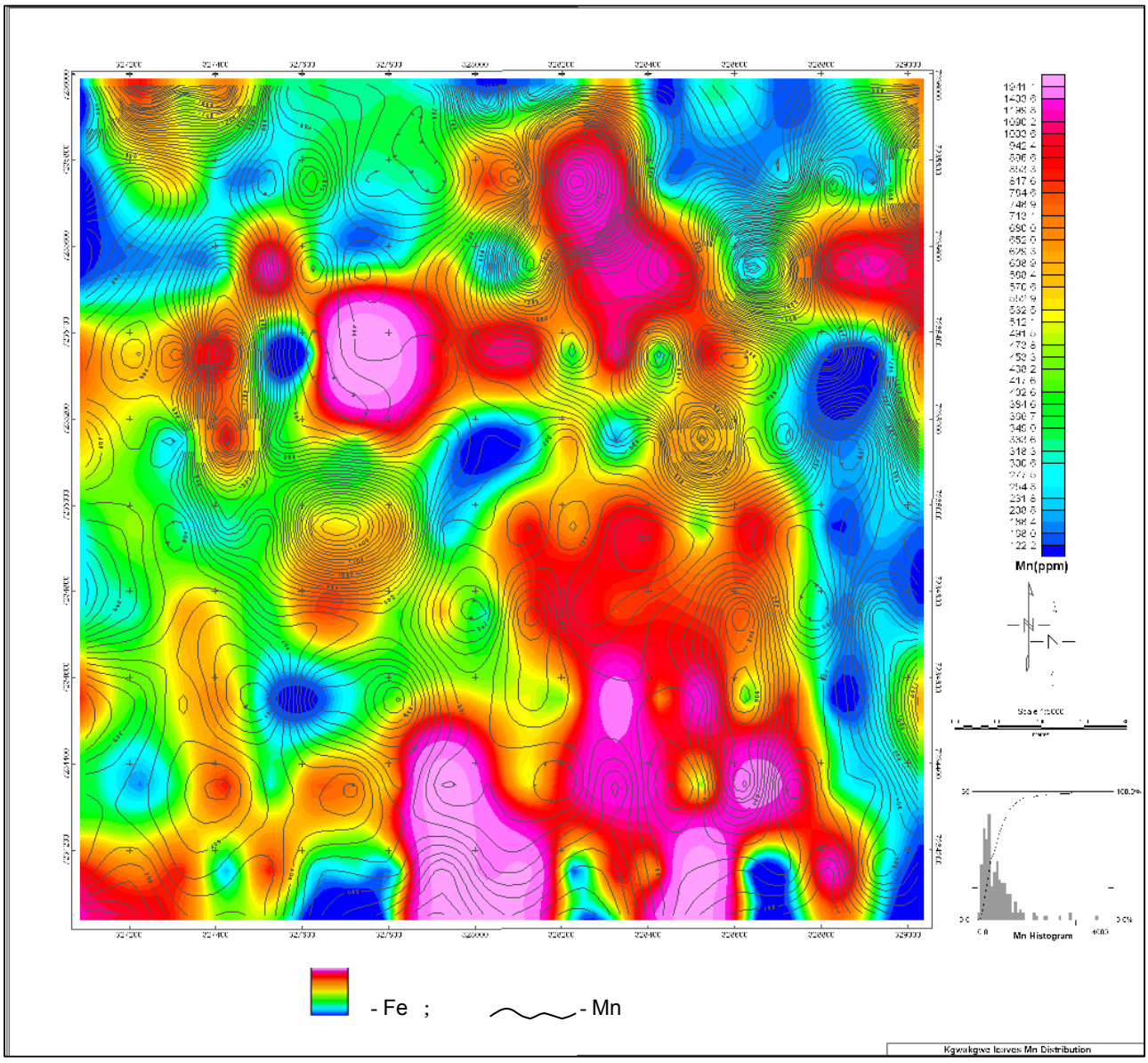

Figure 4.84: Map of spatial distribution of iron concentration and manganese concentration overlay in the leaves of plants from the study area

4.5 GENERAL ENVIRONMENTAL IMPLICATIONS

4.5.1 Effect of manganese and iron on soils and vegetation

Scatter plots of the organic carbon in comparison to electrical conductivity and pH were plotted (Figures 4.85 and 4.86), and the spatial map of TOC with EC overlay presented in Figures 4.87. The scatter plot of pH and TOC shows an exponential type of distribution. The TOC increases as the pH increases, implying a linear relationship between TOC and pH. The EC is very low for some of the samples then it steadily increases until it reaches a plateau around 120 μScm^{-1}. The sample with no organic carbon shows EC values ranging between 40 μScm^{-1} and 100 μScm^{-1}.

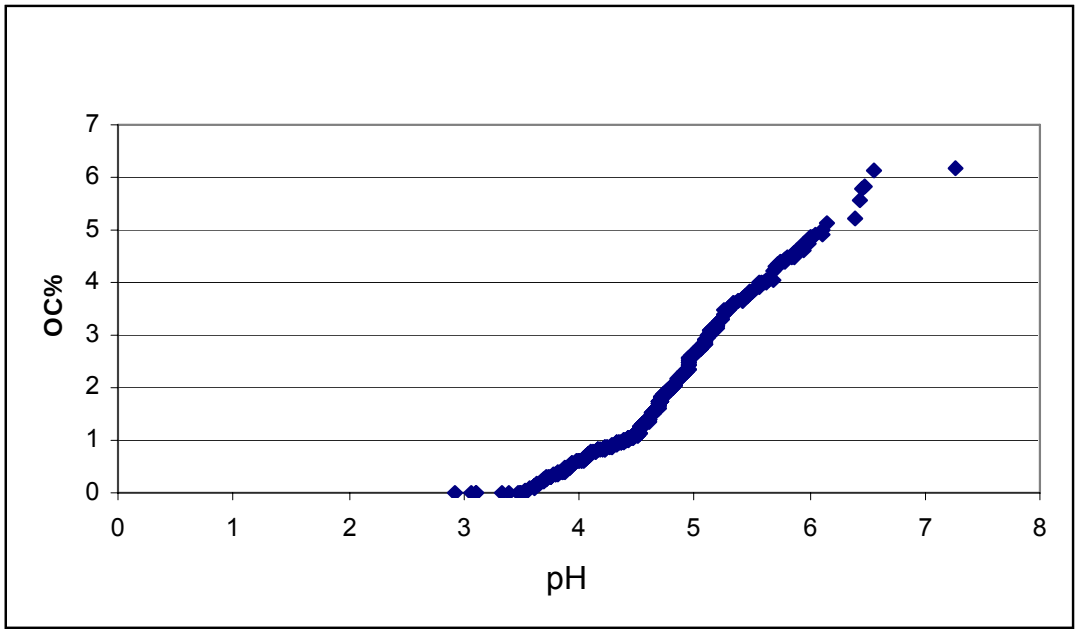

Figure 4.85: Scatter plot of pH and total organic carbon content values in samples of leaves from the study area

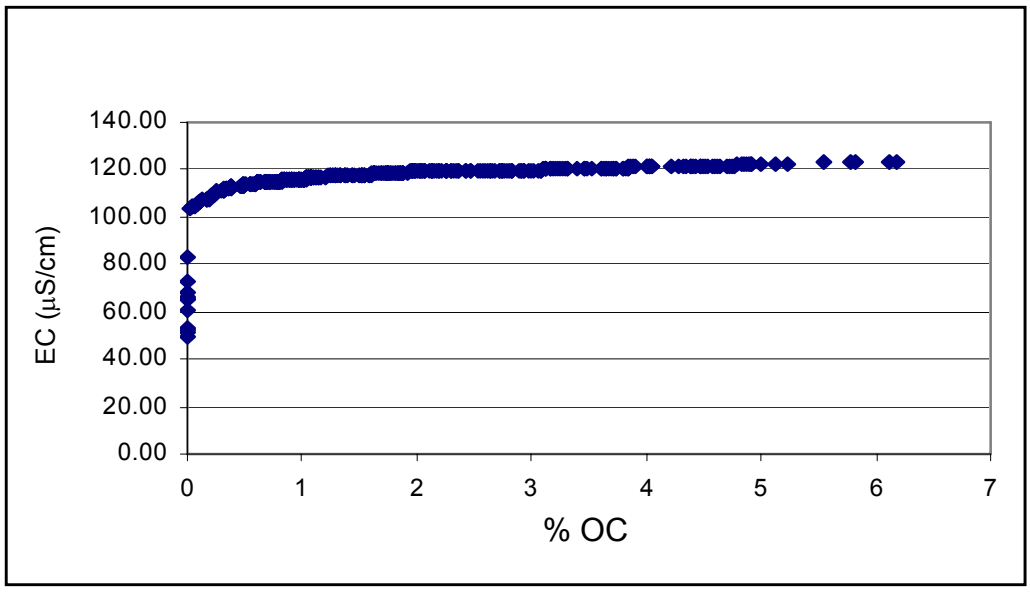

Figure 4.86: Scatter plot of total organic carbon and electrical conductivity of soil samples from the study area

The Fe concentration values in samples of leaves and in soil samples from the study area were plotted and the graph presented in Figure 4. 88. The graph indicated one major population with a couple of outliers. Similarly, Mn concentration values in samples of leaves and in soil samples from the study area were graphically presented in Figure 4.89. The plot reflected one major population and two subpopulations with a couple of outliers.

Looking at all the gridded maps of spatial distribution of Fe concentration levels and pH overlay in soils (Figure 4.90), spatial distribution of Mn concentration levels and pH overlay in soils (Figure 4.91), spatial distribution soil pH and electrical conductivity overlay in soils (Figure 4.92), spatial distribution of soil CEC and EC (Figure 4.93), and the spatial distribution of the soil CEC and TOC

(Figure 4.94), it is could be suggested that both Fe and Mn concentration levels are influenced by the soil pH and EC, and possibly by themselves.

From the the overlay of the CEC to the EC (Figure 4.93), three zones of low values in the northern part of the area and two zones of high and anomalous values in the southern part of the study area are noticed. Two of the low EC zones in the northern part coincide with low to medium CEC values; the one other low EC zone in the south western part of the area coincides with a CEC high zone. The CEC hallow in the central part of the area coincides with low to medium EC values.

The CEC was overlain with total organic carbon and electrical conductivity (Figure 4.94). The organic carbon is very low in the northern part of the study area, high and anomalous values are found in the southern part of the area. The low organic carbon values in the northern part coincide with high CEC and the high organic carbon values in the south western part of the area coincide with low CEC values. One area to note is in the northeastern part of the area, the low organic carbon values overlie high and anomalous CEC values. There is one pocket in the central south western part of the study area where high organic carbon and high CEC coincide. The area around the mine is generally very low in both CEC and organic carbon.

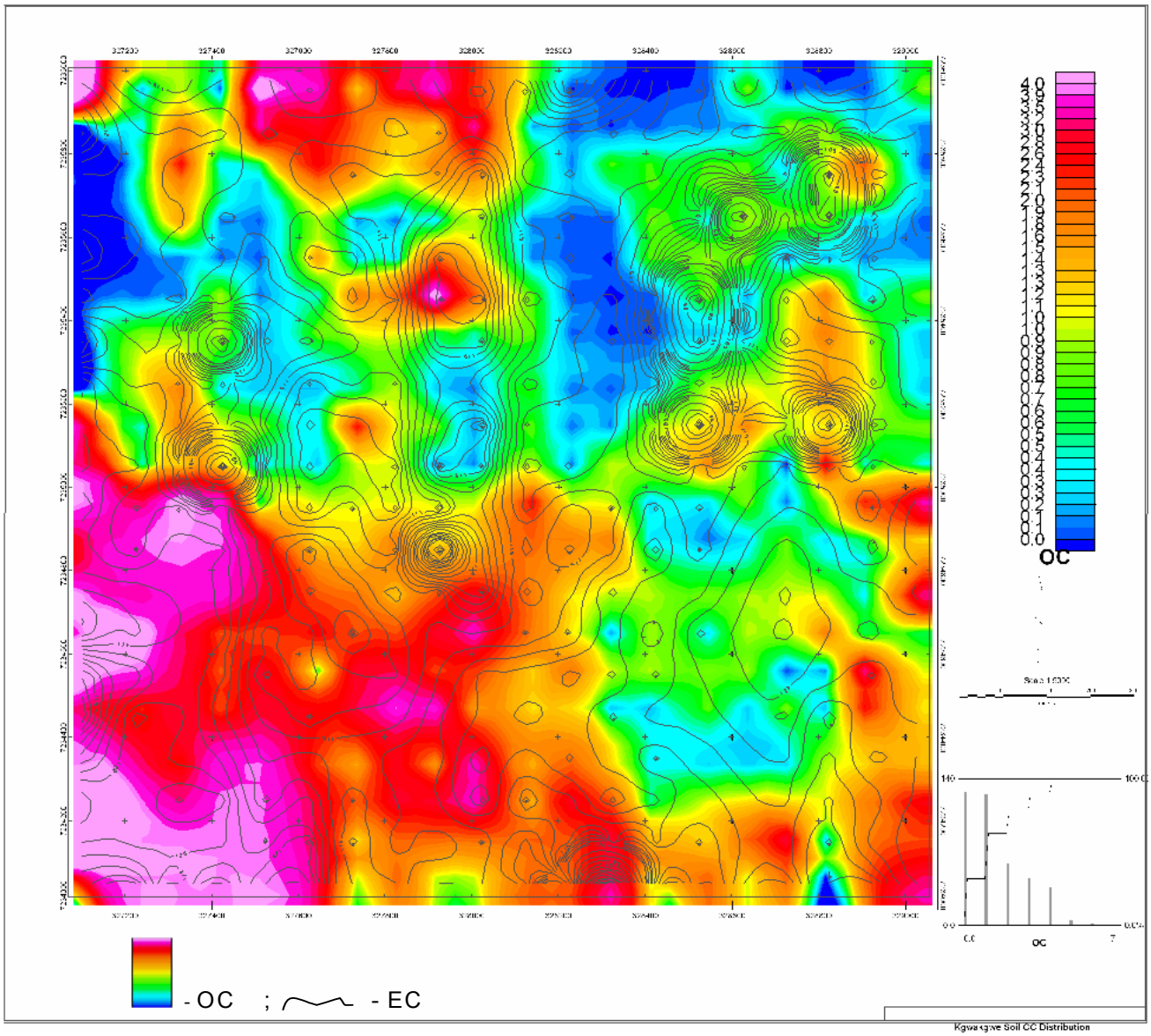

Figure 4.87: Contoured map of spatial distribution of total organic carbon content and electrical conductivity overlay in soils of the study area

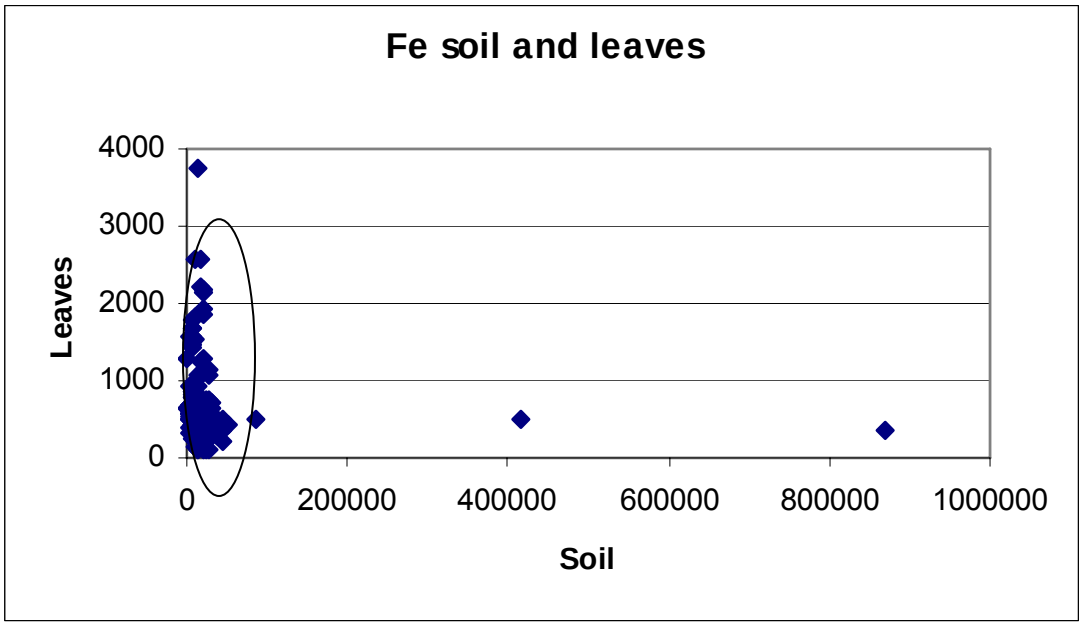

Figure 4.88: Scatter plot of iron concentration values in samples of leaves and soil samples from the study area

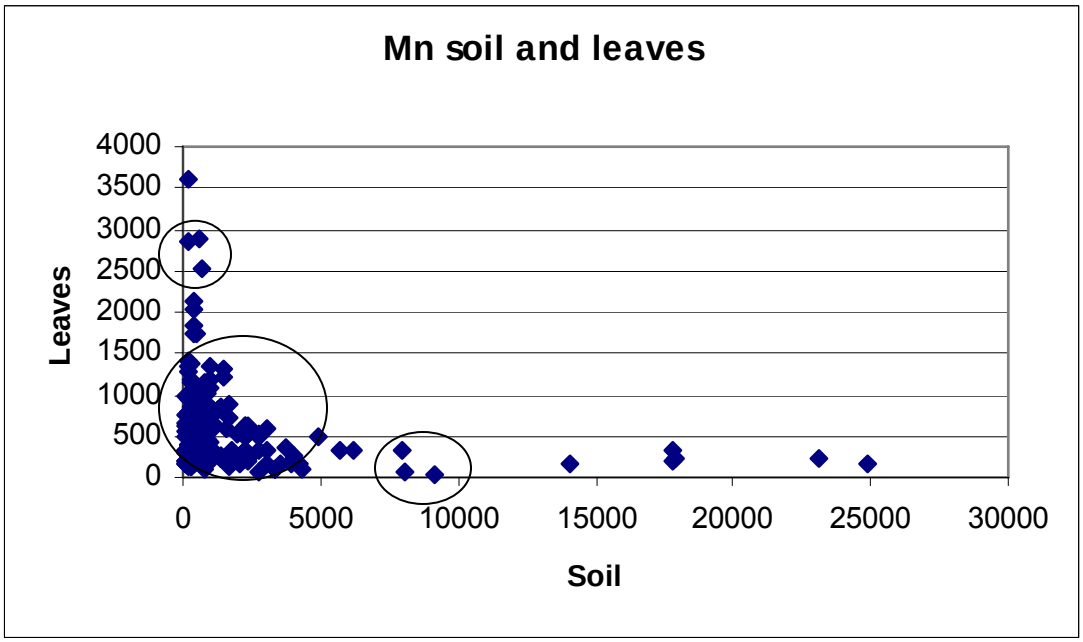

Figure 4.89: Scatter plot of manganese concentration values in samples of leaves and soil samples from the study area

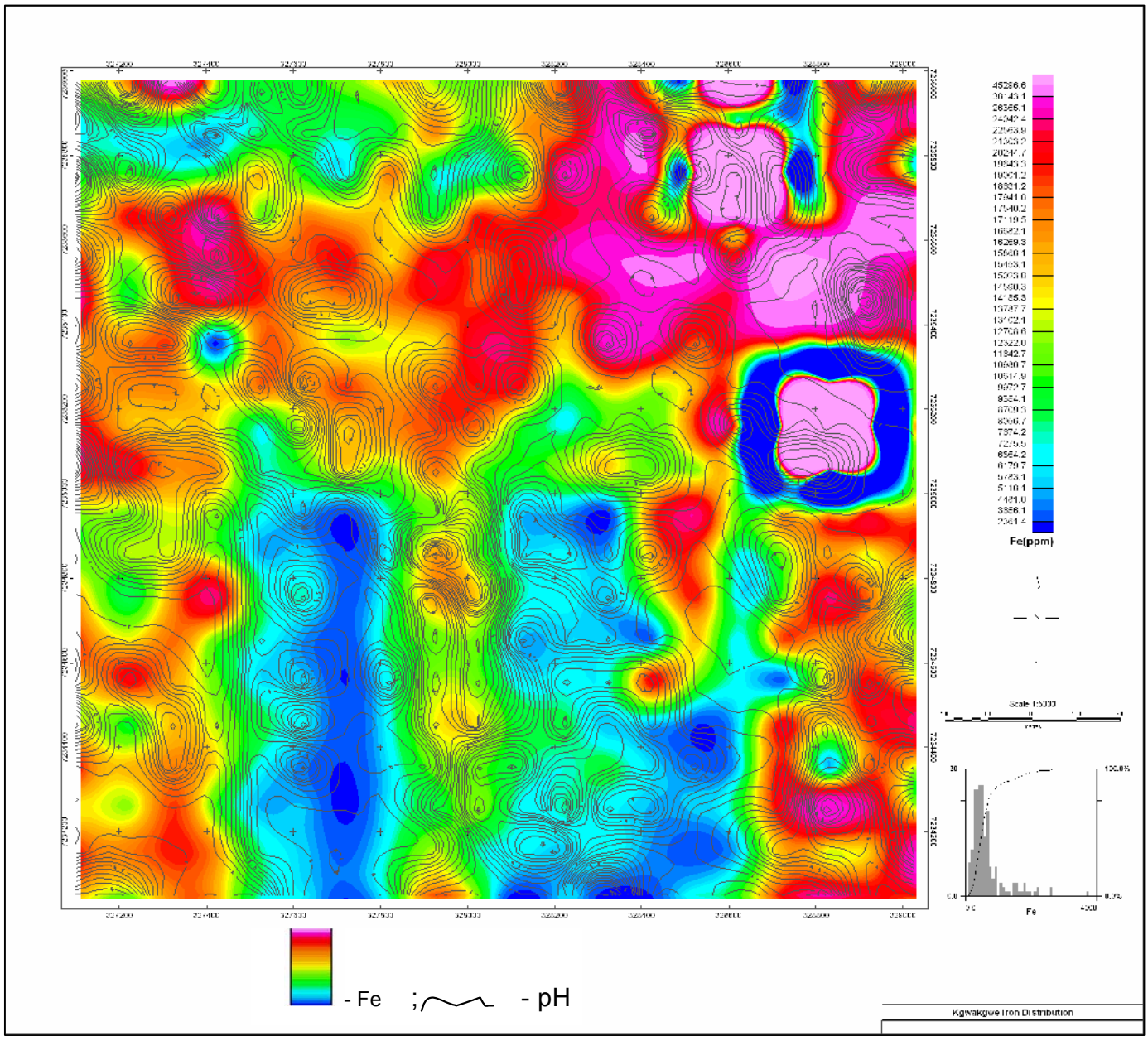

Figure 4.90: Map of spatial distribution of iron concentration levels and pH overlay in soils of the study area

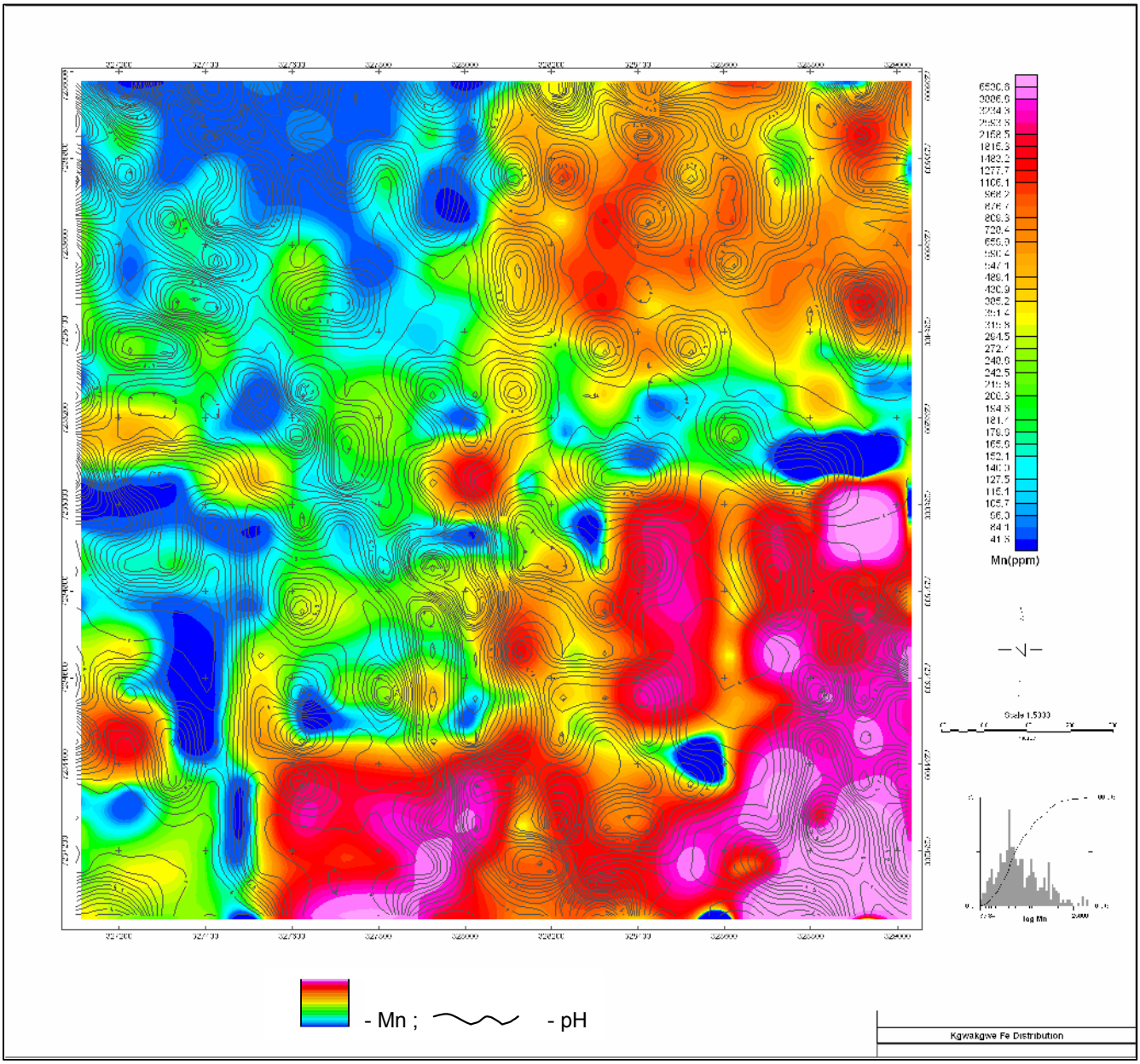

Figure 4.91: Map of spatial distribution of manganese concentration levels and pH overlay in soils of the study area

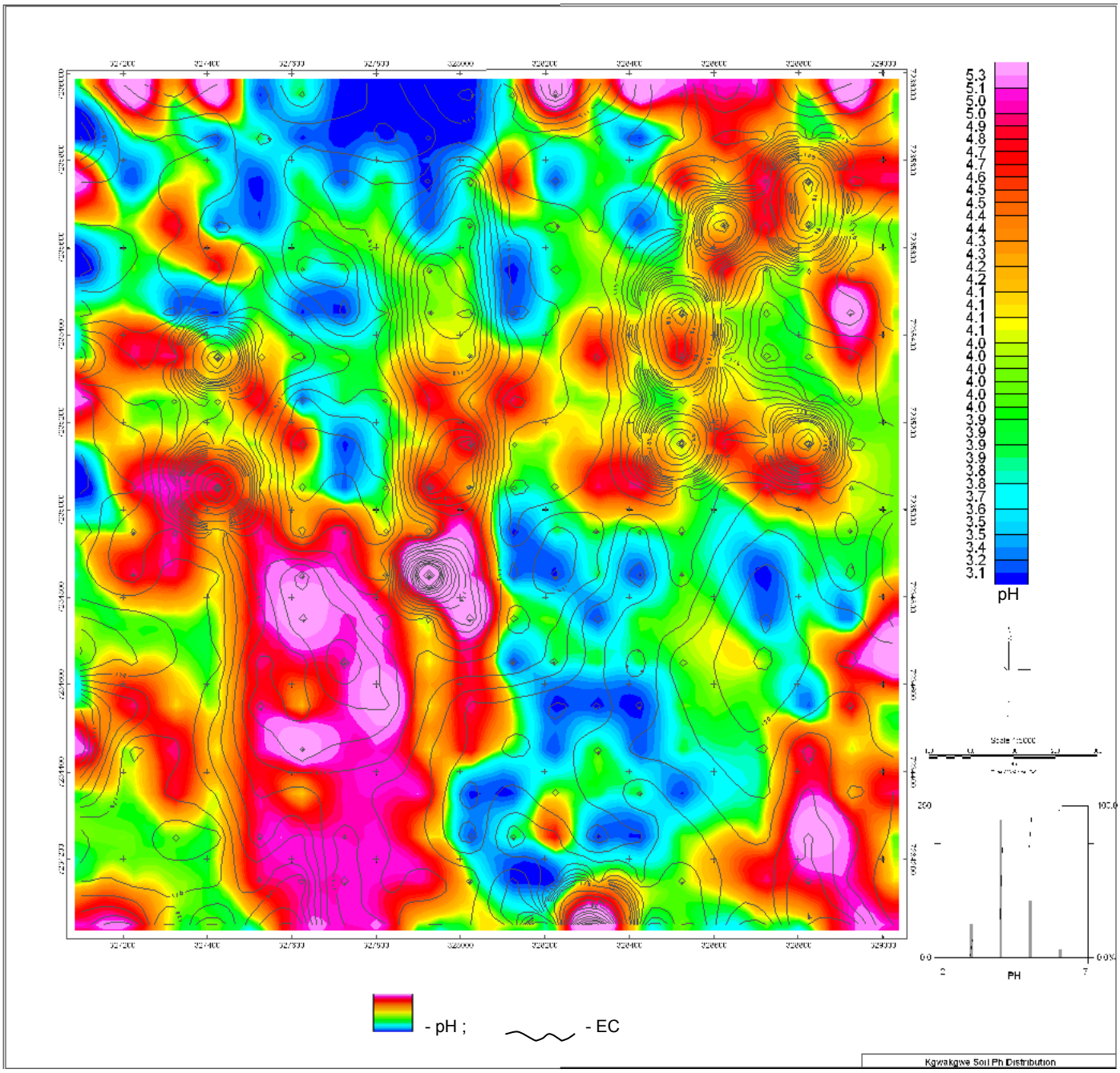

Figure 4.92: Map of spatial distribution soil pH and electrical conductivity overlay in soils of the study area

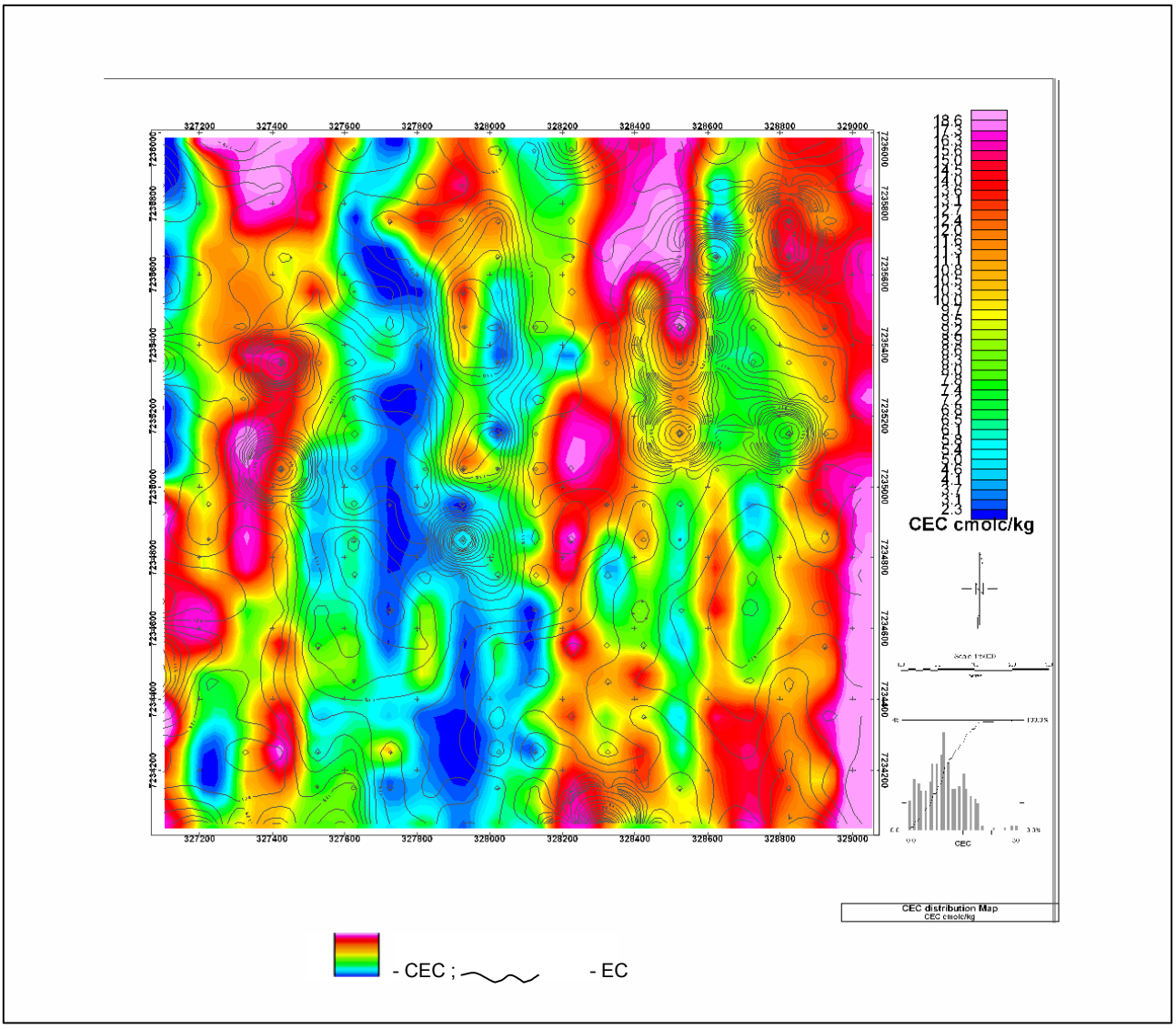

Figure 4.93: Map of spatial distribution soil cation exchange capacity and electrical conductivity overlay in soils of the study area

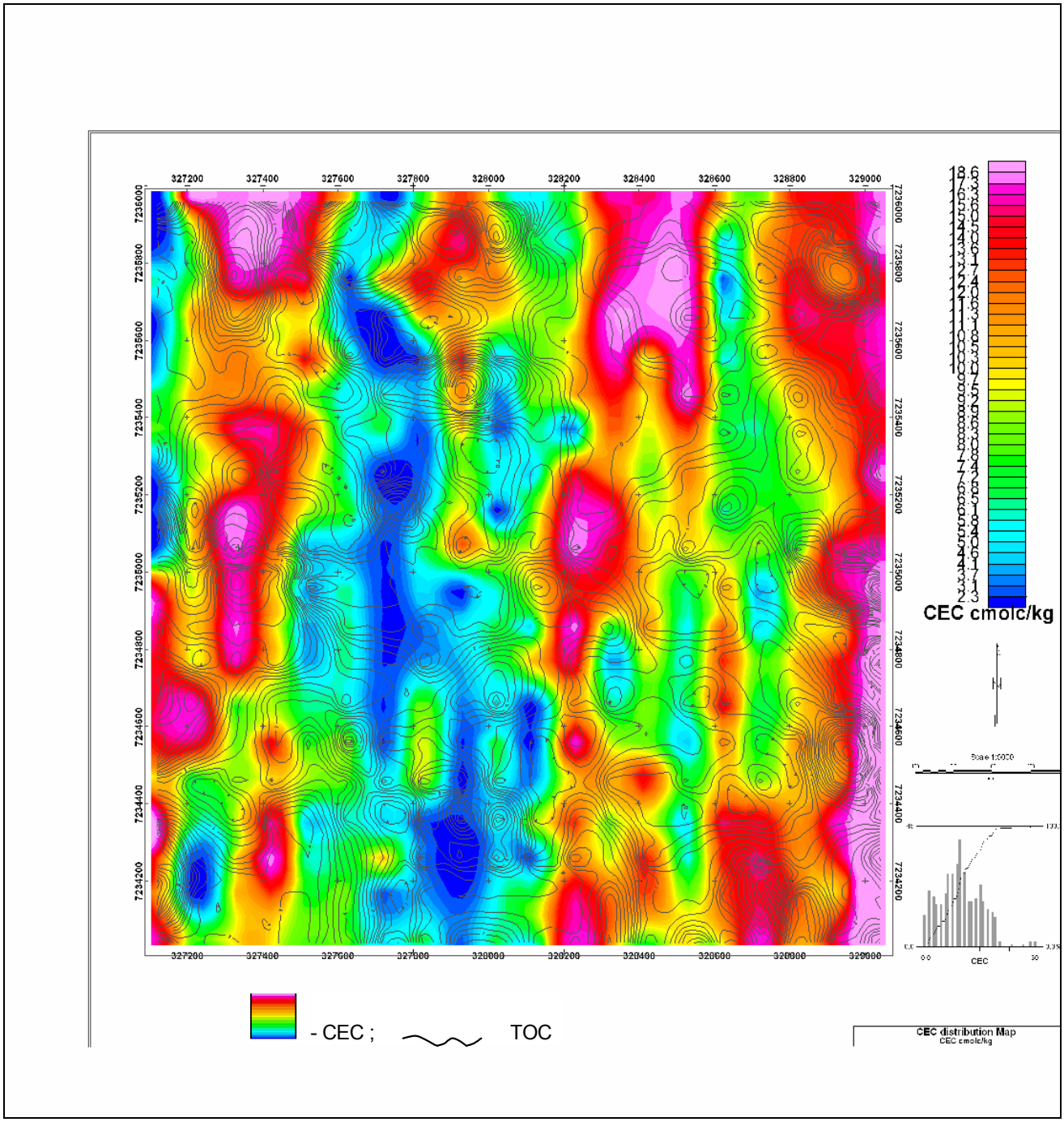

Figure 4.94: Map of spatial distribution soil cation exchange capacity and total organic carbon overlay in soils of the study area

The Fe and Mn show the anomalies in different parts of the study area as reflected in the maps presented in this work area. Where Mn is high, the Fe is low and vice versa this could be attributed to the mobility properties of the elements or simply to the location of the manganese mineralisation. The processing of assay data provided contour map, which can be used for overlaying and comparison of the location of the anomalies. The Mn is high at the mine working and there is another anomalous area in the northwestern part of the map area. The iron on the other hand is very low in the mine working area and is high on the northern part of the map area. This could be due to the mobility properties on the elements. The distribution patterns of Fe and Mn in the leaves is very similar to the patterns in the soils.

According to studies conducted by Shroeder, Dobson and Kane (1987); Eckel and Langley, (1988), and Rope, Arthur, Craig and Craig (1988), natural concentration levels of Mn in soils range from 40 mg kg^{-1} to 900 mg kg^{-1} with an estimated mean of 330 mg kg^{-1}. However, results obtained for concentration levels of Mn in the Kgwakgwe soils indicate that the levels of Mn accumulation in soils in the study area were significantly higher than mean concentration levels. In this regard, the soils at Kgwakgwe are highly contaminated with Mn.

4.5.2 Effect on aquatic systems

Mine drainage water and water enriched with leached ions of heavy metals have been known to affect the quality of aquatic organisms and the quality of water received by the downstram communities (Al, Bowles and Jambor, 1994; and

Egbu, 2000). Although water analyses and characterisation were not conducted as part of the study, it is worthwhile to mention some possible effects mining activities may be having on surrounding aquatic systems. Mining activities are reported to have several adverse hydrogeological impacts, including alteration of local surface and sub surface water environments, in terms of both quality and quantity of the water (Ashton, Love, Mahachi and Dirks, 2001).

Surface water is generally affected in several ways compared to sub surface water. Surface water and runoffs during wet weather storms, or water from other sources such as used batteries, vehicle brake pad dust, exhaust, oil, grease, tyre and fuel discharges, soild waste disposal areas, pesticide residues, and illegal and inappropriate disposal practices may contain Mn and Fe ions. These ions resulting from mining, commercial, industrial, agricultural and domestic activities are conveyed to water bodies within the environment (Egbu, 2000; Hudson-Edwards, Schell and Macklin, 1999). Eutrophication, pH fluctuations and decreased oxygen content affect both the quality and quantity of surface water. Acidic saline conditions promote dissolution of Mn and Fe ions and their migration in waterways whereby upon saturation, they get deposited (Pulles, Howie, Otto and Easton, 1996). According to Pulles (1992), some of the main contaminant sources of aquatic systems due to mining activities have not been effectively contained because of cost effective measures taken by mining companies.

Studies on effluent quality conducted by the Department of Mines (1998) of Botswana revealed concentration levels for Fe and Mn to exceed the recommended values set by the World Health Organisation. The high concentration of Fe and Mn in effluent may be as a result of seepage from mine workings, stockpiles, and exposed orebodies. On days of rainstorms, leaching activities are greatly intensified (Adelekan, 2000; Al and Bowles, 1995; Allan, 1995), and consequent increase in concentration levels of the ions of Mn and Fe in aquatic systems is obvious.

The occurrence of mines close to dolomitic terrains such as the dolomites of the Rammonedi Formation near the study area are of special concern to populations that depend on the dolomitic well fields for water supplies. Leaching of ions associated with Mn may contaminate sub surface waters. Seepage of ions from open pits, tailings and mining waste disposal areas affect the water quality, and could possibly change the rate and direction of sub surface water flow (Brink, Van Schalkwyk, Partridge, Midgley, Ball and Geldenhuis, 1990; Hawkes and Webb, 1979).

4.5.3 Effect of manganese pollution on human beings and animals

There are grave concerns of Mn contamination in the environment having a direct effect on human beings and animals. Fine Mn and Fe particles in soils, sediment, exposed outcrops and orebodies can be air blown to areas of human habitation. In a study carried out by USA-EPA (1995), it was demonstrated that

particle rejection by the pulmonary system is proportional to its size as shown in Figure 4.95. Particulate air matter of size > 10 μm can easily be ejected from the nasal chamber; consequently it does not have any significant chances of penetrating the lungs. Results from this study showed that > 13 wt % of particles in the study area were < 10 μm. It thus implies that at least 13 % of the particles within the Kgwakgwe study area might be inhaled into the respiratory system of human beings living within the vicinity. Other factors such as tidal volume, full volume capacity and residual volume of lungs, breathing frequency, particle morphology, particle chemistry and particle mineralogy may also have a direct bearing on the relative amount of PAM deposited in the pulmonary airspace of the lungs.

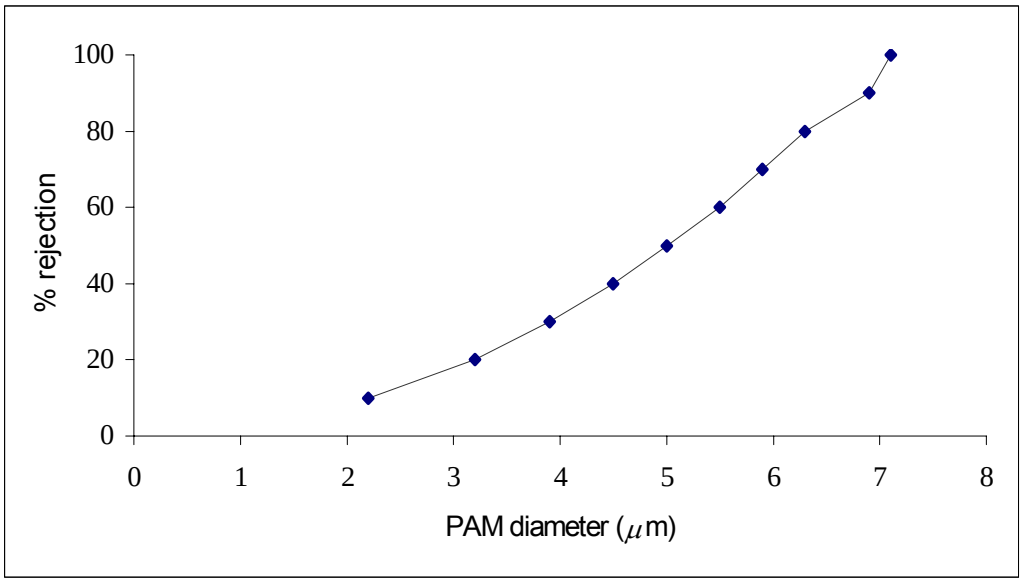

Figure 4.95: Percentage particle rejection by pulmonary system of human beings based on particulate air matter diameter (Based on USA-EPA, 1995).

Human exposure to excess Mn dust particles particularly MnO_2 and Mn_3O_4 have been reported to cause inflammatory response in the lungs, which can result in, impaired lung function (Lauwerys, Roels, Genet, Toussaint, Bouchearta and Cooman, 1985; Lucchini, Selis, Folio, Apostoli, Mutti, Vanoni, Iregren and Alessio, 1995; Zayed, Gẻrin, Loranger, Sierra, Bẻgin and Kennedy, 1994). Inhalation as well as ingestion of Mn dust particles eventually leads to maganic pneumonia, male reproductive effects (decreased libido, impotence and decreased fertility), manganism and neurobehavioral effects (Lucchini *et. al.*, 1995; WHO, 1987; 1999).

Some studies have reported that for populations living within the vicinity of ferromanganese plant, Mn exposure of > I μgm^{-3} is very contributory to increase in the rate of acute respiratory disease (USA-EPA, 1984). In another study, abortions and stillbirths have been reported (International Program on Chemical Safety, 1981). Some other researchers have linked high levels of Mn occurrences to crimes (Masters, Hone and Doshi, 1998; Masters, Way, Hone, Grelotti, Gonzalez and Jones, 1998b), although this remains a controversial subject yet to be well substantiated. Iron occurs as an integral element associated with Mn orebodies. Although it is a very essential component of the blood, it may have some adverse effects. In the oxidation of Fe, acidic solutions could be created which tend to decrease adsorption and promote mobility of metals in soils, water and sediments. Iron is known to cause siderosis, and

scarring of the lungs. Experimental work conducted on ore miners in Newfoundland indicated that Fe is carcinogenic (Langer, 1999).

Animals living within such mining areas are likely to suffer from respiratory problems associated with PAM. Mammals especially sheep and cattle could be more affected than birds, which migrate due to forced changes in climatic conditions. Another unfortunate impact is animal illhealth and calf mortality as a result of geophagia (Elsenbroek and Naser, 2002).

4.6 ASPECTS OF POLLUTION MANAGEMENT AND LAND USE

4.6.1 Manganese and iron contamination at Kgwakgwe

At the end of minerals exploitation of any given mine, the closure and decommissioning phases have to be executed. Quite often, mine related environmental impacts as explained by Ashton *et. al.* (2001), continue to occur several years after the mine has stopped operating. Noticeable impacts at the end of ore mining of a given deposit include landscape scarring due to unrehabilitated waste rock dumps, mine tailings, discard dumps, old shafts and underground fires. Waters remain polluted, wind blown dusts and dispersal of contaminated solid waste are other features which occur after the ore exploitation phase as explained by Johnson, Cooke and Stevenson (1994).

Mining activities at Kgwakgwe could be identified to be responsible for the widespread biophysical and chemical soil disturbances, which are associated with accelerated soil erosion (Figure 4.96). Both Fe and Mn are in very high

levels of concentrations in the soils. However, Mn is more deleterious than Fe, and hence the path of Mn contamination of soils is further explained in detail.

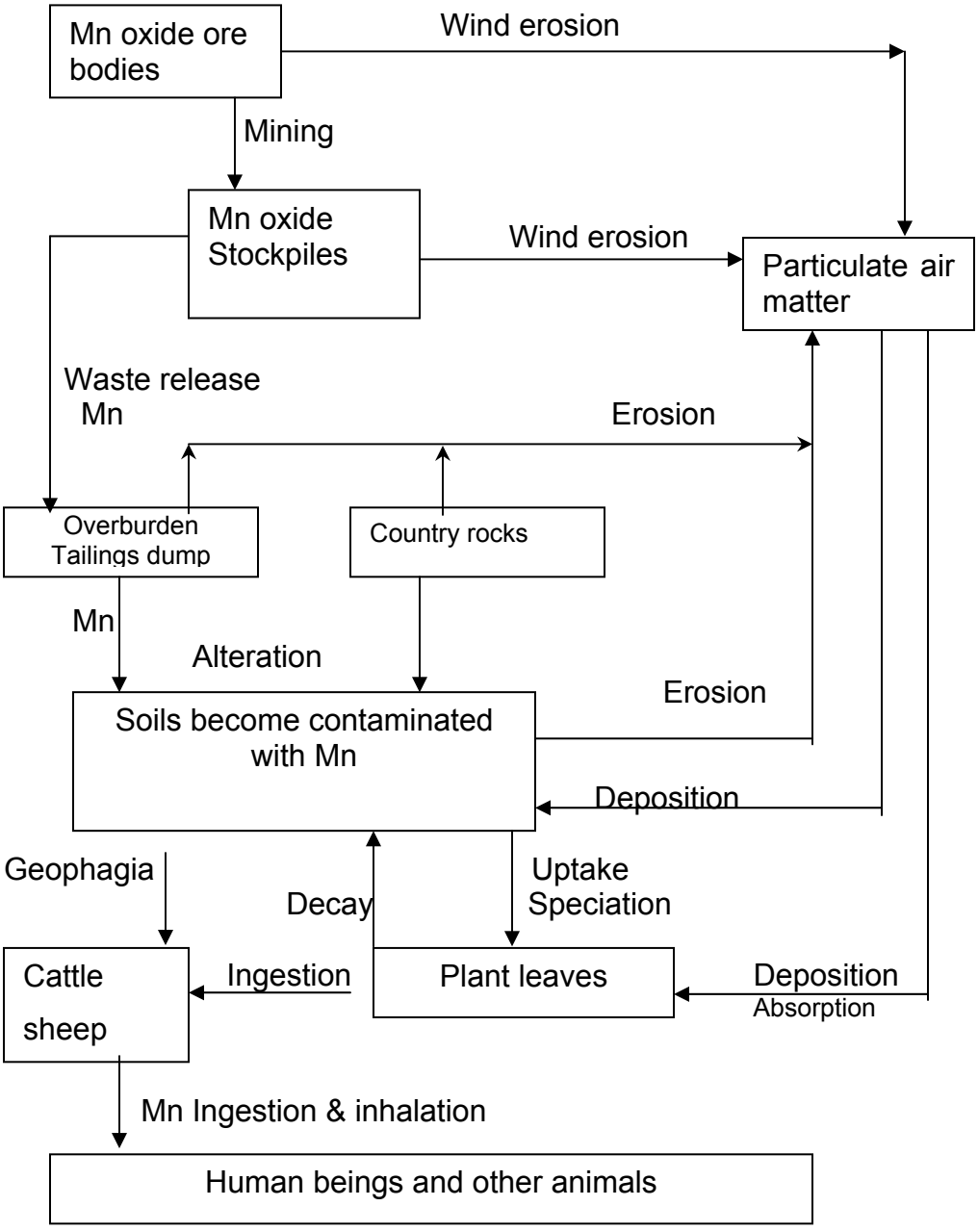

Figure 4.96: Schematic diagram showing biophysical and chemical processes and relationships of environmental constituents at the Kgwakgwe Mn oxide mine study area.

At Kgwakgwe, the Mn oxide ore bodies, Mn oxide stockpiles, waste consisting of tailings dump and overburden and exposed country rocks (rhyolite, dolerite and shales) through wind erosion release PAM rich in Mn particles into the atmosphere which are transported over a short distance and deposited on soils and leaves of plants. Through chemical alteration processes such as leaching and seepage, Mn ions are released migrating from sources to surrounding soils.

Enzootic geophagia (Elsenbroek and Neser, 2002) of cattle, calves and sheep on exposed Mn rich surfaces is also noted, and the cadavers resulting from such act are buried in the soils. Through deposition and absorption of Mn rich PAM on leaves of plants and uptake of Mn by plants, they become concentrated with Mn ions in their system. Human beings and animals feeding on both plants and cattle also receive more than the normal Mn body requirements.

Soils and associated contaminants have been transported by air and water to other surrounding areas. This may have caused changes in the fauna and flora of the environment. Soil erosion resulting from mining activities could enhance a variety of terrestrial ecological changes in the disturbed environments. These ecological changes could possibly lead to the invasion of alien plant and animal species (Zar, 1984).

4.6.2 Possible remediation measures

In Southern African countries like most other countries, all mining activities are considered to likely affect significantly the environment (Chenje, 2000; Weaver and Caldwell, 1999). In recent years, several government and government related institutions demand that elaborate environmental impact assessment (EIA) studies to be undertaken before mining activities can commence (Bradshaw and Johnson, 1992; Reichman, 2000; Ripley *et. al*., 1996). Unfortunately some mining activities in several countries especially the developing nations (including Botswana) have been executed to completion without EIA studies. In such cases, the mining companies have abandoned mined and disturbed lands and the mining environment left without reclamation/rehabilitation. At Kgwakgwe, no EIA studies were carried out before mining of Mn oxide ore. Consequently, the mining company abandoned the area leaving mine workings unfilled and contaminated lands not reclaimed. In this vein, different remediation techniques related to Mn contamination of soils are examined with the possibility of suggesting suitable techniques for the Kgwakgwe scenario.

Before any remediation exercise to treat contaminated soils could be carried out, consideration should be made on the following points as highlighted by Chen (2000), Iskador and Adriano (1997), Pierzynski (1997), and USA-EPA (1990):

- Short term effectiveness
- Long term effectiveness

- Reduction in toxicity and mobility of contaminant
- Reduction in volume of contaminant
- Cost for undertaking the remediation exercise
- Compliance with national Government, Local Government, Councils and Regulatory agencies in terms of standards and guidelines
- Environmental benefit
- Acceptability of remediation measures by both Governments and the local community.

If the above cited conditions are fulfilled, plans are set for the remediation exercise. Chen (2000) mentioned three types of remediation techniques in treating contaminated soils and these are engineering, chemical and biological. Another approach is suggested by the USA-EPA (1997) in which four *in situ* technologies are discussed and these are electrokinetic remediation, phytoremediation, soil flushing and solidification/stabilisation. There are close similarities in the approach of Chen (2000) to that of USA-EPA (1997).

In the method of applying engineering remediation techniques, which is closely related to electrokinetic remediation and remediation by biotechnology, for the effective treatment of contaminated soils, Chen and Lee (1997) suggested that the polluted surface soil be removed and replaced by non contaminated soil. The removed contaminated soil is washed with some chemical extraction or chelating agent. The chemical remediation approach involves the addition of chemical

materials to the contaminated soil in order to reduce the concentration of the contaminant. Some materials that could be added include lime, manure, compost and plenty of phosphate. They increase soil pH and reduce solubility of metals (Chen, 2000). In the remediation approach (Cunningham and Berti, 1993; Cunningham *et. al*., 1995), which embraces phytomining and phytostabilisation, plants are used to reduce the contaminant concentration and promote soil stability (Baker, 1995; Baker and Brooks, 1989; Brooks, 1997; 1998).

Another form of remediation worth mentioning is the naturally occurring biodegradation technique applied to contaminated soils. This technique is principally used for petroleum hydrocarbon contamination in unsaturated zone soils, and has been explained extensively in a document prepared by the Wisconsin Department of Natural Resources (1997). Although this technique is presently applicable to petroleum hydrocarbon contamination, it is the opinion of the author that the technique could also be extended to treat Mn contaminated soils, provided the Mn is in its ionic state. However, the suggestion needs to be further researched upon.

Considering the different approaches to remediation of contaminated soils in terms of cost benefit, and the degree of Mn contamination, the engineering remediation approach is cost effective provided the area is not extensive. Both chemical and biological approaches are feasible if the area is large and the purpose for which the land has to be used will be economically rewarding. At

Kgwakgwe, the Local Government may not have sufficient funds to undertake such remediative efforts. However, the mine workings could be filled with earth, and the surface planted with grass. This initiative was started by the mining company in a localised section of the mine but stopped possibly because of cost of carrying out the exercise including the buying the grass (which was not indigenous to the environment).

4.6.3 Possible land uses

The discussions and suggestions in this section were based mostly on field visits but also on the laboratory results and interpretation of the MSS image. Nine first level land use and land cover classification derived by Anderson, Hardy, Roach and Witmer (1976) are implemented in USA and these are: urban or built up land, agricultural land, rangeland, forest land, water, wetland, barren land, Tundra and Perennial snow or ice. Considering the environmental set up and the development plans for the Kanye District in which Kgwakgwe falls into, the land in the study area could be applied for Urban or built up land and/or agricultural land.

Emphasis of this study was laid on the mining impact on soils close to the Mn oxide ore mining areas. That notwithstanding, suggestions on possible land uses made include the mining areas as well as the study area. In the mining areas, due to high Mn contamination of the soils, there were several areas, which had no vegetation cover and have become dead zones as described by Bertsch and

Seaman (1999). This phenomenon has been observed at other mining areas such as Selebi Phikwe, Botswana (Ekosse *et. al*., 2003; 2003b) and Sudbury, Canada (Coggans, Bowles, Robertson and Jambor, 1999; Hantong-Fong, Bowles and Stuparyk, 1997). In areas where dead zones occur, the soils could be reclaimed using suggested remediative techniques mentioned in 3.6.2 of this thesis. However it may be a very expensive undertaking for the Local Government of Kanye.

In these areas at the abandoned mine, which have become dead zones, it will be very difficult to execute land reclamation through revegetation, even though it is understood that the most important aspect of reclaiming mined lands to their natural or pre-mining state is through the development and establishment of quality vegetation cover (Gillis, 1991). At the mining sites in Kgwakgwe, the physical characteristics of the soil (particle size and PSD, shape, pore space volume, soil pH, EC, soil colour and soil texture), soil chemistry, soil mineralogy and the soil microbiology have completely changed.

According to Anderson *et. al.* (1976) in considering land classification and landuse for agriculture, four subclasses have been suggested and these are croplands and pasture; orchards, groves, vineyards, nurseries, and ornamental horticulture; confined feeding operations; and other agricultural land. In terms of land use, most of the neighbouring lands within the study area are presently used for subsistence agriculture with livestock rearing. Unfortunately, the soils within

the study area are presently contaminated with both Mn and Fe. The predominance of these ions in the soils make the land generally unsuitable for commercial agriculture, though some form of subsistence agriculture (classified as other agricultural land) could be considered. The subsistence agriculture should probably be carried out on the soils located on the small floodplain levees along the streams. However crop yield will most possibly be very poor if no remediation exercise is carried out prior to farming.

Anderson *et. al*. (1976) highlights seven subclasses for land classification for urban or built up land and these are residential; commercial, and services; industrial; transportation, communications and utilities; industrial and commercial complexes; mixed urban and built up land; and other urban and built up land. Because of the adverse health effects of Mn on human beings, the land may not be suitable for residential purposes. There are several factors, which influence the establishment of industries. Among these factors are manpower needs, proximity to raw materials and capital, which are fundamentally crucial in establishing industries. Furthermore industries tend to generate waste, which may not be conducive to the environment. Therefore, the site may not be suitable for the establishment of industries. Dynamic structures such as transportation, communications and utilities are essential services required by society, and at Kgwakgwe these facilities already exist, although the management is not very efficient.

Considering the population of the Kanye area (which includes Kgwakgwe), the available shopping complexes, and the distance of Kgwakgwe from the shopping facilities, there is need to set a commercial facility within the study area. This facility will also serve the neighbouring settlements and villages, which presently do not have any shopping facilities. The inhabitants have to go to Kanye township or Lobatse located about 60 Km away, and more often Gaborone, which is located about 100 km away. Legislative, economic and political factors will definitely be taken into consideration before a final decision is arrived at by the stakeholders who in this case include national and local governments, and the community.

CHAPTER FIVE

CONCLUSIONS AND RECOMMENDATIONS

The Kgwakgwe area, within the periphery of the Kanye township in southeastern Botswana has an abandoned Mn mine from which Mn oxide ore was mined for over thirty years intermittently. Growing concerns that the mining activities may be having a direct influence on the soils around the abandoned mine were primarily investigated in this study. Its aim was to achieve a better understanding of the environmental physico-chemistry, environmental mineralogy, and environmental chemistry of the soils close to the mined lands. With the aid of different spatial presentation techniques, generated data were interpreted contextually in terms of establishing more specifically the influence of Mn and to a lesser extent Fe on the soils and the surrounding environments.

5.1 PHYSICO CHEMICAL ASPECTS

The PSD of soil samples revealed the average wt % of the soil fractions as follows:

- the < 4 μ m fraction was between o.3 wt % and 30.58 wt %,
- the < 53 μ m fraction was between 11.05 wt % and 109.80 wt %.

Soil pH ranged from 2.92 to 7.26 with very acidic soils located close to the mine workings. Electrical conductivity values were significantly low, and the range was from 49.1 $\mu S cm^{-1}$ to 123.5 $\mu S cm^{-1}$. Soils with low pH correspondingly had low EC. The results are indicative of increase in soil acidity due to mining of Mn oxide

ore in an Fe rich environment, at the Kgwakgwe area. Correspondingly, soils of higher EC were closer to the mine compared to those with lower EC values, which were further away from the mine. Dark brown to reddish brown soil colour was indicative of very high Fe and Mn levels in the soils. The observation is indicative of both Fe and Mn containing minerals enriching the soils of the study area. High acidity favoured the leaching of Mn and Fe ions from exposed geological outcrops constituting manganiferous and ferruginous shales as well as Mn oxide ore to the soils, consequently they remain in solution and are bioavailabe for plant uptake.

5.2 MINERALOGICAL ASPECTS

Bulk soil samples consisted of quartz, SiO_2; haematite, $Fe2O_3$; goethite, $Fe^{+3}O(OH)$; bixbyte, Mn_2O_3; braunite, $Mn^{+2}Mn_6^{+3}SiO_{12}$ ramsdellite, MnO_2 pyrolusite MnO_2 cryptomelane $K_{2-x}Mn_8O_{16}$ sanidine $K(Si_3Al)O_8$ microcline, $KAlSi_3O_8$; whereas the < 4 μ m fraction was made of kaolinite, $Al_2Si_2O_5(OH)_4$ illite, $KAl_2Si_3AlO_{10}(OH)_2$; and muscovite $KAl_2Si_3AlO_{10}(OH)_2$.

Hand specimens of coarse fractions of soil samples were viewed with a microscope and physical tests performed on the samples for hardness, cleavage, fracture, colour, streak, lustre, and crystal appearance depict characteristics of quartz, Mn and Fe bearing minerals and feldspars. Grains were poorly sorted, with subangular grains located further from the plant, which is indicative of

windblown particles transported at a short distance. Morphologies of fine soil particles viewed with the SEM revealed kaolinite, goethite and Mn particles.

Ambient temperature, wind and aquatic transportation of Mn particles and Mn and Fe ions, and chemical alteration due to the acidic milieu created favourable conditions for the neomineralisation of Fe bearing and Mn bearing minerals in the soils. The occurrence of both the manganiferous and ferruginous minerals in the soils of the study area and only ferruginous minerals in the soils of the control site demonstrated soil contamination due to Mn oxide ore mining activities.

5.3 ASPECTS OF MANGANESE AND IRON CHEMISTRY

The range of concentration levels of Fe in soils was from 1116 μg g^{-1} to 870766 μg g^{-1} with a mean of 17593 μg g^{-1} and for Mn in soils was 35 μg g^{-1} to 24907 μg g^{-1} with a mean of 1088 μg g^{-1}. For the leaves, the range of concentration levels of Fe contained in them was from 101.2 μg g^{-1} to 3758 μg g^{-1} with a mean of 637 μg g^{-1} and for Mn in leaves was from 26.2 μg g^{-1} to 3611.5 μg g^{-1} with a mean of 598.4 μg g^{-1}. The TOC values were between 0 wt % to 7.9 wt %.

High acidity of soils is reflected by on-going neomineralisation activities which at some places are depicted by the formation of dead zones. Low soil pH promotes the leaching and precipitation of ions including those of Mn and Fe. Other observable phenomena were stunted growth of plants, and the yellowing of their

leaves as a result of high concentrations of heavy metals in their organic systems.

For the soil samples, the processing of assay data provided contour maps, which was used for overlaying and comparison of the location of the anomalies. The gridded soil maps for Fe and Mn show anomalies in different parts of the study area. Where Mn is high, the Fe is low and vice versa. This observed phenomenon could be attributed to the mobility properties of the elements or simply to the proximity to the Mn oxide orebodies and mining sites.

With the leaves of plants sampled, the Mn was high at the mine working and there is another anomalous area in the northwestern part of the study area. Iron on the other hand is very low in the mine working area and is high on the northern part of the study area. One very distinct feature is that where Mn is high, the Fe is low and vice versa. This could be due to the mobility properties on the elements and availability of their ions for plant uptake. It should be noted that the distribution patterns of Fe and Mn in the leaves are very similar to the patterns for the soils.

5.4 RESPONSES TO QUERIES

The findings obtained from field observations; physico-chemical, mineralogical and chemical analyses; and the spatial presentation and interpretation of the data depict the following responses to queries introduced in Chapter one:

- The results of soil samples studied depict that the physico-chemical properties of the soils (more specifically soil PSD, soil pH, EC and colour) around the abandoned Kgwakgwe Mn mine, confirm that the mining activities have negatively affected the soil physico-chemical status. Noticeable alterations of the physico-chemical properties of the soil, and clay fraction of soil due to mining activities in terms of PS, PSD, pH, EC, as well as soil colour were reported and discussed.
- Minerals identification and characterisation tests performed on soil samples further confirm that both Mn bearing and Fe bearing minerals from the Mn oxide ore, the manganiferous and ferruginous shales and other related geological materials have contaminated the soils which are found close to the abandoned mine. New mineral phases were formed in the soil. The new minerals augmented concentrations of Mn and Fe in the physical environment. The soils were enriched with both new minerals and ionic Mn and Fe from mining activities.
- The concentrations of Mn and Fe in the Mn oxide orebodies and related geological materials is considered from the results of mineralogical studies to be significantly high as expected because of Mn mineralisation.
- The concentrations of Mn and Fe in soils were significantly high and need to be addressed by stakeholders.
- There was a direct relationship of the mineralogy of the soil to that of the ore bodies. This implies that soil constituents were partly from ore bodies either by weathering or contamination.

- The concentrations of Mn and Fe in samples of leaves from plants in the study area were significantly high and need to be addressed by stakeholders.
- Based on physico-chemistry, mineralogy, and chemistry regarding mineral genesis, the protore rock that led to the formation of the kaolin and present Mn oxide ore could have been manganiferous shale rich in rhodochrosite. Meteoric fluids reacted with the protore rock and Mn oxides were formed in a slightly acidic environment. Further oxidation of MnO led to the formation of the MnO_2 minerals. The feldspars from the feldspar rich rocks were altered to kaolinite.
- Based on physico-chemistry, mineralogy, and chemistry regarding the soils around the abandoned Mn oxide mine, the soils were primarily formed from the weathering of the feldspar rich country rocks. Eventually as mining took place, they became contaminated with Mn and the levels of Fe contained in them also rose higher.
- Laboratory results were indicative of contamination of the environmental quality due to mining activities.
- Contamination of the physical environment has occurred, and it should be contained by the application of some suggested remediative measures.
- Spatial presentation of analytical results for physico-chemistry, mineralogy, and chemistry of soils depict the surfacial extent to which Mn contamination has taken place.

- The findings of this study determine that the soils around the abandoned Kgwakgwe Mn oxide mine are not suitable for agro-pastoral activities. However very small scale subsistence farming can be practised along the banks of the small streams. The area could conveniently be used as a shopping complex; a decision which could be arrived at after consultation with the interested parties.
- There are grave concerns on possible health and environmental hazards of Mn contamination and/or pollution around Kgwakgwe abandoned Mn oxide mine
- Possible health and environmental hazards of Mn contamination and/or pollution around Kgwakgwe area include Mn and Fe effects on soils and vegetation, aquatic systems, human beings and animals. Examples of the negative effects have been given and where applicable comparison made with available cases in published literature.

Furthermore, a model of the Mn interplay in the soils and environment around the Kgwakgwe abandoned Mn oxide mine has been postulated.

5.5 RECOMMENDATIONS

The recommendations are to the community, the National and Local Governments, and researchers. The three categories of recommendations are listed below.

5.5.1 Recommendations to the community

- The population should desist from allowing their cattle and sheep to graze close to the abandoned mine. Such a move will control enzootic geophagia, which already is known to be occurring in the area.
- Any form of farming should be subsistence, and close to the stream banks where there will be adequate water and are no dead zones.
- As much as possible, the population should avoid staying outdoors where risk exposure to Mn contaminated air is quite high.
- The people of Kgwakgwe should report to Health Authorities for regular check-ups of their health state. The medical visits will include checking the cardio-pulmonary system, the circulatory system, and urine.
- People considered to be frail in health should consider relocation to other township areas away from the exposed Mn particles.

5.5.2 Recommendation to the National and Local Governments

- Risk based medical examinations should be conducted annually.
- Environmental control measures should be implemented.
- An occupational exposure (Occupational Hygiene) programme should be compiled and implemented for former mine workers.
- Policy and procedures with regard to managing the contamination should be compiled and implemented.

- National and Local Governments and related agencies should work as a team in monitoring pollution activities around the Kgwakgwe Mn oxide ore abandoned mine.
- The interested parties should apply environmental management techniques such as phytomining, phytostabilisation, phytoremediation and biotechnology to regain areas where dead zones have developed.
- The agencies should implement health monitoring programmes geared at ensuring quality lifestyle for sustainable development.
- Applied research efforts should be encouraged by authorising bodies.
- Expansion of the Kgwakgwe township should be regulated in such a way that the growing population is least exposed to Mn contamination.

5.5.4 Further research

- Studies on contaminant hydrology may be carried out to determine the spatial extent and degree of contamination of water bodies within the study area.
- A study to characterise the different species of heavy metals in the area may aid in evaluating the physical quality of the environment.
- Studies on health hazards and related sicknesses due to exploitation of Mn oxide ore may aid in setting guidelines on types of exposure and contact period workers may be allowed to bear, and further allowable limits for human beings residing in the area.

- Further research on Mn mineral dust released and its effects to the population and environment needs to be conducted.
- The relationship of Mn, violence and crime may also be investigated at Kgwakgwe.

5.6 CONCLUDING REMARKS

The study has considered the physico-chemistry, mineralogy and chemistry of soils, and the chemistry of leaves of plants around the Kgwakgwe Mn oxide abandoned mine, southeastern Botswana. Appropriate land management is essential for the sustainable development of natural resources. Unfortunately at Kgwakgwe no EIA studies were carried out prior to mining activities. It has advanced certain recommendations that may bring solution to some of the existing environmental pollution problems at Kgwakgwe. The findings of the study may serve as useful guidelines in interpreting particularly the soil status and in general the physical environmental quality of Kgwakgwe and possibly similar settings around the world.

REFERENCES

Adelekan I. O. (2000) A survey of rainstorms as weather hazards in southern Nigeria. *The Environmentalist*. **20**, 33-39.

Aldiss, D.T., Tombale, A.R., Mapeo, R.M.B., Chiepe, M. (1989) The Geology of the Kanye Area. *Bulletin Of the Geoogical Survey Department of Botswana.* **33**, 170 pp.

Al T. A. and Bowles D. W. (1995) Storm-water hydrograph separation of run off from the Kidd Creek mine tailings impoundment, Timmins, Ontario. Paper presented at the Conference of Mining and the Environment held at Sudbury, Canada. 28 May – 1 June 1995. 9pp.

Al T. A., Bowles D. W., and Jambor J. L. (1994) The geochemistry of mine-waste pore water affected by the combined disposal of natrojarosite and base-metal sulphide tailings at Kidd Creek, Timmins, Ontario, Canada. *Can. Geotech. Journal*. 31, 502-512.

Allan R. J. (1995) Impact of mining activities on the terrestial and aquatic environment with emphasis on mitigation and remedial measures. In: salmons W., Frostener U., and Mader P. (Editors) Heavy metals: Problems and solutions. Springer. 119-139.

Alloway B.J. (1990) Heavy Metals in Soils. New York: Halsted Press.

Alloway B. J. and Ayres D. C. (1997) Chemical principles of environmental pollution. Blackie Academic and Professional. 2nd Edition, 395pp.

Anderson J. R., Hardy E. E., Roach J. T. and Witmer R. E. A (1976) A landuse and landcover classification system for use with remote sensor data. US Geological Survey Professional Paper 964.

Ashton P. J., Love D., Mahachi H., and Dirks P. H. G. M. (2001) An overview of the impact of mining and mineral processing operations on water resources and water quality in the Zambezi, Limpopo and Olifants catchments in southern Africa. Contract report to the Mining, Minerals and Sustainable Development (Southern Africa) project, by CSIR-Environmentek, Pretoria, South Africa and Geology Department, University of Zimbabwe, Harare, Zimbabwe. Report No. ENV-P-C 2001-042. 336 pp.

Bailey S. W. (1980) Structures of layer silicates. 115 pp. In: Brindley G. W., and Brown G. (Editors) Crystal structures of clay minerals and their x-ray identification. Mineralogical Society, England.

Barnard R. O., Buys A. J., Coetzee J. G. K., Du Preez C. C., meyer J. H., Van der Merwe A. J., Van Vuuren J. A. J. and Volschenk J. E. (1990) Handbook of standard soil testing methods for advisory purposes. *Soil Science Society of South Africa.* 120 pp.

Barret E. C. and Curtis L. F. (1997) Introduction to environmental remote sensing. Third edition. Chapman and Hall. 426 pp.

Barrick K. A., Schoettle A. W (1996) A comparison of the foliar nutrient status of elfinwood and symmetrically formed tall trees, Colorado Front Range, USA. *Canadian Journal of Botany.* **74**, 1461-1475.

Bertsch P. M. and Seaman J. C. (1999) Characterisation of complex mineral assemblages: implications for contaminant transport and environmental remediation. *PNAS Online*. **96**, 3350-3357.

Bhalotra Y. P. R. (1987) *Elements of climate: Climate of Botswana II*. Unpublished Report. Department of Meteorological Service of Botswana, Gaborone.

Bioremediation (2003) Bioremediation of gasoline-contaminated soil. Environmental Inc, UAI Group. http://www.uaienvironmental.com/biovent.asp. 2 pp.

Bohn H.L., mcNeal B. L., and O'Connor G. A. (2001) Soil Chemistry. 3rd Edition. John Wiley & Sons. 307 pp.

Bosch P. J. A., Ericksson P. G. and Snyman C. P. (1993) The Wolkberg Group in the northern Transvaal: palaeoenvironment derived from sedimentology and geochemistry. *South African Journal of Geology*. **96**, 190 – 204.

Botswana Range Inventory Monitoring Project (2001) Botswana Range Inventory Monitoring Project Phase II: The Biomass Map of Botswana, Growing Season 2000/2001. Ministry of Agriculture, Private Bag 003, Gaborone, Botswana.

Bowles D. W., Jambor J. L., Appleyard E. C., Reardon E. J., and Cherry J. A. (1992) Temporal observations of the geochemistry and mineralogy of a sulphide-rich mine-tailings impoundment, Health Steale Mines. New Brunswick. *Exploration Mining Geology*. **1**, 251- 264.

Bradshaw A. and Johnson M. (1992) Revegetation of metalliferous mine waste: the range of practical techniques used in Western Europe. Minerals, Metals and the environment. Applied Science, Elsevier, London and New York. 481-491

Brink A. B., Van Schalkwyk A., Partridge T. C., Midgley D. C., Ball J. M. and Geldenhuis S. J. (1990) The changing impact of urbanisation and mining on the geological environment. *South African Journal of Science.* **86**, 434-440.

Butuzova G., Drits V., Morozov A. and Gorschkov A (1990) Process of formation of iron-manganese oxyhydroxides in the Atlantis – II and Thetis Deeps of the Red Sea. In: (Editors) Parnell J., Lianjun Y., and Changming C. *Sediment hosted mineral deposits*. Special Publication of the International Association of Sedimentologists. **2**, 57 – 72.

Cairncross B., Beukes N. J. and Gutzmer J. (1997) The manganese adventure. South African manganese fields. Associated Ore and Metal Corporation , Johannesbure, South Africa. 236 pp.

Carney J. N., Adliss D. T., and Lock N. P. (1994) The geology of Botswana. *Bulletin of the Geological Survey Department, Botswana*. **37**, 113 pp.

Chaney R. L., Brown S. L., Li Y. M., Angle J. S., Homer F. A. and Green C. E. (1995) Potential use of metal hyperaccumulators. *Mining and Environmental Management.* **3**, 9-11.

Chaney R. L., Malik M., Li Y. M., Brown S. L., Brewer E. P., Angle J. S. and Baker A. J. M. (1997) Phytoremediation of soil metals. http://www.soils.wise.edu/ 10pp.

Chen Z. and Lee D. Y. (1997) Evaluation of remediation techniques on two cadmium polluted soils in Taiwan. In: Iskandar A. and Adriano D. C. (Editors) Remediation of soils contaminated with metals. Science Reviews. Northwood, UK. 209-223.

Chen Z. (2000) Relationship between heavy metal concentrations in soils of Taiwan and uptake by crops. Food and Fertiliser Technology Center, Taipei. 13 pp.

Chenje M. (2000) State of the environment in the Zambesi basin 2000. Report by the Southern African Development Community (SADC-ELMS), World Conservation Union (IUCN), Zambezi River Authority (ZRA) and Southern African Research and Documentation Centre – Musokotwane Environment Resource Centre for Southern Africa (SARDC- IMERCSA), Maseru, Lusaka, Harare. 334 pp.

Crépin J and Johnson R.L. (1993) Soil sampling for environmental assessment. In Carter R. M. (Ed) *Soil sampling and methods of analyses*.

Coggans C. J., Bowles D. W., Robertson W. D., and Jambor J. L. (1999) The hydrogeochemistry of nickel mine tailings impoundment – Copper Cliff, Ontario. Part B – Case studies and research topics: Fillipek L. H. and Plumlee G. S. (Editors) *Reviews in Economic Geology: Environmental Geochemistry of mineral deposits*. **6B**, 447-465.

Comis D. (1996) Green remediation. *Journal of Soil and Water Conservation*. **51**, 184-187.

Cunningham S. D. and Berti W. R. (1993) remediation of contaminated soils with green plants: an overview. *In vitro cellular and Developmental Biology Plant*. **29**, 207-212.

Cunningham S. D., Berti W. R. and Huang J. W. (1995) Phytoremediation of contaminated soils. *Trends Biotechnology*. **13**, 393-398.

Cunningham S. D. and Lee C. R. (1995) Phytoremediation: Plant-Based Remediation of Contaminated Soils and Sediments. In Skipper, H. D., & Turco, R. F. (Editors) Bioremediation: Science and Applications. Wisconsin: Soil Science Society of America, Inc., American Society of Agronomy, Inc., Crop Science Society of America, Inc. 145-147 pp.

Department of Mines (1998) Air pollution control. 1998 annual report. Department of Mines of Botswana, Gaborone, Botswana. 47 pp.

Dixon J. B. (1989) Kaolin, serpentine group minerals. In Dixon J. B. (Editor), *Minerals in the environment*. 2nd Edition. Soil Science Society of America. Book Series **1**, 467-523.

Egbu A. U. (2000) Constraints to effective pollution control and management in Nigeria. *The Environmentalist*. **20**, 13-17.

Eckel W. P. and Langley W. D. (1988) A background based ranking technique for assessment of elemental enrichment in soils at hazardous waste sites. Superfund 88. Proceedings of the 9th National Conference held in Silverspring MD, USA, 28-30 November 1988. 282-286.

Eijkelkamp (2003) Calcimeter. www.eijkelkamp.com. 2 pp

Ekosse G. (2001) Provenance of the Kgwakgwe kaolin deposit in southeastern Botswana and its possible utilization *Applied Clay Science*. **20**, 137-152.

Ekosse G. and Modisi M. P. (1999) Mineralogical characterization, genesis and possible economic applications of goethite occurrences at the Lower

Transvaal Supergroup, Kgwakgwe, Botswana. *Botswana Journal of Earth Sciences***. 4**, 6-12.

Ekosse G. and Nkoma J. S. (2002) Electron microscopy and complementary techniques in the study of kaolinite formation from localised muscovite. Proceedings of the International Conference on Electron Microscopy, Durban, South Africa. *ICEM* **15**, 1079-1080.

Ekosse G. and Vink B. (1998) The Kgwakgwe manganese oxides in the Kanye area, southeastern Botswana - evidence for a shallow aqueous palaeo-environment. *Botswana Notes and Records*. **30**, 147-156.

Ekosse G. and Vink B. (2001) The Geology and Mineralogy of the Manganiferous, Ferrugenous and Argillaceous Sediments in the Kgwakgwe Basin, Lower Transvaal Supergroup, Kanye area, Botswana. *Botswana Journal of Earth Sciences*. **5**, 11-20.

Ekosse G., van den Heever D. and de Jager L. (2003) Environmental physico-chemistry of tailings dump and soils around the Selebi Phikwe Ni-Cu mine area, Botswana. *International Journal of Environmental Studies* **60**, 2.

Ekosse G., van den Heever D., de Jager L. and Totolo O. (2003b) Environmental mineralogy of soils around Selebi Phikwe nickel-copper plant, Botswana. *International Journal of Environmental Studies* **60**, 251-262.

Ekosse G., van den Heever D., de Jager L. and Totolo O. (2003) Environmental chemistry and mineralogy of particulate air matter around the Selebi Phikwe Ni-Cu mine area, Botswana. *International Journal of Minerals Engineering*. **17**, 349-353.

Elsenbroek J. H. and Neser J. A. (2002) An environmental application of regional geochemical mapping in understanding enzootic geophagia of calves in the Reivilo area, South Africa. *Environmental Geochemistry and Health*. **24**, 159-181.

ERDAS IMAGINE (1992) Field guide 3rd edition.628pp ERDAS, Inc.

Fellman C. (1996) Clays and pottery. http:www.acad.Carleton.edu. 4 pp.

Fouche P. S (1979) Kalkbehoefte. Fertilizer Society of South Africa Journal1, 25-28.

Gaspe A., Messer P. and Young P. (1994) Clay testing. A manual on clay/non-clay measuring technique. *Intermediate Technology Publications.* 17 pp.

Gillis A. M. (1991) Bringing back the land. *Bioscience*. *41*, 68-71.

Goodchild M. F. (1992) Scale in Remote Sensing and GIS. 216pp.

Hantong-Fong C. J., Bowles D. W. and Stuparyk R. A. (1997) Evaluation of low sulphur tailings in the prevention of acid mine drainage. *4th International Conference on Acid Mine Drainage, Vancouver, B. C., Canada.* 31 May – 6 June 1997.Conference Proceedings **2**, 835-847.

Harris D. C. (1999) quantitative chemical analysis. 5th edition. 762-765

Hawkes R. A. W. and Webb J. S. (1979) Geochemistry in Mineral Exploration.

Helyar K.R. (2002) The symptoms and effects on plants of nutrient disorders in acid soils. Farrer Center, Agricultural Research Centre, Wollongbar, NSW 2480, Australia.

Hudson-Edwards K., Schell C., and Macklin M. G. (1999) Mineralogy and geochemistry of alluvium contaminated by metal mining in the Rio Tinto area, southwest Spain. *Applied Geochemistry*. **14**, 1015-1030.

Hughes J.C. and Brown G. (1979) A crystallinity index for soil kaolins and its relation to parent rock, climate and soil maturity. *Journal of Soil Science.* **30**, 557-563.

ICDD (1986) International Centre for Diffraction Data. *Mineral Powder Diffraction File Databook*. Pp 1394.

ILWIS 3.0 (2002) Academic User's Guide. International Institute for Aerospace Survey and Earth Sciences (ITC) Enschede, The Netherlands. Pp 530.

Inglethorpe S. D., Morgan D. J., Highley D. E. and Bloodworth A. J. (1993) Industrial minerals laboratory manual: Bentonite. British Geological Survey Technical Report **WG/93/20**. 116 pp.

International Program on Chemical Safety (1981) Environmental health criteria 17. Manganese. IPCS INCHEM HOME. 89 pp.

Iron and manganese (2002) Iron and manganese fact sheet. Bureau of Reclamation, Technical Service Center. Water Treatment Engineering and Research Group D-8230, Denver, Colorado, USA. 2pp.

Iskandar A. and Adriano D. C. (1997) Remediation of soils contaminated with metals. A review of current practices in the USA. In Iskandar A. and

Adriano D. C. (Editors) Remediation of soils contaminated with metals. Science Reviews. Northwood, UK. 67-84.

Jackson P. E. (2000) Ion chromatography in environmental analysis. In : R. A. Meyers (Editor) Encyclopedia of Analytical Chemistry. John Wiley & Sons, Chichester. 2779-2801

Jewell M.C., Hensley P. J., Barry D.A. and Acworth I. (1993) Site investigation and monitoring techniques for contaminated sites and potential waste disposal sites. In Fell R., Philips T., Gerrad C., (Eds) Geotechnical management of waste and contamination.

Johnson M. S., Cooke J. A., and Stevenson J. K. W. (1994) Revegetation of metalliferous wastes and land after metal mining. In: Hester R. E. and Harrison R. M. (Editors) *Mining and its environmental impact*. Royal Society of Chemistry, Cambridge, Britain.

Jones J. B. and Case V. W. (1990) Sampling, Handling and Analyzing Plant Tissue Samples, In; Soil Testing and Plant Analysis, 3rd Ed., R.L. Westerman, Ed., Soil Science Society of America, Inc., Madison WI, pp.389 – 427.

Kralik M. (1999) A rapid procedure for environmental sampling and evaluation of polluted sediments. *Applied Geochemistry*. **14**, 807-816.

Langer A. M. (1999) Characterisation and measurement of the industrial environment mineralogy; Methods of study and evaluation of occupational respiratory diseases.

Lanzincka P. (1992) Manganese deposits in the global lithogenic system: Quantitative approach. *Ore Geology Review*. **7**, 279-356.

Lauwerys R., Roels H., Genet P., Toussaint G., Bouchearta A., Cooman S. (1985) Fertility of male workers exposed to mercury vapour or manganese dust: a questionnaire study. *American Journal of Industrial Medicine*. **7**, 171-176.

Lucchini R., Selis L., Folio D., Apostoli P., Mutti A., Vanoni O., Iregren A. and Alessio L. (1995) Neurobehavioural effects of manganese in workers from ferroalloy plant after temporary cessation of exposure. *Scandinavian Journal of Work and Environmental Health*. **21**, 143-149.

Ma C. and Eggleton R. A. (1999) Cation exchange capacity of kaolinite. Clays and Clay Minerals. **47**, 174-180.

Masters R., Hone B. and Doshi A. (1998) Environmental pollution, neurotoxicity and criminal violence. In Rose J. (Editor) Environmental toxicity current developments. Gordon and Breach, London, UK. 13-48.

Masters R. D., Way B., Hone T. B., Grelotti D. J., Gonzalez D. and Jones D. (1998b) Neurotoxicity and violence. *Vermont Law Review*. **22**, 358-382

Mazibuko B. (1997) The geology of the Kgwakgwe area south of Kanye. Unpublished BSc thesis. University of Botswana, Gaborone, Botswana. 78 pp.

Mestdagh M. M., Herbillion A. J., Rodrique L. and Rouxhet G. (1982) Evaluation du role due fer structurel sur la crystallinite des kaolinite. *Bulletin of Mineralogy*. **105**, 457 – 466.

Metrohm News (2004) Sulphate analysis of concrete using ion chromatography. Quality assurance in the laboratory. Metrohm , UK, Ltd.

Miller, J.C. and Miller, J.N, (1994) Statistics for analytical chemistry, 3rd edition. Ellis Horwood, Chichester, UK.

Mitchell A. J. B. (1976) Soil description and analysis from Eastern Botswana. Land Res. Div. Min. of Overseas Dev. Tolworth, England. Supplementary Report 6.

Modisi M. P. (1995) The origin of Chert Breccia around Kanye. *Botswana Notes and Records.* **27**, 299-308.

Munsell Soil Colour Book (1992) The Munsell soil colour book. Colour charts. Munsell Colour Company Inc., MD 2128, USA.

Murray H. H. (1986) Clays. Ullman's Encyclopedia of Industrial Chemistry. Weinheim. 5th Edition. 109-136.

National Census (1991) National population and housing census report. Botswana Government, Gaborone, Botswana.

Nedelkoska T. V. and Doran P. M. (2000) Characteristics of heavy metal uptake by plant species with potential for phytoremediation and phytomining. *Minerals Engineering* **13**, 549-561.

Okalebo J. R., Gathua K. W., and Woomer P. L. (1993) Laboratory methods of soil and plant analysis: A working manual. *Soil Science Society of East Africa, Technical Publication*. **1**, 88 pp.

Ostwald J. (1993) Manganese oxide mineralogy, petrography and genesis, Pilbara Manganese Group, western Australia. *Mineralium Deposita*. **28**, 198 – 208.

Page A. L., Miller, R. H. and Keeney, D. R. (1982) Methods of Soil Analysis, Part 2. Chemical and Microbiological Properties, 2nd Ed. America Society of Agronomy Inc. USA.

Parham W. E. (1966) Lateral variation of clay mineral assemblages in modern and ancient sediments. In : Heller L.and Weiss A. Proceedings of the International Clay Conference, Jerusalem, Israel. 1, 135 – 145.

Park C. (1987) Acid Rain. London: Methuen.

Park H., Kim Y, Lee D. W., Lee S. and Lee K. (2002) ion chromatographic determination of inorganicanions in environmental samples of Korea. *Analytical Sciences*. **18**, 343-346

Pettijohn E. J. (1975) Sedimentary rocks. Harper & Row, New York, USA. 628 pp.

Pierzynski G. M. (1997) Strategies for remediating trace elements contaminated sites. Iskandar A. and Adriano D. C. (Editors) Remediation of soils contaminated with metals. Science Reviews. Northwood, UK. 67-84.

Pracejus B. (1989) Nature and formation of supergene manganese deposits on Groote Eylandt. M. T. Australia. Unpublished PhD thesis. University of Adelaide, Australia. 231 pp.

Principles of Geographic Information System (2000) 230 pp. ITC Educational Textbook Series. 170pp International Institute for Aerospace Survey and Earth Sciences (ITC) Enschede, The Netherlands.

Principles of Remote Sensing (2000) ITC Educational Textbook Series. 170pp International Institute for Aerospace Survey and Earth Sciences (ITC) Enschede, The Netherlands.

Ptacek C. J. and Bowles D. W. (1992) Influence of siderite on the pore-water chemistry of inactive mine tailings impoundments. In Environmental Geochemistry of sulphide oxidation. Alpers C. N., and Bowles D. W. (Eds) ACS symposium series 550, 1730189.

Pulles W. (1992) Water pollution: its management and control in the South African gold mining industry. *Journal of the South African Institute of Mining and Metallurgy*. **99**, 197-200.

Pulles W., Howie D., Otto D. and Easton J. (1996) A manual on mine water treatment and management practices in South Africa. Appendix 1. Literature reviews. Water Commission Report 527/1/96. 188 pp.

Purdey M. Ecosystems supporting clusters of sporadic TSEs demonstrate excesses of the radical generating divalent cation manganese and deficiencies of antioxidant co factors Cu, Se, Fe, Zn. Does a foreign cation substitution at PrP's Cu domain initiate TSE? Med Hypotheses 2000; 54(2): 278-306.

Reemelwaal A. (1988) General soil legend of Botswana. FAO/UNDP/Gov't of Botswana. Field document. BOT/85/11.

Reichman S. (2000) Understanding metal toxicity in plants. Ameef literature review award. http://www.ameef.com.au. 4 pp.

Ringrose S. and Matheson W. (1991) Classification of Woody Vegetation Cover in South East Botswana Kalahari, *Global Ecology and biogeography Letter*. **1**,176-181.

Ripley E. A., Redmann R. E., and Crowder A. A. (1996) Environmental effects of mining. St Lucie Press, Delray Beach, Fl, USA. 113-133.

Roane T.M., Perpper, and Miller (1994) Microbial remediation of metals. In Craford, L., Ronolad & Cfawford, L., Don. (Ed.). Bioremediation Principles and Applications (pp. 312-340). 1960. Great Britain: Cambridge University Press.

Rope S. K., Arthur W. J., Craig T. H. and Craig E. H. (1988) Nutrient and trace elements in soil and desert vegetation of southern Idaho. *Environmental Monitoring and Assessment*. **10**, 1-24.

Salt D. E., Blaylock M., Kumar P.B. A. N., Dushenkov S., Ensley B. D., Chet I. and Raskin I. (1996) Phytoremediation: A novel strategy for the removal of toxic metals from the environment using plants. *Bio/Technology.* **13**, 468-474.

Shaw S. C., Groat L. A., Jambor J. L., Bowles D. W., Hantong-Fong C. J. and Stuparyk R. A. (1998) Mineralogical study of base metal tailings with various sulphide contents, oxidised in laboratory columns and field lysmeters. *Environmental Geology*. **33**, 209-217.

Shroeder W. H., Dobson M., and Kane D. M. (1987) Toxic trace elements associated with airborne particulate matter: a review. *Journal of the Air Pollution Control Association*. **37**, 1267-1285.

Sisler J. F. (1996) Spatial and seasonal patterns and long term variability of the composition of the haze in the USA; an analysis of data from the IMPROVE network. ISSN; 0737-5352-32. CIRA, Colorado State University, Fort Collins, CO 80523, USA.

Sisler J. F. and Huffinan D. (1993) Spatial and temporal patterns and the chemical composition of the haze in the USA; An analysis of data from the improve network 1988-1991. ISSN no 0737-5352-26. CIRA Foothills Campus, Colorado State University, Fort Collins, CO 80523, USA.

Skidmore A. (2002) Environmental Modelling With GIS and Remote Sensing. Taylor and Francis, 11 New Fetter Lane, London EC4P 4EE.

Smith K. A. (1990) Manganese and cobalt. In Alloway B. J. (Editor) Heavy metals in soils. Blackie and Sons, Inc. Glassgow.197-236.

Taitel-Goldman N., Heller-Kallai L. and Sass E. (1995) Clay minerals and feldspars in argillaceous strata of the Judea Group in the Jerusalem Hills. *Israel Journal of Earth Sciences*. **44**, 71 – 79.

Tan K. H. (1996) Sample preparation. In Dekker M. (Ed), *Soil sample preparation and analysis*.14pp.

Tan K. H. (1998) Principles of soil chemistry. Mariel Dekker Inc. USA. 521 pp.

Taylor R. M. (1987) Non silicate oxides and hydroxides. In: Newman A. C. (Editor) Chemistry of clays and clay minerals. Mineralogical Society. Monograph **6**, 129 – 201. Longman, England.

Timberlake J. (1980) Vegetation map of south east Botswana. Ministry of Agriculture, Botswana, Gaborone.

USA-EPA (1984) Health assessment document for manganese. Cincinnati, Ohio US Environmental Protection Agency. Office of Research and Development. EPA-600/8-83-013F.

USA-EPA (1990) Summary of treatment technology effectiveness for contaminated soils. Washington D. C., USA. EPA/540/2-89/053. 510 pp.

USA-EPA (1995) National air quality studies and trends. Office of Air and Radiation of the United States of America – Environmental Protection Agency. 10 pp.

USDA (1996) United States Department of Agriculture. Particle size analysis. *Soil Survey Laboratory Methods Manual*. Soil Investigation Report. **42** (3), 31-111.

Van Reeuwijk L. P. (1993) procedures for soil analysis. *Int. Soil Ref. & Info. Centre. Wageningen, The Netherlands*. *Tech. Paper* **9**, 100 pp.

Van den Heever D. J. and Frey B. J. (1996) Human aspects of certain metals in tissue of the African sharptooth catfish, *Clarias gariepinus*, kept in treated sewage effluent and the Krugersdrift Dam: chromium and mercury. *Water SA* 22, 73-78.

Vink B. and Ekosse G. (2002) Manganese occurrences in Botswana. In Ngowi A. Feldman C., B, Matshediso B., Mathiba J., and Segawa J. (Editors) proceedings of the 1st Botswana International Conference on Mining. Challenges facing the mineral industry in developing countries. 20-22 November 2002, 117-123.

Vitosh M. L, Warncke D. D and Lucas R. E. (1994) Secondary and Micronutrients for Vegetables and Field Crops. *Extension Bulletin* E-486.

Weaver C. (1989) Clays, muds and shales. Elsevier. 819 pp.

Wisconsin Department of Natural Resources (1997) Naturally occurring biodegradation as a remedial action option for soil contamination. Interim Guidance (revised). Wisconsin Department of Natural Resources , Emergency and Remedial Response Program. Wisconsin, USA. PUBL-SW-515-95. 16 pp.

Weaver A. V. B. and Caldwell P. (1999) Environmental Impact Assessment for mining projects. In Petts J. (Editor) Handbook of Environmental Impact Assessment: *Volume 2: Environmental Impact assessment in practice: impacts and limitations*. Blackwell science, Oxford, United Kingdom. **2**, 377-403.

World Health Organisation(1984) Guidelines for drinking water quality. Vol 2. Health criteria and other supporting information. 335 pp.

WHO (1987) Manganese. In: Air quality guidelines for Europe. Copenhagen, World Health Organisation Regional Office for Europe. European Series 23, 262-271.

WHO (1993) Guidelines for drinking water quality. 2nd Edition. World Health Organisation, Geneva.

WHO (1999) World Health Organisation air quality guidelines for Europe. Copenhagen, World Health Organisation Regional Office for Europe. 2nd Edition.

Zar, J.H. (1984) Biostatistical Analysis, Prentice Hall, Eaglewood Cliffs, NJ.

Zayed J., Gẻrin G., Loranger S., Sierra P., Bẻgin D. and Kennedy G. (1994) Occupational and environmental exposure of garage workers and taxi drivers to airborne manganese arising from the use of methylcyclopentadienyl manganese tricarbonyl in unleaded gasoline. *American Industrial Hygiene association Journal*. **55**, 53-58.

APPENDIX A

Table 2.1: Sample number, sample code and XY coordinates of points where soil and vegetation samples were obtained

Number Sample	Sample code	X	Y	Sample Number	Sample code	X	Y
1	A1-1	329023.25	7234057	201	C1-1	328023.3	7234057
2	A1-2	329023.25	7234157	202	C1-2	328023.3	7234157
3	A1-3	329023.25	7234257	203	C1-3	328023.3	7234257
4	A1-4	329023.25	7234357	204	C1-4	328023.3	7234357
5	A1-5	329023.25	7234457	205	C1-5	328023.3	7234457
6	A1-6	329023.25	7234557	206	C1-6	328023.3	7234557
7	A1-7	329023.25	7234657	207	C1-7	328023.3	7234657
8	A1-8	329023.25	7234757	208	C1-8	328023.3	7234757
9	A1-9	329023.25	7234857	209	C1-9	328023.3	7234857
10	A1-10	329023.25	7234957	210	C1-10	328023.3	7234957
11	B1-1	329023.25	7235057	211	D1-1	328023.3	7235057
12	B1-2	329023.25	7235157	212	D1-2	328023.3	7235157
13	B1-3	329023.25	7235257	213	D1-3	328023.3	7235257
14	B1-4	329023.25	7235357	214	D1-4	328023.3	7235357
15	B1-5	329023.25	7235457	215	D1-5	328023.3	7235457
16	B1-6	329023.25	7235557	216	D1-6	328023.3	7235557
17	B1-7	329023.25	7235657	217	D1-7	328023.3	7235657
18	B1-8	329023.25	7235757	218	D1-8	328023.3	7235757
19	B1-9	329023.25	7235857	219	D1-9	328023.3	7235857
20	B1-10	329023.25	7235957	220	D1-10	328023.3	7235957
21	A2-1	328923.25	7234057	221	C2-1	327923.3	7234057
22	A2-2	328923.25	7234157	222	C2-2	327923.3	7234157
23	A2-3	328923.25	7234257	223	C2-3	327923.3	7234257
24	A3-4	328923.25	7234357	224	C2-4	327923.3	7234357
25	A2-5	328923.25	7234457	225	C2-5	327923.3	7234457
26	A2-6	328923.25	7234557	226	C2-6	327923.3	7234557
27	A2-7	328923.25	7234657	227	C2-7	327923.3	7234657
28	A2-8	328923.25	7234757	228	C2-8	327923.3	7234757
29	A2-9	328923.25	7234857	229	C2-9	327923.3	7234857
30	A2-10	328923.25	7234957	230	C2-10	327923.3	7234957
31	B2-1	328923.25	7235057	231	D2-1	327923.3	7235057
32	B2-2	328923.25	7235157	232	D2-2	327923.3	7235157
33	B2-3	328923.25	7235257	233	D2-3	327923.3	7235257
34	B2-4	328923.25	7235357	234	D2-4	327923.3	7235357
35	B2-5	328923.25	7235457	235	D2-5	327923.3	7235457
36	B2-6	328923.25	7235557	236	D2-6	327923.3	7235557
37	B2-7	328923.25	7235657	237	D2-7	327923.3	7235657

38	B2-8	328923.25	7235757	238	D2-8	327923.3	7235757
39	B29	328923.25	7235857	239	D2-9	327923.3	7235857
40	B2-10	328923.25	7235957	240	D2-10	327923.3	7235957
41	A3-1	328823.25	7234057	241	C3-1	327823.3	7234057
42	A3-2	328823.25	7234157	242	C3-2	327823.3	7234157
43	A3-3	328823.25	7234257	243	C3-3	327823.3	7234257
44	A3-4	328823.25	7234357	244	C3-4	327823.3	7234357
45	A3-5	328823.25	7234457	245	C3-5	327823.3	7234457
46	A3-6	328823.25	7234557	246	C3-6	327823.3	7234557
47	A3-7	328823.25	7234657	247	C3-7	327823.3	7234657
48	A3-8	328823.25	7234757	248	C3-8	327823.3	7234757
49	A3-9	328823.25	7234857	249	C3-9	327823.3	7234857
50	A3-10	328823.25	7234957	250	C3-10	327823.3	7234957
51	B3-1	328823.25	7235057	251	D3-1	327823.3	7235057
52	B3-2	328823.25	7235157	252	D3-2	327823.3	7235157
53	B3-3	328823.25	7235257	253	D3-3	327823.3	7235257
54	B3-4	328823.25	7235357	254	D3-4	327823.3	7235357
55	B3-5	328823.25	7235457	255	D3-5	327823.3	7235457
56	B3-6	328823.25	7235557	256	D3-6	327823.3	7235557
57	B3-7	328823.25	7235657	257	D3-7	327823.3	7235657
58	B3-8	328823.25	7235757	258	D3-8	327823.3	7235757
59	B3-9	328823.25	7235857	259	D3-9	327823.3	7235857
60	B3-10	328823.25	7235957	260	D3-10	327823.3	7235957
61	A4-1	328723.25	7234057	261	C4-1	327723.3	7234057
62	A4-2	328723.25	7234157	262	C4-2	327723.3	7234157
63	A4-3	328723.25	7234257	263	C4-3	327723.3	7234257
64	A4-4	328723.25	7234357	264	C4-4	327723.3	7234357
65	A4-5	328723.25	7234457	265	C4-5	327723.3	7234457
66	A4-6	328723.25	7234557	266	C4-6	327723.3	7234557
67	A4-7	328723.25	7234657	267	C4-7	327723.3	7234657
68	A4-8	328723.25	7234757	268	C4-8	327723.3	7234757
69	A4-9	328723.25	7234857	269	C4-9	327723.3	7234857
70	A4-10	328723.25	7234957	270	C4-10	327723.3	7234957
71	B4-1	328723.25	7235057	271	D4-1	327723.3	7235057
72	B4-2	328723.25	7235157	272	D4-2	327723.3	7235157
73	B4-3	328723.25	7235257	273	D4-3	327723.3	7235257
74	B4-4	328723.25	7235357	274	D4-4	327723.3	7235357
75	B4-5	328723.25	7235457	275	D4-5	327723.3	7235457
76	B4-6	328723.25	7235557	276	D4-6	327723.3	7235557
77	B4-7	328723.25	7235657	277	D4-7	327723.3	7235657
78	B4-8	328723.25	7235757	278	D4-8	327723.3	7235757
79	B4-9	328723.25	7235857	279	D4-9	327723.3	7235857
80	B4-10	328723.25	7235957	280	D4-10	327723.3	7235957
81	A5-1	328623.25	7234057	281	C5-1	327623.3	7234057
82	A5-2	328623.25	7234157	282	C5-2	327623.3	7234157
83	A5-3	328623.25	7234257	283	C5-3	327623.3	7234257

84	A5-4	328623.25	7234357	284	C5-4	327623.3	7234357
85	A5-5	328623.25	7234457	285	C5-5	327623.3	7234457
86	A5-6	328623.25	7234557	286	C5-6	327623.3	7234557
87	A5-7	328623.25	7234657	287	C5-7	327623.3	7234657
88	A5-8	328623.25	7234757	288	C5-8	327623.3	7234757
89	A5-9	328623.25	7234857	289	C5-9	327623.3	7234857
90	A5-10	328623.25	7234957	290	C5-10	327623.3	7234957
91	B5-1	328623.25	7235057	291	D5-1	327623.3	7235057
92	B5-2	328623.25	7235157	292	D5-2	327623.3	7235157
93	B5-3	328623.25	7235257	293	D5-3	327623.3	7235257
94	B5-4	328623.25	7235357	294	D5-4	327623.3	7235357
95	B5-5	328623.25	7235457	295	D5-5	327623.3	7235457
96	B5-6	328623.25	7235557	296	D5-6	327623.3	7235557
97	B5-7	328623.25	7235657	297	D5-7	327623.3	7235657
98	B5-8	328623.25	7235757	298	D5-8	327623.3	7235757
99	B5-9	328623.25	7235857	299	D5-9	327623.3	7235857
100	B5-10	328623.25	7235957	300	D5-10	327623.3	7235957
101	A6-1	328523.25	7234057	301	C6-1	327523.3	7234057
102	A6-2	328523.25	7234157	302	C6-2	327523.3	7234157
103	A6-3	328523.25	7234257	303	C6-3	327523.3	7234257
104	A6-4	328523.25	7234357	304	C6-4	327523.3	7234357
105	A6-5	328523.25	7234457	305	C6-5	327523.3	7234457
106	A6-6	328523.25	7234557	306	C6-6	327523.3	7234557
107	A6-7	328523.25	7234657	307	C6-7	327523.3	7234657
108	A6-8	328523.25	7234757	308	C6-8	327523.3	7234757
109	A6-9	328523.25	7234857	309	C6-9	327523.3	7234857
110	A6-10	328523.25	7234957	310	C6-10	327523.3	7234957
111	B6-1	328523.25	7235057	311	D6-1	327523.3	7235057
112	B6-2	328523.25	7235157	312	D6-2	327523.3	7235157
113	B6-3	328523.25	7235257	313	D6-3	327523.3	7235257
114	B6-4	328523.25	7235357	314	D6-4	327523.3	7235357
115	B6-5	328523.25	7235457	315	D6-5	327523.3	7235457
116	B6-6	328523.25	7235557	316	D6-6	327523.3	7235557
117	B6-7	328523.25	7235657	317	D6-7	327523.3	7235657
118	B6-8	328523.25	7235757	318	D6-8	327523.3	7235757
119	B6-9	328523.25	7235857	319	D6-9	327523.3	7235857
120	B6-10	328523.25	7235957	320	D6-10	327523.3	7235957
121	A7-1	328423.25	7234057	321	C7-1	327423.3	7234057
122	A7-2	328423.25	7234157	322	C7-2	327423.3	7234157
123	A7-3	328423.25	7234257	323	C7-3	327423.3	7234257
124	A7-4	328423.25	7234357	324	C7-4	327423.3	7234357
125	A7-5	328423.25	7234457	325	C7-5	327423.3	7234457
126	A7-6	328423.25	7234557	326	C7-6	327423.3	7234557
127	A7-7	328423.25	7234657	327	C7-7	327423.3	7234657
128	A7-8	328423.25	7234757	328	C7-8	327423.3	7234757
129	A7-9	328423.25	7234857	329	C7-9	327423.3	7234857

130	A7-10	328423.25	7234957	330	C7-10	327423.3	7234957
131	B7-1	328423.25	7235057	331	D7-1	327423.3	7235057
132	B7-2	328423.25	7235157	332	D7-2	327423.3	7235157
133	B7-3	328423.25	7235257	333	D7-3	327423.3	7235257
134	B7-4	328423.25	7235357	334	D7-4	327423.3	7235357
135	B7-5	328423.25	7235457	335	D7-5	327423.3	7235457
136	B7-6	328423.25	7235557	336	D7-6	327423.3	7235557
137	B7-7	328423.25	7235657	337	D7-7	327423.3	7235657
138	B7-8	328423.25	7235757	338	D7-8	327423.3	7235757
139	B7-9	328423.25	7235857	339	D7-9	327423.3	7235857
140	B7-10	328423.25	7235957	340	D7-10	327423.3	7235957
141	A8-1	328323.25	7234057	341	C8-1	327323.3	7234057
142	A8-2	328323.25	7234157	342	C8-2	327323.3	7234157
143	A8-3	328323.25	7234257	343	C8-3	327323.3	7234257
144	A8-4	328323.25	7234357	344	C8-4	327323.3	7234357
145	A8-5	328323.25	7234457	345	C8-5	327323.3	7234457
146	A8-6	328323.25	7234557	346	C8-6	327323.3	7234557
147	A8-7	328323.25	7234657	347	C8-7	327323.3	7234657
148	A8-8	328323.25	7234757	348	C8-8	327323.3	7234757
149	A8-9	328323.25	7234857	349	C8-9	327323.3	7234857
150	A8-10	328323.25	7234957	350	C8-10	327323.3	7234957
151	B8-1	328323.25	7235057	351	D8-1	327323.3	7235057
152	B8-2	328323.25	7235157	352	D8-2	327323.3	7235157
153	B8-3	328323.25	7235257	353	D8-3	327323.3	7235257
154	B8-4	328323.25	7235357	354	D8-4	327323.3	7235357
155	B8-5	328323.25	7235457	355	D8-5	327323.3	7235457
156	B8-6	328323.25	7235557	356	D8-6	327323.3	7235557
157	B8-7	328323.25	7235657	357	D8-7	327323.3	7235657
158	B8-8	328323.25	7235757	358	D8-8	327323.3	7235757
159	B8-9	328323.25	7235857	359	D8-9	327323.3	7235857
160	B8-10	328323.25	7235957	360	D8-10	327323.3	7235957
161	A9-1	328223.25	7234057	361	C9-1	327223.3	7234057
162	A9-2	328223.25	7234157	362	C9-2	327223.3	7234157
163	A9-3	328223.25	7234257	363	C9-3	327223.3	7234257
164	A9-4	328223.25	7234357	364	C9-4	327223.3	7234357
165	A9-5	328223.25	7234457	365	C9-5	327223.3	7234457
166	A9-6	328223.25	7234557	366	C9-6	327223.3	7234557
167	A9-7	328223.25	7234657	367	C9-7	327223.3	7234657
168	A9-8	328223.25	7234757	368	C9-8	327223.3	7234757
169	A9-19	328223.25	7234857	369	C9-9	327223.3	7234857
170	A9-10	328223.25	7234957	370	C9-10	327223.3	7234957
171	B9-1	328223.25	7235057	371	D9-1	327223.3	7235057
172	B9-2	328223.25	7235157	372	D9-2	327223.3	7235157
173	B9-3	328223.25	7235257	373	D9-3	327223.3	7235257
174	B9-4	328223.25	7235357	374	D9-4	327223.3	7235357
175	B9-5	328223.25	7235457	375	D9-5	327223.3	7235457

176	B9-6	328223.25	7235557	376	D9-6	327223.3	7235557
177	B9-7	328223.25	7235657	377	D9-7	327223.3	7235657
178	B9-8	328223.25	7235757	378	D9-8	327223.3	7235757
179	B9-9	328223.25	7235857	379	D9-9	327223.3	7235857
180	B9-10	328223.25	7235957	380	D9-10	327223.3	7235957
181	A10-1	328123.25	7234057	381	C10-1	327123.3	7234057
182	A10-2	328123.25	7234157	382	C10-2	327123.3	7234157
183	A10-3	328123.25	7234257	383	C10-3	327123.3	7234257
184	A10-4	328123.25	7234357	384	C10-4	327123.3	7234357
185	A10-5	328123.25	7234457	385	C10-5	327123.3	7234457
186	A10-6	328123.25	7234557	386	C10-6	327123.3	7234557
187	A10-7	328123.25	7234657	387	C10-7	327123.3	7234657
188	A10-8	328123.25	7234757	388	C10-8	327123.3	7234757
189	A10-9	328123.25	7234857	389	C10-9	327123.3	7234857
190	A10-10	328123.25	7234957	390	C10-10	327123.3	7234957
191	B10-1	328123.25	7235057	391	D10-1	327123.3	7235057
192	B10-2	328123.25	7235157	392	D10-2	327123.3	7235157
193	B10-3	328123.25	7235257	393	D10-3	327123.3	7235257
194	B10-4	328123.25	7235357	394	D10-4	327123.3	7235357
195	B10-5	328123.25	7235457	395	D10-5	327123.3	7235457
196	B10-6	328123.25	7235557	396	D10-6	327123.3	7235557
197	B10-7	328123.25	7235657	397	D10-7	327123.3	7235657
198	B10-8	328123.25	7235757	398	D10-8	327123.3	7235757
199	B10-9	328123.25	7235857	399	D10-9	327123.3	7235857
200	B10-10	328123.25	7235957	400	D10-10	327123.3	7235957

APPENDIX B

Table 3.2; Particle size distribution of soil samples from the study area

Sample code and size fraction	Percent fraction	Sample code and size fraction	Percent fraction	Sample code and size fraction	Percent fraction	Sample code and size fraction	Percent fraction
A1-1 500 μm	57.10	B1-1 500 μm	12.90	C1-1 500 μm	49.58	D1-1 500 μm	12.22
< 53 μm	34.35	< 53 μm	85.37	< 53 μm	45.57	< 53 μm	82.20
< 4 μm	8.44	< 4 μm	1.62	< 4 μm	4.70	< 4 μm	5.51
A1-2 500 μm	59.72	B1-2 500 μm	18.29	C1-2 500 μm	38.09		
< 53 μm	38.44	< 53 μm	79.10	< 53 μm	56.50	D1-2 500 μm	75.53
< 4 μm	1.64	< 4 μm	2.55	< 4 μm	5.24	< 53 μm	5.55
A1-3 500 μm	61.75	B1-3 500 μm	13.78	C1-3 500 μm	55.85		
< 53 μm	34.15	< 53 μm	83.20	< 53 μm	39.71	D1-3 500 μm	78.03
< 4 μm	4.01	< 4 μm	2.95	< 4 μm	4.39	< 53 μm	4.49
A1-4 500 μm	31.68	B1-4 500 μm	7.85	C1-4 500 μm	42.49	D1-4 500 μm	15.95
< 53 μm	62.29	< 53 μm	82.45	< 53 μm	51.24	< 53 μm	79.13
< 4 μm	5.68	< 4 μm	4.78	< 4 μm	6.17	< 4 μm	4.76
A1-5 500 μm	38.28	B1-5 500 μm	15.41	C1-5 500 μm	63.79	D1-5 500 μm	41.97
< 53 μm	58.24	< 53 μm	79.46	< 53 μm	33.23	< 53 μm	54.40
< 4 μm	3.32	< 4 μm	4.96	< 4 μm	2.92	< 4 μm	3.55
A1-6 500 μm	22.22	B1-6 500 μm	10.13	C1-6 500 μm	21.71	D1-6 500 μm	34.70
< 53 μm	69.17	< 53 μm	84.83	< 53 μm	71.88	< 53 μm	58.30
< 4 μm	8.38	< 4 μm	4.90	< 4 μm	6.28	< 4 μm	3.92
A1-7 500 μm	51.09	B1-7 500 μm	9.78	C1-7 500 μm	73.82	D1-7 500 μm	9.98
< 53 μm	38.15	< 53 μm	82.84	< 53 μm	24.93	< 53 μm	85.81
< 4 μm	10.42	< 4 μm	7.30	< 4 μm	1.23	< 4 μm	4.18
A1-8 500 μm	20.38	B1-8 500 μm	8.70	C1-8 500 μm	30.62	D1-8 500 μm	11.92
< 53 μm	76.74	< 53 μm	90.15	< 53 μm	65.65	< 53 μm	83.90
< 4 μm	2.55	< 4 μm	1.13	< 4 μm	3.65	< 4 μm	4.19
A1-9 500 μm	20.40	B1-9 500 μm	18.48	C1-9 500 μm	22.32	D1-9 500 μm	9.44
< 53 μm	75.49	< 53 μm	78.36	< 53 μm	72.87	< 53 μm	84.76
< 4 μm	3.83	< 4 μm	3.08	< 4 μm	4.73	< 4 μm	5.64
A1-10 500 μm	22.47	B1-10 500 μm	17.21	C1-10 500 μm	15.51	D1-10 500 μm	29.66
< 53 μm	76.92	< 53 μm	78.07	< 53 μm	76.09	< 53 μm	65.58
< 4 μm	0.30	< 4 μm	4.70	< 4 μm	8.32	< 4 μm	4.69
A2-1 500 μm	19.74	B2-1 500 μm	13.64	C-2-1 500 μm	49.23	D2-1 500 μm	18.28
< 53 μm	76.72	< 53 μm	82.31	< 53 μm	44.23	< 53 μm	77.86
< 4 μm	3.49	< 4 μm	3.99	< 4 μm	6.97	< 4 μm	3.77
A22 500 μm	19.26	B2-2 500 μm	17.58	C-2-2 500 μm	53.79	D2-2 500 μm	15.59
< 53 μm	79.13	< 53 μm	80.05	< 53 μm	41.50	< 53 μm	82.75
< 4 μm	1.33	< 4 μm	2.35	< 4 μm	4.52	< 4 μm	1.56
A2-3 500 μm	20.79	B2-3 500 μm	18.36	C-2-3 500 μm	56.17	D2-3 500 μm	16.16
< 53 μm	53.42	< 53 μm	78.63	< 53 μm	39.28	< 53 μm	78.13
< 4 μm	25.55	< 4 μm	2.98	< 4 μm	4.82	< 4 μm	5.64

A2-4 500 μm	16.90	B2-4 500 μm	11.81	C-24 500 μm	49.10	D2-4 500 μm	17.25
< 53 μm	72.99	< 53 μm	83.23	< 53 μm	45.09	< 53 μm	80.42
< 4 μm	9.91	< 4 μm	4.88	< 4 μm	5.71	< 4 μm	2.24
A2-5 500 μm	25.35	B2-5 500 μm	8.15	C-25 500 μm	46.43	D2-5 500 μm	59.64
< 53 μm	66.82	< 53 μm	83.53	< 53 μm	50.38	< 53 μm	37.26
< 4 μm	7.32	< 4 μm	4.89	< 4 μm	3.09	< 4 μm	3.07
A2-6 500 μm	23.01	B2-6 500 μm	10.94	C2-6 500 μm	19.35	D2-6 500 μm	23.05
< 53 μm	69.96	< 53 μm	83.99	< 53 μm	75.27	< 53 μm	70.05
< 4 μm	6.62	< 4 μm	4.86	< 4 μm	5.25	< 4 μm	6.61
A2-7 500 μm	50.09	B2-7 500 μm	10.90	C2-7 500 μm	48.26	D2-7 500 μm	14.99
< 53 μm	48.90	< 53 μm	84.50	< 53 μm	47.02	< 53 μm	80.29
< 4 μm	1.04	< 4 μm	4.54	< 4 μm	4.52	< 4 μm	4.62
A2-8 500 μm	15.88	B2-8 500 μm	20.48	C2-8 500 μm	26.48	D2-8 500 μm	6.17
< 53 μm	76.57	< 53 μm	77.22	< 53 μm	69.38	< 53 μm	89.87
< 4 μm	7.28	< 4 μm	2.31	< 4 μm	4.05	< 4 μm	3.91
A2-9 500 μm	29.83	B2-9 500 μm	15.03	C2-9 500 μm	19.60	D2-9 500 μm	4.06
< 53 μm	65.26	< 53 μm	73.24	< 53 μm	75.67	< 53 μm	84.70
< 4 μm	4.80	< 4 μm	11.65	< 4 μm	4.60	< 4 μm	11.05
A2-10 500 μm	55.64	B210 500 μm	26.17	C210 500 μm	16.70	D210 500 μm	50.57
< 53 μm	37.31	< 53 μm	71.06	< 53 μm	78.40	< 53 μm	48.31
< 4 μm	6.88	< 4 μm	2.71	< 4 μm	4.80	< 4 μm	0.83
A3-1 500 μm	28.68	B3-1 500 μm	12.72	C3-1 500 μm	38.94	D3-1 500 μm	12.31
< 53 μm	66.48	< 53 μm	83.97	< 53 μm	51.37	< 53 μm	82.30
< 4 μm	4.73	< 4 μm	3.22	< 4 μm	9.64	< 4 μm	5.27
A3-2 500 μm	31.28	B3-2 500 μm	16.98	C3-2 500 μm	63.38	D3-2 500 μm	12.68
< 53 μm	44.80	< 53 μm	78.97	< 53 μm	32.55	< 53 μm	79.76
< 4 μm	23.62	< 4 μm	3.99	< 4 μm	3.53	< 4 μm	7.34
A3-3 500 μm	29.09	B3-3 500 μm	21.31	C3-3 500 μm	60.40	D3-3 500 μm	10.81
< 53 μm	51.98	< 53 μm	76.14	< 53 μm	18.31	< 53 μm	82.10
< 4 μm	18.46	< 4 μm	2.50	< 4 μm	21.22	< 4 μm	7.00
A3-4 500 μm	46.99	B3-4 500 μm	13.28	C3-4 500 μm	50.34	D3-4 500 μm	15.62
< 53 μm	51.34	< 53 μm	84.98	< 53 μm	45.46	< 53 μm	80.11
< 4 μm	1.51	< 4 μm	1.68	< 4 μm	4.01	< 4 μm	4.11
A3-5 500 μm	21.02	B3-5 500 μm	17.64	C3-5 500 μm	53.38	D3-5 500 μm	39.86
< 53 μm	72.12	< 53 μm	109.80	< 53 μm	43.97	< 53 μm	56.30
< 4 μm	6.63	< 4 μm	2.83	< 4 μm	2.52	< 4 μm	3.80
A3-6 500 μm	25.95	B3-6 500 μm	12.33	C3-6 500 μm	19.60	D3-6 500 μm	20.15
< 53 μm	69.54	< 53 μm	83.52	< 53 μm	74.71	< 53 μm	72.59
< 4 μm	4.29	< 4 μm	4.05	< 4 μm	5.58	< 4 μm	7.73
A3-7 500 μm	34.84	B3-7 500 μm	10.83	C3-7 500 μm	43.89	D3-7 500 μm	7.68
< 53 μm	61.80	< 53 μm	84.03	< 53 μm	52.94	< 53 μm	89.97
< 4 μm	3.21	< 4 μm	5.12	< 4 μm	3.10	< 4 μm	7.73
A3-8 500 μm	28.14	B3-8 500 μm	16.13	C3-8 500 μm	20.16	D3-8 500 μm	11.89
< 53 μm	62.48	< 53 μm	80.42	< 53 μm	73.87	< 53 μm	81.47
< 4 μm	9.23	< 4 μm	3.38	< 4 μm	5.77	< 4 μm	6.68
A3-9 500 μm	14.49	B39 500 μm	20.94	C3-9 500 μm	19.55	D3-9 500 μm	4.30
< 53 μm	79.47	< 53 μm	73.68	< 53 μm	75.57	< 53 μm	89.43
< 4 μm	5.77	< 4 μm	5.24	< 4 μm	4.81	< 4 μm	6.15

A3-10 500 μm	17.61	B3-10 500 μm	34.04	C3-10 500 μm	11.35	D3-10 500 μm	24.58
< 53 μm	72.43	< 53 μm	63.88	< 53 μm	83.16	< 53 μm	67.21
< 4 μm	9.38	< 4 μm	2.03	< 4 μm	5.37	< 4 μm	5.40
A4-1 500 μm	50.57	B4-1 500 μm	13.07	C4-1 500 μm	53.99	D4-1 500 μm	10.78
< 53 μm	48.31	< 53 μm	83.31	< 53 μm	42.39	< 53 μm	88.07
< 4 μm	0.83	< 4 μm	3.60	< 4 μm	3.56	< 4 μm	1.10
A4-2 500 μm	32.13	B4-2 500 μm	12.24	C4-2 500 μm	44.23	D4-2 500 μm	12.07
< 53 μm	60.95	< 53 μm	83.69	< 53 μm	50.50	< 53 μm	79.46
< 4 μm	6.65	< 4 μm	3.85	< 4 μm	5.17	< 4 μm	8.30
A4-3 500 μm	62.10	B4-3 500 μm	18.37	C4-3 500 μm	39.05	D4-3 500 μm	14.73
< 53 μm	28.89	< 53 μm	79.75	< 53 μm	57.37	< 53 μm	78.97
< 4 μm	8.90	< 4 μm	1.82	< 4 μm	3.49	< 4 μm	6.22
A4-4 500 μm	39.86	B4-4 500 μm	7.95	C4-4 500 μm	34.78	D4-4 500 μm	15.21
< 53 μm	56.30	< 53 μm	85.07	< 53 μm	58.30	< 53 μm	76.49
< 4 μm	3.80	< 4 μm	6.90	< 4 μm	6.81	< 4 μm	6.01
A4-5 500 μm	28.80	B4-5 500 μm	10.91	C4-5 500 μm	57.79	D4-5 500 μm	57.73
< 53 μm	89.54	< 53 μm	83.69	< 53 μm	30.21	< 53 μm	38.23
< 4 μm	4.76	< 4 μm	5.19	< 4 μm	11.90	< 4 μm	4.00
A4-6 500 μm	46.13	B4-6 500 μm	11.75	C4-6 500 μm	22.07	D4-6 500 μm	20.85
< 53 μm	50.29	< 53 μm	83.24	< 53 μm	72.86	< 53 μm	70.28
< 4 μm	3.47	< 4 μm	4.97	< 4 μm	4.96	< 4 μm	6.27
A4-7 500 μm	33.54	B4-7 500 μm	11.84	C4-7 500 μm	50.87	D4-7 500 μm	9.39
< 53 μm	61.91	< 53 μm	84.18	< 53 μm	46.63	< 53 μm	83.57
< 4 μm	4.29	< 4 μm	3.91	< 4 μm	2.48	< 4 μm	6.92
A4-8 500 μm	53.72	B4-8 500 μm	15.30	C4-8 500 μm	16.73	D4-8 500 μm	6.72
< 53 μm	44.10	< 53 μm	83.77	< 53 μm	77.24	< 53 μm	90.20
< 4 μm	2.67	< 4 μm	0.90	< 4 μm	5.89	< 4 μm	3.00
A4-9 500 μm	60.99	B4-9 500 μm	14.27	C4-9 500 μm	17.44	D4-9 500 μm	6.53
< 53 μm	37.49	< 53 μm	80.41	< 53 μm	77.37	< 53 μm	87.68
< 4 μm	1.51	< 4 μm	5.29	< 4 μm	5.05	< 4 μm	5.69
A4-10 500 μm	50.48	B4-10 500 μm	17.62	C4-10 500 μm	17.51	D4-10 500 μm	32.61
< 53 μm	46.44	< 53 μm	76.64	< 53 μm	77.13	< 53 μm	64.92
< 4 μm	2.67	< 4 μm	5.53	< 4 μm	5.30	< 4 μm	2.37
A5-1 500 μm	32.94	B5-1 500 μm	14.65	C5-1 500 μm	41.58	D5-1 500 μm	17.77
< 53 μm	57.81	< 53 μm	83.62	< 53 μm	53.11	< 53 μm	71.98
< 4 μm	9.11	< 4 μm	1.68	< 4 μm	5.18	< 4 μm	8.15
A5-2 500 μm	55.88	B5-2 500 μm	24.46	C5-2 500 μm	56.45	D5-2 500 μm	13.47
< 53 μm	35.54	< 53 μm	73.68	< 53 μm	40.19	< 53 μm	77.15
< 4 μm	8.39	< 4 μm	1.83	< 4 μm	3.32	< 4 μm	5.93
A5-3 500 μm	31.09	B5-3 500 μm	14.34	C5-3 500 μm	52.63	D5-3 500 μm	15.42
< 53 μm	27.29	< 53 μm	84.61	< 53 μm	33.82	< 53 μm	79.20
< 4 μm	7.70	< 4 μm	1.02	< 4 μm	11.91	< 4 μm	5.34
A5-4 500 μm	52.31	B5-4 500 μm	11.21	C5-4 500 μm	63.77	D5-4 500 μm	19.09
< 53 μm	39.28	< 53 μm	82.03	< 53 μm	32.19	< 53 μm	78.73
< 4 μm	8.26	< 4 μm	6.67	< 4 μm	3.90	< 4 μm	5.50
A5-5 500 μm	39.68	B5-5 500 μm	12.18	C5-5 500 μm	40.77	D5-5 500 μm	18.74
< 53 μm	51.16	< 53 μm	84.15	< 53 μm	55.09	< 53 μm	76.13
< 4 μm	8.93	< 4 μm	3.32	< 4 μm	3.99	< 4 μm	5.06

A5-6 500 μm	37.45	B5-6 500 μm	11.04	C5-6 500 μm	31.28	D5-6 500 μm	20.00
< 53 μm	55.08	< 53 μm	84.44	< 53 μm	62.95	< 53 μm	74.57
< 4 μm	7.34	< 4 μm	4.46	< 4 μm	5.64	< 4 μm	5.33
A5-7 500 μm	41.36	B5-7500 μm	12.68	C5-7 500 μm	54.15	D5-7 500 μm	11.05
< 53 μm	53.01	< 53 μm	82.93	< 53 μm	43.16	< 53 μm	84.7
< 4 μm	5.46	< 4 μm	4.33	< 4 μm	2.60	< 4 μm	3.48
A5-8 500 μm	43.48	B5-8 500 μm	16.00	C5-8 500 μm	18.87	D5-8 500 μm	8.03
< 53 μm	45.74	< 53 μm	80.15	< 53 μm	74.67	< 53 μm	87.25
< 4 μm	10.63	< 4 μm	3.75	< 4 μm	6.41	< 4 μm	2.83
A5-9 500 μm	45.56	B5-9 500 μm	19.74	C5-9 500 μm	18.68	D5-9 500 μm	7.58
< 53 μm	44.97	< 53 μm	76.72	< 53 μm	66.49	< 53 μm	83.51
< 4 μm	9.29	< 4 μm	3.49	< 4 μm	4.73	< 4 μm	5.51
A5-10 500 μm	71.14	B5-10 500 μm	22.89	C5-10 500 μm	11.41	D5-10 500 μm	24.11
< 53 μm	26.79	< 53 μm	71.77	< 53 μm	81.20	< 53 μm	69.95
< 4 μm	1.92	< 4 μm	5.11	< 4 μm	7.33	< 4 μm	5.88
A6-1 500 μm	45.05	B6-1 500 μm	10.92	C6-1 500 μm	38.30	D6-1 500 μm	20.10
< 53 μm	43.78	< 53 μm	85.31	< 53 μm	58.41	< 53 μm	73.62
< 4 μm	11.06	< 4 μm	3.73	< 4 μm	3.22	< 4 μm	6.22
A6-2 500 μm	61.73	B6-2 500 μm		C6-2 500 μm	66.19	D6-2 500 μm	18.70
< 53 μm	32.01	< 53 μm	67.79	< 53 μm	31.57	< 53 μm	78.44
< 4 μm	6.22	< 4 μm	2.36	< 4 μm	2.19	< 4 μm	2.70
A6-3 500 μm	75.31	B6-3 500 μm	21.77	C6-3 500 μm	30.83	D6-3 500 μm	14.95
< 53 μm	20.63	< 53 μm	75.74	< 53 μm	66.34	< 53 μm	80.59
< 4 μm	3.96	< 4 μm	2.41	< 4 μm	2.77	< 4 μm	4.32
A6-4 500 μm	51.79	B6-4 500 μm	11.10	C6-4 500 μm	53.82	D6-4 500 μm	26.96
< 53 μm	41.48	< 53 μm	84.97	< 53 μm	27.02	< 53 μm	68.48
A6-5 500 μm	66.26	B6-5 500 μm	7.76	C6-5 500 μm	35.71	D6-5 500 μm	27.27
< 53 μm	26.92	< 53 μm	88.29	< 53 μm	59.62	< 53 μm	68.51
< 4 μm	6.71	< 4 μm	3.86	< 4 μm	4.52	< 4 μm	4.10
A6-6 500 μm	52.04	B6-6 500 μm	12.13	C6-6 500 μm	48.58	D6-6 500 μm	18.92
< 53 μm	44.97	< 53 μm	82.81	< 53 μm	47.47	< 53 μm	80.01
< 4 μm	2.88	< 4 μm	4.97	< 4 μm	3.85	< 4 μm	0.91
A6-7 500 μm	51.65	B6-7 500 μm	10.71	C6-7 500 μm	25.87	D6-7 500 μm	8.75
< 53 μm	45.25	< 53 μm	84.68	< 53 μm	63.22	< 53 μm	87.81
< 4 μm	3.12	< 4 μm	4.43	< 4 μm	10.82	< 4 μm	2.98
A6-8 500 μm	72.86	B6-8 500 μm	9.76	C6-8 500 μm	55.61	D6-8 500 μm	12.75
< 53 μm	22.07	< 53 μm	84.54	< 53 μm	41.41	< 53 μm	84.47
< 4 μm	4.96	< 4 μm	5.66	< 4 μm	2.90	< 4 μm	2.65
A6-9 500 μm	65.17	B6-9 500 μm	21.77	C6-9 500 μm	34.58	D6-9 500 μm	8.62
< 53 μm	27.52	< 53 μm	73.77	< 53 μm	57.88	< 53 μm	85.75
< 4 μm	7.19	< 4 μm	4.40	< 4 μm	7.46	< 4 μm	5.56
A6-10 500 μm	50.33	B6-10 500 μm	20.52	C6-10 500 μm	41.42	D6-10 500 μm	14.96
< 53 μm	45.80	< 53 μm	75.23	< 53 μm	55.91	< 53 μm	76.09
< 4 μm	3.64	< 4 μm	4.14	< 4 μm	2.52	< 4 μm	8.85
A7-1 500 μm	53.56	B7-1 500 μm	15.49	C7-1 500 μm	51.65	D7-1 500 μm	12.13
< 53 μm	44.87	< 53 μm	66.93	< 53 μm	45.25	< 53 μm	81.35
< 4 μm	1.41	< 4 μm	17.41	< 4 μm	3.12	< 4 μm	6.42
A7-2 500 μm	61.29	B7-2 500 μm	15.18	C7-2 500 μm	45.80	D7-2 500 μm	80.74

< 53 μm	32.94	< 53 μm	70.47	< 53 μm	50.33	< 53 μm	17.76
< 4 μm	5.68	< 4 μm	14.17	< 4 μm	3.64	< 4 μm	1.43
A7-3 500 μm	82.87	B7-3 500 μm	17.51	C7-3 500 μm	36.41	D7-3 500 μm	18.97
< 53 μm	12.81	< 53 μm	79.42	< 53 μm	60.66	< 53 μm	72.76
< 4 μm	4.24	< 4 μm	3.14	< 4 μm	2.82	< 4 μm	8.18
A7-4 500 μm	63.28	B7-4 500 μm	14.74	C7-4 500 μm	53.05	D7-4 500 μm	6.81
< 53 μm	29.96	< 53 μm	79.82	< 53 μm	43.83	< 53 μm	89.83
< 4 μm	6.67	< 4 μm	4.08	< 4 μm	3.05	< 4 μm	3.30
A7-5 500 μm	40.77	B7-5 500 μm	17.57	C7-5 500 μm	37.49	D7-5 500 μm	17.02
< 53 μm	55.09	< 53 μm	77.70	< 53 μm	58.06	< 53 μm	78.08
< 4 μm	3.99	< 4 μm	4.68	< 4 μm	4.33	< 4 μm	4.77
A7-6 500 μm	55.61	B7-6 500 μm	5.45	C7-6 500 μm	44.97	D7-6 500 μm	4.92
< 53 μm	41.41	< 53 μm	89.94	< 53 μm	52.04	< 53 μm	92.87
< 4 μm	2.90	< 4 μm	4.60	< 4 μm	2.88	< 4 μm	4.80
A7-7 500 μm	51.65	B7-7 500 μm	31.41	C7-7 500 μm	28.39	D7-7 500 μm	18.86
< 53 μm	45.25	< 53 μm	61.19	< 53 μm	66.05	< 53 μm	79.51
< 4 μm	3.12	< 4 μm	7.33	< 4 μm	5.49	< 4 μm	1.60
A7-8 500 μm	58.54	B7-8 500 μm	10.90	C7-8 500 μm	45.86	D7-8 500 μm	5.08
< 53 μm	37.24	< 53 μm	80.18	< 53 μm	50.17	< 53 μm	91.50
< 4 μm	4.20	< 4 μm	5.52	< 4 μm	3.88	< 4 μm	3.65
A7-9 500 μm	57.37	B7-9 500 μm	27.44	C7-9 500 μm	63.70	D7-9 500 μm	5.63
< 53 μm	39.05	< 53 μm	66.60	< 53 μm	35.57	< 53 μm	89.54
< 4 μm	3.49	< 4 μm	5.90	< 4 μm	0.55	< 4 μm	4.76
A7-10 500 μm	63.50	B7-10 500 μm	12.04	C7-10 500 μm	27.42	D7-10 500 μm	28.80
< 53 μm	34.58	< 53 μm	81.80	< 53 μm	60.82	< 53 μm	68.60
< 4 μm	1.87	< 4 μm	6.00	< 4 μm	9.98	< 4 μm	2.57
A8-1 500 μm	36.80	B8-1 500 μm	11.62	C8-1 500 μm	57.63	D8-1 500 μm	12.20
< 53 μm	32.55	< 53 μm	83.90	< 53 μm	39.30	< 53 μm	70.25
< 4 μm	30.58	< 4 μm	4.34	< 4 μm	3.01	< 4 μm	17.39
A8-2 500 μm	31.87	B8-2 500 μm	28.62	C8-2 500 μm	48.26	D8-2 500 μm	18.48
< 53 μm	59.08	< 53 μm	66.81	< 53 μm	47.02	< 53 μm	67.15
< 4 μm	8.85	< 4 μm	4.55	< 4 μm	4.52	< 4 μm	14.15
A8-3 500 μm	54.00	B8-3 500 μm	18.92	C8-3 500 μm	60.98	D8-3 500 μm	14.14
< 53 μm	35.13	< 53 μm	76.67	< 53 μm	36.73	< 53 μm	82.79
< 4 μm	10.42	< 4 μm	4.26	< 4 μm	2.12	< 4 μm	3.14
A8-4 500 μm	43.51	B8-4 500 μm	22.30	C8-4 500 μm	45.43	D8-4 500 μm	16.04
< 53 μm	40.12	< 53 μm	71.15	< 53 μm	50.93	< 53 μm	80.15
< 4 μm	16.29	< 4 μm	5.83	< 4 μm	3.53	< 4 μm	3.75
A8-5 500 μm	19.60	B8-5 500 μm	14.61	C8-5 500 μm	28.68	D8-5 500 μm	15.15
< 53 μm	74.71	< 53 μm	83.58	< 53 μm	66.49	< 53 μm	70.15
< 4 μm	5.58	< 4 μm	1.75	< 4 μm	4.74	< 4 μm	14.49
A8-6 500 μm	26.72	B8-6 500 μm	25.66	C8-6 500 μm	50.46	D8-6 500 μm	13.47
< 53 μm	67.80	< 53 μm	70.18	< 53 μm	46.74	< 53 μm	83.46
< 4 μm	5.29	< 4 μm	4.06	< 4 μm	2.66	< 4 μm	3.15
A8-7 500 μm	60.04	B8-7 500 μm	17.61	C8-7 500 μm	29.72	D8-7 500 μm	14.24
< 53 μm	35.88	< 53 μm	76.25	< 53 μm	64.58	< 53 μm	81.05
< 4 μm	6.87	< 4 μm	5.80	< 4 μm	5.53	< 4 μm	4.66
A8-8 500 μm	45.01	B8-8 500 μm	17.36	C8-8 500 μm	50.34	D8-8 500 μm	5.11

< 53 μm	47.93	< 53 μm	76.86	< 53 μm	47.11	< 53 μm	90.61
< 4 μm	7.01	< 4 μm	4.38	< 4 μm	2.48	< 4 μm	4.27
A8-9 500 μm	59.87	B8-9 500 μm	10.93	C8-9 500 μm	60.27	D8-9 500 μm	44.81
< 53 μm	32.26	< 53 μm	83.47	< 53 μm	37.53	< 53 μm	50.62
< 4 μm	8.08	< 4 μm	5.24	< 4 μm	2.16	< 4 μm	4.44
A8-10 500 μm	36.42	B8-10 500 μm	30.71	C8-10 500 μm	49.86	D8-10 500 μm	48.15
< 53 μm	55.55	< 53 μm	66.87	< 53 μm	48.03	< 53 μm	47.27
< 4 μm	8.01	< 4 μm	2.37	< 4 μm	2.04	< 4 μm	4.45
A9-1 500 μm	45.32	B9-1 500 μm	82.92	C9-1 500 μm	45.50	D9-1 500 μm	17.79
< 53 μm	39.39	< 53 μm	78.92	< 53 μm	51.47	< 53 μm	77.64
< 4 μm	15.27	< 4 μm	4.03	< 4 μm	2.95	< 4 μm	4.35
A9-2 500 μm	51.98	B9-2 500 μm	8.25	C9-2 500 μm	46.71	D9-2 500 μm	13.89
< 53 μm	32.73	< 53 μm	87.56	< 53 μm	50.57	< 53 μm	79.71
< 4 μm	15.17	< 4 μm	3.85	< 4 μm	2.71	< 4 μm	6.27
A9-3 500 μm	47.93	B9-3 500 μm	21.68	C9-3 500 μm	69.02	D9-3 500 μm	13.79
< 53 μm	45.01	< 53 μm	75.00	< 53 μm	29.27	< 53 μm	80.94
< 4 μm	7.01	< 4 μm	3.08	< 4 μm	1.67	< 4 μm	5.22
A9-4 500 μm	39.52	B9-4 500 μm	7.97	C9-4 500 μm	54.94	D9-4 500 μm	23.57
< 53 μm	52.32	< 53 μm	84.46	< 53 μm	42.85	< 53 μm	74.66
< 4 μm	8.07	< 4 μm	7.25	< 4 μm	2.17	< 4 μm	1.66
A9-5 500 μm	16.68	B9-5 500 μm	28.93	C9-5 500 μm	30.85	D9-5 500 μm	65.91
< 53 μm	55.51	< 53 μm	64.20	< 53 μm	65.17	< 53 μm	31.43
< 4 μm	27.78	< 4 μm	5.97	< 4 μm	3.85	< 4 μm	4.22
A9-6 500 μm	44.11	B9-6 500 μm	11.78	C9-6 500 μm	53.05	D9-6 500 μm	39.37
< 53 μm	48.43	< 53 μm	82.96	< 53 μm	44.03	< 53 μm	57.38
< 4 μm	7.32	< 4 μm	4.90	< 4 μm	2.68	< 4 μm	3.20
A9-7 500 μm	31.61	B9-7 500 μm	13.06	C9-7 500 μm	38.54	D9-7 500 μm	13.90
< 53 μm	56.08	< 53 μm	81.59	< 53 μm	57.25	< 53 μm	81.00
< 4 μm	12.20	< 4 μm	3.68	< 4 μm	4.30	< 4 μm	4.02
A9-8 500 μm	44.42	B9-8 500 μm	12.70	C9-8 500 μm	48.85	D9-8 500 μm	14.49
< 53 μm	46.29	< 53 μm	82.68	< 53 μm	48.26	< 53 μm	79.47
< 4 μm	9.22	< 4 μm	4.25	< 4 μm	2.60	< 4 μm	5.77
A9-9 500 μm	41.58	B9-9 500 μm	17.47	C9-9 500 μm	36.89	D9-9 500 μm	16.90
< 53 μm	53.11	< 53 μm	78.68	< 53 μm	59.87	< 53 μm	72.99
< 4 μm	5.18	< 4 μm	3.68	< 4 μm	3.17	< 4 μm	9.91
A9-10 500 μm	31.05	B9-10 500 μm	9.07	C9-10 500 μm	50.48	D9-10 500 μm	15.51
< 53 μm	57.30	< 53 μm	87.03	< 53 μm	46.44	< 53 μm	72.87
< 4 μm	11.51	< 4 μm	3.50	< 4 μm	2.67	< 4 μm	4.73
A10-1 500 μm	43.26	B10-1 500 μm	12.20	C10-1 500 μm	62.12	D10-1 500 μm	15.55
< 53 μm	56.33	< 53 μm	83.33	< 53 μm	34.92	< 53 μm	79.83
< 4 μm	5.44	< 4 μm	4.39	< 4 μm	2.90	< 4 μm	7.32
A10-2 500 μm	38.68	B10-2 500 μm	12.98	C10-2 500 μm	51.87	D10-2 500 μm	14.73
< 53 μm	56.35	< 53 μm	99.29	< 53 μm	45.65	< 53 μm	73.43
< 4 μm	4.87	< 4 μm	2.78	< 4 μm	2.40	< 4 μm	11.69
A10-3 500 μm	48.29	B10-3 500 μm	28.89	C10-3 500 μm	37.92	D10-3 500 μm	18.00
< 53 μm	48.70	< 53 μm	66.62	< 53 μm	59.02	< 53 μm	70.03
< 4 μm	3.02	< 4 μm	4.16	< 4 μm	2.93	< 4 μm	11.82
A10-4 500 μm	42.67	B10-4 500 μm	15.97	C10-4 500 μm	48.78	D104 500 μm	10.62

< 53 μm	53.66	< 53 μm	80.57	< 53 μm	48.00	< 53 μm	83.06
< 4 μm	3.47	< 4 μm	3.34	< 4 μm	3.20	< 4 μm	6.22
A10-5 500 μm	40.20	B10-5 500 μm	24.26	C10-5 500 μm	41.92	D10-5 500 μm	8.21
< 53 μm	55.17	< 53 μm	71.97	< 53 μm	52.78	< 53 μm	86.43
< 4 μm	4.36	< 4 μm	3.70	< 4 μm	3.60	< 4 μm	5.18
A10-6 500 μm	47.15	B10-6 500 μm	30.14	C10-6 500 μm	63.50	D10-6 500 μm	15.71
< 53 μm	50.76	< 53 μm	66.52	< 53 μm	34.58	< 53 μm	78.14
< 4 μm	2.21	< 4 μm	2.66	< 4 μm	1.87	< 4 μm	5.86
A10-7 500 μm	66.66	B10-7 500 μm	19.23	C10-7 500 μm	63.65	D10-7 500 μm	15.18
< 53 μm	31.15	< 53 μm	77.81	< 53 μm	32.87	< 53 μm	81.67
< 4 μm	1.85	< 4 μm	2.34	< 4 μm	3.43	< 4 μm	3.00
A10-8 500 μm	60.17	B10-8 500 μm	12.64	C10-8 500 μm	45.04	D10-8 500 μm	13.90
< 53 μm	33.85	< 53 μm	86.80	< 53 μm	52.48	< 53 μm	81.00
< 4 μm	5.57	< 4 μm	0.53	< 4 μm	2.45	< 4 μm	4.02
A10-9 500 μm	38.50	B10-9 500 μm	14.04	C10-9 500 μm	69.40	D10-9 500 μm	15.52
< 53 μm	61.53	< 53 μm	83.54	< 53 μm	27.16	< 53 μm	81.17
< 4 μm	3.35	< 4 μm	2.05	< 4 μm	3.39	< 4 μm	3.27
A10-10 500 μm	32.62	B10-10 500 μm	21.80	C10-10 500 μm	57.88	D10-10 500 μm	4.93
< 53 μm	61.36	< 53 μm	75.50	< 53 μm	39.47	< 53 μm	90.22
< 4 μm	5.29	< 4 μm	2.70	< 4 μm	2.61	< 4 μm	4.78

Table 3.5: The pH and electrical conductivity values of samples from the study area

Sample code	**pH**	**EC** μScm^{-1}	**Sample code**	**pH**	**EC** μScm^{-1}	**Sample code**	**pH**	**EC** μScm^{-1}	**Sample code**	**pH**	**EC** μScm^{-1}
A11	5.7	119.7	B11	4.51	116.5	C11	4.49	117	D11	4.53	107
A12	4.37	120.5	B12	4.3	117.9	C12	4.53	115.9	D12	5.06	103.7
A13	4.8	119.6	B13	4.45	115.5	C13	3.11	122.3	D13	4.39	114.5
A14	5.99	119.9	B14	4.27	115.2	C14	3.79	121	D14	4.86	106.8
A15	4.99	119.9	B15	4.31	117.6	C15	5.07	118.2	D15	4.6	104.8
A16	4.57	120.8	B16	4.36	116.7	C16	5.29	119.5	D16	4.47	109.9
A17	6.47	120	B17	4.17	118.6	C17	5.17	115.3	D17	4.04	107.4
A18	5.19	117.5	B18	5.05	114.9	C18	6.15	107.8	D18	4.23	107.5
A19	4.69	120.1	B19	4.96	115.4	C19	5.3	111.5	D19	3.47	116.9
A110	4.08	120.2	B110	4.39	117.7	C110	5.86	113	D110	3.82	112.1
A21	5.19	115.6	B21	4.82	119.1	C21	4.61	117.9	D21	5.1	104.7
A22	5.45	119.7	B22	4.69	121.4	C22	5.12	115.7	D22	4.66	111.2
A23	5.69	117.9	B23	4.55	120.6	C23	4.25	117.3	D23	5.04	112.5
A24	4.35	120.6	B24	5.1	119.2	C24	5.05	116.8	D24	4.93	107.4
A25	4.33	119	B25	6.03	112.3	C25	4.74	117.7	D25	4.55	106.3
A26	5.43	117.9	B26	4.9	119.3	C26	4.62	116.3	D26	4.39	105.9
A27	5.24	121.1	B27	4.5	119.7	C27	4.83	116.9	D27	3.71	112.2
A28	3.65	120.5	B28	5.69	120.8	C28	4.71	117	D28	3.54	116.5
A29	4.96	115.4	B29	4.59	117.1	C29	7.26	83	D29	3.54	118.7

A210	4.46	115.9	B210	6.39	119.5	C210	4.8	121.1	D210	2.92	115.6
A31	4.96	115.6	B31	5.1	120.1	C31	5.79	115.2	D31	4.43	121.4
A32	5.15	114.3	B32	4.77	66.2	C32	5.8	117.3	D32	4.86	118.6
A33	6.56	115	B33	4.71	119.6	C33	5.51	116.6	D33	4.74	118
A34	5.42	116.1	B34	4.73	119.9	C34	5.51	117.7	D34	4.29	115.7
A35	5.79	115.5	B35	4.81	115.2	C35	5.56	114.5	D35	4.31	117.7
A36	3.98	120.7	B36	4.79	116.2	C36	6.05	112.1	D36	4.79	114.5
A37	4.42	120.6	B37	4.52	65.6	C37	5.86	113.6	D37	4.81	115.9
A38	4.71	119.5	B38	4.66	60.9	C38	5.85	117.4	D38	4.9	115.3
A39	4.62	120.1	B39	4.64	119.4	C39	4.37	120.8	D39	3.74	118.4
A310	4.29	119.7	B310	4.65	121.1	C310	4.06	121.1	D310	3.1	117.8
A41	4.98	119.9	B41	5.08	119.7	C41	5.62	115.2	D41	3.49	117.6
A42	5.42	118.2	B42	4.64	119.2	C42	5.56	112.9	D42	3.07	119.9
A43	4.71	119.4	B43	4.66	113.5	C43	5.59	113.3	D43	4.42	115.4
A44	4.5	120.5	B44	4.64	122	C44	5.94	116.1	D44	4.06	114.9
A45	4.46	121.8	B45	4.91	120	C45	5.99	114.9	D45	3.81	120.6
A46	4.41	121.5	B46	4.71	119.5	C46	5.87	113.8	D46	4.09	120.8
A47	4.13	122.5	B47	5.48	119.6	C47	5.98	108.8	D47	4.19	114.5
A48	3.97	122.9	B48	5.49	121.8	C48	5.14	112.4	D48	3.64	113.9
A49	3.88	121.1	B49	4.74	120	C49	5.39	115.1	D49	3.67	117.8
A410	4.21	119.3	B410	5.09	116.6	C410	5.74	114.6	D410	3.93	117.9
A51	4.6	115.8	B51	4.96	119.5	C51	5.18	121.6	D51	4	121.4
A52	4.51	115.5	B52	5.36	119.6	C52	5.11	123	D52	5.43	121.3
A53	4.33	115.3	B53	4.92	113.4	C53	5.51	119.2	D53	3.92	119.3
A54	4.04	115.7	B54	4.43	118.6	C54	4.99	117.6	D54	4.84	111.5
A55	4.62	115.3	B55	4.66	117.1	C55	6.01	112.3	D55	3.88	115.9
A56	4.29	119.6	B56	5.01	113.6	C56	4.83	115.7	D56	4.46	120.4
A57	4.61	118.7	B57	4.7	72.4	C57	5.22	116.1	D57	4.06	118.9
A58	4.17	117.5	B58	4.78	118.8	C58	6.12	111.3	D58	4.35	115.6
A59	3.92	119.1	B59	5.16	118.6	C59	5.87	109.4	D59	3.99	116.4
A510	3.61	119.5	B510	5.46	113.9	C510	4.31	121.3	D510	4.45	120.4
A61	4.41	115.1	B61	4.88	119.2	C61	4.1	121.6	D61	4.08	115.1
A62	4.53	114.6	B62	4.46	52.4	C62	5.53	117.6	D62	4.39	116.3
A63	4.07	116.9	B63	4.55	118.9	C63	5.71	114.2	D63	5.76	112.5
A64	3.94	117.5	B64	5.71	65.6	C64	5.91	115	D64	4.15	117.7
A65	4.92	119.1	B65	4.92	49.1	C65	5.45	114.4	D65	4.92	114.6
A66	4.86	119	B66	4.64	112.7	C66	5.22	111.1	D66	4.42	114.9
A67	4.18	121	B67	4.7	119.8	C67	5.65	112.2	D67	3.69	116.9
A68	4.96	117.5	B68	5.61	113.9	C68	5.23	116.6	D68	3.33	117.5
A69	4.56	115.5	B69	4.77	119.5	C69	5.49	114.9	D69	4.23	115.3
A610	4.3	115.9	B610	5.63	120.5	C610	5.25	114.7	D610	3.54	116.4
A71	4.22	115	B71	5.2	115.6	C71	4.62	117.6	D71	5.2	53.6
A72	4.73	119.7	B72	4.85	116.7	C72	4.69	121.9	D72	4.85	116.7
A73	3.91	119.2	B73	4.7	118.6	C73	4.05	123.5	D73	4.7	118.6
A74	4.44	115.7	B74	4.47	116.9	C74	4.72	119.4	D74	4.47	67.9
A75	3.66	119.5	B75	4.31	119	C75	4.61	117.6	D75	3.93	121.2

A76	3.93	116.1	B76	4.77	114.9	C76	4.32	119.9	D76	5.03	118.5
A77	4.21	115.5	B77	3.5	115.4	C77	4.61	121.3	D77	3.5	115.4
A78	4.05	117.9	B78	4.72	118.9	C78	4.57	119.5	D78	4.72	118.9
A79	3.71	122.2	B79	3.61	119.3	C79	4.09	120.1	D79	3.61	119.4
A710	4.09	120.8	B710	6.46	117.4	C710	4.31	121	D710	6.43	117.4
A81	6.11	51	B81	5.33	117.6	C81	4.46	121	D81	5.33	117.6
A82	4.59	121.6	B82	4.47	118.1	C82	4.65	120.7	D82	4.47	118.1
A83	3.9	122	B83	4.67	118.1	C83	4.73	123	D83	4.67	118.1
A84	4.02	117.9	B84	5.2	119.1	C84	5.26	119.9	D84	5.2	119.1
A85	4.55	116.2	B85	4.9	118.9	C85	5.03	121.6	D85	3.76	122.7
A86	3.83	120.8	B86	4.63	116.7	C86	4.71	120.4	D86	4.7	117.5
A87	4.4	119.4	B87	4.37	118.3	C87	4.62	120	D87	5.13	119.8
A88	3.76	121.5	B88	4.54	117.9	C88	4.41	120.4	D88	4.54	117.9
A89	4.09	115.8	B89	4.69	119.3	C89	5.05	120.3	D89	4.69	119.3
A810	4.61	114.6	B810	4.79	114.5	C810	5.53	120.9	D810	4.79	114.5
A91	4.04	119.1	B91	4.49	119.6	C91	5.73	116.2	D91	5.01	120.1
A92	3.92	118.3	B92	4.53	118.6	C92	4.56	121.4	D92	4.67	119.2
A93	5.1	116.9	B93	4.45	116.4	C93	4.86	120.9	D93	4.45	116.4
A94	4.49	120.5	B94	4.02	117.1	C94	4.67	121.2	D94	5.29	117.9
A95	3.95	119.7	B95	4.63	115.3	C95	4.01	123.5	D95	4.24	119.2
A96	3.8	120.7	B96	4.41	118.3	C96	5.11	116.2	D96	4.41	118.3
A97	4.16	115.6	B97	4.16	115.9	C97	4.45	122.3	D97	4.78	118
A98	4.15	115.5	B98	3.76	119.5	C98	4.22	121.9	D98	3.78	119.5
A99	3.39	112.5	B99	4.95	118.9	C99	5.1	116.6	D99	4.95	118.9
A910	4.35	114.5	B910	6	106.6	C910	4.97	116.8	D910	6.03	116.6
A101	4.02	119.2	B101	4.09	121.1	C101	5.21	117.5	D101	3.9	119.9
A102	3.69	120.7	B102	4.71	119.5	C102	4.69	120.8	D102	4.71	119.5
A103	4.11	113.8	B103	5.14	119.6	C103	4.51	121.7	D103	5.13	119.6
A104	3.86	117.7	B104	4.94	114.9	C104	4.32	118.6	D104	4.93	114.9
A105	4.52	120.9	B105	3.62	119.6	C105	5.88	114.3	D105	4.68	119.2
A106	4.47	119.5	B106	3.89	116.1	C106	4.58	115.9	D106	3.89	116.1
A107	3.72	114.7	B107	4.74	118.3	C107	4.15	122.2	D107	4.74	118.3
A108	4.14	119.3	B108	5.95	119.2	C108	4.22	121.7	D108	5.95	119.2
A109	3.56	118.6	B109	4.83	117.8	C109	4.79	119.4	D109	3.57	122.9
A1010	3.86	119.6	B1010	4.95	119.1	C1010	4.55	120.1	D1010	4.95	119.1

Table 3.7: Value/chroma, hue and colour of soil samples from the study area

Sample code	Value/chroma	Hue	Colour	Sample code	Value/chroma	Hue	Colour
A11	A3/1	2.5YR	Dark Reddish Grey	C11	C4/4	5YR	Reddish Brown
A12	A3/4	7.5YR	Dark Red	C12	C4/4	5YR	Reddish Brown
A13	A4/4	7.5YR	Dark Red	C13	C4/3	5YR	Reddish Brown
A14	A3/4	5YR	Dark Reddish Brown	C14	C4/4	5YR	Reddish Brown
A15	A3/6	2.5YR	Dark Red	C15	C4/4	5YR	Reddish Brown

A16	A3/4	2.5YR	Dark Red	C16	C3/4	5YR	Dark Reddish Brown
A17	A3/4	2.5YR	Dark Reddish Brown	C17	C4/3	5YR	Reddish Brown
A18	A4/4	5YR	Reddish Brown	C18	C4/3	5YR	Reddish Brown
A19	A4/4	2.5YR	Reddish Brown	C19	C3/4	5YR	Dark Reddish Brown
A110	A3/6	2.5YR	Dark Red	C110	C3/4	5YR	Dark Reddish Brown
A21	A3/1	5YR	Very Dark Grey	C21	C4/4	5YR	Reddish Brown
A22	A3/1	5YR	Very Dark Grey	C22	C4/4	5YR	Reddish Brown
A23	A4/2	7.5YR	Brown	C23	C4/4	2.5YR	Reddish Brown
A24	A3/4	5YR	Dark Reddish Brown	C24	C5/4	7.5YR	Brown
A25	A3/6	2.5YR	Dark Red	C25	C3/4	7.5YR	Dark Brown
A26	A3/4	2.5YR	Dark Reddish Brown	C26	C4/4	7.5YR	Brown
A27	A3/6	2.4YR	Dark Brown	C27	C4/3	5YR	Reddish Brown
A28	A4/4	2.5YR	Reddish Brown	C28	C3/4	7.5YR	Dark Brown
A29	A3/4	5YR	Dark Reddish Brown	C29	C4/4	5YR	Reddish Brown
A210	A3/6	2.5YR	Dark Red /twice	C210	C4/4	5YR	Reddish Brown
A31	A4/2	5YR	Dark Reddish Grey	C31	C4/4	7.5YR	Brown
A32	A3/2	5YR	Dark Reddish Brown	C32	C4/4	5YR	Reddish Brown
A33	A4/2	5YR	Dark Reddish Grey	C33	C4/4	5YR	Reddish Brown
A34	A3/4	7.5YR	Dark Brown	C34	C4/4	7.5YR	Brown
A35	A3/6	7.5YR	Dark Red	C35	C3/4	5YR	Dark Reddish Brown
A36	A3/4	2.5YR	Dark Reddish Brown	C36	C4/4	5YR	Reddish Brown
A37	A3/4	5YR	Dark Reddish Brown	C37	C4/2	5YR	Dark Reddish Grey
A38	A3/6	2.5YR	Dark Red	C38	C4/4	5YR	Reddish Brown
A39	A3/6	7.5YR	Dark Brown	C39	C4/4	5YR	Reddish Brown
A310	A4/6	5YR	Yellowish Red	C310	C3/4	5YR	Dark Reddish Brown
A41	A4/2	5YR	Dark Reddish Grey	C41	C4/4	5YR	Reddish Brown
A42	A4/4	5YR	Reddish Brown	C42	C4/4	5YR	Reddish Brown
A43	A4/4	5YR	Reddish Brown	C43	C4/6	4YR	Yellowish Red
A44	A4/4	5YR	Reddish Brown	C44	C4/3	5YR	Reddish Brown
A45	A4/4	5YR	Reddish Brown	C45	C3/4	5YR	Dark Reddish Brown
A46	A4/4	5YR	Reddish Brown	C46	C4/4	5YR	Reddish Brown
A47	A3/4	5YR	Dark Reddish Brown	C47	C3/3	5YR	Dark Reddish Brown
A48	A4/2	5YR	Dark Reddish Grey	C48	C3/4	5YR	Dark Reddish Brown
A49	A4/4	5YR	Reddish Brown	C49	C4/6	7.5YR	Strong Brown
A410	A3/4	5YR	Dark Reddish Brown	C410	C4/4	5YR	Reddish Brown
A51	A4/6	5YR	Yellowish red	C51	C4/3	5YR	Reddish Brown
A52	A4/4	7.5YR	Brown	C52	C4/4	5YR	Reddish Brown
A53	A3/4	5YR	Reddish Brown	C53	C4/3	5YR	Reddish Brown
A54	A4/4	5YR	Reddish Brown	C54	C3/4	5YR	Dark Reddish Brown
A55	A4/6	7.5YR	Strong Brown	C55	C3/4	5YR	Dark Reddish Brown
A56	A3/4	5YR	Reddish Brown	C56	C4/4	5YR	Reddish Brown
A57	A4/4	7.5YR	Brown	C57	C3/4	5YR	Dark Reddish Brown
A58	A4/4	5YR	Reddish Brown	C58	C3/4	5YR	Dark Reddish Brown
A59	A3/4	7.5YR	Brown	C59	C4/4	5YR	Reddish Brown
A510	A4/4	7.5YR	Brown	C510	C4/4	5YR	Reddish Brown
A61	A4/3	2.5YR	Reddish Brown	C61	C3/3	5YR	Dark Reddish Brown
A62	A4/4	7.5YR	Brown	C62	C3/3	5YR	Dark Reddish Brown
A63	A4/4	7.5YR	Brown	C63	C4/3	5YR	Reddish Brown

A64	A4/4	7.5YR	Brown	C64	C3/2	5YR	Dark Reddish Brown
A65	A4/4	7.5YR	Brown	C65	C3/3	5YR	Dark Reddish Brown
A66	A4/3	2.5YR	Reddish Brown	C66	C4/4	5YR	Reddish Brown
A67	A4/3	2.5YR	Reddish Brown	C67	C4/4	5YR	Reddish Brown
A68	A4/3	2.5YR	Reddish Brown	C68	C4/2	5YR	Dark Reddish Grey
A69	A4/4	7.5YR	Brown	C69	C3/3	5YR	Dark Reddish Brown
A610	A4/3	2.5YR	Reddish Brown	C610	C3/2	5YR	Dark Reddish Grey
A71	A4/4	7.5YR	Brown	C71	C3/3	5YR	Dark Reddish Brown
A72	A4/3	7.5YR	Brown	C72	C3/3	5YR	Dark Reddish Brown
A73	A4/4	7.5YR	Brown	C73	C4/4	2.5YR	Reddish Brown
A74	A4/3	5YR	Reddish Brown	C74	C4/2	5YR	Dark Reddish Grey
A75	A3/4	7.5YR	Brown	C75	C4/4	5YR	Reddish Brown
A76	A3/4	7.5YR	Brown	C76	C4/4	2.5YR	Reddish Brown
A77	A4/3	2.5YR	Reddish Brown	C77	C4/4	5YR	Reddish Brown
A78	A3/4	5YR	Dark Reddish Brown	C78	C5/2	5YR	Reddish Green
A79	A4/4	7.5YR	Brown	C79	C4/3	5YR	Reddish Brown
A710	A4/4	7.5YR	Brown	C710	C4/3	5YR	Reddish Brown
A81	A4/3	7.5YR	Brown	C81	C4/3	5YR	Reddish Brown
A82	A4/3	7.5YR	Brown	C82	C3/3	5YR	Dark Reddish Brown
A83	A5/4	5YR	Reddish Brown	C83	C3/4	5YR	Dark Reddish Brown
A84	A4/4	5YR	Reddish Brown	C84	C3/3	5YR	Dark Reddish Brown
A85	A4/4	5YR	Reddish Brown	C85	C4/3	5YR	Reddish Brown
A86	A5/4	5YR	Reddish Brown	C86	C4/3	5YR	Reddish Brown
A87	A5/6	5YR	Yellowish Red	C87	C4/3	5YR	Reddish Brown
A88	A5/4	5YR	Reddish Brown	C88	C3/3	7.5YR	Dark Brown
A89	A4/6	7.5YR	Strong Brown	C89	C3/3	5YR	Dark Reddish Brown
A810	A5/4	5YR	Reddish Brown	C810	C4/2	5YR	Dark Reddish Grey
A91	A5/4	5YR	ReddishBrown	C91	C3/3	5YR	Dark Reddish Brown
A92	A4/6	7.5YR	Strong Brown	C92	C3/3	5YR	Dark Reddish Brown
A93	A4/4	5YR	ReddishBrown	C93	C4/4	5YR	Reddish Brown
A94	A5/4	5YR	ReddishBrown	C94	C3/4	5YR	Dark Reddish Grey
A95	A4/4	5YR	ReddishBrown	C95	C3/3	5YR	Dark Reddish Brown
A96	A5/4	5YR	ReddishBrown	C96	C4/4	5YR	Reddish Brown
A97	A4/4	7.5YR	Brown	C97	C3/4	5YR	Dark Reddish Brown
A98	A5/4	5YR	ReddishBrown	C98	C4/2	5YR	Dark Reddish Grey
A99	A5/4	5YR	ReddishBrown	C99	C3/3	5YR	Dark Reddish Brown
A910	A6/4	7.5YR	Light Brown	C910	C4/2	5YR	Dark Reddish Grey
A101	A4/3	5YR	Reddish Brown	C101	C4/3	5YR	Reddish Brown
A102	A4/6	2.5YR	Red	C10-2	C4/3	5YR	Dark Reddish Brown
A103	A4/4	5YR	Reddish Brown	C10-3	C3/3	5YR	Dark Reddish Brown
A104	A5/4	7.5YR	Brown	C10-4	C3/2	5YR	Dark Reddish Brown
A105	A4/6	5YR	Yellowish Red	C10-5	C4/3	5YR	Reddish Brown
A106	A5/4	7.5YR	Brown	C10-6	C4/3	5YR	Dark Reddish Brown
A107	A5/4	5YR	Reddish Brown	C10-7	C4/4	5YR	Reddish Brown
A108	A5/4	7.5YR	Brown	C10-8	C4/3	5YR	Reddish Brown
A109	A4/3	7.5YR	Brown	C10-9	C4/3	5YR	Reddish Brown
A10-10	A5/4	5YR	Reddish Brown	C10-10	C3/3	5YR	Dark Reddish Brown
B11	B4/6	2.5YR	Red	D11	D4/6	5YR	Yellowish Red

B12	B4/4	2.5YR	Reddish Brown	D12	D4/4	5YR	Reddish Brown
B13	B4/6	5YR	Yellowish Red	D13	D4/3	5YR	Reddish Brown
B14	B3/6	2.5YR	Dark Red	D14	D3/4	5YR	Dark Reddish Brown
B15	B3/6	2.5YR	Dark Red	D15	D4/3	7.5YR	Brown
B16	B3/6	2.5YR	Dark Red	D16	D4/4	5YR	Reddish Brown
B17	B4/6	2.5YR	Red	D17	D4/4	5YR	Reddish Brown
B18	B4/6	2.5YR	Red	D18	D3/3	5YR	Dark Reddish Brown
B19	B3/6	2.5YR	Dark Red	D19	D3/1	2.4YR	Dark Reddish Grey
B110	B3/6	2.5YR	Dark Red	D110	D3/2	7.5YR	Dark Brown
B21	B3/6	5YR	Dark Reddish Brown	D21	D3/4	5YR	Reddish Brown
B22	B4/6	2.5YR	Red	D22	D4/6	5YR	Yellowish Red
B23	B4/6	5YR	Yellowish Red	D23	D4/4	5YR	Reddish Brown
B24	B3/6	2.5YR	Dark Red	D24	D3/6	2.5YR	Dark Brown
B25	B3/4	5YR	Dark Reddish Brown	D25	D3/3	5YR	Dark Reddish Brown
B26	B3/4	5YR	Dark Reddish Brown	D26	D4/4	5YR	Reddish Brown
B27	B4/4	2.5YR	Reddish Brown	D27	D4/4	5YR	Reddish Brown
B28	B3/6	2.5YR	Reddish Brown	D28	D4/3	5YR	Reddish Brown
B29	B3/6	2.5YR	Dark Red	D29	D4/4	7.5YR	Brown
B210	B3/6	2.5YR	Dark Red	D210	D3/1	5YR	Very Dark Grey
B31	B4/6	2.5YR	Red	D31		5YR	Yellowish Red
B32	B4/6	5YR	Yellowish Red	D32	D4/6	5YR	Yellowish Red
B33	B4/4	2.5YR	Reddish Brown	D33	D3/4	5YR	Dark Reddish Brown
B34	B3/6	2.5YR	Dark Red	D34	D4/4	5YR	Reddish Brown
B35	B3/6	2.5YR	Dark Red	D35	D4/4	5YR	Reddish Brown
B36	B3/6	2.5YR	Dark Red	D36	D4/4	5YR	Reddish Brown
B37	B3/6	2.5YR	Dark Red	D37	D3/4	5YR	Dark Reddish Brown
B38	B3/6	2.5YR	Dark Red	D38	D3/4	5YR	Dark Reddish Brown
B39	B4/6	2.5YR	Red	D39	D4/4	5YR	Reddish Brown
B310	B3/6	2.5YR	Dark Red	D310	D3/2	5YR	Dark Reddish Brown
B41	B3/6	2.5YR	Dark Red	D41	D4/4	5YR	Reddish Brown
B42	B4/4	2.5YR	Reddish Brown	D42	D4/4	5YR	Reddish Brown
B43	B3/6	2.5YR	Dark Red	D43	D3/3	5YR	Yellowish Red
B44	B3/6	2.5YR	Dark Red	D44	D4/4	5YR	Reddish Brown
B45	B3/6	2.5YR	Dark Red	D45	D3/3	5YR	Dark Reddish Brown
B46	B4/6	5YR	Yellowish Red	D46	D4/4	5YR	Reddish Brown
B47	B3/6	2.5YR	Dark Red	D47	D4/4	5YR	Reddish Brown
B48	B3/6	2.5YR	Dark Red	D48	D4/3	5YR	Reddish Brown
B49	B4/6	2.5YR	Red	D49	D3/3	5YR	Dark Reddish Brown
B410	B4/6	2.5YR	Red	D410	D3/3	5YR	Dark Reddish Brown
B51	B4/6	2.5YR	Red	D51	D4/4	5YR	Reddish Brown
B52	B3/4	2.5YR	Dark Reddish Brown	D52	D4/6	2.5YR	Reddish Brown
B53	B3/4	2.5YR	Dark Reddish Brown	D53	D4/4	5YR	Reddish Brown
B54	B4/4	5YR	Reddish Brown	D54	D3/4	5YR	Dark Reddish Brown
B55	B4/4	5YR	Dark Red	D55	D3/4	5YR	Dark Reddish Brown
B56	B4/4	5YR	Dark Red	D56	D4/4	5YR	Reddish Brown
B57	B5/7	2.5YR	Red	D57	D4/4	2.5YR	Reddish Brown
B58	B3/6	2.5YR	Dark Red	D58	D4/3	5YR	Reddish Brown
B59	B3/6	2.5YR	Dark Red	D59	D3/2	5YR	Dark Reddish Brown

B510	B3/6	2.5YR	Dark Red	D510	D3/2	5YR	Dark Reddish Brown
B61	B4/4	2.5YR	Reddish Brown	D61	D4/4	5YR	Reddish Brown
B62	B3/6	2.5YR	Dark Red	D62	D3/4	5YR	Dark Reddish Brown
B63	B3/6	2.5YR	Dark Red	D63	D3/4	5YR	Dark Reddish Brown
B64	B3/6	5YR	Dark Red	D64	D4/4	5YR	Reddish Brown
B65	B3/6	5YR	Dark Red	D65	D4/4	5YR	Reddish Brown
B66	B4/6	2.5YR	Red	D66	D4/3	5YR	Reddish Brown
B67	B3/6	2.5YR	Dark Red	D67	D4/3	5YR	Reddish Brown
B68	B3/4	2.5YR	Dark Reddish Brown	D68	D5/4	5YR	Reddish Brown
B69	B3/6	2.5YR	Dark Red	D69	D3/3	5YR	Dark Reddish Brown
B610	B3/6	2.5YR	Dark Red	D610		5YR	Dark Reddish Brown
B71	B4/6	2.5YR	Red	D71	D4/6	5YR	Yellowish Red
B72	B4/6	2.5YR	Red	D72	D4/3	5YR	Reddish Brown
B73	B3/6	2.5YR	Dark Red	D73	D4/4	5YR	Reddish Brown
B74	B4/6	2.5YR	Red	D74	D4/4	5YR	Reddish Brown
B75	B4/3	5YR	Reddish Brown	D75		5YR	Reddish Brown
B76	B4/4	2.5YR	Reddish Brown	D76	D4/3	5YR	Reddish Brown
B77	B4/4	2.5YR	Reddish Brown	D77	D4/4	5YR	Reddish Brown
B78	B3/6	2.5YR	Dark Red	D78	D4/4	5YR	Reddish Brown
B79	B3/6	2.5YR	Dark Red	D79	D4/4	5YR	Reddish Brown
B710	B3/4	2.5YR	Dark Reddish Brown	D710	D3/2	5YR	Dark Reddish Brown
B81	B4/6	2.5YR	Red	D81	D4/3	5YR	Yellowish Red
B82	B4/6	2.5YR	Red	D82	D4/4	7.5YR	Brown
B83	B4/6	2.5YR	Red	D83	D3/4	5YR	Dark Reddish Brown
B84	B4/6	2.5YR	Red	D84	D4/4	5YR	Reddish Brown
B85	B4/4	2.5YR	Reddish Brown	D85	D4/4	5YR	Dark Reddish Brown
B86	B3/6	2.5YR	Dark Red	D86	D4/4	5YR	Reddish Brown
B87	B3/6	2.5YR	Dark Red	D87	D4/4	5YR	Reddish Brown
B88	B4/4	2.5YR	Reddish Brown	D88	D3/3	5YR	Dark Reddish Brown
B89	B3/6	2.5YR	Dark Red	D89	D4/4	5YR	Reddish Brown
B810	B3/6	2.5YR	Dark Red	D810	D4/4	5YR	Reddish Brown
B91	B3/6	2.5YR	Dark Red	D91	D3/6	2.5YR	Dark Red
B92	B3/6	2.5YR	Dark Red	D92	D3/4	5YR	Dark Reddish Brown
B93	B3/6	2.5YR	Dark Red	D93	D3/6	2.5YR	Dark Red
B94	B3/6	2.5YR	Dark Red	D94	D3/4	5YR	Dark Reddish Brown
B95	B3/6	2.5YR	Dark Red	D95	D4/2	5YR	Dark Reddish Grey
B96	B3/6	2.5YR	Dark Red	D96	D4/3	5YR	Reddish Brown
B97	B3/6	2.5YR	Dark Red	D97	D3/4	5YR	Reddish Brown
B98	B3/4	2.5YR	Dark Reddish Brown	D98	D3/4	7.5YR	Reddish Brown
B99	B4/6	2.5YR	Brown	D99	D4/3	7.5YR	Dark Reddish Grey
B910	B3/6	2.5YR	Dark Red	D910	D3/4	5YR	Reddish Brown
B101	B4/6	2.5YR	Red	D101	D3/6	2.5YR	Dark Red
B102	B3/6	2.5YR	Dark Red	D102	D4/3	5YR	Reddish Brown
B103	B3/6	2.5YR	Dark Red	D103	D4/6	2.5YR	Red
B104	B3/6	2.5YR	Dark Red	D104	D4/4	5YR	Reddish Brown
B105	B4/6	2.5YR	Red	D105	D3/3	5YR	Dark Reddish Brown
B106	B3/6	2.5YR	Dark Red	D106	D3/3	5YR	Dark Reddish Brown
B107	B4/6	2.5YR	Red	D107	D3/4	5YR	Dark Reddish Brown

B108	B3/6	2.5YR	Dark red	D108	D5/3	7.5YR	Brown
B109	B3/6	2.5YR	Dark Red	D109	D5/3	7.5YR	Brown
B1010	2.5/4	2.5YR	Dark Reddish Brown	D1010	D3/3	5YR	Dark Reddish Brown

Table 3.9: Mineralogy of the < 53 μm fraction of soil samples as determined by X-ray diffraction (note +++ is major, ++ is minor, + is trace)

Sample No	Microcline	Sanidine	Hematite	Goethite	Bixbyite	Braunite	Ramsdellite	Pyrolusite	Cryptomelane
1	+			++				+++	
2	+			++					
3			+++		+				+
4			+++				+		
5			+++						
6			+++				+		
7		+							+++
8		+							+++
9	+				+				+++
10									+++
11					+++				
12		++			++				
13	++		+++			+		+	
14			+++						
15			+++						
16			+++						
17	+				+		+		+++
18				++					+++
19						+			+++
20		+					+		+++
21			+++						
22	+		+++					+	
23			+++	+					+
24			+++						
25				++					
26				+++			+	+	+
27		++					++		
28	+					+++		+	
29			+			+++			+
30	+					+++			
31			+++			++			
32		+	+++					+	
33		+	+++					++	
34	+		+++				+		
25	++			+	++				

36		++	++						
37				++		+++			+
38			+			+++	+		
39	+			+		+++		+	+
40		+				+++			++
41		+	+++	++					
42		+	+++	++					
43		+	+++	+++					
44		+	+++	+++					
45		++		+++			+		
46		++		++			+		
47		+		+		+		+	+
48		+			++		+++	+	
49		++				+	+++		
50		+				+	+++		
51		+	+++				+++		
52	+		+++					++	
53	+		+++						
54	+		++	++					
55		++	+						
56		++	+	+	+				
57		+				++	+		+++
58	++		+					+	+++
58					+		++		+++
60						++	+	+	+++
61	++		+++	+					
62	+		+++	++					
63	++		+++	+					+
64		++	+++		+				
65	+					++	+		
66							++	+	
67							+	+++	
68				+					+++
69				+					+++
70			+						+++
71			+++						+++
72			+++						
73			+++						
74			+++						
75		+				+++		+	
76						+++		+	
77						+++			+
78						+++	++		
79						+++	+		
80						+++		++	

81						+++			+
82			+++	+					
83			+++	+					
84			+++	+					
85			+++	+					
86		+			+		++		
87	+								+++
88		++							+++
89		+							+++
90		+							+++
91	++			++				+	
92		+	+++						
93		+	+++						
94		+	+++						+++
95		+	+++						+++
96	+						+		+++
97	+						+		+++
98			+			+			+
99					+			++	+
100					++			+	+
101	+					+++			
102	+					+++	+		
103	+					+++			
104	+					+++			+
105		+		++	+				
106		+							
107		++				+++		+	
108		+				+++	+	++	
109			++			+++		+	
110			+			+++			++
111		+		++			+		
112		+		++			+		
113		+		++			+		
114		+		++			+		
115		+		++			+		
116						+++		+	
117						+++			+
118						+++		+	
119						+++			
120	+		+++				+		
121	+		+++						
122	+		+++						
123	+		+++						
124				+		+			
125				+		+			

126				+		+			
127	+								+++
128	+								+++
129	+								+++
130			+++	+					+++
131			+++	+					
132			+++	+					
133			+++	+					
134	+				+		+		
125	+				+		+		
136	+				+		+		
137						+			+++
138						+			+++
139						+			+++
140						+			+++
141		+				+		+	
142		+				+		+	
143		++				+		+	
144		++				+		+	
145		++				+		++	
146		++				+		+	
147						+++	++		
148						+++	+		+
149						+++	+		++
150						+++	+	++	
151		+		+					++
152	+		+++						
153	+		+++						
154	+		+++						
155		++	+++						
156	+				+			++	
157				++		+++			
158					++	+++	+		
158						+++		++	
160						+++	+		++
161		++	++	+				+	
162	++		+++						
163	+		+++						
164	+		+++						
165	+		+++	++					
166		++	++		+				
167		++	+		++				+++
168		+		++					+++
169		+							+++
170		+							+++

171			++	+		+			
172			++	+	++				
173			+	+		++			
174			+	+	+				
175			+	+		++			
176			+		++				
177			+			++			+++
178		+							+++
179		+							+++
180		+							+++
180		+				++		+	
181	+		+++						
182	+		+++						
183	+		+++						
184	+		+++						
185				++			++		+
186				+		++	+		
187		+				+++			
188		+				+++			
189		+				+++			
190		+				+++		+	
191	+		+++						
192		+	+++						
193	+		+++						
194	+		+++	+					
195	+		+	+					
196	+					++			
197		+				+++			
198		+				+++			
199		+				+++			
200		+				+++			
201		++	+	+					
202	+		+++						
203	+		+++						
204	+		+++						
205	+		+++						
206	+	+				++			+++
207							++		+++
208						++	+		+++
209							++		+++
210		+			++				
211	++					+		++	
212		+	+++						
213		+	+++						
214		+	+++						

215		+	+++						
216		+							+++
217					++				+++
218						+			+++
219					+	++			+++
220			++	+	++				
221			+	+		++			
222			+	+	+				
223			+	+		++			
224		+	+	+					
225		+	+		++				
226		+				+++			
227		+				+++			
228		+				+++			
229		+				+++			
230		+	+++	+		++			
231			+++	+					
232			+++	+					
233			+++	+					
234				+					
225			+	+++	+		++		
236					+	+++	+		++
237						+++			
238						+++			
239						+++			
240			+++			++			
241		+	+++						
242		+	+++						
243		+	+++						
244		+		++					
245		+							
246			++						
247			+						+++
248									+++
249									+++
250									+++
251			++						
252				++	+	++			
253				+	+		++		
254				+	+	+			
255				+	+		++		
256		+							+++
257		+							+++
258		+							+++
258		+							+++

260			+++						
261			+++						
262			+++						
263			+++						
264		++		++					
265		+					+++		
266		+				+++			
267						+++			
268						+++			
269						+++			
270			+++	++	+	++			
271			+++	+	+		++		
272			+++	+	+	+			
273			+++	+	+		++		
274	+				+				
275		+			+				
276	+			+	+				
277						+++	++		
278						+++	+		
279						+++	++		
280						+++	+		
281	+		+++						
282	+		+++						
283	+		+++						
284	+		+++						
285		++	+	++					
286		+	+		++				
287		+	+	+					+++
288		+	+		++				+++
289		++							+++
290		++							+++
291	++		+++						
292	+		+++						
293	+		+++						
294	+		+++						
295		++	++						
296		++		+					
297					+				+++
298				+					+++
299				+	+				+++
300									+++
301			+++						
302			+++						
303			+++						
304			+++						

305	++	+	++						
306	+	+		++					
307	+	+	+			+++			
308	+	+		++		+++			
309						+++			
310		++				+++			
311			+++	++	+	++			
312			+++	+	+		++		
313			+++	+	+	+			
314			+++	+	+		++		
315	+++	+	+		++	+			
316	+++	+	+		++	+			
317	+++	+	+		++	+++			
318		++				+++			
319		++				+++			
320		++				+++			
321			+++	+	+	+		++	+
322			+++	++	+	+		++	
323			+	+++	+	+		++	
324			+++	+++	+	+		++	
325	+++	+	+		++	+			
326	+++	+	+		++	+			
327	+++	+	+		++	++			
328	+								+++
329	+								+++
330	+								+++
331			+++						+
332		++	+++						
333		+	+++						
334		+	+++						
325	+++	+	+		++	++			
336	+++	+	+		++	++			
337	+++	+	+		++	++			
338		+++	+	+					
339	+								+++
340	+								+++
341	+								+++
342	+								+++
343	+	+	+		++	+			
344	+	+	+		++	+			
345	+	+	+		++	+			
346		+	+	+		++	+		
347	+					+++			
348	+					+++			
349	+					+++			

350	+					+++			
351			+++	+					
352			+++	+					
353			+++	+					
354			+++	+					
355									
356	++	+							
357	+								+++
358		++							+++
358		+							+++
360	+			++					+++
361		+	+++						
362	++		+++						
363	+		+++						
364	+		+++						
365	+	+	+		++	+			
366		+	+	+		++	+		
367	++								+++
368	+								+++
369	+								+++
370	++								+++
371			+	+	+		++	+	
372				+	+	+		++	+
373			+	+	+		+	+	
374				+	+	+		+	+
375		+	+	+		++	+		
376			+	+	+		++	+	
377		++				+++			
378		++				+++			
379		++				+++			
380		++				+++			
380	+	+	+		++	+			
381		+	+	+		++	+		
382	+	+	+		++	+			
383		+	+	+		++	+		
384	+	+	+		++	+			
385		+	+	+		++	+		
386	+	+	+		++	+			
387		+	+	+		++	+		
388	+	+	+		++	+			
389		+	+	+		++	+		
390	++		+++						
391	++		+++						
392	++		+++						
393	++		+++						

394	+	+	+		++	+			
395		+	+	+		++	+		
396	+	+	+		++	+			
397		+	+	+		++	+		
398	++					+++			
399	++					+++			
400	++					+++			

Table 3.11: Mineralogy of the < 4 μm fraction of soil samples as determined by X-ray diffraction (note +++ is major, ++ is minor, + is trace)

Sample No	Muscovite	Ilite	Kaolinite
1		+	+
2			
3	+	+	+
4		+	
5	+	+	
6		+++	
7	+		+++
8			++
9	+		+++
10			+
11	+++		
12	++		+
13		+++	
14		+++	+
15		+++	
16		+++	
17	+		+++
18			++
19			+++
20			++
21		+++	
22		+++	
23		+++	+
24		+++	
25	+		
26			+
27	+		
28	+		
29		+	+
30			
31	+	+++	

32		+++	
33		+++	
34		+++	
25	++		
36		++	
37	+		+
38		+	
39			+
40			++
41		+++	
42		+++	
43		+++	
44		+++	
45	+		
46	+		
47			+
48	++		
49	+		
50	+		
51		+++	+
52		+++	
53		+++	+
54		++	
55		+	
56	+	+	
57			++
58		+	+++
58	+		+++
60			++
61	+	+	
62		+++	
63		+++	+
64	+	+	
65		+	
66	+		
67	+		+
68			+++
69			+++
70		+	+
71		+++	+++
72		+++	
73		+++	
74		+++	
75	+		
76	+		

77			+
78		+	
79		+	
80		+	
81			+
82		+++	
83		+++	
84		+++	
85		+++	
86	+		
87			++
88			+++
89			+
90			++
91	+		
92		+++	
93		+++	
94		+++	+++
95		+++	+++
96			+++
97			+++
98		+	+
99	+		+
100	++		+
101	+	+	+
102		+	
103		+	
104			+
105	+		
106		+	
107			+
108			+
109		++	
110		+	++
111			+
112			+
113			+
114			+
115			
116			
117			+
118		+	
119		+	
120		+++	+
121		+++	+

122		+++	
123		+++	++
124		+	+
125		+	+
126			+
127			+++
128			+++
129			+++
130		+++	+++
131		+++	
132		+++	
133		+++	
134	+		
125	+		
136	+		
137			+++
138			+++
139			+++
140		++	+++
141		+	
142		+	
143		+	
144		+	
145		++	
146		+	
147		++	
148			+
149			++
150			
151			++
152		+++	
153		+++	
154		+++	
155		+++	
156	+		
157			
158	++		
158			
160			++
161		++	
162		+++	
163		+++	
164		+++	
165		+++	
166	+	++	

167	++	+	+++
168			+++
169			+++
170			+++
171		++	
172	++	++	
173		+	
174	+	+	
175		+	
176	++	+	
177		+	+++
178			+++
179			+++
180			+++
180			
181		+++	+
182		+++	++
183		+++	
184		+++	++
185			+
186	+		
187	++		
188		+	
189	++		
190			
191		+++	
192		+++	
193		+++	
194		+++	
195		+	
196			+
197			++
198			+
199			++
200			+
201		+	++
202		+++	
203		+++	++
204		+++	
205		+++	
206			+++
207			+++
208			+++
209			+++
210	++		

211			
212		+++	
213		+++	
214		+++	
215		+++	
216			+++
217	++		+++
218			+++
219	+		+++
220	++	++	
221		+	
222	+	+	
223		+	
224		+	
225	++	+	
226			
227	+		
228		+	
229		+	
230		+++	
231		+++	
232		+++	
233		+++	
234			
225	+	+	
236	+		++
237			+
238			++
239			+
240		+++	++
241		+++	
242		+++	
243		+++	
244			+
245			+
246		++	
247		+	+++
248			+++
249			+++
250			+++
251		++	
252	+		
253	+		
254	+		
255	+		

256			+++
257			+++
258			+++
258			+++
260		+++	
261		+++	
262		+++	
263		+++	
264			+
265			++
266			+
267			++
268			+
269			+
270	+	+++	
271	+	+++	
272	+	+++	
273	+	+++	
274	+		
275	+		
276	+		+
277			++
278		+	
279			++
280		+	
281		+++	
282		+++	
283		+++	
284		+++	
285		+	
286	++	+	
287		+	+++
288	++	+	+++
289			+++
290			+++
291		+++	
292		+++	
293		+++	
294		+++	
295		++	
296			
297	+		+++
298			+++
299	+		+++
300			+++

301		+++	
302		+++	
303		+++	
304		+++	
305		++	
306			+
307		+	++
308			+
309			++
310			+
311	+	+++	
312	+	+++	
313	+	+++	
314	+	+++	
315	++	+	
316	++	+	
317	++	+	
318		+	
319		+	
320		+	
321	+	+++	+
322	+	+++	
323	+	+	
324	+	+++	
325	++	+	
326	++	+	
327	++	+	
328			+++
329			+++
330			+++
331		+++	+
332		+++	
333		+++	
334		+++	
325	++	+	
336	++	+	
337	++	+	
338		+	
339			+++
340			+++
341			+++
342			+++
343	++	+	
344	++	+	
345	++	+	

346		+	+
347			++
348			++
349			++
350			+++
351		+++	
352		+++	
353		+++	
354		+++	
355			+
356			++
357			+++
358			+++
358			+++
360			+++
361		+++	
362		+++	
363		+++	
364		+++	
365	++	+	
366		+	
367			+++
368			+++
369			+++
370			+++
371	+	+	
372	+		+
373	+	+	
374	+		+
375		+	
376	+	+	
377			+
378			++
379			+
380			++
380	++	+	
381		+	
382	++	+	
383		+	
384	++	+	
385		+	
386	++	+	
387		+	
388	++	+	
389		+	

390		+++	
391		+++	
392		+++	
393		+++	
394	++	+	
395		+	
396	++	+	
397		+	
398			++
399			+
400			++

Table 3.14: Concentration levels of iron, manganese and total organic carbon in soils in the study area

Sample Number	Fe, conc. (μg g^{-1})	%rsd	s.d	Mn, conc. (μg g^{-1})	%rsd	s.d	TOC (wt %)
A1-1	19790.13	5.7	1128.04	9150.01	0.2	18.30	3.07
A1-2	26253.24	0.4	105.013	8016.51	1.8	144.30	2.26
A1-3	12917.38	3.4	439.19	2787.92	3.8	105.94	3.84
A1-4	13095.62	1.2	157.15	3351.98	7.2	241.35	1.76
A1-5	23482.24	1.6	375.716	3323.49	5.6	186.12	1.83
A1-6	14227.68	2.1	298.78	3348.41	6.3	210.95	1.38
A1-7	13088.21	4	523.53	4326.8	3.9	168.75	0
A1-8	11688.05	6.4	748.035	782.85	0.7	5.48	4.01
A1-9	19018.9	6.7	1274.27	1626.81	0.7	11.39	0.94
A1-10	17321.6	1.4	242.50	307.99	2.2	6.78	4.91
A2-1	21256.5	4.9	1041.57	3038.51	4.6	139.77	2.46
A2-2	14800.44	1	148	24907.56	1.6	398.52	2.75
A2-3	23946.24	3.1	742.33	14056.24	2.7	379.52	2.34
A3-4	18362.03	7.5	1377.15	3968.21	4.1	162.70	1.36
A2-5	20196.03	5.4	1090.57	4225.99	4.2	177.49	3.28
A2-6	20315.97	3.2	650.11	3506.72	5.6	196.38	4.02
A2-7	16354.77	2.2	359.80	2060.41	4.5	92.72	0.9
A2-8	17657.91	1.4	247.21	2317.09	3.2	74.15	0.97
A2-9	13281.23	6.3	836.72	1969.26	2.9	57.11	0.75
A2-10	20329.16	3.4	691.19	17776.5	8.3	1475.45	3
A3-1	24721.99	1.9	469.72	17901.99	1	179.02	0.1
A3-2	13526.24	3.2	432.84	23073.27	0.6	138.44	0
A3-3	30099.1	1.4	421.39	2300.41	2.1	48.31	1.81
A3-4	3281.7	3.4	111.58	4002.28	7.6	304.17	1.62
A3-5	14499.81	2.9	420.49	2500.84	3	75.0252	0.96
A3-6	14178.69	8.4	1191.01	4002.28	7.6	304.17	0.81
A3-7	16295.35	1.6	260.726	1717.78	24.8	426.01	2.36

A3-8	23157.95	2.3	532.63	2111.79	10.1	213.29	1.76
A3-9	15942.75	0.6	95.66	2138.38	9	192.45	0.81
A3-10	14396.89	7.8	1122.96	1333.63	9.6	128.03	1.07
A4-1	20329.16	3.4	691.19	17776.5	8.3	1475.45	2.64
A4-2	15861.51	2.2	348.95	2741.62	2	54.83	3.24
A4-3	21464.94	1.7	364.90	6169.78	2	123.40	1.02
A4-4	20450.33	1.5	306.76	7972.25	0.7	55.81	0.91
A4-5	21256.5	4.9	1041.57	3038.51	4.6	139.77	1.15
A4-6	2658.84	2.6	69.13	1128.56	1.7	19.19	0.97
A4-7	19520.29	0.9	175.68	5736.96	3.5	200.79	1.22
A4-8	10822.1	8	865.77	1802	10.3	185.61	1.51
A4-9	11782.08	5.6	659.79	2294.61	9	206.51	1.13
A4-10	15740.83	7.4	1164.82	2217.72	8.3	184.07	0.86
A5-1	9898.75	3.1	306.86	821.2	11.5	94.44	1.97
A5-2	5303.96	0.6	31.82	808.53	3.3	26.68	2.2
A5-3	9231.55	0.9	83.08	3773.56	2	75.47	1.88
A5-4	5352.74	3.7	198.05	709.49	0.6	4.26	0.83
A5-5	6098.01	0.8	48.78	670.28	1.9	12.73	0.96
A5-6	6879.16	1.8	123.82	583.3	0.5	2.92	1.68
A5-7	6147.74	2.1	129.10	294.03	1.4	4.11	1.63
A5-8	6009.71	0.6	36.06	283.43	3.9	11.05	1.26
A5-9	6992.4	2.9	202.78	259.42	3.1	8.04	0.39
A5-10	10531.06	1.6	168.50	619.15	1.7	10.53	1.29
A6-1	7415.98	2.7	200.23	763.39	1.8	13.74	2.12
A6-2	2614.16	8.2	214.36	4889.23	1.5	73.34	1.05
A6-3	5653.75	3.9	220.49	2709.51	0.6	16.28	1.73
A6-4	3576.58	6.7	239.63	298.17	2.5	7.45	0.84
A6-5	2547.42	3.4	86.61	69.34	1.6	1.11	1.49
A6-6	11782.08	5.6	659.80	2294.61	9	206.51	1.54
A6-7	15740.83	7.4	1164.82	2217.72	8.3	184.07	0.58
A6-8	20137.18	0.9	181.23	2789.41	8.9	248.26	1.59
A6-9	18314.53	3	549.44	2317.09	3.2	74.15	0.7
A6-10	24440.73	0.1	24.44	1969.26	2.9	57.11	0.25
A7-1	2468.17	6.8	167.84	648.65	1.2	7.78	1.76
A7-2	4330.5	1.6	69.29	1601.4	2	32.03	1.02
A7-3	4893.42	2.8	137.02	1004.36	5.2	52.23	0.67
A7-4	5850.62	3.7	216.47	897.62	1.3	11.67	0.8
A7-5	5064.97	0.8	40.52	283.12	3.1	8.78	0.97
A7-6	21256.5	4.9	1041.57	3038.51	4.6	139.77	1.07
A7-7	2658.84	2.6	69.13	1128.56	1.7	19.19	1.05
A7-8	11782.08	5.6	659.80	2294.61	9	206.51	1.11
A7-9	15740.83	7.4	1164.82	2217.72	8.3	184.07	0.62
A7-10	18314.53	3	549.44	2317.09	3.2	74.15	0.79
A8-1	1116.59	1.2	13.40	768.68	1.3	9.99	3.83
A8-2	7316.76	1.4	102.43	1702.47	2.9	49.37	3.6
A8-3	6344.06	2.9	183.98	882.28	6.1	53.82	2.64

A8-4	9004.84	1.4	126.07	654.82	6.1	39.94	1.43
A8-5	5064.97	0.8	40.52	283.12	3.1	8.78	0.92
A8-6	6991.04	0.5	34.96	689.69	1.7	11.72	1.03
A8-7	5565.33	3.8	211.48	524.5	2	10.49	0.89
A8-8	5356.17	0.8	42.85	1017.57	1.9	19.33	1.54
A8-9	4884.93	2.9	141.66	240.08	1	2.40	2.78
A8-10	1871.24	7.3	136.60	127.16	6.2	7.88	1.86
A9-1	5850.62	3.7	216.47	897.62	1.3	11.67	2.05
A9-2	5356.17	0.8	42.85	1017.57	1.9	19.33	2.36
A9-3	7800.7	0.7	54.60	1423.6	3.4	48.40	3.1
A9-4	7188.54	3.3	237.22	1637.27	1.8	29.47	2.02
A9-5	8675.32	0.2	17.35	406.72	1.5	6.10	1.76
A9-6	6979.56	2.1	146.57	453.38	1.1	4.99	2.06
A9-7	5728.41	1.3	74.47	346.76	0.3	1.04	1.53
A9-8	6918.42	1.3	89.97	396.86	0.8	3.17	1.75
A9-19	6712.27	1	67.12	623.61	0.6	3.74	2.16
A9-10	5002.74	3.5	175.096	159.84	5.4	8.63	1.51
A10-1	1116.59	1.2	13.40	768.68	1.3	9.99	2.9
A10-2	6782.02	3.9	264.50	974.39	1.4	13.64	2.3
A10-3	6814.28	1.9	129.47	312.48	1.4	4.37	1.03
A10-4	8238.12	0.7	57.67	998.65	3.6	35.95	1.01
A10-5	9050.15	1.5	135.75	1447.44	2	28.95	1.24
A10-6	6393.65	1.3	83.12	180.78	5.1	9.22	1.64
A10-7	4940.49	5	247.02	1444.44	2	28.89	2.25
A10-8	7689.99	2.3	176.87	944.62	5.4	51.01	2.65
A10-9	6203.21	1.4	86.84	244.16	1.9	4.64	2.47
A10-10	5350.77	3.4	181.93	296.24	5	14.81	2.11
B1-10	12099.44	6.1	738.07	258.37	1.9	4.91	0.36
B1-2	15613.95	8.2	1280.34	199.84	0.4	0.80	1.07
B1-3	11488.57	6.2	712.29	108.6	2.6	2.82	0.69
B1-4	19867.23	3.1	615.88	360.412	4.8	17.30	0.33
B1-5	23859.93	0.8	190.88	882.27	1.7	14.99	1.01
B1-6	23908.99	3.3	788.99	799.85	1.5	11.99	0.67
B1-7	43537.69	5.7	2481.65	731.11	1.2	8.77	0
B1-8	7887.87	2	157.757	107.12	1.4	1.50	0.31
B1-9	20002.96	3.1	620.09	434.18	2.4	10.42	0.12
B1-10	18456.61	4.9	904.37	861.84	0.9	7.76	1.33
B2-1	10891.51	1.2	130.70	196.2	2.4	4.71	0.9
B2-2	16204.73	0.7	113.43	81.31	1.3	1.06	1.1
B2-3	13326.48	2.6	346.49	92.63	1.1	1.02	1.08
B2-4	18110.89	1.9	344.12	290.116	1.4	4.06	1.07
B2-5	27886.59	0.9	250.98	1415.56	8.2	116.08	0.5
B2-6	30211.66	5	1510.58	681.99	0.8	5.46	0.2
B2-7	37931.94	1.4	531.05	457.56	1.3	5.95	0.48
B2-8	23859.93	0.8	190.88	882.27	1.7	14.99	3.39
B29	27886.59	0.9	250.98	1415.56	8.2	116.08	0.04

B2-10	17189.23	0.4	68.76	355.89	0.7	2.49	0.56
B3-1	10431.62	1	104.32	232.33	2.7	6.27	3.19
B3-2	870766	1.4	12190.72	85.19	1.2	1.02	1.82
B3-3	10237.69	1.3	133.09	531.25	2.7	14.34	2.12
B3-4	17869.14	1.7	303.77	148.36	1.6	2.37	2.02
B3-5	37931.94	1.4	531.04	457.56	1.3	5.95	2.11
B3-6	45369.51	19.7	8937.79	827.16	1.9	15.72	0.9
B3-7	14916.58	5.9	880.08	744.7	2.1	15.64	1.2
B3-8	19611.84	3.8	745.25	382.47	3.4	13.00	1.08
B3-9	17243.06	1.6	275.89	478.16	4.6	21.99	1.01
B3-10	18727.59	2.8	524.37	248.85	2.7	6.719	0.97
B4-1	11955.56	6.3	753.20	240.41	1.9	4.57	0.83
B4-2	11430.12	5.9	674.38	133.3	0.8	1.07	1.96
B4-3	12413.59	4.5	558.61	128.5	2.3	2.96	1.43
B4-4	20037.39	3.1	621.16	484.45	3.6	17.44	1.29
B4-5	45369.51	19.7	8937.79	827.16	1.9	15.716	1.07
B4-6	51145.52	37.6	19230.72	816.94	2.7	22.06	0.87
B4-7	23824.58	2.2	524.14	476.23	0.6	2.86	1.02
B4-8	13207.31	1	132.07	238.64	2.3	5.489	0.29
B4-9	13568.72	2.8	379.92	261.8	2.3	6.02	1.51
B4-10	5234.45	13	680.48	681.15	1.4	9.54	0.67
B5-1	10843.47	8.3	900.01	264.55	0.1	0.26	1.97
B5-2	14721.66	5.4	794.97	226.61	1.5	3.40	2.2
B5-3	14285.9	5.7	814.30	151.19	1.4	2.12	1.88
B5-4	22288.61	2.3	512.64	269.44	1.4	3.77	0.83
B5-5	23824.58	2.2	524.14	476.23	0.6	2.86	0.96
B5-6	22058.69	2.9	639.70	545.86	0.3	1.64	1.68
B5-7	43786.61	10.2	4466.23	986.99	1.4	13.82	1.63
B5-8	414465.25	2.8	11605.03	898.74	2.7	24.26	1.26
B5-9	17135.65	5.8	993.87	491	3.8	18.66	0.39
B5-10	84948.88	7.5	6371.17	896.47	3.4	30.48	1.29
B6-1	11625.61	1.5	174.38	417.4	3.9	16.28	2.12
B6-2	19038.86	1	190.39	200.06	5.3	10.60	1.05
B6-3	14999.29	4	599.97	127.92	2.3	2.94	1.73
B6-4	18224.23	0.7	127.57	423.28	1.6	6.77	0.84
B6-5	23824.58	2.2	524.14	476.23	0.6	2.857	1.49
B6-6	33657.84	3.5	1178.02	1025.54	0.6	6.15	1.54
B6-7	22376.08	1.9	425.15	633.63	2.2	13.94	0.58
B6-8	14402.48	0.9	129.62	340.21	7.5	25.52	1.59
B6-9	24980.58	2	499.62	556.02	0.5	2.78	0.7
B6-10	19243.15	1.3	250.16	407.43	4	16.30	0.25
B7-1	10822.84	2.2	238.10	226.87	1.5	3.40	1.76
B7-2	10728.27	5.3	568.40	130.77	0.5	0.65	1.02
B7-3	13121.12	4.4	577.33	109.84	0.3	0.33	0.67
B7-4	26292.01	3.4	893.93	776.85	2.3	17.87	0.8
B7-5	28337.67	1.3	368.39	344.99	1	3.45	0.97

B7-6	31172.2	2.3	716.96	938.48	1.8	16.89	1.07
B7-7	16401.64	2.6	426.44	603.9	3.2	19.32	1.05
B7-8	28800.06	3.4	979.20	1112.49	2.5	27.81	1.11
B7-9	27735.49	2.8	776.59	743.93	1.5	11.15	0.62
B7-10	14640.54	2.6	380.65	626.08	4.5	28.17	0.79
B8-1	15221.1	4.5	684.95	235.08	2.3	5.41	1
B8-2	11221.3	3.1	347.86	177.76	0.9	1.599	0.97
B8-3	16090.01	6.9	1110.21	412.25	3	12.37	0.46
B8-4	28337.67	1.3	368.39	344.99	1	3.45	0.34
B8-5	23450.07	0.2	46.90	1319.34	1.7	22.43	0.77
B8-6	29798.45	2.8	834.36	1051.38	1	10.51	0.85
B8-7	23450.07	0.2	46.90	1319.34	1.7	22.43	0.93
B8-8	23145.54	4.1	948.97	712.63	2.4	17.10	1.4
B8-9	27060.06	2.8	757.68	402.11	1.7	6.84	0.88
B8-10	24114.82	2.2	530.53	342.47	0.5	1.71	0.84
B9-1	13002.71	2.9	377.08	466.93	2.1	9.80	0.83
B9-2	6646.34	10	664.63	95.4	4.6	4.39	0.92
B9-3	10070.31	5.2	523.66	174.35	2.3	4.01	0.03
B9-4	14475.02	3.3	477.68	202.7	1.4	2.8	0
B9-5	16401.64	2.6	426.44	603.9	3.2	19.32	0.72
B9-6	26033.33	2.5	650.83	901.15	1	9.01	0.54
B9-7	21229.38	3.1	658.11	293.69	3.8	11.16	0.22
B9-8	26670.87	6.3	1680.26	1021.58	1	10.21	0.31
B9-9	17027.91	2.9	493.81	365.11	2	7.30	0.61
B9-10	19328.04	3.9	753.79	334.43	2.2	7.36	0.49
B10-1	9930.77	5.1	506.47	156.08	1	1.56	1.44
B10-2	10239.47	6.3	645.09	467.66	0.7	3.27	1.33
B10-3	20468.39	2.7	552.65	392.63	2.3	9.03	1.29
B10-4	21651.53	5.9	1277.44	389.14	3	11.67	1.04
B10-5	20468.39	2.7	552.65	392.63	2.3	9.03	1.31
B10-6	20231.62	3.5	708.11	426.26	2.3	9.80	0.99
B10-7	18579.93	6.1	1133.38	663.16	0.5	3.32	0.75
B10-8	9752.8	7.9	770.47	198.09	1.5	2.97	1.08
B10-9	16401.64	2.6	426.44	603.9	3.2	19.32	0.62
B10-10	13882.41	4.6	638.59	241.42	3.5	8.45	1.71
C1-1	12372.48	1.4	173.22	1382.03	3.2	44.22	1.77
C1-2	7562.104	4.8	362.98	1169.47	1.9	22.22	2.05
C1-3	12446.43	1	124.46	3956.43	0.7	27.69	4.92
C1-4	11103.84	2.1	233.18	3219.32	2.4	77.26	4.75
C1-5	14319.95	0.8	114.56	322.23	4.6	14.82	1.62
C1-6	11484.34	1.7	195.23	125.3	1	1.25	2.21
C1-7	11976.91	1.6	191.63	268.95	2.2	5.92	4.57
C1-8	14801.19	1.3	192.42	346.05	1.6	5.54	3.46
C1-9	11076.37	1.9	210.45	302.44	7.9	23.89	1.79
C1-10	12840.25	2.4	308.17	134.76	0.8	1.08	1.51
C2-1	18482.5	1.4	258.76	2196.08	1.3	28.55	1.98

C2-2	13107.5	2.6	340.80	5220.37	2.1	109.63	2.07
C2-3	8522.5	2.7	230.11	3174.66	1.4	44.45	3.02
C2-4	11697.5	1	116.98	1493.91	2.8	41.83	1.98
C2-5	13950	1	139.5	279.82	2.9	8.11	4.41
C2-6	12507.5	2.1	262.66	523.81	1.8	9.43	2.58
C2-7	11027.5	1.8	198.50	173.81	4	6.95	3.11
C2-8	16400	1.1	180.4	301.06	1	3.01	2.67
C2-9	16415	2.2	361.13	238.33	0.4	0.95	1.61
C2-10	11355	0.9	102.19	129.06	6.8	8.78	1.83
C3-1	8388.61	2.9	243.27	7411.71	0.9	66.71	2.73
C3-2	7626.901	2.8	213.55	1400.26	1.5	21.00	2.81
C3-3	6581.25	4.4	289.57	3595.66	0.9	32.361	3.17
C3-4	6271.8	4.6	288.50	1606.11	0.6	9.64	3.05
C3-5	7163.22	3.4	243.55	193.09	2.4	4.63	4.02
C3-6	7268.89	0.1	7.27	273.24	1.6	4.37	3.71
C3-7	9157.33	2.1	192.30	121.23	5.2	6.30	2.91
C3-8	8072.9	2.9	234.11	219.98	2.2	4.84	1.92
C3-9	7042.86	0.9	63.38	148.99	1.9	2.83	2
C3-10	7908.37	0.8	63.27	206.16	1.6	3.298	1.97
C4-1	2619.01	2.3	60.24	7023.02	4.8	337.11	1.05
C4-2	3063.06	1.6	49.00	1254.97	0.4	5.02	1.99
C4-3	1521.08	2	30.42	1662.54	1.8	29.93	2.12
C4-4	2293.96	0.5	11.47	1809.48	1.5	27.14	1.63
C4-5	2481.19	1.4	34.74	220.78	1.3	2.87	3.74
C4-6	2206.46	3.1	68.40	267.09	1.2	3.20	3.81
C4-7	2701.95	3	81.06	155.94	0.7	1.09	2.06
C4-8	3004.23	3.7	111.16	302.46	3	9.07	2.59
C4-9	2438.64	1.9	46.33	150.62	2.9	4.37	1.25
C4-10	2590.95	3.5	90.68	100.38	3.7	3.71	1.36
C5-1	6118.01	5.6	342.61	3355.96	0.6	20.14	3.61
C5-2	5557.23	2.6	144.49	1156.56	2.2	25.44	3.16
C5-3	5359.92	1.1	58.96	2695.16	0.9	24.26	3.7
C5-4	3979.49	2	79.59	2095.22	0.6	12.57	2.93
C5-5	6549.22	0.7	45.84	177.52	0.8	1.42	3.63
C5-6	5702.99	5.4	307.96	66.78	4.5	3.00	0.84
C5-7	4476.06	2.4	107.45	198.5	2.6	5.16	3.65
C5-8	7862.45	3.4	267.32	305.75	3.2	9.78	2.54
C5-9	5891.61	2.3	135.51	206.24	0.8	1.65	1.52
C5-10	4898.4	0.5	24.49	217.29	1.9	4.13	1.77
C6-1	7468	4.5	336.06	206.45	3.1	6.39995	4.76
C6-2	7812.87	2.3	179.69	261.7	3.9	10.23	4.32
C6-3	4974.16	7.5	373.062	261.27	5.7	14.89	4.83
C6-4	6883.29	3.4	234.031	203.26	2	4.07	4.79
C6-5	8867.83	0.9	79.81	652.38	3.7	24.14	3.11
C6-6	5863.54	1.7	99.68	433.83	3.6	15.62	3.46
C6-7	7469.22	0.7	52.28	310.91	5.4	16.79	2.43

C6-8	8014.48	1.9	152.28	80.14	2.1	1.68	3.32
C6-9	4799.82	4.3	206.39	131.99	4.7	6.20	3.32
C6-10	7334.2	0.4	29.34	45.24	6.2	2.80	0.71
C7-1	16189.53	3.1	501.88	231.3	1.1	2.54	4.03
C7-2	16627.77	2.3	382.44	163.07	12.9	21.04	4.43
C7-3	10494.16	2.8	293.84	202.64	5	10.13	4.51
C7-4	14453.24	1	144.53	193.32	3.2	6.186	4.88
C7-5	12830.24	1.7	218.11	54.34	3.6	1.96	2.02
C7-6	11339.86	1.1	124.74	38.21	5.7	2.17797	2.89
C7-7	11265.92	2.7	304.18	35.84	3.4	1.22	2.25
C7-8	24121.92	1.2	289.46	89.18	3.1	2.76	4.21
C7-9	11773.22	3.6	423.83	153.52	2.7	4.14	4.59
C7-10	12203.22	2.4	292.88	53.98	8.1	4.37	4.01
C8-1	17403.74	0.5	87.02	248.34	0.9	2.23	4.89
C8-2	19619.51	1.1	215.81	332.45	0.9	2.99	4.5
C8-3	19178.85	1.3	249.33	238.13	1.1	2.62	3.73
C8-4	17240.88	1.4	241.37	241.92	1.1	2.66	2.77
C8-5	15353.54	1.6	245.66	117.528	0.3	0.35	3.91
C8-6	16126.94	4.5	725.71	57.99	3.1	1.798	3.64
C8-7	17993.82	2.2	395.86	41.69	2.3	0.96	3.83
C8-8	16594	2.7	448.04	43.59	3.9	1.70	4.63
C8-9	13552.77	1.8	243.95	191.3	0.8	1.53	4.04
C8-10	13905.26	0.8	111.24	82.39	1.4	1.15	5.13
C9-1	12306.8	2.5	307.67	256.06	1.5	3.84	4.39
C9-2	17383.29	1.7	295.52	326.32	0.9	2.94	4.84
C9-3	12294.6	7.7	946.68	110.15	3.4	3.74	4.62
C9-4	15508.65	0.5	77.54	204.34	0.1	0.20	3.11
C9-5	9427.76	7.2	678.79	1935.64	1.2	23.22	2.75
C9-6	20692.64	2.5	517.32	183.03	3.6	6.59	4.48
C9-7	13678.9	3.1	424.05	389.77	1.9	7.41	5.82
C9-8	7872.48	6.7	527.46	98.09	1.4	1.37	3.72
C9-9	13118.09	1.4	183.65	162.16	0.3	0.49	4.39
C9-10	11830.61	3	354.92	54.18	5.1	2.76	3.21
C10-1	14983.05	5.1	764.14	354.79	1.1	3.90	3.22
C10-2	18754.52	3.3	618.90	191.65	2.6	4.98	7.91
C10-3	14243.07	3	427.29	205.23	1.2	2.46	6.11
C10-4	18591.87	0.2	37.18	220.09	1.5	3.30	4.27
C10-5	13099.75	1.9	248.90	819.6	1.1	9.01	3.27
C10-6	15855.12	0.9	142.70	465.09	4.1	19.07	5.55
C10-7	18231.86	1.5	273.48	305.59	0.7	2.14	4.73
C10-8	14893.71	1.8	268.09	104.6	2.2	2.30	4.34
C10-9	11169.87	6.4	714.87	198.32	1.4	2.78	3.79
C10-10	12216.85	0.9	109.95	72.39	5	3.62	4.05
D1-1	11142.07	5.7	635.10	2075.3	2.3	47.73	0.97
D1-2	17728.3	2.6	460.94	199.41	0.4	0.79	0.32
D1-3	19738.31	1.8	355.29	211.9	2.4	5.08	0.48

D1-4	22396.08	3.8	851.05	266.91	2.6	6.94	0.61
D1-5	18329.45	2.3	421.58	173.7	1	1.74	2.17
D1-6	18231.86	1.5	273.48	305.59	0.7	2.14	1.62
D1-7	19815.16	1	198.15	62.98	6.3	3.97	1.88
D1-8	7627.83	5.2	396.65	130.19	1.6	2.08	2.25
D1-9	9596.73	7.4	710.16	64.56	4.6	2.97	4.99
D1-10	11430.08	1.3	148.59	48.73	3.8	1.85	2.82
D2-1	17739.82	4.5	798.29	388.2	1.3	5.05	0
D2-2	18703.71	3.3	617.22	158.46	0.9	1.43	1.59
D2-3	18252.21	3.5	638.83	201.06	4.6	9.25	0.31
D2-4	14249.81	6.7	954.74	109.14	6.1	6.66	0.99
D2-5	20404.33	3	612.13	141.91	1.5	2.13	5.23
D2-6	21848.26	2.4	524.36	213.51	0.9	1.92	2.72
D2-7	9347.74	4.8	448.69	63.19	1.1	0.70	0
D2-8	7326.5	6.1	446.92	70.39	0.5	0.35	2.55
D2-9	17728.3	2.6	460.94	199.41	0.4	0.80	1.46
D2-10	13079.06	3.2	418.53	99.59	3.3	3.29	4.7
D3-1	11959.51	4.5	538.18	182.64	1.6	2.92	1.66
D3-2	16993.76	1.1	186.93	256.84	4.3	11.04	1.4
D3-3	15671.04	3.4	532.82	249.4	1.4	3.49	1.32
D3-4	13769.6	1.4	192.77	139.1	1.5	2.09	1.97
D3-5	17887.98	3.1	554.53	122.18	5	6.11	2.82
D3-6	14130.21	6	847.81	68.57	4.2	2.88	0.59
D3-7	14537.08	1.7	247.13	149.12	3.5	5.22	0.62
D3-8	17728.3	2.6	460.93	199.41	0.4	0.80	1.09
D3-9	9057.43	4	362.30	75.31	1.6	1.20	1.86
D3-10	14102.62	1.4	197.44	75.18	7.9	5.942	3.85
D4-1	14825.65	7	1037.80	171.25	0.6	1.02	1.32
D4-2	14873.69	0.9	133.86	205.47	2	4.11	3.8
D4-3	19149.7	7.6	1455.38	218.85	0.6	1.31	0.86
D4-4	12224.53	3.7	452.31	139.27	2.6	3.62	1.14
D4-5	17168.54	3.9	669.57	117.04	0.2	0.23	2.82
D4-6	20211.98	3.1	626.57	91.86	5	4.59	0.24
D4-7	15399.32	1	153.99	73.64	2.3	1.69	0.39
D4-8	6391.87	7.5	479.39	77.36	0.8	0.62	2.42
D4-9	8002.01	2.1	168.04	80.96	6	4.86	2.97
D4-10	11195.26	4.4	492.59	71	6.2	4.402	1.72
D5-1	10392.29	3.8	394.91	132.27	4.1	5.42	0.64
D5-2	13431.63	2.2	295.50	176.98	1.7	3.01	0.59
D5-3	16348.13	1.2	196.18	140.85	2.4	3.38	0.48
D5-4	15876.57	3.1	492.17	202.49	1.5	3.045	1.04
D5-5	15753.82	4.9	771.94	211.33	0.8	1.69	0.17
D5-6	18282.21	3.2	585.03	287.97	0.7	2.02	2.29
D5-7	17082.96	3.8	649.15	105.67	3	3.17	1.36
D5-8	9858.92	4.4	433.79	73.96	9.6	7.10	3.07
D5-9	9198.92	10.7	984.28	94.46	2.9	2.74	3.88

D5-10	9739.58	4.6	448.02	73.37	2.2	1.61	4.46
D6-1	7780.72	10.8	840.32	468.4	1.7	7.96	0.98
D6-2	6916.57	8.7	601.74	106.74	5.3	5.66	1.06
D6-3	18274.49	3.7	676.16	51.506	8.5	4.38	0.16
D6-4	17927.88	2.2	394.41	120.33	3	3.61	0
D6-5	19288.25	6.1	1176.58	157.11	5.2	8.17	0.88
D6-6	18769.81	2.2	412.93	127.43	6.2	7.90	0.71
D6-7	11235.57	5.6	629.19	93.72	6.1	5.717	0.38
D6-8	15422.85	4.9	755.72	72.91	1.8	1.31	0.09
D6-9	7856.52	15.2	1194.19	66.78	1.1	0.73	4.54
D6-10	9446.16	10.3	972.95	87.21	6	5.23	6.18
D7-1	16771.84	5.4	905.68	349.91	1.6	5.60	1.88
D7-2	14115	0.2	28.23	118.19	7	8.27	1.51
D7-3	14215.08	3.9	554.39	182.86	5.6	10.24	0.62
D7-4	1242.41	4.5	55.91	241.62	0.5	1.21	1.07
D7-5	23068.6	0.7	161.48	142.97	1.2	1.71	1.08
D7-6	23065.46	3.9	899.56	151.64	2	3.03	0
D7-7	26630.86	2.7	719.03	147.87	1.7	2.51	0.11
D7-8	9776.79	2.7	263.97	147.51	4.1	6.048	0
D7-9	5426.22	7.1	385.26	47.72	1.7	0.81	1.61
D7-10	12581.79	2.3	289.38	60.01	1.6	0.96	0.72
D8-1	16694.44	2.5	417.36	41.733	9.3	3.88	1.93
D8-2	14741.35	1.9	280.08	398.8	0.8	3.19	2.61
D8-3	17233	3.8	654.85	163	6.1	9.94	2.32
D8-4	18867.83	1.6	301.88	155.3	4.2	6.52	1.86
D8-5	18338.18	2.3	421.78	197.36	2.7	5.33	0.91
D8-6	20582.28	3.1	638.05	154.8	3.9	6.04	0.77
D8-7	19719.71	2.9	571.87	181.81	1.6	2.91	2.75
D8-8	8119.88	3.9	316.67	62.04	5.4	3.35	3.53
D8-9	7014.43	9.2	645.33	57.33	8.9	5.10	2.94
D8-10	27638.53	2.7	746.24	49.47	5.4	2.67	1.04
D9-1	21544.36	2.3	495.52	63.69	9	5.73	0.11
D9-2	15189.56	2.5	379.74	573.52	0.8	4.59	0
D9-3	17053.45	3.2	545.71	172.94	1.3	2.25	1.07
D9-4	17254.25	2.4	414.10	243.79	1.5	3.66	1.25
D9-5	9510.35	4.5	427.97	107.58	6.5	6.99	0.63
D9-6	12533.81	0.8	100.27	75.6	8.2	6.20	0.9
D9-7	20376.42	2.2	448.28	104.74	6.2	6.49	0
D9-8	10170.93	4.4	447.52	125.22	3.4	4.28	0.06
D9-9	7159.75	2.3	164.67	203.84	0.8	1.63	0.37
D9-10	16503.3	1.5	247.55	53.27	8.8	4.69	0.49
D10-1	21740.71	3.8	826.15	68.87	3.2	2.20	3.47
D10-2	20489.06	2.6	532.72	500.44	1.7	8.51	3.67
D10-3	17630.25	3.6	634.69	161.86	4	6.47	0.36
D10-4	16879.41	1.7	286.95	175.64	2.7	4.74	0.54
D10-5	23135.89	1	231.36	228.93	2.5	5.72	0.46

D10-6	18788.13	5.2	976.98	207.4	5.4	11.20	0.83
D10-7	12498.39	5.3	662.41	214.53	4.1	8.79	0.73
D10-8	9391.97	9	845.28	55.46	5.9	3.27	0.55
D10-9	7134.55	1.2	85.61	99.13	6.3	6.25	0.16
D10-10	12155.4	6	729.32	108.22	5.4	5.84	5.78

Table 3.15: Concentration levels of iron and manganese in leaves in the study area

Sample Number	Fe, conc. (μg g^{-1})	%rsd	s.d	Mn, conc. (μg g^{-1})	%rsd	s.d
2	471.59	0.5	2.36	499.44	1	4.99
4	1295.85	2.6	33.69	585.49	2.5	14.64
6	1295.85	2.6	33.69	585.49	2.5	14.64
8	605.29	1.3	7.87	131.35	3.2	4.20
10	477.59	1.3	6.21	177.46	0.3	0.53
12	1445.21	3	43.36	437.35	2.2	9.62
14	2175.28	2.5	54.38	751.27	0.8	6.01
16	764.71	1.2	9.18	970.81	2.2	21.36
18	2585.17	1.6	41.36	603.7	2	12.07
20	671.16	2.9	19.46	674.1	5.5	37.07
	296.43	2.2	148.0	324.5	1.3	4.22
22	658.09	1.4	9.21	375.13	2	7.50
24	444.89	2.6	11.574	232.9	2.8	6.52
26	706.41	4.2	29.67	232.79	3.6	8.38
28	897.28	1	8.97	245.11	3.5	8.58
30	444.89	2.6	11.57	232.9	2.8	6.52
32	334.61	0.5	1.67	231.14	2.1	4.85
34	702.38	0.7	4.92	95.83	6.8	6.52
36	1067.02	0.5	5.34	1158.33	3.2	37.07
38	915.95	2.4	21.98	170.08	3.2	5.44
40	633.45	1.7	10.77	414.72	1.5	6.22
42	108.75	1.3	1.41	1333.76	1.6	21.34
44	448.26	2.2	9.86	372.99	2.4	8.95
46	426.19	4.6	19.60	80.1	5.7	4.57
48	125.46	2.1	2.63	175.57	3.9	6.85
50	264.34	7.5	19.82	108.67	4.5	4.89
52	272.93	4.4	12.00	162.53	0.7	1.13
54	1501.65	4.3	64.57	131.27	2.2	2.89
56	854.51	0.1	0.85	995.6	1.3	12.94
58	1458.84	6.2	90.45	332.53	1.6	5.32
60	573.46	3.8	21.79	247.93	3	7.4379
62	389.46	3.1	12.07	166.94	7.6	12.69
64	138.88	3.7	5.14	1329.1	1.5	19.93
66	438.42	2.1	9.21	898.62	1.8	16.17
68	238.83	1	2.39	575.48	0.7	4.03

70	208.54	2.7	5.63	664.15	1.9	12.61
72	1077.04	0.8	8.62	255.54	2.8	7.15
74	910.16	1.6	14.56	393.4	1.5	5.90
76	2148.31	1.2	25.78	539.58	0.4	2.16
78	269.56	5.4	14.56	277.69	3.7	10.27
80	260.9	4.2	10.96	120.37	0.9	1.08
82	294.95	1.9	5.60	234.03	1.7	3.98
84	862.12	0.5	4.31	1723.5	2.2	37.92
86	916.89	0.2	1.83	341.36	0.7	2.39
88	921.81	3.1	28.58	764.37	1.4	10.70
90	400.07	0.8	3.20	940.86	1.8	16.93
92	712.18	4	28.49	522.12	2.4	12.53
94	549.73	2.4	13.19	575.01	1.7	9.78
96	2575.92	0.2	5.15	202.66	4.7	9.52
98	644.84	1.6	10.32	166.21	5	8.31
100	291.58	6.5	18.95	287.56	3.6	10.35
102	350.36	2.6	9.11	2878.38	1.1	31.66
104	346.24	2.6	9.00	387.77	3.3	12.79
106	416.77	1.5	6.25	1424.69	1.2	17.09
108	506.68	4	20.27	789.88	1.4	11.06
110	357.16	2.6	9.29	379.7	1.7	6.45
112	1936.07	4.2	81.31	596.67	2	11.93
114	632.59	1.2	7.59	919.49	1.4	12.87
116	674.78	1.3	8.77	770.41	2.3	17.72
118	699.89	2.3	16.098	220.97	1.6	3.53
120	410.72	2.4	9.86	319.64	2.7	8.63
122	393.29	2.3	9.04	603.24	1.9	11.46
124	257.18	3.5	9.00	1207.5	1	12.08
126	402.24	1.2	4.87	636.71	2.8	17.83
128	405.84	1.9	7.711	837.47	1.9	15.91
130	236.2	1.9	4.49	865.9	0.9	7.793
132	526.74	4.9	25.81	609.33	1	6.09
134	1583.18	7	110.82	283.27	1.3	3.68
136	647.1	2.4	15.53	1167.57	0.8	9.34
138	617.49	1.2	7.41	208.48	2.3	4.80
140	646.25	1.2	7.76	65.96	4.7	3.10
142	615.08	0.8	4.92	1002.18	1.3	13.03
144	639.99	1.7	10.88	1371.62	0.8	10.97
146	412.5	3.4	14.03	1828.55	2.8	51.20
148	307.2	4.8	14.75	773.02	1.8	13.91
150	255.91	2.9	7.42	978.54	2.8	27.40
152	787.42	1.9	14.96	158.68	1.7	2.70
154	727.35	3.2	23.28	1181.52	2	23.63
158	1830.6	3.4	62.24	1163.53	3.3	38.40
160	616.67	1.6	9.87	745.85	0.6	4.48
162	656.11	1.6	10.50	111.29	9.1	10.13
164	295.74	2.6	7.69	1103.26	1.6	

166	439.85	3.2	14.07	485.32	1.1	5.33
168	278.81	2.3	6.41	1010.79	3.1	31.33
170	483.97	2.2	10.65	594.94	1.4	8.33
172	306.47	4.8	14.71	657.86	1.6	10.53
174	1120.87	1.1	12.33	311.45	1.9	5.92
176	865.03	1.5	12.97	915.48	4	36.62
178	3758.09	1	37.58	1278.07	2.1	26.84
180	679.15	4.4	29.88	292.74	0.7	2.049
182	498.42	3.9	19.44	2116.25	1.4	29.63
184	359.66	2.6	12.96	485.97	3.2	15.55
186	538.65	3.1	11.15	524.82	0.5	2.62
188	673.89	0.3	2.02	812.71	2.1	17.07
190	226.06	0.7	1.58	886.38	2.7	23.93
192	502.61	0.4	2.01	156.15	6.7	10.46
194	629.99	2.8	17.64	1083.2	2.5	27.08
196	1824.83	2.9	52.92	363.21	2.7	9.81
198	348.75	2.3	8.02	647	1.2	7.764
200	306.19	0.8	2.45	238.7	3.7	8.83
202	515.72	2.7	13.92	1729.15	1.1	19.02
204	403.4	3	12.10	1181.35	0.7	8.27
206	371.91	6.4	23.80	501.74	0.7	3.51
208	126.97	4.1	5.21	299.14	0.7	2.09
210	383.06	3.3	12.64	454.67	1.6	7.27
212	436.4	2.3	10.04	26.2	2.8	0.73
214	691.32	0.8	5.53	1020.15	3.5	35.71
216	838.94	3.2	26.85	187.35	1.6	2.99
218	461.37	5.6	25.84	843.57	1.3	10.97
220	1240.76	0.6	7.44	148.58	1	1.49
222	779.92	0.7	5.46	2516.5	1.5	37.74
224	340.38	3.4	11.58	2844.1	0.6	17.06
226	463.91	0.4	1.86	577.82	2.3	13.28
228	230.72	3.8	8.77	601.61	1.4	8.42
230	353.55	2.2	7.78	190.45	2.4	4.57
232	629.83	1.5	9.44	359.09	2.4	8.62
234	349.94	1.7	5.949	821.25	0.6	4.93
236	577.88	3.1	17.91	628.2	2.9	2.9
238	101.27	8.1	8.20	351.26	1.9	6.67
240	242.01	8.2	19.84	266.3	3.1	8.26
242	517.2	0.7	3.62	256.32	3.2	8.20
244	592.32	1.8	10.66	644.42	1.4	9.02
246	926.16	1.7	15.74	420.39	1.5	6.31
248	526.71	4	21.07	386.85	0.9	3.48
250	1157.18	1.1	12.73	636.92	0.8	5.10
252	452.48	1	4.52	803.26	1.2	9.64
254	406.19	0.5	2.03	2024.09	0.6	12.14
256	386.19	3.4	13.13	326.11	0.6	1.96
258	197.99	4.8	9.50	330.65	2	6.61

260	197.99	4.8	9.50	330.65	2	6.61
262	536.28	1.9	10.19	336.78	1.6	5.39
264	283.57	7.6	21.55	714.42	0.9	6.44
266	697.25	2.5	17.43	314.58	2.8	8.81
268	529.18	1.6	8.467	743.21	4.3	31.96
270	1562.13	4.4	68.73	516.12	2	10.32
272	342.37	3.5	11.98	447.46	3.8	17.00
274	413.17	4.6	19.00	3611.5	0.8	28.89
276	539.84	0.4	2.16	290.32	0.9	2.61
278	164.48	1.4	2.30	308.74	4.3	13.27
280	246.74	2.7	6.66	321.15	1.6	5.14
282	530.04	3.8	20.14	264.47	2	5.29
284	385.1	2.2	8.47	741.34	1.4	10.38
286	727.8	5	36.39	90.05	4.5	4.05
288	491.76	5.4	26.56	791.62	4.6	36.41
290	1522.47	3.8	57.85	550.98	0.8	4.41
292	468.42	0.8	3.75	570.18	1.3	7.41
294	271.04	8.3	22.50	209.73	6.3	13.21
296	110.48	1.9	2.10	353.28	1.2	4.24
298	743.31	1.1	8.18	404.98	0.8	3.24
300	297.26	1	2.97	338.28	1.1	3.72
302	262.38	4.2	11.026	880.76	2.4	21.14
304	324.01	4.5	14.58	265.06	2.2	5.83
306	122.92	9.4	11.55	148.72	0.7	1.04
308	531.39	1.2	6.38	333.77	3.1	10.35
310	655.55	3.4	22.29	368.63	2.1	7.74
312	503.38	3.4	17.11	350.87	2	7.02
314	635.34	1.9	12.07	94.55	2	1.89
316	560.25	1.8	10.08	1295.42	2	25.91
318	320.91	6	19.25	200.78	1.6	3.21
320	493.23	2.7	13.32	333.8	3.4	11.35
322	335.32	3.5	11.74	177.69	0.5	0.89
324	525.2	2.6	13.66	867.23	2	17.34
326	196.99	2.7	5.319	659.18	1.6	10.55
328	307.45	5.1	15.68	486.04	2.5	12.15
330	924.54	1.7	15.72	312.6	1.7	5.31
332	1798.92	6	107.93	921.82	2.4	22.12
334	1663.26	5.2	86.49	959.89	2	19.20
336	1070.75	1.9	20.34	242.03	4	9.68
338	653.82	2.2	14.38	179.22	3.7	6.63
340	1859.82	1.6	29.76	712.74	3.1	22.09
342	376.98	1.6	6.03	854.51	1.9	16.24
344	439.38	3	13.18	395.27	2.6	10.28
346	424.3	2.7	11.46	557.71	3.9	21.75
348	380.26	2.5	9.51	623.16	1.1	6.85
350	360.74	1.5	5.41	295.78	1.6	4.73
352	403.46	0.8	3.23	243.07	3.9	9.48

354	375.28	2.6	9.76	738.76	1.6	11.82
356	691.2	2.4	16.59	192.8	1.6	3.08
358	516.5	0.8	4.13	586.44	1.8	10.56
360	1684.62	1.9	32.01	445.05	1.7	7.56
362	176.46	3	5.29	651	1.1	7.161
364	322.82	2.2	7.10	174.82	2.3	4.02
366	200.38	2.1	4.21	396.43	1.1	4.36
368	544.88	2.2	11.99	307.72	1	3.08
370	526.77	5.3	27.92	482.35	4.1	19.78
372	548.36	2.1	11.51	440.38	2	8.81
374	728.15	1.8	13.11	549.12	1.5	8.24
376	467.56	2.9	13.56	171.7	0.4	0.69
378	281.88	2.7	7.61	456.82	0.4	1.83
380	2196.94	2.2	48.33	861.27	3	25.84
382	241.43	2.6	6.28	829.39	1.4	11.61
384	281.22	5.2	14.62	337.96	1.5	5.07
386	120.21	3.4	4.09	648.64	1.2	7.78
388	660.91	1.6	10.57	318.04	0.6	1.91
390	561.6	2	11.23	359.35	2.9	10.42
392	371.43	1.2	4.46	534.18	0.7	3.74
394	520.95	3.1	16.15	655.64	1.1	7.21
396	253.41	4.3	10.90	132.9	3.1	4.12
398	507.78	4.4	22.34	169.43	2.2	3.73
400	533.28	4	21.33	346.04	1.6	5.54

Table 3.19: Concentration levels of exchangeable bases in soil samples obtained from the study area

Sample code	Na $cmol_c kg^{-1}$	K $cmol_c kg^{-1}$	Ca $cmol_c kg^{-1}$	Mg $cmol_c kg^{-1}$	Sample code	Na $cmol_c kg^{-1}$	K $cmol_c kg^{-1}$	Ca $cmol_c kg^{-1}$	Mg $cmol_c kg^{-1}$
A1-1	1.1	2.9	9.7	12.3	C1-1	0.3	0.9	2.4	2.1
A1-2	0.4	1.1	7.9	11.7	C1-2	0.2	0.6	2.1	2.0
A1-3	0.9	2.7	9.4	12.1	C1-3	0.2	0.6	2.0	2.3
A1-4	1.0	2.6	9.8	11.7	C1-4	0.2	0.5	1.9	2.0
A1-5	0.4	0.9	7.8	10.9	C1-5	0.3	0.7	2.1	2.3
A1-6	0.4	0.8	7.1	9.9	C1-6	0.2	0.8	2.8	2.3
A1-7	0.3	0.9	6.6	10.0	C1-7	0.2	0.5	2.1	2.8
A1-8	0.4	0.9	6.7	9.9	C1-8	0.3	0.9	2.5	2.1
A1-9	0.3	0.9	6.6	8.9	C1-9	0.3	0.8	2.4	2.0
A1-10	0.4	0.8	6.5	8.8	C1-10	0.2	0.3	2.1	1.9
B1-1	0.2	0.5	4.8	6.9	D1-1	0.2	0.5	2.8	2.4
B1-2	0.2	0.4	4.6	5.8	D1-2	0.1	0.3	0.4	0.5
B1-3	0.2	0.6	4.8	7.1	D1-3	0.1	0.2	3.4	2.5
B1-4	0.2	0.3	3.8	5.6	D1-4	0.1	0.3	0.9	1.5

B1-5	0.2	0.9	4.6	8.1	D1-5	0.3	0.2	0.8	1.4
B1-6	0.2	0.4	6.6	7.3	D1-6	0.2	0.3	0.7	1.5
B1-7	0.2	0.4	6.7	7.4	D1-7	0.2	0.5	2.8	4.4
B1-8	0.2	0.3	3.9	5.7	D1-8	0.3	0.4	3.9	6.7
B1-9	0.3	0.9	6.5	8.4	D1-9	0.2	0.4	3.8	4.4
B1-10	0.3	1.0	6.2	8.6	D1-10	0.2	0.5	2.7	2.3
A2-1	0.2	0.8	4.6	8.1	C2-1	0.1	0.3	0.8	1.7
A2-2	0.3	0.5	4.8	4.4	C2-2	0.1	0.3	0.7	0.5
A2-3	0.2	0.3	3.7	5.6	C2-3	0.1	0.3	0.3	0.7
A3-4	0.3	1.0	6.3	8.5	C2-4	0.1	0.3	0.7	0.3
A2-5	0.3	0.5	4.7	4.1	C2-5	0.1	0.2	0.3	0.3
A2-6	0.3	0.6	4.8	4.2	C2-6	0.1	0.3	0.9	0.4
A2-7	0.2	0.7	4.9	4.4	C2-7	0.1	0.3	1.1	0.7
A2-8	0.3	0.5	5.1	4.6	C2-8	0.1	0.3	0.9	1.2
A2-9	0.2	0.4	4.1	3.9	C2-9	0.1	0.2	1.1	1.4
A2-10	0.3	0.5	3.8	4.5	C2-10	0.1	0.2	0.3	0.5
B2-1	0.2	0.5	3.6	6.1	D2-1	0.1	0.2	0.3	0.4
B2-2	0.2	0.3	2.1	3.9	D2-2	0.2	0.3	2.0	3.7
B2-3	0.1	0.3	2.1	4.1	D2-3	0.1	0.3	1.1	3.1
B2-4	0.2	0.4	2.2	4.3	D2-4	0.1	0.3	2.2	4.1
B2-5	0.2	0.4	2.2	4.6	D2-5	0.2	0.4	2.1	4.3
B2-6	0.2	0.4	2.3	4.6	D2-6	0.2	0.3	2.2	4.6
B2-7	0.3	0.6	2.5	4.7	D2-7	0.2	0.3	2.1	3.7
B2-8	0.1	0.3	2.1	4.3	D2-8	0.2	0.3	1.9	3.5
B29	0.2	0.3	1.9	4.5	D2-9	0.2	0.5	3.2	6.6
B2-10	0.3	0.5	2.2	5.1	D2-10	0.2	0.3	2.2	4.5
A3-1	0.1	0.3	2.3	4.5	C3-1	0.2	0.4	3.8	4.3
A3-2	0.2	0.3	1.9	4.1	C3-2	0.1	0.3	0.9	1.3
A3-3	0.1	0.3	3.3	4.5	C3-3	0.1	0.3	0.7	1.1
A3-4	0.1	0.2	3.3	4.9	C3-4	0.1	0.2	0.9	0.5
A3-5	0.1	0.2	3.1	4.6	C3-5	0.1	0.2	3.1	3.9
A3-6	0.1	0.2	3.2	5.2	C3-6	0.1	0.2	3.3	4.3
A3-7	0.2	0.3	1.8	3.5	C3-7	0.2	0.3	1.7	3.4
A3-8	0.1	0.2	3.1	4.1	C3-8	0.1	0.3	0.9	1.3
A3-9	0.2	0.3	1.7	3.7	C3-9	0.1	0.3	0.7	0.9
A3-10	0.1	0.2	3.2	5.3	C3-10	0.1	0.4	0.9	1.9
B3-1	0.2	0.4	2.8	3.3	D3-1	0.2	0.3	3.7	2.3
B3-2	0.1	0.2	3.7	5.3	D3-2	0.1	0.3	1.1	1.3
B3-3	0.1	0.3	1.1	3.1	D3-3	0.1	0.3	0.8	0.9
B3-4	0.2	0.3	1.5	3.6	D3-4	0.1	0.3	0.6	0.7
B3-5	0.2	0.3	1.6	3.9	D3-5	0.2	0.4	1.1	1.7
B3-6	0.1	0.2	3.3	5.3	D3-6	0.1	0.3	0.8	0.6
B3-7	0.2	0.5	3.2	6.7	D3-7	0.1	0.2	3.1	4.6
B3-8	0.2	0.4	3.9	6.9	D3-8	0.2	0.3	4.0	7.0
B3-9	0.3	0.6	2.5	4.7	D3-9	0.1	0.3	2.2	4.1
B3-10	0.2	0.3	3.8	5.6	D3-10	0.2	0.4	3.8	4.3

A4-1	0.3	1.0	6.3	8.7	C4-1	0.1	0.4	0.8	1.9
A4-2	0.2	0.9	4.5	8.3	C4-2	0.1	0.3	0.5	0.7
A4-3	0.2	0.5	3.6	5.9	C4-3	0.1	0.3	3.1	4.3
A4-4	0.3	0.6	2.7	4.7	C4-4	0.2	0.4	1.1	1.6
A4-5	0.2	0.4	2.8	2.3	C4-5	0.1	0.2	3.3	2.6
A4-6	0.2	0.3	2.4	2.5	C4-6	0.1	0.3	0.7	0.6
A4-7	0.2	0.3	2.1	1.8	C4-7	0.1	0.2	0.6	0.7
A4-8	0.2	0.4	1.8	2.9	C4-8	0.1	0.3	0.8	0.7
A4-9	0.1	0.3	0.9	1.5	C4-9	0.1	0.3	0.6	0.9
A4-10	0.1	0.3	0.6	1.0	C4-10	0.1	0.2	0.5	0.8
B4-1	0.2	0.3	1.9	3.3	D4-1	0.1	0.2	0.4	0.7
B4-2	0.2	0.3	1.7	2.9	D4-2	0.1	0.2	0.3	0.8
B4-3	0.2	0.4	2.7	3.8	D4-3	0.1	0.2	0.3	0.6
B4-4	0.2	0.2	2.1	2.9	D4-4	0.2	0.4	2.4	3.2
B4-5	0.2	0.3	2.6	4.1	D4-5	0.2	0.3	1.9	2.6
B4-6	0.2	0.4	2.1	4.5	D4-6	0.1	0.2	0.3	0.5
B4-7	0.2	0.3	2.1	3.7	D4-7	0.1	0.2	0.3	0.3
B4-8	0.2	0.3	2.5	4.3	D4-8	0.2	0.4	2.3	4.6
B4-9	0.3	0.4	2.8	4.6	D4-9	0.1	0.2	0.9	1.8
B4-10	0.2	0.3	1.9	2.8	D4-10	0.1	0.2	0.3	0.7
A5-1	0.2	0.3	2.2	4.1	C5-1	0.2	0.3	1.8	2.7
A5-2	0.2	0.3	2.3	4.4	C5-2	0.1	0.2	1.9	2.8
A5-3	0.2	0.3	2.7	4.6	C5-3	0.2	0.3	1.5	2.1
A5-4	0.4	0.5	3.7	5.6	C5-4	0.2	0.3	1.3	1.9
A5-5	0.3	0.4	2.8	4.3	C5-5	0.2	0.3	1.8	2.7
A5-6	0.2	0.4	2.0	4.4	C5-6	0.2	0.3	1.9	2.7
A5-7	0.2	0.3	2.9	4.8	C5-7	0.2	0.3	1.4	1.9
A5-8	0.2	0.3	2.7	4.5	C5-8	0.2	0.3	1.7	2.0
A5-9	0.2	0.3	2.3	4.3	C5-9	0.2	0.3	1.9	2.0
A5-10	0.3	0.4	2.8	4.1	C5-10	0.2	0.3	1.6	2.0
B5-1	0.2	0.3	1.9	2.9	D5-1	0.2	0.4	1.1	1.7
B5-2	0.2	0.3	1.4	1.9	D5-2	0.2	0.3	1.8	2.8
B5-3	0.3	0.3	1.8	2.9	D5-3	0.2	0.3	1.6	1.9
B5-4	0.2	0.3	1.5	2.0	D5-4	0.1	0.2	0.9	1.8
B5-5	0.2	0.4	2.4	3.3	D5-5	0.1	0.3	0.9	1.9
B5-6	0.1	0.2	1.1	1.8	D5-6	0.2	0.4	2.5	3.4
B5-7	0.2	0.4	1.3	1.7	D5-7	0.2	0.3	0.8	1.0
B5-8	0.1	0.2	0.3	0.4	D5-8	0.1	0.1	0.3	0.3
B5-9	0.1	0.2	1.0	1.8	D5-9	0.1	0.3	0.8	1.8
B5-10	0.1	0.3	0.9	1.7	D5-10	0.2	0.3	2.8	4.1
A6-1	0.2	0.3	2.2	4.2	C6-1	0.2	0.3	2.0	2.9
A6-2	0.2	0.3	2.0	2.6	C6-2	0.2	0.3	1.9	2.3
A6-3	0.1	0.2	0.9	1.7	C6-3	0.1	0.2	0.8	1.7
A6-4	0.2	0.3	0.7	1.2	C6-4	0.1	0.2	0.9	0.8
A6-5	0.2	0.4	2.3	3.2	C6-5	0.2	0.3	1.9	2.7
A6-6	0.2	0.3	0.7	1.0	C6-6	0.2	0.3	2.1	2.6

A6-7	0.2	0.3	1.5	1.9	C6-7	0.2	0.3	1.1	1.8
A6-8	0.1	0.2	0.8	1.4	C6-8	0.1	0.2	0.5	0.7
A6-9	0.2	0.3	0.8	1.1	C6-9	0.2	0.2	0.5	0.6
A6-10	0.2	0.3	1.3	1.5	C6-10	0.1	0.2	0.5	0.8
B6-1	0.2	0.3	2.2	4.3	D6-1	0.1	0.2	0.5	0.7
B6-2	0.3	0.4	2.8	4.2	D6-2	0.3	0.3	1.9	2.7
B6-3	0.2	0.4	2.1	4.4	D6-3	0.2	0.3	2.4	4.3
B6-4	0.2	0.3	2.4	4.3	D6-4	0.2	0.3	2.5	4.4
B6-5	0.4	0.9	6.7	9.8	D6-5	0.2	0.3	1.9	2.8
B6-6	0.5	0.9	6.8	9.9	D6-6	0.4	0.5	3.9	5.7
B6-7	0.6	0.8	7.7	9.7	D6-7	0.2	0.3	2.6	4.3
B6-8	0.6	0.7	7.9	9.8	D6-8	0.3	0.5	3.2	6.7
B6-9	0.5	0.8	6.9	9.9	D6-9	0.3	0.5	3.9	6.2
B6-10	0.4	0.7	6.7	9.6	D6-10	0.5	0.8	7.1	9.9
A7-1	0.2	0.3	2.1	2.6	C7-1	0.2	0.3	2.6	4.3
A7-2	0.2	0.3	2.5	4.3	C7-2	0.2	0.3	2.3	4.1
A7-3	0.2	0.4	2.9	4.4	C7-3	0.5	0.9	6.7	9.9
A7-4	0.2	0.3	2.1	2.5	C7-4	0.3	0.5	3.8	6.7
A7-5	0.3	0.5	3.9	6.3	C7-5	0.2	0.3	2.8	4.3
A7-6	0.2	0.3	2.3	2.4	C7-6	0.3	0.5	3.9	6.3
A7-7	0.3	0.5	3.9	5.9	C7-7	0.3	0.4	3.7	5.8
A7-8	0.2	0.3	2.9	4.3	C7-8	0.3	0.5	2.9	4.3
A7-9	0.2	0.4	2.4	4.4	C7-9	0.2	0.3	2.9	4.0
A7-10	0.2	0.3	2.9	4.3	C7-10	0.2	0.3	2.8	4.3
B7-1	0.2	0.3	3.2	4.5	D7-1	0.2	0.4	2.7	4.3
B7-2	0.3	0.5	2.9	4.8	D7-2	0.2	0.4	2.9	4.1
B7-3	0.2	0.3	2.1	2.8	D7-3	0.2	0.3	1.9	2.8
B7-4	0.3	0.4	2.7	4.8	D7-4	0.3	0.5	3.9	6.6
B7-5	0.3	0.4	2.7	4.5	D7-5	0.3	0.4	2.8	4.3
B7-6	0.2	0.3	2.2	2.8	D7-6	0.3	0.4	2.9	3.3
B7-7	0.4	0.7	6.7	9.7	D7-7	0.3	0.4	2.7	4.8
B7-8	0.4	0.7	6.9	9.8	D7-8	0.3	0.5	3.9	6.7
B7-9	0.4	0.6	6.7	9.6	D7-9	0.5	0.8	7.7	8.7
B7-10	0.3	0.5	3.8	6.7	D7-10	0.5	0.6	7.6	8.5
A8-1	0.2	0.4	2.4	4.3	C8-1	0.2	0.3	2.9	4.3
A8-2	0.2	0.4	2.5	4.4	C8-2	0.2	0.4	2.3	4.1
A8-3	0.3	0.4	2.7	4.7	C8-3	0.2	0.3	2.8	4.2
A8-4	0.2	0.3	2.1	2.6	C8-4	0.3	0.4	2.9	4.7
A8-5	0.2	0.4	2.3	4.3	C8-5	0.3	0.4	2.9	4.6
A8-6	0.3	0.4	3.1	4.7	C8-6	0.3	0.4	2.8	4.5
A8-7	0.2	0.3	1.2	1.8	C8-7	0.2	0.3	1.4	1.9
A8-8	0.1	0.2	0.5	0.8	C8-8	0.4	0.6	6.8	9.7
A8-9	0.2	0.3	1.4	1.8	C8-9	0.4	0.6	6.6	9.9
A8-10	0.2	0.3	2.5	4.3	C8-10	0.4	0.7	6.9	9.7
B8-1	0.2	0.3	2.8	4.9	D8-1	0.4	0.6	6.7	9.8
B8-2	0.4	0.6	6.7	9.5	D8-2	0.5	0.8	6.8	9.8

B8-3	0.2	0.4	2.3	4.0	D8-3	0.2	0.3	2.9	4.1
B8-4	0.2	0.3	2.5	4.3	D8-4	0.2	0.4	3.5	4.4
B8-5	0.2	0.3	2.9	4.7	D8-5	0.2	0.4	2.4	4.2
B8-6	0.4	0.7	6.8	9.8	D8-6	0.3	0.5	2.6	4.3
B8-7	0.5	0.8	6.8	9.9	D8-7	0.2	0.3	2.9	4.2
B8-8	0.3	0.5	3.9	6.7	D8-8	0.4	0.7	6.9	9.8
B8-9	0.2	0.3	2.9	4.9	D8-9	0.5	0.8	6.7	9.9
B8-10	0.2	0.4	3.7	4.4	D8-10	0.5	0.7	6.8	8.9
A9-1	0.4	0.7	6.1	9.7	C9-1	0.2	0.3	2.3	2.4
A9-2	0.2	0.4	3.7	4.1	C9-2	0.1	0.2	0.3	0.4
A9-3	0.2	0.4	2.8	4.4	C9-3	0.1	0.4	0.6	0.7
A9-4	0.2	0.3	2.9	4.8	C9-4	0.2	0.3	1.5	1.9
A9-5	0.2	0.3	2.9	4.3	C9-5	0.2	0.3	1.1	1.8
A9-6	0.5	0.6	6.7	8.9	C9-6	0.3	0.5	3.8	6.8
A9-7	0.2	0.4	2.5	4.3	C9-7	0.4	0.6	6.8	9.5
A9-8	0.2	0.4	3.7	4.2	C9-8	0.2	0.3	2.9	4.3
A9-9	0.5	0.8	6.8	9.7	C9-9	0.2	0.3	3.2	4.4
A9-10	0.2	0.3	2.9	4.3	C9-10	0.2	0.3	2.8	4.3
B9-1	0.5	0.8	6.9	9.7	D9-1	0.2	0.3	3.3	4.7
B9-2	0.4	0.7	6.8	9.5	D9-2	0.2	0.3	3.6	4.7
B9-3	0.3	0.5	3.8	6.7	D9-3	0.2	0.3	2.9	4.4
B9-4	0.1	0.4	0.5	0.7	D9-4	0.2	0.3	3.1	4.4
B9-5	0.2	0.3	3.6	4.7	D9-5	0.2	0.3	3.4	4.9
B9-6	0.2	0.3	3.7	4.2	D9-6	0.2	0.3	3.5	4.2
B9-7	0.2	0.3	2.8	4.4	D9-7	0.2	0.4	3.1	4.7
B9-8	0.2	0.3	3.7	4.6	D9-8	0.2	0.3	2.7	4.4
B9-9	0.2	0.3	1.7	1.9	D9-9	0.2	0.3	3.6	4.6
B9-10	0.2	0.3	2.9	4.2	D9-10	0.5	0.8	7.1	9.7
A10-1	0.2	0.3	1.7	1.8	C10-1	0.2	0.4	3.7	4.4
A10-2	0.2	0.3	1.5	2.1	C10-2	0.2	0.3	3.4	5.1
A10-3	0.1	0.4	0.6	0.6	C10-3	0.2	0.3	2.9	4.4
A10-4	0.2	0.3	3.5	4.2	C10-4	0.5	0.7	6.8	8.8
A10-5	0.1	0.2	0.5	0.8	C10-5	0.2	0.3	3.4	4.2
A10-6	0.1	0.2	0.3	0.3	C10-6	0.2	0.3	3.1	4.6
A10-7	0.1	0.2	0.3	0.4	C10-7	0.3	0.5	3.8	6.7
A10-8	0.2	0.3	3.6	4.8	C10-8	0.2	0.4	3.7	4.6
A10-9	0.1	0.3	0.9	1.1	C10-9	0.3	0.5	3.6	6.6
A10-10	0.2	0.3	3.5	3.9	C10-10	0.3	0.5	3.7	6.6
B10-1	0.3	0.4	3.1	4.2	D10-1	0.3	0.5	3.7	6.7
B10-2	0.3	0.3	2.9	4.2	D10-2	0.1	0.2	0.5	0.8
B10-3	0.1	0.3	0.9	1.0	D10-3	0.1	0.2	0.5	0.9
B10-4	0.2	0.3	1.5	2.1	D10-4	0.3	0.3	3.0	4.2
B10-5	0.2	0.3	3.5	4.1	D10-5	0.2	0.3	1.5	2.2
B10-6	0.2	0.3	2.9	4.2	D10-6	0.1	0.3	0.9	1.9
B10-7	0.2	0.3	3.4	4.1	D10-7	0.2	0.3	3.5	3.9
B10-8	0.3	0.3	3.3	4.0	D10-8	0.2	0.3	1.5	1.9

B10-9	0.2	0.3	1.5	2.2	D10-9	0.2	0.3	2.9	4.4
B10-10	0.1	0.3	1.1	1.4	D10-10	0.1	0.2	0.4	0.6

Table 3.21: Cation exchange capacity of soil samples from the study area

Sample code	X	Y	CEC (meq^{-100g})	Sample code	X	Y	CEC (meq^{-100g})
A1-1	329023.25	7234057	29.2	C1-1	7234057	7234057	7.3
A1-2	329023.25	7234157	28.5	C1-2	328023.3	7234157	6.4
A1-3	329023.25	7234257	29.1	C1-3	328023.3	7234257	5.9
A1-4	329023.25	7234357	28.1	C1-4	328023.3	7234357	6.7
A1-5	329023.25	7234457	26.7	C1-5	328023.3	7234457	7.2
A1-6	329023.25	7234557	23.1	C1-6	328023.3	7234557	8.9
A1-7	329023.25	7234657	20.0	C1-7	328023.3	7234657	6.6
A1-8	329023.25	7234757	20.9	C1-8	328023.3	7234757	7.4
A1-9	329023.25	7234857	18.2	C1-9	328023.3	7234857	7.6
A1-10	329023.25	7234957	18.0	C1-10	328023.3	7234957	6.9
B1-1	329023.25	7235057	16.1	D1-1	328023.3	7235057	9.4
B1-2	329023.25	7235157	14.7	D1-2	328023.3	7235157	1.3
B1-3	329023.25	7235257	17.3	D1-3	328023.3	7235257	5.3
B1-4	329023.25	7235357	14.6	D1-4	328023.3	7235357	2.8
B1-5	329023.25	7235457	15.5	D1-5	328023.3	7235457	3.6
B1-6	329023.25	7235557	16.6	D1-6	328023.3	7235557	4.4
B1-7	329023.25	7235657	16.2	D1-7	328023.3	7235657	10.7
B1-8	329023.25	7235757	14.5	D1-8	328023.3	7235757	12.6
B1-9	329023.25	7235857	18.6	D1-9	328023.3	7235857	10.5
B1-10	329023.25	7235957	17.7	D1-10	328023.3	7235957	8.9
A2-1	328923.25	7234057	15.3	C2-1	327923.3	7234057	3.3
A2-2	328923.25	7234157	10.0	C2-2	327923.3	7234157	2.4
A2-3	328923.25	7234257	14.2	C2-3	327923.3	7234257	1.5
A3-4	328923.25	7234357	17.3	C2-4	327923.3	7234357	2.6
A2-5	328923.25	7234457	11.4	C2-5	327923.3	7234457	1.4
A2-6	328923.25	7234557	12.6	C2-6	327923.3	7234557	2.3
A2-7	328923.25	7234657	13.3	C2-7	327923.3	7234657	3.5
A2-8	328923.25	7234757	14.5	C2-8	327923.3	7234757	4.6
A2-9	328923.25	7234857	10.8	C2-9	327923.3	7234857	5.5
A2-10	328923.25	7234957	15.6	C2-10	327923.3	7234957	1.3
B2-1	328923.25	7235057	16.6	D2-1	327923.3	7235057	13.0
B2-2	328923.25	7235157	10.3	D2-2	327923.3	7235157	10.2
B2-3	328923.25	7235257	11.4	D2-3	327923.3	7235257	9.4
B2-4	328923.25	7235357	12.2	D2-4	327923.3	7235357	11.1
B2-5	328923.25	7235457	13.7	D2-5	327923.3	7235457	12.7
B2-6	328923.25	7235557	14.2	D2-6	327923.3	7235557	15.1
B2-7	328923.25	7235657	15.5	D2-7	327923.3	7235657	10.6

B2-8	328923.25	7235757	11.5	D2-8	327923.3	7235757	10.1
B29	328923.25	7235857	13.1	D2-9	327923.3	7235857	16.4
B2-10	328923.25	7235957	14.7	D2-10	327923.3	7235957	13.6
A3-1	328823.25	7234057	11.4	C3-1	327823.3	7234057	7.1
A3-2	328823.25	7234157	13.6	C3-2	327823.3	7234157	4.7
A3-3	328823.25	7234257	11.0	C3-3	327823.3	7234257	3.1
A3-4	328823.25	7234357	11.3	C3-4	327823.3	7234357	2.1
A3-5	328823.25	7234457	11.7	C3-5	327823.3	7234457	10.3
A3-6	328823.25	7234557	12.4	C3-6	327823.3	7234557	10.9
A3-7	328823.25	7234657	10.5	C3-7	327823.3	7234657	9.9
A3-8	328823.25	7234757	11.1	C3-8	327823.3	7234757	4.3
A3-9	328823.25	7234857	10.7	C3-9	327823.3	7234857	3.6
A3-10	328823.25	7234957	12.3	C3-10	327823.3	7234957	5.7
B3-1	328823.25	7235057	7.6	D3-1	327823.3	7235057	7.1
B3-2	328823.25	7235157	12.9	D3-2	327823.3	7235157	4.7
B3-3	328823.25	7235257	9.5	D3-3	327823.3	7235257	3.1
B3-4	328823.25	7235357	10.8	D3-4	327823.3	7235357	2.1
B3-5	328823.25	7235457	11.6	D3-5	327823.3	7235457	4.3
B3-6	328823.25	7235557	12.4	D3-6	327823.3	7235557	2.0
B3-7	328823.25	7235657	16.7	D3-7	327823.3	7235657	11.5
B3-8	328823.25	7235757	15.8	D3-8	327823.3	7235757	15.6
B3-9	328823.25	7235857	13.8	D3-9	327823.3	7235857	11.2
B3-10	328823.25	7235957	14.2	D3-10	327823.3	7235957	7.2
A4-1	328723.25	7234057	17.9	C4-1	327723.3	7234057	5.5
A4-2	328723.25	7234157	15.1	C4-2	327723.3	7234157	2.6
A4-3	328723.25	7234257	16.3	C4-3	327723.3	7234257	11.6
A4-4	328723.25	7234357	15.5	C4-4	327723.3	7234357	4.8
A4-5	328723.25	7234457	8.6	C4-5	327723.3	7234457	5.4
A4-6	328723.25	7234557	7.9	C4-6	327723.3	7234557	2.3
A4-7	328723.25	7234657	6.7	C4-7	327723.3	7234657	2.4
A4-8	328723.25	7234757	8.8	C4-8	327723.3	7234757	2.7
A4-9	328723.25	7234857	4.6	C4-9	327723.3	7234857	2.9
A4-10	328723.25	7234957	3.8	C4-10	327723.3	7234957	2.1
B4-1	328723.25	7235057	9.6	D4-1	327723.3	7235057	2.5
B4-2	328723.25	7235157	8.9	D4-2	327723.3	7235157	3.1
B4-3	328723.25	7235257	7.6	D4-3	327723.3	7235257	1.6
B4-4	328723.25	7235357	6.9	D4-4	327723.3	7235357	7.6
B4-5	328723.25	7235457	10.1	D4-5	327723.3	7235457	6.6
B4-6	328723.25	7235557	12.4	D4-6	327723.3	7235557	1.8
B4-7	328723.25	7235657	9.8	D4-7	327723.3	7235657	1.2
B4-8	328723.25	7235757	10.5	D4-8	327723.3	7235757	12.8
B4-9	328723.25	7235857	11.8	D4-9	327723.3	7235857	5.2
B4-10	328723.25	7235957	8.9	D4-10	327723.3	7235957	2.0
A5-1	328623.25	7234057	10.2	C5-1	327623.3	7234057	8.3
A5-2	328623.25	7234157	13.6	C5-2	327623.3	7234157	9.0
A5-3	328623.25	7234257	14.5	C5-3	327623.3	7234257	7.5

A5-4	328623.25	7234357	16.9	C5-4	327623.3	7234357	6.3
A5-5	328623.25	7234457	11.8	C5-5	327623.3	7234457	8.7
A5-6	328623.25	7234557	12.5	C5-6	327623.3	7234557	9.3
A5-7	328623.25	7234657	15.6	C5-7	327623.3	7234657	6.6
A5-8	328623.25	7234757	14.6	C5-8	327623.3	7234757	7.2
A5-9	328623.25	7234857	13.5	C5-9	327623.3	7234857	7.8
A5-10	328623.25	7234957	11.6	C5-10	327623.3	7234957	7.3
B5-1	328623.25	7235057	9.3	D5-1	327623.3	7235057	4.0
B5-2	328623.25	7235157	6.7	D5-2	327623.3	7235157	8.0
B5-3	328623.25	7235257	8.5	D5-3	327623.3	7235257	6.4
B5-4	328623.25	7235357	6.9	D5-4	327623.3	7235357	5.2
B5-5	328623.25	7235457	7.7	D5-5	327623.3	7235457	5.6
B5-6	328623.25	7235557	5.8	D5-6	327623.3	7235557	7.6
B5-7	328623.25	7235657	4.7	D5-7	327623.3	7235657	3.2
B5-8	328623.25	7235757	2.3	D5-8	327623.3	7235757	1.2
B5-9	328623.25	7235857	4.8	D5-9	327623.3	7235857	5.2
B5-10	328623.25	7235957	5.3	D5-10	327623.3	7235957	10.6
A6-1	328523.25	7234057	10.2	C6-1	327523.3	7234057	8.6
A6-2	328523.25	7234157	8.4	C6-2	327523.3	7234157	7.4
A6-3	328523.25	7234257	5.5	C6-3	327523.3	7234257	5.5
A6-4	328523.25	7234357	4.9	C6-4	327523.3	7234357	3.9
A6-5	328523.25	7234457	7.7	C6-5	327523.3	7234457	9.4
A6-6	328523.25	7234557	4.6	C6-6	327523.3	7234557	7.8
A6-7	328523.25	7234657	6.8	C6-7	327523.3	7234657	6.3
A6-8	328523.25	7234757	5.9	C6-8	327523.3	7234757	3.6
A6-9	328523.25	7234857	5.4	C6-9	327523.3	7234857	3.4
A6-10	328523.25	7234957	6.1	C6-10	327523.3	7234957	3.9
B6-1	328523.25	7235057	10.6	D6-1	327523.3	7235057	3.7
B6-2	328523.25	7235157	11.5	D6-2	327523.3	7235157	9.4
B6-3	328523.25	7235257	12.6	D6-3	327523.3	7235257	10.2
B6-4	328523.25	7235357	13.1	D6-4	327523.3	7235357	13.3
B6-5	328523.25	7235457	19.2	D6-5	327523.3	7235457	8.4
B6-6	328523.25	7235557	18.7	D6-6	327523.3	7235557	15.3
B6-7	328523.25	7235657	19.5	D6-7	327523.3	7235657	10.3
B6-8	328523.25	7235757	18.8	D6-8	327523.3	7235757	16.7
B6-9	328523.25	7235857	17.8	D6-9	327523.3	7235857	15.8
B6-10	328523.25	7235957	18.9	D6-10	327523.3	7235957	17,7
A7-1	328423.25	7234057	8.9	C7-1	327423.3	7234057	10.2
A7-2	328423.25	7234157	13.5	C7-2	327423.3	7234157	13.1
A7-3	328423.25	7234257	14.2	C7-3	327423.3	7234257	19.8
A7-4	328423.25	7234357	9.5	C7-4	327423.3	7234357	16.7
A7-5	328423.25	7234457	15.1	C7-5	327423.3	7234457	10.1
A7-6	328423.25	7234557	8.6	C7-6	327423.3	7234557	15.7
A7-7	328423.25	7234657	9.3	C7-7	327423.3	7234657	9.8
A7-8	328423.25	7234757	10.1	C7-8	327423.3	7234757	10.8
A7-9	328423.25	7234857	12.5	C7-9	327423.3	7234857	10.4

A7-10	328423.25	7234957	10.2	C7-10	327423.3	7234957	10.8
B7-1	328423.25	7235057	10.1	D7-1	327423.3	7235057	12.6
B7-2	328423.25	7235157	9.7	D7-2	327423.3	7235157	14.3
B7-3	328423.25	7235257	8.8	D7-3	327423.3	7235257	15.4
B7-4	328423.25	7235357	9.8	D7-4	327423.3	7235357	16.7
B7-5	328423.25	7235457	9.4	D7-5	327423.3	7235457	11.3
B7-6	328423.25	7235557	8.9	D7-6	327423.3	7235557	10.3
B7-7	328423.25	7235657	18.0	D7-7	327423.3	7235657	9.7
B7-8	328423.25	7235757	18.9	D7-8	327423.3	7235757	15.4
B7-9	328423.25	7235857	17.8	D7-9	327423.3	7235857	19.6
B7-10	328423.25	7235957	15.2	D7-10	327423.3	7235957	19.3
A8-1	328323.25	7234057	12.0	C8-1	327323.3	7234057	10.0
A8-2	328323.25	7234157	12.4	C8-2	327323.3	7234157	11.4
A8-3	328323.25	7234257	9.3	C8-3	327323.3	7234257	10.8
A8-4	328323.25	7234357	8.6	C8-4	327323.3	7234357	9.8
A8-5	328323.25	7234457	11.6	C8-5	327323.3	7234457	9.3
A8-6	328323.25	7234557	9.9	C8-6	327323.3	7234557	8.9
A8-7	328323.25	7234657	6.6	C8-7	327323.3	7234657	7.8
A8-8	328323.25	7234757	3.4	C8-8	327323.3	7234757	17.7
A8-9	328323.25	7234857	7.6	C8-9	327323.3	7234857	18.6
A8-10	328323.25	7234957	13.6	C8-10	327323.3	7234957	17.6
B8-1	328323.25	7235057	14.7	D8-1	327323.3	7235057	18.9
B8-2	328323.25	7235157	16.6	D8-2	327323.3	7235157	19.8
B8-3	328323.25	7235257	11.3	D8-3	327323.3	7235257	10.4
B8-4	328323.25	7235357	13.3	D8-4	327323.3	7235357	16.8
B8-5	328323.25	7235457	14.8	D8-5	327323.3	7235457	11.2
B8-6	328323.25	7235557	17.9	D8-6	327323.3	7235557	12.6
B8-7	328323.25	7235657	19.9	D8-7	327323.3	7235657	10.8
B8-8	328323.25	7235757	15.3	D8-8	327323.3	7235757	17.9
B8-9	328323.25	7235857	14.8	D8-9	327323.3	7235857	19.9
B8-10	328323.25	7235957	16.7	D8-10	327323.3	7235957	18.9
A9-1	328223.25	7234057	17.0	C9-1	327223.3	7234057	8.3
A9-2	328223.25	7234157	16.0	C9-2	327223.3	7234157	1.3
A9-3	328223.25	7234257	12.4	C9-3	327223.3	7234257	2.6
A9-4	328223.25	7234357	14.4	C9-4	327223.3	7234357	7.8
A9-5	328223.25	7234457	10.0	C9-5	327223.3	7234457	6.7
A9-6	328223.25	7234557	18.8	C9-6	327223.3	7234557	15.8
A9-7	328223.25	7234657	12.0	C9-7	327223.3	7234657	17.4
A9-8	328223.25	7234757	16.0	C9-8	327223.3	7234757	9.9
A9-19	328223.25	7234857	19.9	C9-9	327223.3	7234857	10.8
A9-10	328223.25	7234957	13.6	C9-10	327223.3	7234957	9.0
B9-1	328223.25	7235057	19.9	D9-1	327223.3	7235057	11.4
B9-2	328223.25	7235157	17.8	D9-2	327223.3	7235157	11.0
B9-3	328223.25	7235257	15.4	D9-3	327223.3	7235257	9.5
B9-4	328223.25	7235357	2.3	D9-4	327223.3	7235357	10.0
B9-5	328223.25	7235457	11.3	D9-5	327223.3	7235457	11.5

B9-6	328223.25	7235557	10.7	D9-6	327223.3	7235557	10.6
B9-7	328223.25	7235657	8.9	D9-7	327223.3	7235657	12.7
B9-8	328223.25	7235757	9.9	D9-8	327223.3	7235757	8.8
B9-9	328223.25	7235857	6.9	D9-9	327223.3	7235857	9.9
B9-10	328223.25	7235957	8.8	D9-10	327223.3	7235957	19.9
A10-1	328123.25	7234057	6.2	C10-1	327123.3	7234057	16.7
A10-2	328123.25	7234157	7.4	C10-2	327123.3	7234157	11.8
A10-3	328123.25	7234257	2.0	C10-3	327123.3	7234257	13.4
A10-4	328123.25	7234357	10.4	C10-4	327123.3	7234357	18.6
A10-5	328123.25	7234457	3.6	C10-5	327123.3	7234457	10.3
A10-6	328123.25	7234557	1.1	C10-6	327123.3	7234557	14.4
A10-7	328123.25	7234657	1.2	C10-7	327123.3	7234657	15.7
A10-8	328123.25	7234757	11.1	C10-8	327123.3	7234757	14.8
A10-9	328123.25	7234857	4.8	C10-9	327123.3	7234857	15.1
A10-10	328123.25	7234957	9.6	C10-10	327123.3	7234957	15.0
B10-1	328123.25	7235057	9.0	D10-1	327123.3	7235057	2.8
B10-2	328123.25	7235157	8.6	D10-2	327123.3	7235157	3.7
B10-3	328123.25	7235257	4.8	D10-3	327123.3	7235257	3.9
B10-4	328123.25	7235357	7.5	D10-4	327123.3	7235357	8.8
B10-5	328123.25	7235457	9.9	D10-5	327123.3	7235457	7.4
B10-6	328123.25	7235557	8.8	D10-6	327123.3	7235557	4.5
B10-7	328123.25	7235657	9.6	D10-7	327123.3	7235657	3.2
B10-8	328123.25	7235757	8.6	D10-8	327123.3	7235757	6.8
B10-9	328123.25	7235857	7.8	D10-9	327123.3	7235857	2.8
B10-10	328123.25	7235957	5.6	D10-10	327123.3	7235957	1.9

Table 3.23: Percent base saturation of soil samples from the study area

No	Exchangeable bases (%)	No	Exchangeable bases (%)	No	Exchangeable bases (%)	No	Exchangeable bases (%)
1	89.04	101	67.65	201	78.08	301	62.79
2	74.04	102	60.71	202	76.56	302	63.51
3	86.25	103	52.73	203	86.44	303	50.91
4	89.32	104	48.98	204	68.66	304	51.28
5	74.91	105	79.22	205	75.00	305	54.26
6	78.79	106	47.83	206	68.54	306	66.67
7	89.00	107	57.35	207	84.85	307	53.97
8	85.65	108	42.37	208	78.38	308	41.67
9	91.76	109	44.44	209	72.37	309	44.12
10	91.67	110	54.09	210	65.22	310	41.03
11	77.02	111	66.04	211	62.77	311	40.54
12	74.83	112	66.96	212	99.10	312	55.32
13	73.41	113	56.35	213	116.98	313	70.59
14	67.81	114	54.96	214	100.00	314	55.64
15	89.03	115	92.71	215	75.00	315	61.91

16	87.35	116	96.79	216	61.36	316	68.63
17	90.74	117	96.41	217	73.83	317	71.85
18	69.66	118	91.06	218	89.68	318	64.07
19	86.56	119	101.69	219	83.81	319	68.99
20	90.96	120	92.06	220	64.04	320	103.39
21	89.54	121	58.43	221	87.88	321	72.55
22	99.91	122	54.07	222	66.67	322	52.67
23	69.01	123	55.63	223	93.33	323	90.91
24	93.06	124	53.68	224	53.85	324	67.66
25	84.21	125	72.85	225	64.29	325	75.25
26	78.57	126	60.47	226	73.91	326	70.06
27	76.69	127	113.98	227	62.86	327	104.08
28	72.41	128	76.24	228	54.35	328	74.07
29	79.63	129	59.20	229	50.91	329	71.15
30	58.33	130	75.49	230	84.62	330	70.37
31	62.65	131	81.19	231	7.69	331	60.327
32	63.12	132	87.63	232	60.78	332	53.15
33	57.89	133	61.36	233	48.94	333	33.77
34	58.19	134	83.67	234	60.36	334	67.67
35	54.02	135	84.04	235	55.12	335	69.03
36	52.82	136	61.79	236	48.34	336	66.99
37	52.26	137	97.22	237	59.43	337	84.54
38	59.13	138	94.18	238	58.42	338	74.03
39	52.67	139	97.19	239	64.02	339	90.31
40	55.10	140	74.34	240	52.94	340	89.12
41	63.16	141	60.83	241	122.54	341	77.00
42	47.79	142	60.48	242	55.32	342	61.40
43	74.55	143	87.09	243	70.97	343	69.44
44	75.22	144	60.47	244	80.95	344	84.69
45	68.376	145	62.069	245	70.874	345	88.172
46	70.16	146	85.859	246	72.48	346	89.89
47	55.24	147	53.03	247	56.57	347	48.72
48	67.57	148	47.06	248	60.46	348	98.87
49	55.14	149	48.68	249	55.56	349	94.09
50	71.55	150	53.67	250	57.89	350	100.56
51	88.16	151	55.78	251	91.59	351	92.59
52	72.09	152	93.61	252	59.57	352	90.40
53	48.42	153	61.06	253	67.74	353	72.11
54	51.85	154	54.89	254	80.95	354	50.59
55	51.72	155	54.73	255	79.07	355	64.29
56	71.77	156	98.88	256	90.00	356	61.11
57	63.47	157	90.45	257	69.56	357	70.37
58	72.15	158	74.51	258	73.72	358	99.44
59	58.69	159	56.08	259	59.82	359	89.95
60	69.72	160	52.09	260	90.83	360	89.42

61	91.06	161	99.41	261	58.18	361	62.65
62	92.05	162	52.50	262	61.54	362	76.92
63	62.58	163	62.90	263	67.24	363	69.23
64	53.55	164	56.94	264	68.75	364	50.00
65	66.28	165	77.00	265	94.81	365	50.75
66	68.35	166	88.83	266	73.91	366	72.15
67	65.67	167	61.67	267	66.67	367	99.42
68	60.27	168	53.15	268	70.37	368	77.78
69	60.87	169	89.45	269	65.52	369	75.00
70	52.63	170	56.62	270	76.19	370	84.44
71	59.37	171	89.95	271	56.00	371	74.56
72	57.30	172	97.75	272	45.16	372	80.00
73	93.42	173	73.38	273	75.00	373	82.10
74	78.26	174	73.91	274	81.58	374	80.00
75	71.29	175	77.88	275	75.76	375	76.52
76	58.06	176	78.50	276	61.11	376	77.36
77	64.29	177	86.52	277	75.00	377	66.12
78	69.52	178	88.89	278	58.59	378	86.36
79	68.64	179	59.42	279	57.69	379	87.88
80	58.43	180	86.36	280	65.00	380	90.95
81	66.67	181	64.52	281	60.24	381	52.09
82	52.94	182	55.41	282	55.56	382	76.27
83	53.79	183	85.00	283	54.67	383	58.21
84	60.35	184	78.85	284	58.73	384	90.32
85	66.10	185	44.44	285	57.47	385	78.64
86	56.00	186	81.82	286	54.84	386	56.94
87	52.56	187	83.33	287	57.57	387	71.97
88	52.74	188	80.18	288	58.33	388	60.13
89	52.59	189	50.00	289	56.41	389	72.85
90	65.52	190	82.29	290	56.16	390	74.00
91	56.99	191	88.89	291	85.00	391	90.00
92	56.72	192	89.53	292	63.75	392	43.24
93	62.35	193	47.92	293	62.50	393	43.59
94	57.97	194	54.67	294	57.69	394	88.64
95	81.81	195	81.81	295	57.14	395	56.75
96	55.17	196	86.36	296	85.52	396	71.11
97	76.59	197	83.33	297	71.87	397	86.87
98	43.47	198	91.86	298	66.67	398	57.35
99	64.58	199	53.85	299	57.69	399	78.57
100	56.60	200	51.79	300	69.81	400	68.42

Table 3.26: Chloride, sulphate and carbonate concentrations in soil samples from the study area

Sample code	Cl^- ($mgkg^{-1}$)	SO_4^{-2} ($mgkg^{-1}$)	CO_3^{-2} ($CaCO_3$ equiv) gkg^{-1}	Sample code	Cl^- ($mgkg^{-1}$)	SO_4^{-2} ($mgkg^{-1}$)	CO_3^{-2} ($CaCO_3$ equiv) gkg^{-1}
A1-1	6.2	15.3	34.1	C1-1	7.7	19.1	44.1
A1-2	5.3	13.1	31.3	C1-2	10.3	26.1	55.3
A1-3	7.8	19.3	44.4	C1-3	7.7	19.1	43.7
A1-4	7.6	18.9	43.6	C1-4	7.8	19.4	42.9
A1-5	5.6	13.9	32.8	C1-5	7.1	17.8	41.8
A1-6	7.4	18.1	42.9	C1-6	7.6	8.8	21.0
A1-7	7.5	18.1	42.7	C1-7	7.7	19.1	44.4
A1-8	7.9	19.6	43.6	C1-8	7.6	8.7	21.3
A1-9	6.2	15.3	35.8	C1-9	7.8	19.4	42.7
A1-10	6.0	15.1	34.7	C1-10	7.7	19.0	42.1
B1-1	7.7	19.2	43.9	D1-1	7.8	19.3	42.9
B1-2	6.1	15.1	34.6	D1-2	6.4	16.0	37.1
B1-3	7.8	19.2	43.9	D1-3	6.1	15.2	34.8
B1-4	5.5	13.7	33.3	D1-4	5.8	14.3	34.9
B1-5	5.6	13.9	34.1	D1-5	6.2	15.3	34.9
B1-6	5.6	14.0	34.7	D1-6	6.2	15.4	35.3
B1-7	0.2	2.1	11.1	D1-7	6.2	15.2	35.7
B1-8	9.2	23.1	52.7	D1-8	8.8	21.1	49.1
B1-9	6.0	15.1	34.9	D1-9	8.1	20.4	45.0
B1-10	7.8	19.3	44.9	D1-10	7.8	19.2	44.8
A2-1	7.7	19.1	39.9	C2-1	6.3	15.5	35.1
A2-2	7.8	19.3	42.3	C2-2	7.0	17.4	39.9
A2-3	5.6	13.8	33.3	C2-3	8.3	20.7	44.8
A3-4	6.3	15.5	36.2	C2-4	7.8	19.2	44.8
A2-5	6.0	15.0	34.9	C2-5	11.9	27.2	56.1
A2-6	5.9	14.9	34.8	C2-6	7.6	18.8	43.1
A2-7	6.9	17.3	40.1	C2-7	7.8	19.3	43.8
A2-8	6.8	16.3	36.9	C2-8	6.8	16.3	36.7
A2-9	7.5	18.1	43.1	C2-9	6.8	16.4	36.9
A2-10	6.0	15.1	34.8	C2-10	7.8	19.4	44.8
B2-1	6.6	15.1	34.9	D2-1	6.4	15.6	36.1
B2-2	9.1	23.0	51.3	D2-2	6.3	15.1	34.8
B2-3	7.1	17.8	40.2	D2-3	6.3	15.0	35.3
B2-4	6.9	17.2	40.1	D2-4	7.1	17.9	42.2
B2-5	5.3	13.1	32.3	D2-5	6.0	14.9	35.1
B2-6	4.0	10.5	24.8	D2-6	5.9	14.9	35.2
B2-7	4.6	11.4	26.6	D2-7	8.1	21.0	46.3
B2-8	5.7	13.2	32.9	D2-8	8.6	21.4	46.8
B2-9	5.5	12.9	31.3	D2-9	6.3	15.1	36.0
B2-10	7.3	18.1	43.7	D2-10	8.4	21.2	46.0

A3-1	6.3	15.2	36.7	C3-1	8.5	21.5	46.9
A3-2	7.7	19.1	44.9	C3-2	8.6	21.5	45.8
A3-3	3.9	10.5	26.7	C3-3	8.9	22.2	47.7
A3-4	10.9	28.7	57.1	C3-4	8.8	22.1	49.9
A3-5	7.0	17.5	40.2	C3-5	8.4	21.3	48.8
A3-6	6.9	17.3	40.0	C3-6	8.4	21.2	48.9
A3-7	6.8	16.3	36.2	C3-7	8.1	20.6	44.8
A3-8	5.4	13.1	31.1	C3-8	8.8	22.2	48.7
A3-9	7.1	18.2	43.4	C3-9	8.7	22.0	48.1
A3-10	7.0	17.6	41.0	C3-10	8.6	21.7	46.2
B3-1	8.0	20.3	43.8	D3-1	7.9	19.8	44.8
B3-2	ND	42.5	57.3	D3-2	6.9	17.2	39.9
B3-3	8.1	20.5	44.8	D3-3	7.0	17.5	40.1
B3-4	6.4	16.4	37.1	D3-4	7.2	17.8	40.8
B3-5	2.3	5.3	16.1	D3-5	6.3	16.1	36.7
B3-6	ND	43.5	51.9	D3-6	6.1	16.2	34.9
B3-7	7.1	18.1	43.2	D3-7	6.1	16.1	36.1
B3-8	6.1	15.2	12.2	D3-8	6.3	15.4	35.7
B3-9	6.4	16.0	36.0	D3-9	8.1	20.7	45.8
B3-10	6.1	15.3	12.8	D3-10	7.1	17.8	41.1
A4-1	6.1	15.1	35.3	C4-1	11.0	29.6	59.1
A4-2	7.0	17.6	40.3	C4-2	10.8	26.1	56.2
A4-3	6.0	14.9	35.1	C4-3	11.7	30.4	54.3
A4-4	6.0	15.0	35.0	C4-4	11.5	30.0	50.5
A4-5	5.9	15.1	35.7	C4-5	11.5	29.8	48.9
A4-6	6.0	15.0	36.1	C4-6	11.4	29.1	50.1
A4-7	5.9	15.1	34.8	C4-7	11.6	29.9	49.7
A4-8	8.1	20.5	45.7	C4-8	10.8	26.8	25.9
A4-9	7.8	19.5	44.9	C4-9	11.7	30.1	48.9
A4-10	6.9	17.7	40.0	C4-10	11.6	29.6	49.7
B4-1	7.8	19.6	45.1	D4-1	7.0	17.6	40.1
B4-2	7.9	19.9	44.8	D4-2	7.1	17.9	41.1
B4-3	7.7	19.5	46.2	D4-3	6.2	15.4	34.8
B4-4	6.0	14.9	34.6	D4-4	8.3	20.6	44.9
B4-5	ND	42.8	51.3	D4-5	6.5	16.7	37.5
B4-6	ND	45.2	58.9	D4-6	6.0	15.0	35.3
B4-7	5.7	14.1	34.7	D4-7	6.9	17.3	41.1
B4-8	7.7	19.6	45.1	D4-8	9.6	23.8	51.2
B4-9	7.7	19.4	45.0	D4-9	9.7	24.1	54.3
B4-10	11.1	26.8	50.1	D4-10	7.8	19.9	45.1
A5-1	8.2	21.0	47.9	C5-1	9.1	22.8	49.3
A5-2	9.5	23.4	50.1	C5-2	10.6	27.1	50.1
A5-3	10.4	26.8	49.8	C5-3	10.7	26.9	49.7
A5-4	9.3	22.8	54.8	C5-4	9.5	23.1	44.4
A5-5	9.6	23.7	54.1	C5-5	10.1	25.9	49.7
A5-6	9.5	23.1	52.9	C5-6	9.9	24.8	50.3

A5-7	9.4	23.1	52.0	C5-7	10.1	25.7	54.2
A5-8	9.3	22.9	54.1	C5-8	10.6	27.1	52.3
A5-9	9.5	23.2	54.9	C5-9	10.5	27.0	51.9
A5-10	8.1	20.4	44.9	C5-10	10.9	29.3	50.1
B5-1	8.3	21.1	46.3	D5-1	7.9	19.7	45.1
B5-2	7.5	18.4	42.8	D5-2	7.3	18.1	43.1
B5-3	7.5	18.5	42.1	D5-3	6.8	16.9	38.9
B5-4	5.8	14.0	34.1	D5-4	6.9	17.1	39.1
B5-5	5.7	13.9	33.1	D5-5	6.9	16.8	36.8
B5-6	5.8	14.0	33.4	D5-6	6.2	15.6	35.1
B5-7	1.8	3.6	14.3	D5-7	6.6	16.6	36.1
B5-8	1.9	3.9	16.1	D5-8	8.1	20.5	44.8
B5-9	7.6	16.9	38.8	D5-9	8.1	20.6	44.9
B5-10	ND	45.7	49.6	D5-10	8.1	20.4	45.6
A6-1	9.8	24.8	50.3	C6-1	10.3	26.1	55.5
A6-2	10.7	26.5	46.1	C6-2	10.4	26.4	54.9
A6-3	9.9	24.8	41.8	C6-3	11.5	30.1	51.0
A6-4	10.7	25.9	40.9	C6-4	10.8	26.3	49.6
A6-5	10.9	27.1	55.1	C6-5	10.0	25.1	51.9
A6-6	7.8	19.8	45.0	C6-6	10.8	26.2	50.5
A6-7	6.9	17.8	38.7	C6-7	9.1	23.0	50.7
A6-8	6.0	15.0	34.8	C6-8	9.0	22.6	48.7
A6-9	6.3	16.2	37.1	C6-9	11.3	29.9	50.1
A6-10	5.8	14.8	12.1	C6-10	10.9	28.1	50.9
B6-1	7.8	19.9	44.8	D6-1	8.8	22.1	46.1
B6-2	6.1	15.3	25.3	D6-2	8.9	22.7	41.3
B6-3	7.0	17.6	40.1	D6-3	6.2	15.6	35.1
B6-4	6.1	15.2	35.1	D6-4	6.3	16.2	37.8
B6-5	5.7	13.6	32.4	D6-5	6.1	15.1	34.8
B6-6	4.0	10.1	24.7	D6-6	6.2	15.6	35.9
B6-7	6.2	15.6	35.2	D6-7	7.8	19.8	44.1
B6-8	7.1	17.9	41.6	D6-8	7.0	17.5	40.0
B6-9	6.8	16.9	38.8	D6-9	8.8	22.2	49.1
B6-10	7.2	15.6	35.8	D6-10	8.1	20.7	44.3
A7-1	11.1	30.1	41.1	C7-1	6.6	16.1	36.7
A7-2	10.7	26.1	48.5	C7-2	6.8	16.8	36.0
A7-3	10.8	26.4	40.3	C7-3	8.0	20.2	46.1
A7-4	10.6	26.0	47.2	C7-4	7.2	17.8	42.4
A7-5	10.6	25.9	48.1	C7-5	7.8	19.6	44.8
A7-6	5.9	14.9	35.4	C7-6	7.9	19.8	44.0
A7-7	5.1	12.8	30.1	C7-7	7.9	19.8	46.1
A7-8	7.8	18.8	41.1	C7-8	5.6	14.1	33.2
A7-9	7.1	17.7	39.9	C7-9	7.9	19.7	44.0
A7-10	7.7	19.5	41.3	C7-10	7.8	19.6	45.1
B7-1	7.9	19.9	44.2	D7-1	7.1	17.9	41.1
B7-2	7.9	20.0	45.6	D7-2	6.8	16.7	36.2

B7-3	7.2	17.6	40.1	D7-3	6.8	16.8	36.7
B7-4	5.1	12.9	29.9	D7-4	7.3	18.0	42.1
B7-5	5.0	12.6	29.1	D7-5	5.6	13.9	34.1
B7-6	5.8	14.8	34.2	D7-6	5.5	13.4	31.1
B7-7	7.0	17.4	40.1	D7-7	8.1	20.3	44.1
B7-8	5.8	14.9	37.1	D7-8	10.3	25.1	41.9
B7-9	5.7	14.6	34.7	D7-9	11.1	30.1	50.2
B7-10	6.9	17.3	41.1	D7-10	7.3	17.9	41.3
A8-1	11.8	30.6	5.1	C8-1	6.3	16.1	35.1
A8-2	10.7	26.0	48.9	C8-2	6.1	16.1	36.7
A8-3	10.9	26.7	43.4	C8-3	6.2	15.9	36.1
A8-4	8.9	22.8	45.2	C8-4	6.4	16.6	36.1
A8-5	10.1	25.7	44.1	C8-5	6.5	16.4	36.9
A8-6	9.9	24.8	40.1	C8-6	6.6	16.4	37.1
A8-7	10.1	25.1	30.8	C8-7	6.2	15.8	35.9
A8-8	10.1	24.9	29.8	C8-8	6.9	16.7	36.8
A8-9	10.4	25.6	30.6	C8-9	7.4	18.1	42.5
A8-10	11.9	30.7	40.1	C8-10	7.6	18.6	40.5
B8-1	7.1	17.8	38.1	D8-1	6.5	16.5	37.6
B8-2	7.9	19.8	40.2	D8-2	6.9	16.8	37.9
B8-3	6.8	17.0	40.7	D8-3	6.3	15.9	35.6
B8-4	4.6	11.3	23.2	D8-4	6.1	15.7	35.1
B8-5	5.0	12.6	24.1	D8-5	6.1	16.8	37.7
B8-6	4.2	10.8	23.9	D8-6	5.9	15.1	35.1
B8-7	4.9	11.0	24.1	D8-7	5.9	15.2	34.8
B8-8	4.9	10.9	22.8	D8-8	9.3	23.2	46.1
B8-9	4.4	10.7	20.1	D8-9	10.4	25.7	47.0
B8-10	4.8	10.8	23.7	D8-10	4.4	10.8	24.8
A9-1	10.8	26.5	40.1	C9-1	7.8	19.4	44.9
A9-2	10.8	26.7	46.8	C9-2	6.4	15.6	35.9
A9-3	10.1	25.1	47.8	C9-3	7.7	19.3	44.8
A9-4	10.2	25.8	47.9	C9-4	7.0	17.5	40.8
A9-5	8.5	21.5	45.7	C9-5	8.4	21.2	44.9
A9-6	10.4	25.8	47.8	C9-6	6.0	15.1	35.0
A9-7	10.8	26.6	47.7	C9-7	7.7	19.4	44.8
A9-8	10.2	25.7	46.9	C9-8	8.5	21.6	47.2
A9-19	10.2	25.8	47.1	C9-9	7.7	19.5	45.1
A9-10	11.7	30.3	56.5	C9-10	7.9	19.9	45.0
B9-1	7.2	18.0	41.1	D9-1	5.8	13.8	30.7
B9-2	9.2	23.1	51.2	D9-2	7.1	17.9	41.1
B9-3	8.0	19.9	45.1	D9-3	6.8	16.5	37.2
B9-4	6.9	17.3	42.1	D9-4	6.8	16.6	37.1
B9-5	6.6	16.2	40.8	D9-5	8.8	21.1	48.9
B9-6	5.6	13.8	31.3	D9-6	7.6	18.1	43.2
B9-7	5.9	14.3	35.2	D9-7	6.0	15.1	34.8
B9-8	5.6	14.0	35.1	D9-8	8.0	20.3	45.0

B9-9	6.7	16.9	41.0	D9-9	9.5	24.6	55.1
B9-10	6.1	15.2	35.9	D9-10	5.8	14.7	33.8
A10-1	11.1	30.2	58.7	C10-1	7.1	18.1	43.2
A10-2	9.7	23.9	52.7	C10-2	6.7	16.7	36.7
A10-3	9.5	22.8	49.1	C10-3	7.1	17.9	43.0
A10-4	8.9	22.1	47.3	C10-4	6.5	15.8	36.1
A10-5	8.2	20.6	45.1	C10-5	7.7	19.2	43.8
A10-6	9.6	23.1	53.1	C10-6	7.1	17.8	40.7
A10-7	11.0	30.0	58.7	C10-7	6.3	15.5	35.1
A10-8	10.5	26.4	56.2	C10-8	7.2	18.1	43.8
A10-9	9.6	23.1	51.3	C10-9	7.9	19.6	45.1
A10-10	10.1	25.7	55.1	C10-10	7.7	18.1	43.1
B10-1	8.1	20.5	45.1	D10-1	6.8	16.4	36.1
B10-2	8.0	20.0	45.0	D10-2	5.8	14.6	34.8
B10-3	6.0	15.1	35.1	D10-3	6.0	15.0	35.1
B10-4	5.9	14.9	34.9	D10-4	6.3	15.9	40.1
B10-5	6.1	15.6	35.8	D10-5	5.4	13.9	30.3
B10-6	6.1	15.5	35.9	D10-6	6.2	15.5	35.1
B10-7	5.8	16.7	38.7	D10-7	7.8	19.5	45.3
B10-8	7.9	19.7	44.1	D10-8	10.1	25.6	55.1
B10-9	7.2	17.8	41.3	D10-9	10.5	27.0	57.1
B10-10	7.7	19.1	45.1	D10-10	7.8	19.5	44.7